



Some pages of this thesis may have been removed for copyright restrictions.

If you have discovered material in AURA which is unlawful e.g. breaches copyright, (either yours or that of a third party) or any other law, including but not limited to those relating to patent, trademark, confidentiality, data protection, obscenity, defamation, libel, then please read our [Takedown Policy](#) and [contact the service](#) immediately

Strategic Development and Physicochemical Analysis of Oral Preparations for Unstable Drugs

Anjumn Shabir
Doctor of Philosophy

Aston University

December 2011

©Anjumn Shabir, 2011, asserts her moral right to be identified as the author of this thesis.

This copy of the thesis has been supplied on the condition that anyone who consults it is understood to recognise that its copyright rests with its author and that no quotation from the thesis and no information derived from it may be published without proper acknowledgment.

Aston University

**Strategic Development and Physicochemical Analysis of Oral Preparations for
Unstable Drugs**

Anjum Shabir

Doctor of Philosophy

Summary

Oral liquid formulations are ideal dosage forms for paediatric, geriatric and patient with dysphagia. Dysphagia is prominent among patients suffering from stroke, motor neurone disease, advanced Alzheimer's and Parkinson's disease. However oral liquid preparations are particularly difficult to formulate for hydrophobic and unstable drugs. Therefore current methods employed in solving this issue include the use of 'specials' or extemporaneous preparations. In order to challenge this, the government has encouraged research into the field of oral liquid formulations, with the EMEA and MHRA publishing list of drugs of interest. The current work investigates strategic formulation development and characterisation of select API's (captopril, gliclazide, melatonin, L-arginine and lansoprazole), each with unique obstacles to overcome during solubilisation, stabilisation and when developing a palatable dosage form. By preparing a validated calibration protocol for each of the drug candidates, the oral liquid formulations were assessed for stability, according to the ICH guidelines along with thorough physicochemical characterisation.

The results showed that pH and polarity of the solvent had the greatest influence on the extent of drug solubilisation, with inclusion of antioxidants and molecular steric hindrance influencing the extent of drug stability.

Captopril, a hydrophilic ACE inhibitor (160 mg.mL^{-1}), undergoes dimerisation with another captopril molecule. It was found that with the addition of EDTA and HP- β -CD, the drug molecule was stabilised and prevented from initiating a thiol induced first order free radical oxidation. The cyclodextrin provided further steric hindrance (1:1 molar ratio) resulting in complete reduction of the intensity of sulphur like smell associated with captopril. Palatability is a crucial factor in patient compliance, particularly when developing a dosage form targeted towards paediatrics. L-arginine is extremely bitter in solution (148.7 g.L^{-1}). The addition of tartaric acid into the 100 mg.mL^{-1} formulation was sufficient to mask the bitterness associated with its guanidium ions.

The hydrophobicity of gliclazide (55 mg.L^{-1}) was strategically challenged using a binary system of a co-solvent and surfactant to reduce the polarity of the medium and ultimately increase the solubility of the drug. A second simpler method was developed using pH modification with L-arginine.

Melatonin has two major obstacles in formulation: solubility ($100 \text{ } \mu\text{g.mL}^{-1}$) and photosensitivity, which were both overcome by lowering the dielectric constant of the medium and by reversibly binding the drug within the cyclodextrin cup (1:1 ratio). The cyclodextrin acts by preventing UV rays from reaching the drug molecule and initiated the degradation pathway.

Lansoprazole is an acid labile drug that could only be delivered orally via a delivery vehicle. In oral liquid preparations this involved nanoparticulate vesicles. The extent of drug loading was found to be influenced by the type of polymer, concentration of polymer, and the molecular weight.

All of the formulations achieved relatively long shelf-lives with good preservative efficacy.

Keywords: HP- β -CD, paediatrics, nanoparticles, PET

ACKNOWLEDGEMENTS

I would like to thank my supervisors, Dr. Afzal Mohammed and Professor Yvonne Perrie for the continued support I received during my PhD. I am very grateful for their enthusiasm, encouragement, motivation, especially their immense knowledge.

I would also like to thank Jiteen Ahmed for his ability to lift ones spirit when things are tough, and when my motivation was nearly lost.

I would also like to thank all of the technical staff and fellow lab mates in the Drug Delivery Group at Aston University.

Most of all I want to thank God, my family and best friend for always supporting me and pushing me to achieve more.

Abuji, Mama, Bhaijaan Abrar and Didi, I dedicate this PhD to you. I could not have done this without any of you.

LIST OF CONTENTS

Title	1
Summary.....	2
Acknowledgements.....	3
List of Contents	4
List of Tables	13
List of Figures	16
Abbreviations	28
Thesis Publications	31
Chapter 1.....	34
1.1. Project scope and significance	35
1.2. Reformulation of medicines	36
1.3. Gastrointestinal physiology and its impact on bioavailability	38
1.4. Drug formulation strategies.....	40
1.4.1. <i>Solubility Enhancement</i>	40
1.4.1.1. <i>pH adjustment</i>	40
1.4.1.2. Solvent and Co-solvents.....	41
1.4.1.2.1. Mechanism of solvent action on drug solubility	41
1.4.2. <i>Cyclodextrins</i>	43
1.4.2.1. Pharmaceutical applications	44
1.4.2.1.1. Solubilisation	44
1.4.2.1.2. Taste masking	45
1.4.2.1.3. Drug stabilisation	46
1.4.2.1.4. Photostability	46

<i>1.4.3. Suspensions</i>	47
1.4.3.1. Particle-Particle Interactions	48
1.4.3.1.1. Electrical Properties of Particles in Suspension	48
1.4.3.1.2. Effect of particle Separation on Particle Interaction.....	49
1.4.3.1.3. Electrolytes.....	50
1.4.3.1.4 Surface Active Agents	51
1.4.3.1.5. Hydrophilic Polymers.....	52
1.4.3.1.6. Nanoparticles	53
1.4.3.1.6. Nanoparticles	54
1.5. Excipients for Inclusion in all Oral Liquid Formulations	54
1.5.1. <i>Preservatives</i>	54
1.5.2. <i>Chemical stabilisers</i>	55
1.6. Development of a Palatable Formulation	57
1.6.1. <i>Sweeteners</i>	57
1.6.2. <i>Flavourings</i>	58
1.7. <i>Rational and aim of the project</i>	58
Chapter 2.....	60
2.1.1. <i>Angiotensin Converting Enzyme (ACE)</i>	61
2.1.2. <i>ACE Inhibitors</i>	61
2.1.3. <i>Captopril</i>	64
2.1.3.1. “Specials” – current state of oral liquid captopril	66
2.1.4. <i>Aims and objectives</i>	66
2.2. Methods and materials	67
2.2.1. <i>Materials</i>	67
2.2.2. <i>Calibration validation</i>	67
2.2.3. <i>Formulation strategies</i>	67
2.2.3.1. <i>Captopril solubilisation</i>	67
2.2.3.2. <i>Addition of an antioxidant</i>	67
2.2.3.2.1. Addition of 0.1 % (w/v) sodium-metabisulphite.....	68
2.2.3.2.2. Addition of 30 % (w/v) glycerol.....	68
2.2.3.2.3. Addition of HP-β-CD	68
2.2.3.3. 5mg.mL ⁻¹ formulation of captopril.....	68

2.2.3.3.1. Addition of EDTA	68
2.2.3.3.2. Addition of HP- β -CD with EDTA	68
2.2.4. <i>Microviscosity of glycerol</i>	69
2.2.5. <i>Conductivity measurements</i>	69
2.2.5.1. Calculation of association constant	69
2.2.5.2. Calculation of Molar conductivities	70
2.2.6. <i>Freeze-drying protocol</i>	71
2.2.7. <i>Proton Nuclear Magnetic resonance Spectroscopy (H^1-NMR)</i>	72
2.2.8. <i>Differential Scanning Calorimetry (DSC)</i>	72
2.2.9. <i>Thermogravimetric analysis (TGA)</i>	72
2.2.10. <i>Fourier Transform Infrared Spectroscopy (FTIR)</i>	72
2.2.11. <i>pH</i>	73
 2.3. Results and Discussion	74
2.3.1. <i>Validation of Calibration Curve</i>	74
2.3.1.1. Linearity	74
2.3.1.2. Precision	74
2.3.1.3. Accuracy	75
2.3.1.4 Limit of detection (LOD) and limit of quantification (LOQ)	75
2.3.2. <i>Formulation development strategy</i>	75
2.3.2. <i>Formulation development strategy</i>	76
2.3.3. <i>Approaches to reduce oxidation</i>	76
2.3.3.1. Influence of addition of antioxidant on the stability of captopril in solution	76
2.3.3.2. Influence of EDTA and glycerol on the stability of captopril in solution	81
2.3.3.3. Influence of addition of sodium metabisulphite on captopril stability in solution	85
2.3.4. <i>Approaches to enhance the organoleptic properties of the formulation</i>	87
2.3.4. <i>Approaches to enhance the organoleptic properties of the formulation</i>	88
2.3.4.1. Influence of HP- β -CD on captopril in solution	88
2.3.4.2. Interaction of HP- β -CD with captopril and its influencing properties	92
2.3.5. <i>Influence of concentration of captopril and its affect on shelf life stability</i>	98
 2.4. Conclusion	100
 Chapter 3.....	101
3.1. Introduction	102
3.1.1. <i>Gliclazide structure and mechanism of action</i>	102

3.1.1. Gliclazide and its therapeutic affects	103
3.1.2. Current dosage forms.....	103
3.1.3. Aim.....	103
 3.2. Materials and Method	105
3.2.1. Materials.....	105
3.2.2. Calibration Validation.....	105
3.2.3. Phase solubility	105
3.2.3.1. Phase solubility with pH modification	105
3.2.4. Oral liquid formulation of gliclazide	106
3.2.4.1. Solubilisation of gliclazide (8 mg.mL^{-1}) with L-arginine (7 mg.mL^{-1})	106
3.2.4.2. Solubilisation of gliclazide (16 mg.mL^{-1}) with 5 % pluronic F127 (w/v) and 15 % ethanol (v/v).....	106
3.2.5. Freeze-drying protocol.....	106
3.2.6. Differential Scanning Calorimetry (DSC).....	107
3.2.7. Thermogravimetric analysis (TGA)	107
3.2.8. Fourier Transform Infrared Spectroscopy (FTIR)	107
3.2.9. Proton Nuclear Magnetic Resonance Spectroscopy ($H^1\text{-NMR}$).....	108
3.2.10. pH	108
 3.3. Results and Discussion	109
3.3.1. Calibration Validation.....	109
3.3.1.1 Linearity.....	109
3.3.1.2 Precision	109
3.3.1.3. Accuracy	110
3.3.1.4 Limit of detection (LOD) and limit of quantification (LOQ)	110
3.3.2. Phase solubility	110
3.3.2. Phase solubility	111
3.3.2.1. Solubilisation of gliclazide with amino acids.....	111
3.3.2.1.1. L-arginine	111
3.3.2.1.2. L-lysine	112
3.3.2.2. Solubilisation of gliclazide with Pluronic F127	115
3.3.2.2. Solubilisation of gliclazide with Pluronic F127	116
3.3.2.2.1. Influence of Pluronic F127 concentration	116
3.3.2.2.2. Influence of pH and pluronic F127 (5 % w/v)	117
3.3.2.2.3. Summary	118
3.3.2.4. Solubilisation of gliclazide in a co-solvent system	119

3.3.2.4.1. Influence of pH and ethanol (15 % v/v)	120
3.3.2.4.1. Influence of pH and ethanol (15 % v/v)	121
3.3.2.5. Solubilisation of gliclazide with 5 % (w/v) F127 and 15 % (v/v) ethanol-water	122
3.3.2.6. Phase solubility summary	122
3.3.3. <i>Formulation and stability of an oral liquid solution of gliclazide</i>	123
3.3.3.1. Gliclazide (8 mg.mL ⁻¹) oral liquid formulation in the presence of 7 mg.mL ⁻¹ L-arginine	123
3.3.3.2. Gliclazide (16 mg.mL ⁻¹) oral liquid formulation in the presence of 15 % (v/v) ethanol and 5 % (w/v) Pluronic F127	123
3.3.4. <i>Physicochemical analysis of gliclazide with L-arginine</i>	124
3.3.4. <i>Physicochemical analysis of gliclazide with L-arginine</i>	125
3.3.4.1. DSC.....	125
3.3.4.2. FTIR analysis	127
3.3.4.2. FTIR analysis	128
3.3.4.3. H ¹ -NMR	131
3.4. Conclusion	133
3.4. Conclusion	134
Chapter 4.....	135
4.1. Introduction and Aims.....	136
4.1.1. <i>Amino Acids</i>	136
4.1.2. <i>Arginine</i>	137
4.1.2.1. Therapeutic effect of Arginine	137
4.1.2.2. Structure and Metabolism	137
4.1.3. <i>Aim</i>	140
4.2. Materials and Method	141
4.2.1. <i>Materials</i>	141
4.2.2. <i>Method</i>	141
4.2.2.1. Protocol for Ninhydrin-UV Calibration of L-arginine.....	141
4.2.2.1.1. Preparation of 1 M sodium phosphate	141
4.2.2.1.2. Preparation of stock solution of L-arginine	141
4.2.2.1.3. Ninhydrin assay	141
4.2.2.2. pH titrations using tartaric acid.....	142

4.2.2.3. Oral liquid formulation recipe of L-arginine.....	142
4.3. Results and Discussion	144
4.3.1. <i>Optimisation of a calibration protocol for the detection and quantification of L-arginine in solution.....</i>	144
4.3.1.1. Preliminary investigations	144
4.3.1.2. Development of Ninhydrin assay	149
4.3.1.3. Ninhydrin mechanism	151
4.3.2. <i>Calibration Validation using a modified ninhydrin assay</i>	153
4.3.2.1. Linearity.....	153
4.3.2.2. Precision	153
4.3.2.3. Accuracy	154
4.3.2.4 Limit of detection (LOD) and limit of quantification (LOQ)	154
4.3.3. <i>Optimisation of an oral liquid formulation for L-arginine: rational for taste masking...154</i>	154
4.3.3. <i>Optimisation of an oral liquid formulation for L-arginine: rational for taste masking ...155</i>	155
4.3.3.1. Influence of Tartaric acid	155
4.3.3.1. Formulation Optimisation.....	157
4.3.4. <i>Stability studies</i>	157
4.4. Conclusion	160
Chapter 5.....	161
5.1. Introduction	162
5.1.1. <i>Structure, biosynthesis and metabolism of melatonin</i>	162
5.1.2. <i>Melatonin and its therapeutic effects</i>	163
5.1.3. <i>Current dosage forms.....</i>	163
5.1.4. <i>Aim.....</i>	165
5.2. Materials and Method	166
5.2.1. <i>Materials.....</i>	166
5.2.2. <i>Method</i>	166
5.2.2.1. Development of a calibration method for melatonin	166
5.2.2.2. pH titration of tartaric acid	166
5.2.2.3. Oral liquid formulation recipe of melatonin	167
5.3. Results and discussion	168
5.3.1. <i>Calibration Validation.....</i>	168

5.3.1.1. Linearity.....	168
5.3.1.2. Precision	169
5.3.1.3. Accuracy	169
5.3.1.4. Limit of detection (LOD) and limit of quantification (LOQ)	169
5.3.1.4. Limit of detection (LOD) and limit of quantification (LOQ)	170
5.3.2. <i>Influence of polarity on the solubilisation of melatonin</i>	170
5.3.3. <i>Organoleptic optimisation of melatonin in solution (1 mg.mL⁻¹)</i>	172
5.3.4. <i>Stability studies</i>	173
5.4. Conclusion	175
Chapter 6.....	176
6.1. Introduction	177
6.2. Materials and Method.....	178
6.2.1. <i>Materials</i>	178
6.2.2. <i>Method</i>	178
6.2.2.1. Preparation of neutraliser	178
6.2.2.2. Preparation of the inoculum	178
6.2.2.3. Harvesting bacteria and C. albicans	179
6.2.2.4. Harvesting A. niger	179
6.2.2.5. Inoculation of pharmaceutical preparation	180
6.2.2.6. Preservative efficacy test.....	180
6.3. Results and discussion.....	181
6.3.1. <i>Preservative activity against Bacteria</i>	181
6.3.1.1. Structure of bacteria	181
6.3.1.2. Self-preserving formulations	184
6.3.1.2.1. Preservation efficacy using acidic medium	184
6.3.1.2.2. Preservative efficacy using chelating agents on Gram-negative bacteria.....	186
6.3.1.2.3. Conclusion.....	187
6.3.1.3. Synergistic effect of EDTA with potassium sorbate.....	187
6.3.1.4. Preservative affects of sodium benzoate	191
6.3.1.4. Preservative affects of sodium benzoate	192
6.3.1.5. Preservative affects of parabens	195
6.3.2. <i>Preservative activity against Fungi</i>	199

6.3.2.1. Fungi structure and classification.....	199
6.3.2.2. Preservative efficacy against C. albicans.....	200
6.3.2.3. Preservative efficacy against A.niger	204
6.4. Conclusion	206
Chapter 7.....	207
7.1. Introduction	208
7.1.1. <i>Therapeutic effect of proton pump inhibitors (PPI's)</i>	208
7.1.1.1. Structure, mechanism of action and metabolism of lansoprazole.....	208
7.1.1.2. Current dosage forms.....	209
7.1.2. <i>Polymeric nanoparticle delivery</i>	209
7.1.2.1. Special consideration for nanoparticles during formulation	210
7.1.3. <i>Aim</i>	211
7.2. Methods and Materials	212
7.2.1. <i>Materials</i>	212
7.2.2. <i>Methods</i>	212
7.2.2.1. Development of a calibration method for lansoprazole	212
7.2.2.2.1. Calibration validation protocol.....	212
7.2.2.2. Nanoparticle preparation using the solvent displacement technique	213
7.2.2.3. Nanoparticle preparation using the emulsion diffusion technique.....	214
7.2.2.5. pH	214
7.2.2.6. Particle sizing	214
7.2.2.7. Planetary-ball milling	214
7.2.2.8. Scanning electron microscopy (SEM)	215
7.2.2.9. Micro-viscosity testing of PCL nanoparticles.....	215
7.2.2.10. Molecular weight analysis of milled polymers using gel permeation chromatography (GPC)	215
7.2.2.11. Wettability profiling	215
7.2.2.13. Freeze-drying preparation of nanoparticles.....	216
7.2.2.14. Differential scanning calorimetry (DSC)	216
7.2.2.15. Thermogravimetric Analysis (TGA)	216
7.2.2.16. Fourier Transform Infrared Spectroscopy (FTIR)	216
7.2.2.17. Proton Nuclear Magnetic Resonance Spectroscopy (H^1 -NMR).....	217
7.2.2.18. In Vitro Release Studies	217

7.2.2.18.1. Nanoparticle preparation	217
2.2.2.18.2. Fasted State	217
7.2.2.18.3. Non-Fasted State	218
7.2.2.19. Statistical analysis	218
 7.3. Results	219
7.3.1. <i>Calibration Validation</i>	219
7.3.1.1 Linearity.....	219
7.3.1.2 Precision	219
7.3.1.3. Accuracy	220
7.3.1.4 Limit of detection (LOD) and limit of quantification (LOQ)	220
7.3.2. <i>Influence of PCL and PLGA polymer ratio on nanoparticle preparation and characterisation using the solvent displacement technique</i>	221
7.3.3. <i>Influence of the mode of preparation of PCL nanoparticles: solvent displacement versus emulsion diffusion method</i>	225
7.3.3.1. Characterisation of lansoprazole loaded PCL nanoparticles	225
7.3.3.2.1. Influence of viscosity.....	226
7.3.3.2.1. Conclusion.....	227
7.3.4. <i>Planetary ball milling</i>	228
7.3.4.1. Implications on physical properties of PCL and PLGA	228
7.3.4.1.1. Impact on molecular weight	228
7.3.4.1.2. Wettability studies: Impact on polymer hydrophobicity	229
7.3.4.1.3. Thermal analysis	233
7.3.4.2. Influence of milled polymers on nanoparticle formation	236
7.3.4.2.1. Milled PCL nanoparticles	236
7.3.4.2.2. Milled PLGA nanoparticles	237
7.3.4.3. Physiochemical analysis of milled PCL and milled PLGA nanoparticles	239
7.3.4.3.1. H ¹ -NMR	239
7.3.4.3.2. FTIR	246
7.3.4.3.3. DSC.....	249
7.3.4.3.3. DSC.....	250
7.3.5. <i>In Vitro release study</i>	253
7.3.5. <i>In Vitro release study</i>	254
7.3.5.1. Implications of the fasted state conditions (0.1 M HCl) on non-milled and milled polymeric nanoparticles	254

7.3.5.2. Implications of the fed state conditions (pH 4.5) on milled and non-milled polymeric nanoparticles	256
7.3.5.3. Fasting versus Fed conditions	257
7.4. Conclusion	258
Chapter 8.....	259
8.1. Summary of research findings	260
8.1.1. <i>Formulation development and physicochemical investigation of a stable aqueous preparation of captopril</i>	260
8.1.2. <i>Solubilisation and physicochemical analysis of gliclazide</i>	261
8.1.3. <i>Solubilisation and formulation of melatonin as a liquid oral dosage form</i>	261
8.1.4. <i>Optimisation of an extraction protocol and development of an oral liquid formulation for L-arginine</i>	262
8.1.5. <i>Preservative Efficacy Test (PET)</i>	262
8.1.6. <i>Solubilisation of a proton pump inhibitor (Lansoprazole) using nano-particulate delivery</i>	263

LIST OF TABLES

Table 1.1.	Cyclodextrin characteristics.....	43
Table 1.2.	Classification of antioxidants.....	55
Table 2.1.	Summary of Calibration Validation of captopril.....	73
Table 2.2.	Conductiometry calculations for captopril with increasing molar concentrations of HP- β -CD.....	87
Table 2.3.	Frequency of bond vibrations attributing to the captopril and HP- β -CD complex formulation.	92
Table 3.1.	Summary of calibration validation of gliclazide.....	106
Table 3.2.	The calculated difference of gliclazide with L-lysine and L-arginine.....	112
Table 3.3.	Summary of the thermokinetic changes occurring when solubilising gliclazide with L-arginine.....	124
Table 3.4.	FTIR analysis of gliclazide in solution once formulated as an oral liquid dosage form, and its bond vibrations and their respective donors.....	128
Table 4.1.	Summary of amino acids based on their difference in structure and physic chemical properties.....	133
Table 4.2.	Urea Cycle disorders.....	135
Table 4.3.	Protocol for the preparation of L-arginine-ninhydrin solutions at various concentrations.....	138
Table 4.4.	Summary of calibration validation of L-arginine.....	150

Table 4.5.	Stability study assessing oragnoleptic properties of the oral liquid formulation of L-arginine (100 mg.mL ⁻¹).....	154
Table 5.1.	Summary of calibration validation of melatonin.....	165
Table 6.1.	'In-house' calibration of known concentrations of bacteria and <i>C. albicans</i>	175
Table 6.2.	Summary of factors enhancing preservative efficacy.....	179
Table 6.3.	Tryptone soya agar plates cultured with bacteria after inoculation with potassium sorbate in the melatonin pharmaceutical preparation.....	186
Table 6.4.	Tryptone soya agar plates cultured with bacteria after inoculation with sodium benzoate in the L-arginine pharmaceutical preparation.....	189
Table 6.5.	Tryptone soya agar plates cultured with bacteria after inoculation with parabens in the Gliclazide-L-arginine pharmaceutical preparation.....	192
Table 6.6.	Tryptone soya agar plates cultured with bacteria after inoculation with parabens in the gliclazide-ethanol (15 % v/v) pharmaceutical preparation.....	194
Table 6.7.	Sabroud dextrose agar plates cultured with <i>C. albicans</i> after inoculation with preservative-free captopril formulations.....	197
Table 6.8.	Sabroud dextrose agar plates cultured with <i>C. albicans</i> after inoculation with formulations containing; potassium sorbate, sodium benzoate, parabens, or parabens in the presence of ethanol (15 % v/v).....	199

Table 6.9.	Sabroud dextrose agar plates cultured with <i>A. niger</i> after inoculation with formulations containing; potassium sorbate, sodium benzoate, parabens, or parabens in the presence of ethanol (15 % v/v).....	201
Table 7.1.	Calibration validation of lansoprazole using a UV spectrophotometer.....	216
Table 7.2.	Characterisation of PCL nanoparticles before and after lansoprazole loading.....	217
Table 7.3.	Characterisation of PLGA nanoparticles with and without lansoprazole loading.....	218
Table 7.4.	Comparison of lansoprazole loaded PCL nanoparticles preparation techniques: solvent displacement vs. emulsion diffusion.....	222
Table 7.5.	Influence of milling on the molecular weight of PCL and PLGA.....	224
Table 7.6.	Wettability profiling of PCL and PLGA before and after milling.....	225
Table 7.7.	Characterisation of nanoparticles prepared using milled PCL (200 rpm, 1 hour).....	232
Table 7.8.	Characterisation of nanoparticles prepared using milled PLGA (200 rpm, 1 hour).	233
Table 7.9.	Analysis of excipient interaction and chemical bond donation with PCL nanoparticles, prepared at a 5:1 polymer-drug ratio.....	243
Table 7.10.	Analysis of excipient interaction and chemical bond donation with PLGA nanoparticles, prepared at a 5:1 polymer-drug ratio.....	245

LIST OF FIGURES

Figure No	Description	Page No
Figure 1.1.	Schematic of the GIT and its relative pH.....	37
Figure 1.2.	Chemical reaction of hydrogen chloride (HCl) in water.....	41
Figure 1.3.	Schematic representation of the lattice structure of water with ethanol.....	42
Figure 1.4.	Structure of (A) β -CD and (B) its derivative HP- β -CD.....	42
Figure 1.5.	Schematic representation of the tongue and the four zones of taste receptors: Sour, bitter, salty and sweet.	44
Figure 1.6.	Schematic representation of photo-stabilising affects of cyclodextrin.....	46
Figure 1.7.	Diagrammatic Representation of the electrical double layer formed around particles in suspension.....	47
Figure 1.8.	Schematic representation of the three possible levels of particle interaction when in suspension.....	49
Figure 1.9.	Diagrammatic representation of the effect of changing electrolyte concentration.....	50
Figure 1.10.	Comparison of the response in shear rate with increasing shear stress for Newtonian flow and pseudoplastic flow.....	52
Figure 1.11.	Typical plot of viscosity against shear rate for a pseudoplastic liquid.....	52

Figure 2.1.	Angiotensin converting enzyme mechanism.....	61
Figure 2.2.	Chemical structures of ACE inhibitors currently on the pharmaceutical market.....	62
Figure 2.3.	Schematic representation of the formulation issues associated with captopril degradation.....	64
Figure 2.4.	Graph of captopril calibration highlighting the linearity of the validation protocol (n=3).....	74
Figure 2.5.	Structure of EDTA.....	76
Figure 2.6.	Stability of captopril in distilled water (1 mg.mL^{-1}) stored under 25°C (40 % humidity) and 40°C (75 % humidity) conditions.....	77
Figure 2.7.	Stability of captopril with 0.1 % EDTA (1 mg.mL^{-1}) stored under 5°C , 25°C (40 % humidity) and 40°C (75 % humidity) conditions.....	77
Figure 2.8.	pH stability of captopril with 0.1 % EDTA (1 mg.mL^{-1}) stored under 5°C , 25°C (40 % humidity) and 40°C (75 % humidity) conditions.....	78
Figure 2.9.	The chelation mechanism of EDTA with captopril.....	78
Figure 2.10.	Conductometry of Captopril with increasing amounts of EDTA.....	79
Figure 2.11.	Viscosity of glycerol in distilled water with increasing concentrations of glycerol.....	81

Figure 2.12.	Six month stability profile of captopril with 30 % (w/v) glycerol (1 mg.mL ⁻¹) stored under 5 °C, 25 °C (40 % humidity) and 40 °C (75 % humidity) conditions.....	82
Figure 2.13.	Schematic representation of the reaction mechanism of glycerol with captopril, forming the degradation product captopril disulphide.....	83
Figure 2.14.	Stability of captopril in 0.1 % (w/v) sodium metabisulphite (1 mg.mL ⁻¹) stored under 25 °C (40 % humidity) and 40 °C (75 % humidity) conditions.....	84
Figure 2.15.	Schematic of sodium metabisulphite converted into its respective ions when placed in water.....	85
Figure 2.16.	Schematic for the degradation pathway of captopril in the presence of sodium metabisulphite.....	85
Figure 2.17.	Investigations of the molar conductivities of captopril on the HP-β-CD molar concentrations.....	88
Figure 2.18.	H ¹ -NMR spectrum of captopril in DMSO, displaying 14 Hydrogen atoms.....	88
Figure 2.19.	H ¹ -NMR spectrum of HP-β-CD in DMSO, displaying 43 Hydrogen atoms.....	89
Figure 2.20.	H ¹ -NMR spectrum of captopril and HP-β-CD in DMSO, displaying 31 Hydrogen atoms.....	89
Figure 2.21.	12 months stability profile of captopril (1 mg.mL ⁻¹) with 0.1 % EDTA and HP-β-CD stored under 5 °C, 25 °C (40 % humidity) and 40 °C (75 % humidity) conditions.....	91

Figure 2.22.	FTIR fingerprint absorption spectrum of captopril formulation with HP- β -CD and its excipients.....	93
Figure 2.23.	Schematic representation of the molecular arrangement of EDTA and HP- β -CD with captopril, predicted using FTIR.....	93
Figure 2.24.	DSC thermogram of a 5 mg.mL ⁻¹ captopril formulation with 0.1 % (w/v) EDTA.....	94
Figure 2.25.	TGA and DSC Thermograms of a 5 mg.mL ⁻¹ captopril formulation composed of 0.1% (w/v) EDTA and HP- β -CD.....	95
Figure 2.26.	12 month stability profile of captopril with 0.1 % (w/v) EDTA (5 mg.mL ⁻¹) stored under 5 °C, 25 °C (40 % humidity), and 40 °C (75 % humidity) conditions.....	96
Figure 2.27.	12 month stability profile of captopril with 0.1 % (w/v) EDTA and HP- β -CD (5 mg.mL ⁻¹) stored under 5 °C, 25 °C (40 % humidity), and 40 °C (75 % humidity) conditions.....	96
Figure 3.1.	Chemical structure of gliclazide. The sulphonylurea backbone is highlighted in red, with the unique side groups of gliclazide highlighted in blue.	99
Figure 3.2.	Calibration graph of gliclazide highlighting the linearity of the validation protocol.....	107
Figure 3.3.	Phase solubility of gliclazide in L-arginine.....	110
Figure 3.4.	Phase solubility of gliclazide with increasing concentrations of L-lysine (10-300 mg.mL ⁻¹).	111

Figure 3.5.	(A) Structure of L-lysine; containing an amine end group with a pKa ₃ 9.28, and (B) structure of L-arginine, containing a guanidinium end group with a pKa ₃ 12.48.....	112
Figure 3.6.	Phase solubility profile of gliclazide with increasing concentrations of surfactant F127, and its respective pH profile.....	113
Figure 3.7.	Phase solubility profile of gliclazide in 5 % F127 (CMC) at varying pH.....	115
Figure 3.8.	Phase solubility of gliclazide with increasing concentrations of ethanol as a co-solvent (10-100 % v/v).....	117
Figure 3.9.	Influence of pH on the phase solubility of gliclazide in 15 % ethanol-water (v/v).....	118
Figure 3.10.	Influence of pH of the phase solubility diagram of gliclazide in 5% (w/v) F127 and 15 % ethanol-water (v/v).....	119
Figure 3.11.	Nine month stability profile of 8 mg.mL ⁻¹ gliclazide with 7 mg.mL ⁻¹ L-arginine stored under 5 °C, 25 °C (40 % humidity) and 40 °C (75 % humidity) conditions.....	121
Figure 3.12.	Nine month stability profile of 16 mg.mL ⁻¹ gliclazide with 5 % (w/v) pluronic F127 and 15 % (v/v) ethanol, stored under 5 °C, 25 °C (40 % humidity) and 40 °C (75 % humidity) conditions.....	121
Figure 3.13.	DSC overlay of xylitol, L-arginine, gliclazide, and gliclazide formulation with L-arginine after being freeze-dried, at a scan rate of 100 °C.min ⁻¹	123
Figure 3.14.	DSC of 40 µL L-arginine solution with dissolved gliclazide in comparison with 40 µL L-arginine solution, at a scan rate of 100 °C.min ⁻¹	124

Figure 3.15.	Respective chemical structures of the excipients used in the formulation of an oral liquid dosage form for gliclazide.....	126
Figure 3.16.	FTIR scans of the respective excipients used in the formulation of an oral liquid dosage form for gliclazide, with a comparative FTIR scan of the formulation.....	127
Figure 3.17.	H^1 -NMR absorption graph for L-arginine using D_2O (reference at 4.77 ppm); 15 protons were detected.	130
Figure 3.18.	H^1 -NMR absorption graph for a 1:1 molar ratio mix of L-arginine with gliclazide using D_2O (reference at 4.77 ppm); 35 protons were detected.....	130
Figure 4.1.	Chemical structures of Arginine and its stereo forms.....	134
Figure 4.2.	Chemical structure of L-arginine: 3-carbon aliphatic straight the distal end of which is capped by a guanidinium group.....	135
Figure 4.3.	HPLC spectra of (A) methanol:water mix at a 1:1 ratio and (B) 0.28 mmol.L ⁻¹ concentration of L-arginine.....	141
Figure 4.4.	HPLC spectra for (A) Solvent front of the mobile phase consisting of 0.1% TFA in water and methanol (70:30 v/v) and (B) 50 μ g.mL ⁻¹ sample of L-arginine.....	143
Figure 4.5.	HPLC spectra for (A) solvent front of the mobile phase containing water and acetonitrile (90:10 v/v) with 0.5 % (v/v) TFA, and (B) 0.08 mmol.L ⁻¹ L-arginine.....	144
Figure 4.6.	Calibration of L-arginine ($\lambda=404$) using phosphate buffered saline at pH 9.....	145

Figure 4.7.	Calibration of L-arginine ($\lambda=404$ nm) using a modified ninhydrin assay with 25 mmol.L ⁻¹ sodium phosphate buffer at pH 4.5.....	146
Figure 4.8.	Lambda max of L-arginine solution after being treated with the modified ninhydrin assay.....	147
Figure 4.9.	Chemical structure of ninhydrin (C ₉ H ₆ O ₄), displaying its main functional groups; ketone and hydroxyl groups.....	147
Figure 4.10.	Mechanism of L-arginine and ninhydrin in the production of Ruhemann's purple.....	148
Figure 4.11.	Calibration of L-arginine ($\lambda=560$ nm) using a modified ninhydrin assay with 25 mmol.L ⁻¹ sodium phosphate buffer at pH 4.5.....	149
Figure 4.12.	The mechanism of reaction of tartaric acid with water.....	152
Figure 4.13.	Influence of increasing concentrations of tartaric acid on the pH of L-arginine in solution.....	152
Figure 4.14.	12 months stability profile of 100 mg.mL ⁻¹ L-arginine with 4 % (w/v) tartaric acid and 0.5 % (v/v) raspberry concentrate stored under 5 °C, 25 °C (40 % humidity) and 40 °C (75 % humidity) conditions...	155
Figure 4.15.	12 months stability profile of 100 mg.mL ⁻¹ L-arginine with 4 % (w/v) tartaric acid and 0.5 % (v/v) raspberry concentrate stored under 5 °C, 25 °C (40 % humidity) and 40 °C (75 % humidity) conditions...	155
Figure 5.1.	Chemical structures of (A) indole and (B) an indolamine (L-tryptophan).....	158
Figure 5.2.	Four-step pathway synthesis of melatonin by the pineal gland.....	160

Figure 5.3.	Graph of melatonin calibration highlighting the linearity of the validation protocol.....	164
Figure 5.4.	Influence of tartaric acid, and the subsequent addition of a preservative (potassium sorbate) and an antioxidant (EDTA), on the pH of the melatonin formulation (1 mg.ml^{-1}).....	168
Figure 5.5.	12 months stability profile of 1 mg/mL melatonin stored under 5°C , 25°C (40 % humidity) and 40°C (75 % humidity) conditions.....	170
Figure 5.6.	12 months stability profile of 1 mg.ml^{-1} melatonin stored under 5°C , 25°C (40 % humidity) and 40°C (75 % humidity) conditions...	170
Figure 6.1.	Schematic representations of (A) Bacterial cell, (B) Gram-negative bacteria cell, and (C) Gram-positive bacteria cell.....	178
Figure 6.2.	Preservative efficacy of captopril formulations at pH 3.4 on Gram-negative and Gram-positive bacteria, after 28 days incubation under 25°C (75 % humidity) conditions.....	181
Figure 6.3.	Schematic representation of the affect of EDTA on a Gram-negative bacteria cell wall.....	184
Figure 6.4.	Preservative efficacy of potassium sorbate in the melatonin formulation against Gram-positive (<i>S. aureus</i>) and Gram-negative (<i>P. aeruginosa</i> and <i>E. coli</i>) bacteria.....	185
Figure 6.5.	A schematic representation of the antimicrobial mechanism of potassium sorbate ($\text{C}_6\text{H}_9\text{O}_2\text{K}$) in the presence of EDTA on a Gram-negative cell.....	187

Figure 6.6.	Preservative efficacy of sodium benzoate in the L-arginine formulation against Gram-positive (<i>S. aureus</i>) and Gram-negative (<i>P. aeruginosa</i> and <i>E. coli</i>) bacteria.....	188
Figure 6.7.	A schematic representation of the antimicrobial mechanism of sodium benzoate on the Gram-negative cell.....	190
Figure 6.8.	Preservative efficacy of propyl- and butyl- paraben in the Gliclazide formulation containing L-arginine against Gram-positive (<i>S. aureus</i>) and Gram-negative (<i>P. aeruginosa</i> and <i>E. coli</i>) bacteria.....	191
Figure 6.9.	Preservative efficacy of propyl- and butyl- paraben in the Gliclazide formulation containing Pluronic F127 and ethanol (15 % v/v) against Gram-positive (<i>S. aureus</i>) and Gram-negative (<i>P. aeruginosa</i> and <i>E. coli</i>) bacteria.....	193
Figure 6.10.	A schematic representation of a eukaryotic cell wall.....	195
Figure 6.11.	Preservative efficacy of captopril formulations containing EDTA (formulation 1) and EDTA with HP β CD (formulation 2) against <i>C. albicans</i>	196
Figure 6.12.	Preservative efficacy of; potassium sorbate (melatonin formulation), sodium benzoate (L-arginine formulation), parabens (gliclazide-L-arginine formulation) and parabens with ethanol (gliclazide-ethanol formulation) against <i>C. albicans</i>	198
Figure 6.13	Inhibition of <i>A. niger</i> by preservative-containing formulations within 28 days of inoculation.....	200
Figure 7.1.	Chemical structures of: (A) Lansoprazole and the monomer units of (B) PLGA (C) PCL, (D) Trehalose and (E) Pluronic F127.....	206

Figure 7.2.	Graph of lansoprazole calibration highlighting the linearity of the validation protocol. (n=3).....	215
Figure 7.3.	Light microscopy of PCL nanoparticles in suspension and viewed on a glass slide and coverslip at 100 x objection.....	219
Figure 7.4.	SEM profiling of PCL-coated nanoparticles after freeze-drying.....	220
Figure 7.5.	Viscosity measurements of PCL nanospheres before and after homogenisation.....	222
Figure 7.6.	Wettability and SEM profiling of PCL (A) before and (B) after milling for 1 hour at 200 rpm.....	227
Figure 7.7.	Wettability and SEM profiling of PLGA (A) before and (B) after milling for 1 hour at 200 rpm.....	228
Figure 7.8.	DSC thermographs of; (A) PLGA, (B) milled PLGA, (C) PCL, (D) milled PCL, (E) lansoprazole and (F) milled lansoprazole.....	230
Figure 7.9.	TGA and DSC thermographs of lansoprazole: (A) un-milled and (B) milled.....	231
Figure 7.10.	H ¹ -NMR spectrum (DMSO-D ₆) of pure pluronic F127.....	236
Figure 7.11.	H ¹ -NMR spectrum (DMSO-D ₆) of pure lansoprazole.....	236
Figure 7.12.	H ¹ -NMR spectrum (DMSO-D ₆) of pure PCL.....	237
Figure 7.13.	H ¹ -NMR spectrum (DMSO-D ₆) of pure PLGA.....	237

Figure 7.14.	H ¹ -NMR spectrum (DMSO-D ₆) of physical mixture of PCL and lansoprazole.....	238
Figure 7.15.	H ¹ -NMR spectrum (DMSO-D ₆) of physical mixture of milled PCL and lansoprazole.....	239
Figure 7.16.	H ¹ -NMR spectrum (DMSO-D ₆) of PCL-coated lansoprazole-loaded nanoparticles.....	239
Figure 7.17.	H ¹ -NMR spectrum (DMSO-D ₆) of physical mixture of PLGA and lansoprazole.....	240
Figure 7.18.	H ¹ -NMR spectrum (DMSO-D ₆) of physical mixture of milled PLGA and lansoprazole.....	241
Figure 7.19.	H ¹ -NMR spectrum (DMSO-D ₆) of PLGA-coated lansoprazole-loaded nanoparticles.....	241
Figure 7.20.	Comparison of FTIR spectrum for trehalose, pluronic F127, lansoprazole (LSP), standard PLGA and PLGA nanoparticles prepared at a 5:1 polymer drug ratio.....	243
Figure 7.21.	FTIR spectra of PCL nanoparticles prepared at a 5:1 polymer-drug ratio.....	244
Figure 7.22.	Comparison of FTIR spectrum for trehalose, pluronic F127, lansoprazole (LSP), standard PLGA and PLGA nanoparticles prepared at a 5:1 polymer drug ratio.....	245

Figure 7.23.	Comparison of FTIR spectrum for trehalose, pluronic F127, lansoprazole (LSP), milled PLGA and milled PLGA nanoparticles prepared at a 5:1 polymer drug ratio.....	246
Figure 7.24.	DSC thermogram of PCL lansoprazole nanoparticles at varying ratios, at a scan rate of $150\text{ }^{\circ}\text{C}.\text{min}^{-1}$	247
Figure 7.25.	DSC thermogram of milled PCL lansoprazole nanoparticles at varying ratios, at a scan rate of $150\text{ }^{\circ}\text{C}.\text{min}^{-1}$	247
Figure 7.26.	DSC thermogram for the milled PLGA nanoparticles at varying ratios, at a scan rate of $150\text{ }^{\circ}\text{C}.\text{min}^{-1}$	248
Figure 7.27.	DSC thermogram for PLGA nanoparticles at varying polymer-drug concentrations, at a scan rate of $150\text{ }^{\circ}\text{C}.\text{min}^{-1}$	249
Figure 7.28.	Release profile of milled and non-milled PCL nanoparticles (5:1 polymer-drug ratio) in the buffer phase when under fasting conditions.....	250
Figure 7.29.	Release profile of milled and non-milled PLGA nanoparticles (5:1 polymer-drug ratio) in the buffer phase when under fasting conditions.....	251
Figure 7.30.	Release profile of PCL and PLGA nanoparticles (5:1 polymer-drug ratio) in the buffer phase, when under fed condition.....	252

ABBREVIATIONS

α	Alpha
β	Beta
γ	Gamma
δ	Delta
ϵ	Epsilon
θ	Contact Angle
λ	Lamda
μl	Micro litre
μm	Micro meter
\AA	Angstrom
ACE	Angiotensin I-Converting Enzyme
ACN	Acetonitrile
ANOVA	Analysis of Variance
API	Active Pharmaceutical Ingredient
ARBs	Angiotensin Receptor Blockers
a_w	Available water
BP	British Pharmacopoeia
CD	Cyclodextrin
CFU	Colony Forming Units
D	Drug
$^{\circ}\text{C}$	Degrees Celsius
D₂O	Deuterated water
DMSO-D₆	Deuterated Dimethyl sulfoxide
DSC	Differential Scanning Calorimetry
EDTA	Ethylenediaminetetraacetic acid disodium salt dihydrate
EMEA	European Medical Agency
FDA	Food and Drug Administration

FT-IR	Fourier Transform Infrared Spectroscopy
g	Gram
GI	Gastro Intestinal
GIT	Gastrointestinal Tract
GRAS	Generally Recognised As Safe
H¹-NMR	Hydrogen – Nuclear Magnetic Resonance
HCl	Hydrogen Chloride
HPLC	High Pressure Liquid Chromatography
HP-β-CD	Hydroxypropyl-beta-cyclodextrin
ICH	International Conference on Harmonisation
K	Constant
K⁺	Potassium ion
L	Litre
LDF	London Dispersion Forces
LOD	Limit of Detection
Log₁₀	Logarithm to the power of 10
LOQ	Limit of Quantification
LPS	Lipopolysaccharide
M	Mole
mAU	Milli Absorbance Unit
mg	Milligram
Mg²⁺	Magnesium ion
MHz	Milli Hertz
min	Minute
mL	Millilitre
mm	Millimetre
MPa.s⁻¹	Milli pascals per second
mTorr	Milli Torr

mV	Millivolt
NaOH	Sodium hydroxide
NCE	New Chemical Entity
nm	Nano meter
PBS	Phosphate Buffered Saline
PCL	Polycaprolactone
PEG	Polyethylene Glycol
PeT	polyethylene terephthalate
PET	Preservative Efficacy Test
PLGA	Polylactide-coglycolide
PPIs	Proton Pump Inhibitors
rpm	Revolutions per minute
s	Seconds
SD	Standard Deviation
SEM	Scanning Electron Microscope
SLN	Solid- lipid nanoparticles
TFA	Trifluoroacetic Acid
Tg	Glass transition
TGA	Thermogravimetric analysis
Tm	Melting temperature
USP	United States Pharmacopoeia
UV	Ultra Violet

THESIS PUBLICATIONS

Peer-reviews Journal Articles:

Shabir A., Alhusban F., Perrie Y., **Mohammed A.** (2011) Effects of ball-milling on PLGA polymer and its implication on Lansoprazole-loaded nanoparticles. *J Basic Clin Pharmacy*, 2 (2): 71-82

Tawfeek H., Khidr S., Samy E., Ahmed S., Murphy M., **Mohammed A.**, **Shabir A.**, Hutcheon, G., Saleem I. (2011) Poly(glycerol adipate-co- ω -pentadecalactone) spray-dried microparticles as sustained release carriers for pulmonary delivery. *Pharmaceut Res*, 28(9): 2086-2097

Shabir A., **Mohammed A.** (2010) Exploring the use of cyclodextrins as carriers in paediatric formulations. *Brit J Clin Pharmacy*, 2: 275-278

Conference Proceedings

Shabir A., Mohammed A., Perrie Y., Begum S.- Poly(DL-lactide-co-glycolide)(PLGA) based nanospheres for the delivery of Lansoprazole. UK-PharmSci Synposium, Septmeber 2011, Nottingham, UK.

Shabir A., Mohammed A., Perrie Y. – Dry-milling of PLGA for use in nanoparticle encapsulation of Lansoprazole. UKICRS Symposium, April 2011, Belfast, Ireland.

Shabir A., Mohammed A., Perrie Y., Begum S. – Poly-caprolactone (PCL) based nanospheres for the delivery of Lansoprazole. UK-PharmSci Symposium, September 2010, Birmingham, UK.

Shabir A., Mohammed A., Perrie Y., Begum S. – Oral liquid nanomedicines for Lansoprazole. British Pharmaceutical Conference, September 2009, Manchester, UK.

Shabir A., Mohammed A. – Development and characterisation of nanoparticulate systems for oral delivery of flurbiprofen. 36th Annual Meeting of the Controlled Release Society, July 2009, Copenhagen, Denmark.

Conference Presentations

Shabir A., Mohammed A. – Poly(DL-lactide-co-glycolide)(PLGA) based nanospheres for the delivery of Lansoprazole. UK-PharmSci, September 2011, Nottingham, UK.

Shabir A., Mohammed A. – Development and characterisation of a nano-particulate systems for the oral delivery of Lansoprazole using milled poly(DL-lactide-co-glycolide). 38th Annual Meeting of the Controlled Release Society, August 2011, Maryland, USA.

CHAPTER 1

Introduction

Papers relating to this chapter

Shabir, A. and Mohammed, A. (2010). Exploring the use of cyclodextrins as carriers in paediatric formulations. *The British Journal of Clinical Pharmacy*, 2: 275-278

CHAPTER 1

Introduction

1.1. Project scope and significance

The United States identified the problem of poor availability of paediatric medication in the 1990's and since 1998 there has been a regulation in place (Federal Register 66632, 1998) requiring all medicines produced to be assessed for safety and efficacy in paediatrics. As such, since 4th January 2002 under the 'best pharmaceuticals for children' act (FDA/Pub L No. 107-109, 2002) the Food and Drug Administration (FDA) require evidence that the medication is both safe and effective. In 2007 the European Medical Agency (EMEA) followed suit in the recognition of the problem and has since devised a priority list of off-patent paediatric medications with the goal of directing the research and development in the direction of the medications deemed the most important and the most in need of reformulation and investigation. The most recent list was released in 2010 (EMA/480197/2010).

Only a small percentage of all of the medications currently available are developed and tested with the paediatric patient segment as the primary target. Current methods employed in managing this problem include the use of; extemporaneous preparation, off-label drugs, unlicensed drugs and via the production of 'specials' (Giam and McLachlan, 2008). Giam and McLachlan (2008) carried out a review to provide an insight into the incidence of extemporaneous preparation. In the United Kingdom the prevalence of extemporaneous preparation was indicated to be around 10% for paediatric administration, with a similar trend being observed across Europe.

Many problems have been related to these 'alternative formulations' for paediatric treatment, mainly associated with unlicensed and off-label drug use. For example the extemporaneous preparation of medications to be administered to children usually involves the use of drugs intended for adult use in which the dose is adjusted for each individual case (Nahata, 1999). In the case of very small children (newborn) the dose may need to be extremely small, causing issues with dosing accuracy and errors, which could result in irritation and toxic effects in paediatric patients. Children are more susceptible to side effects associated with medications and are less well able to cope with accidental overdose when compared to an

adult. Extemporaneous preparation carries with it further problems including: published standards relating to the production of extemporaneous preparations are not available, there is a lack of information regarding the reproducibility of the medication via extemporaneous preparation, and procedures such as crushing tablets which have been designed for the controlled release of the drug can result in large overdoses.

1.2. Reformulation of medicines

Reformulation of existing medicinal products is performed for a variety of reasons. Pharmaceutical companies ‘alter’ their own products so as to allow for re-patenting and in doing so maintain their market exclusivity in that area, to expanding the scope of an existing drug to better target other patient segments (Yoshitani and Cooper, 2007). Also there are many factors of existing formulations which can be improved in an effort to maximise their potential for targeting specific patient groups. Where paediatric reformulations are concerned some of the most common areas for improvement include; increasing the understanding of pharmacokinetics of the drug, improving the drug’s safety and developing an age appropriate formulation.

Reformulation of off-patent medications in an attempt to improve the availability of medication to children is a much more attractive proposition when compared to developing a completely new chemical entity (NCE). Further developing an existing active pharmaceutical ingredient (API) recognised by the FDA, means that all of the data collected via clinical trials associated with the production of a NCE will already have been carried out in order for the FDA advisory committee to approve the product (Bhattaram *et al*, 2005). This will remove much of the cost associated with the formulation of a new drug. Reformulation is generally categorised into three sub classes: (1) the reformulation of a molecular entity, (2) new deliveries and (3) new indications (Yoshitani and Cooper, 2007).

The reformulation of molecular entities involves the modification of an existing API just enough so as that the changed molecule can be patented without compromising its *in vivo* performance. In this way the FDA views the modified API as the same drug under the guidelines regarding bioequivalency. In the area of molecular entity reformulation there are three further subsections which involve: (1) metabolites, (2) polymorphs and (3) chiral switching.

Metabolites are the molecules produced following a chemical reaction in the body, the modification implemented with regards to metabolites is the creation of prodrugs which enter the body in an inactive form and following metabolism the active form of the drug is produced (Yoshitani and Cooper 2007).

Polymorphs which exist with different crystalline structures, waters of hydration, solvents and amorphous forms come into play where reformulation is concerned, as the FDA recognise a modified API so long as there is no change in its physical form and that it is also bioequivalent to the original drug (Yoshitani and Cooper 2007). It is often difficult to produce reformulations which display characteristics that are bioequivalent to the original product as changes in the polymorphism often bring about changes in the solubility of the drug, which in turn can result in changes in the dissolution properties (Williams *et al* 2008).

Chiral switching is implemented in reformulation as the ratio of each chiral version can be changed resulting in a more pure S- enantiomer or a purer R- enantiomer, with each chiral version bringing about very different responses in the body (Fleming and Ma 2002). A more pure mix would produce a more effective response in favour of one or the other enantiomer depending on which was present in the highest concentration. In this way the efficacy of a drug is improved without altering the molecule itself (Yoshitani and Cooper 2007).

Reformulation to produce new delivery methods is fairly self explanatory with factors such as the alteration of the dosage form (from an oral liquid such as a suspension to an oral solid such as a tablet or a capsule). Another approach is alternative route of delivery (a nasal spray to an oral tablet or a capsule). In both cases it is essential that the behaviour of the drug once inside the body is identical to the original formulation (Yoshitani and Cooper 2007).

New indications involve the use of medication to treat a disease or condition not covered in an existing drug patent (Ashburn and Thor 2004). If this is achieved then there are no changes to the existing API but can be used to treat different disease condition. This is a relatively uncommon occurrence as drug companies go to great lengths to protect their products in order to maintain market exclusivity (Yoshitani and Cooper 2007).

1.3. Gastrointestinal physiology and its impact on bioavailability

The oral route remains as the preferred route of drug administration for patients, due to its ease of convenience, good patient compliance, and low medicinal cost (Wong *et al*, 2006). However the human body is a complex system that has a multitude of functions which include: secretion, digestion, absorption and excretion. All medicinal products ingested must pass a range of physiological barriers before the systemic delivery of the drug, particularly the extreme pH conditions encountered through the gastrointestinal tract (GIT) (Figure 1.1). The acidic environment of the stomach is attributed to the presence of gastric fluids, and the secretion of hydrochloric acid from the parietal cells of the stomach. Under fasted conditions the pH of the stomach is ~1.7, with the stomach contents becoming neutralised in the duodenum by the bicarbonate ions through the pancreatic duct, raising the pH steeply to

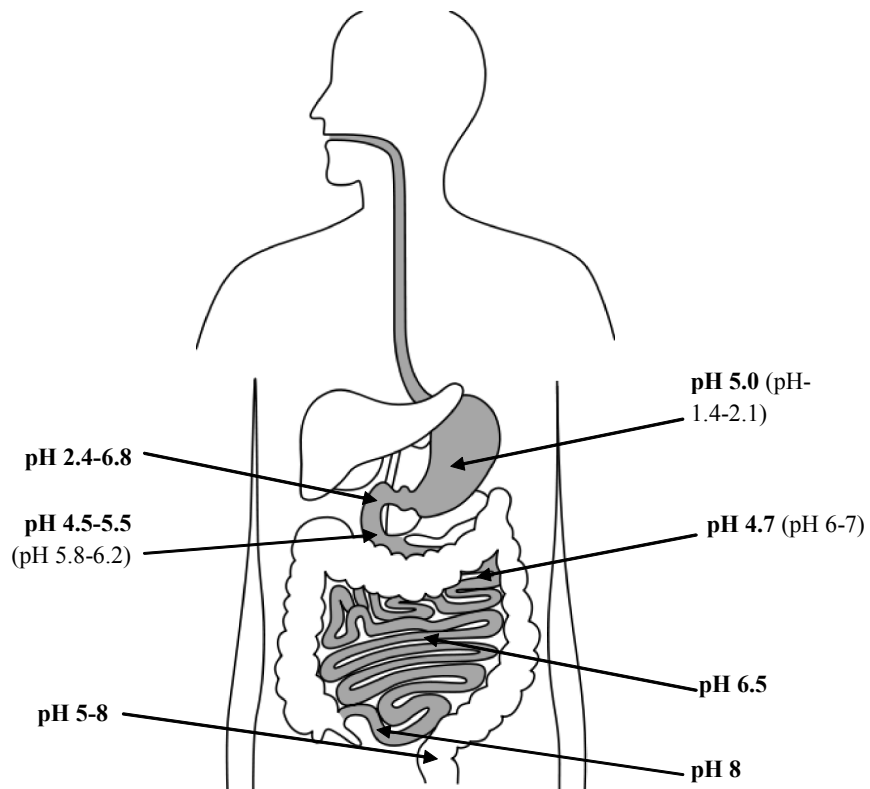


Figure 1.1. Schematic of the GIT and its relative pH. Under fed conditions the pH of the stomach is pH 5, however under faster conditions the pH of the stomach significantly decreases to pH 1.4-2.1. The pH of the duodenum is in the range of pH 2.4-6.8, with the small intestines displaying a relatively alkaline environment (pH 6.5).

~4.6. Between the proximal jejunum and the distal ileum, the pH rises further ~6 to 8. This alkaline environment is due to the secretion of bicarbonate. The ingestion of food has a dramatic affect on the acidity of the stomach, by raising its pH profile briefly to 7, after 6 minutes the pH drops to 5, which reduces further to pH 3 after 1 hour, and returns to the fasted level (pH ~1.7) after 3 hours. As the movement of food transgresses through the proximal jejunum, the pH reduces to 4.5; however the distal portions of the small intestine are not dramatically changed by the presence of food (Avdeef, 2003). As well as pH, other obstacles exerted by the GIT include: degradative enzymes, first pass metabolism and hydrophilic and lipophilic barriers. The physiology of the GIT has a major influence on drug bioavailability and drug absorption. There are a number of physiological factors which can influence drug bioavailability and drug absorption from the GIT.

The surface area of the gastrointestinal (GI) absorption sites vary significantly along the GIT. The small intestine (i.e. duodenum, jejunum and ileum) possesses the largest surface area for absorption in the GI for the majority of active drug candidates and therefore is the site where maximum absorption of API occurs. The large difference in surface area across the GIT results in variation in the rate and extent of absorption of active drug across the GIT.

pH influences both the ionisation and chemical stability of active drug, as the ionisation and stability of active drug ingredients, varies according to the acidity or basicity of the surrounding environment in the GIT. For example, a weakly acidic drug will exist in its unionised form at low pH (such as the stomach), however as the pH of the environment increases the drug will become ionised, and ultimately affect its solubility.

Gastric emptying rate also has a significant effect on drug absorption. Gastric emptying rate is defined as the rate at which a drug in solution leaves the stomach and enters the duodenum. As most active drug ingredients are efficiently absorbed from the small intestine, a reduction in gastric emptying rate is likely to reduce absorption and subsequently delay the onset of the therapeutic/medicinal response. Gastric emptying rate may be influenced by the type of dosage form in which the active drug ingredient is contained, as solid dosage forms show pronounced differences when compared to liquid dosage forms.

The consumption of food can also lead to a reduction in active drug ingredient absorption and bioavailability due to complexation, in which active drug ingredients form a permanent complex/interaction with components in the diet. The formed complex is not able to be absorbed across the GI membrane, therefore a reduction in bioavailability is observed. For example, tetracycline forms a non-absorbable complex with calcium (found in milk and other

dairy products), therefore patients are advised not to consume dairy products at the same time of day as they administer tetracycline.

1.4. Drug formulation strategies

The mainstay for drug delivery research has always been to identify strategies for efficient delivery of drugs in order to improve their therapeutic performance. Since the best option for paediatric administration is the production of an oral liquid formulation, the aqueous solubility of a drug can be a determinate in the dosage form selection with soluble drugs lending themselves easily to the production of solutions. For insoluble drugs however the options are to produce a suspension where the drug remains undissolved, or alternatively to utilise techniques to solubilise the insoluble drug (such as complexation, co-solvency or micelles). In addition, a variety of successful techniques have been developed over the years, which are specific to the drug candidate. These techniques include: liposomes (Dupont, 2002), emulsions (Nakano, 2000), microemulsions (Lawrence and Rees, 2000) and solid dispersions (Leuner and Dressman, 2000).

1.4.1. Solubility Enhancement

Oral solutions can either be complex formulations or simple preparations, involving various types of excipients which include: water, water-soluble organic solvents, water-insoluble organic solvents, organic solvents, surfactants, buffers, sugars, flavours, sweeteners, aromatics and dyes (Strickley, 2004). This simple approach aims to increase the bioavailability of hydrophilic and lipophilic drugs without compromising their chemical stability. Common methods of solubilisation include: pH adjustment, co-solvent/binary system and polarity adjustment.

1.4.1.1. pH adjustment

A common and simple method of drug solubilisation involves the adjustment of the pH of the medium. However this method can only be possible with hydrophobic drugs whose molecular structure enables them to be protonated (base) or deprotonated (acid) (Vemula *et al*, 2010). This is the simplest and most commonly used method to increase water solubility of ionisable compounds, by forming a salt form, which then converts into its respective acid and base forms in the GIT. This method of solubilisation is not suitable for unionisable compounds. A

drug with a basic functional group can be solubilised in acidic solutions at pH values below the pKa of the drug (Strickley, 2004).

1.4.1.2. Solvent and Co-solvents

The main concern in pharmaceutical development is the inability to dissolve relatively hydrophobic (non-polar) drugs in aqueous (polar and mixed polar) solvents. Oral solutions can be simple or complex formulations, involving many types of excipients including water-soluble organic solvents (forming a co-solvent system). Co-solvents are mixtures of miscible solvents, such as ethanol and water, forming a binary system, used to solubilise poorly water-soluble drugs to the required concentration in oral solutions (Strickley, 2004). Other common pharmaceutical solvents include propylene glycol, glycerine and polyethylene glycol (PEG), due to their relatively low toxicity (Vemula *et al*, 2010). The advantage of using a co-solvent system to solubilise hydrophobic drugs is mainly associated with the simplicity and ease of preparation of the formulation. This method of solubilisation has been commonly applied for drug molecules that cannot be solubilised by pH adjustment, as their chemical structures lack ionisable groups. The co-solvent binary system causes a change in the polar condition of the solution, which becomes the governing factor on the extent of solubilisation of a given compound.

The key to co-solvent solubilisation of hydrophobic compounds rests on the polarity of the hydrophobic compound matching the polarity of the solvent mixture (Rubino, 2002; Miyako *et al*, 2010). Polarity can be defined as the ability of a molecular structure to delocalise its electronic charges (Miyako *et al*, 2010). Hence the term polarity refers to the hydrophilicity of the compound; greater the polarity of a compound, greater its hydrophilicity. With regard to solvation of a compound in solution, the polarity of the solvent mixture greatly influences the extent of drug solubilised.

1.4.1.2.1. Mechanism of solvent action on drug solubility

Polar solvents (such as water) can solubilise polar compounds in one of two ways: (1) dissolve ionic salts by separating the cations and the anions of the salt, and (2) its ability to break a covalent bond in solution and produce an ionised form of the compound. The latter method can be observed clearly when dissolving hydrogen chloride (HCl) in water (Figure 1.2). Water is a unique solvent that has a high boiling point, a high dielectric constant (78.36 ϵ), and is polar. The dielectric constant dictates the affect a medium has on the ease with which two oppositely charged species may be separated. Thus the ability of water to

solubilise salts can be explained by their high dielectric constants, with an increase in solvent polarity increasing the dielectric constant of the solution (Gupta, 2005) and resulting in the solubilisation of highly polar compounds (hydrophilic drugs).

Ethanol, a partly polar solvent with a reduced dielectric constant (24.3 ϵ), and low molecular weight, forms a water-alcohol complex (Figure 1.3). Alcohols with larger molecular weights are less polar (due to the increase in carbon backbone), and are less able to compete with water molecules for a place in the water-lattice arrangement formed through hydrogen bonding (Gupta, 2005). From figure 1.3, it can be observed that the hydrogen bond between the hydroxyl group and the water molecule plays a major role in the extent of solubilisation.

Individually the water molecules have a higher dielectric constant than ethanol. However, when arranged in a lattice form through hydrogen bonding the dielectric constant of the overall solution is reduced, thereby enabling less polar molecules to be dissolved within this lattice matrix. The non-polar hydrocarbon region of the co-solvent (ethanol portion) can lower the ability of the aqueous system to squeeze out non-polar compounds by weakening the intermolecular hydrogen bonding network of water. The solubilisation efficiency of the co-solvent system therefore depends upon the extent by which the structure of water is weakened (seedher and Kanojia, 2009). Alternatively, by increasing the hydroxyl groups in the alcohol (such as sugars and glycosides), the solubility of non-polar compounds in water can be increased further.

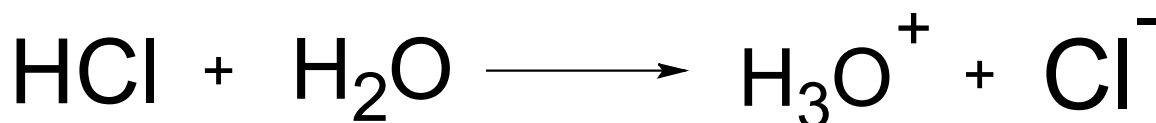


Figure 1.2. Chemical reaction of hydrogen chloride (HCl) in water. The water molecule breaks the covalent bond of H-Cl, forming an ionised chloride ion (Cl^-) and a protonated water molecule.

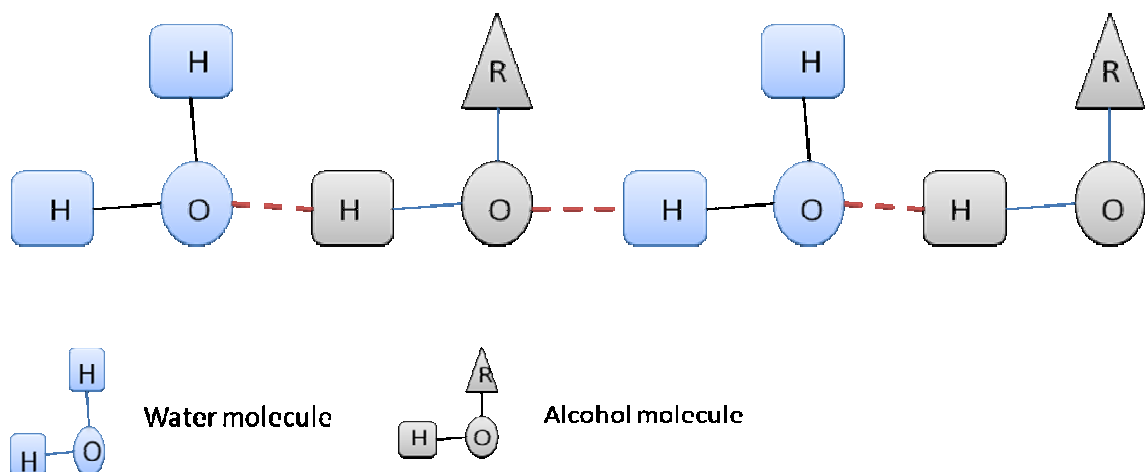


Figure 1.3. Schematic representation of the lattice structure of water with ethanol. The incorporation of ethanol within the lattice matrix reduces the polarity of the aqueous system, thereby enabling less polar molecules to be dissolved within the solution.



Aston University

Illustration removed for copyright restrictions



Aston University

Illustration removed for copyright restrictions

(A)

(B)

Figure 1.4. Structure of (A) β -CD and (B) its derivative HP- β -CD.

1.4.2. Cyclodextrins

Cyclodextrins are cyclic oligosaccharides consisting of six, seven or eight glucose ring molecules forming α -, β - and γ -cyclodextrins respectively (Figure 1.4.) (Kayser *et al*, 2003). Their main advantage is the spontaneous formation of hydrophobic cores with inner diameters ranging from 4.70-11.20 Å (Table 1.1). The cyclodextrins are arranged with their hydrophilic hydroxyl groups on the outside with a lipophilic inner cavity. This cavity allows for

Table 1.1. Cyclodextrin characteristics (taken from Brewster and Loftsson, 2007).



dipolar interactions to be formed between the lipophilic compounds (guest molecule) and the cavity of the cyclodextrin (Forgo *et al*, 2003). The advantages of using cyclodextrins for complexation include; increased uniformity and absorption of poorly soluble drugs that are known for their erratic absorption behaviour and increased drug activity upon oral administration.

1.4.2.1. Pharmaceutical applications

Cyclodextrins have been used in pharmaceuticals to overcome various obstacles exhibited by hydrophilic and hydrophobic drugs, such as solubilisation, taste masking, drug stabilisation, and photostability.

1.4.2.1.1. Solubilisation

Cyclodextrins are naturally water soluble (Table 1.1), with modified cyclodextrins (HP- β -CD) having a greater solubility profile. HP- β -CD owes this solubility to its degree of substitution, which plays a major role in balancing cyclodextrin water solubility and its complexing ability. By increasing the degree of substitution the solubility of the cyclodextrin increases exponentially until a plateau effect is seen at which point the steric hindrances of the host molecule impairs the cyclodextrin solubility efficiency.

1.4.2.1.2. Taste masking

In order for medicinal products to be acceptable by the patient, the preparation must have good organoleptic properties (particularly for oral drug formulations). These include; taste, smell, colour and consistency (gritty/smooth). Taste has been a particular issue when administering drugs to paediatrics therefore taste masking is essential to ensure patient compliance. Taste is associated by four major taste receptors on the tongue; sour, bitter, salty and sweet (Figure 1.5). In order to elicit a taste sensation, a molecule must dissolve or come into contact with the saliva; the molecules then react with the taste receptors on the tongue to give a particular taste sensation. Every molecule is specific to a taste response depending on its sapophore groups (groups of atoms in a molecule of a compound that gives the substance its characteristic taste).

In order to mask unpleasant tastes (such as bitter tasting drugs), the molecule can be bound to a second molecule preventing its sapophores from reaching the taste receptors. Previous research has highlighted the application of cyclodextrins in masking the bitter taste of midazolam (a preoperative anaesthetic commonly prescribed to children) (Marçon *et al*, 2009). Current applications of cyclodextrins in the food industry has seen Japan approving the use of cyclodextrins as ‘modified starch’ in food applications (Prasad *et al*, 1999; Singh *et al*, 2002, Kant *et al*, 2004; Astray *et al*, 2010)

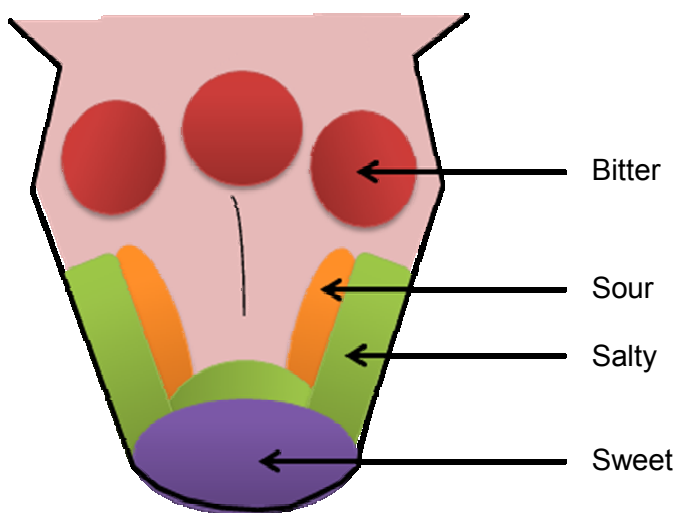


Figure 1.5. Schematic representation of the tongue and the four zones of taste receptors: Sour, bitter, salty and sweet.

1.4.2.1.3. Drug stabilisation

The chemical structure of cyclodextrins allows for molecules to be partly or completely complexed within their hydrophobic core, thereby bringing about enhancement of the stability of the formulation. The strength of this affect depends entirely upon three factors; (1) Van der Waals forces between the guest and the host molecules, (2) the way in which the guest molecule fits into the cavity of the cyclodextrin, and (3) size of the host cavity. Previous studies have looked at the impact of cyclodextrin on the stabilisation of adrimycin (doxorubicin) and daunomycin (daunorubicin), in which it was found that the cavity size of the cyclodextrin greatly impacted the strength of the inclusion complex (Emara *et al*, 2000).

As well as the strength of inclusion complexes, the characteristic nature (ionic and non-ionic) of the cyclodextrins also plays a part in chemical stability, with possible drug degradation occurring between the guest and the hydroxyl groups of the cyclodextrin (Loftsson, 1995). It was found that ionic cyclodextrins formed stronger complexes with non-ionic molecules, and weaker complexes with molecules carrying the same charge as the cyclodextrins (Másson *et al*, 1998). This was a direct result of the changes in the location of the molecules within the cyclodextrin cavity. This was particularly important with modified cyclodextrins (such as HP- β -CD), which have a different structural conformation to its parent cyclodextrin, in order to accommodate for the additional methyl groups, and thus ultimately changing the shape of the cyclodextrin cavity (Másson *et al*, 1998).

1.4.2.1.4. Photostability

The rate of photodegradation depends upon light intensity and the spectrum of light used (Backensfeld *et al*, 1991), thus degradation bi-products can occur in one of two ways: the first being sunlight and the second being exposed to light spectrum from an artificial source, such as a light bulb, which becomes particularly important during product manufacturing. For example, nifedipine undergoes 5-times faster degradation on exposure to sunlight than under fluorescent lamp. Therefore in order to fully test the photostability of a drug, it first becomes necessary to understand the kinetics of photodegradation, and then to confirm and characterise the drug-cyclodextrin inclusion complex formed, and assess whether the part of the drug molecule involved in the first step of drug photodegradation has formed an inclusion with the cyclodextrin cavity. Various studies have been carried out looking at photo-stabilising affects of cyclodextrins (Backensfeld *et al*, 1991; Mielcarek and Daczkowska, 1999; Sortino *et al*, 1999; Bayomi *et al*, 2002), in which it was concluded that modified

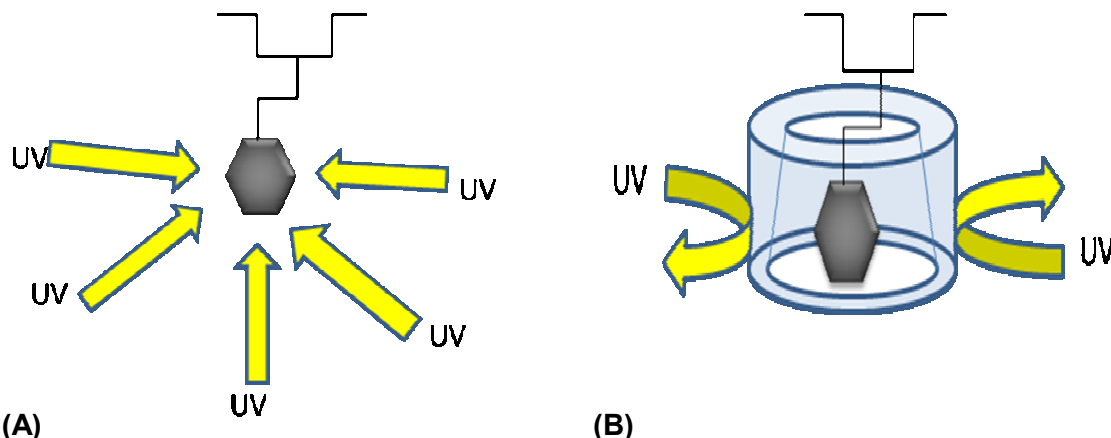


Figure 1.6. Schematic representation of photo-stabilising affects of cyclodextrin. **(A)** In the absence of cyclodextrin, the drug molecule is fully exposed to UV rays. **(B)** However, once complexed within the cyclodextrin core, the complex structure of the cyclodextrin glucose units act as a screen protecting its contents within.

cyclodextrins provided better photo-stabilising affects than their parent counterparts. These findings were attributed to the screening effects of cyclodextrins on light reaching the guest molecule (Figure 1.6).

1.4.3. Suspensions

Suspensions are dispersions of an insoluble drug (or other substance) in an aqueous or non-aqueous continuous phase. A number of dosage form formulation factors are associated with suspensions which can influence the bioavailability of an active drug ingredient. These include particle size and effective surface area of the suspended drug particles, the crystal form of the drug, drug-excipient complexation, (for example formation of a non-absorbable complex between the drug and suspending agent) and the viscosity exhibited by the suspension in the GI fluids (Tezlaff et al., 1978, Werling et al., 2008, Arias et al., 2009).

Suspensions are more complicated formulations than solutions to produce as they are inherently unstable formulations. If the particles in a suspension sediment in a very compact manner then caking can result where homogenous redistribution of the particles into the suspension is impossible. Controlling the interaction between the particles so that any aggregation is reversible or preventing any interaction between particles makes it possible to prevent caking. In order to do this the inclusion of excipients such as; electrolytes, surface active agents and hydrophilic polymers are often added in suspension formulations.

Electrolytes and surface active agents on the whole improve the stability of a suspension by modifying the Zeta potential of the suspended particles (Li et al., 2009, Xu et al., 2004).

1.4.3.1. Particle-Particle Interactions

1.4.3.1.1. Electrical Properties of Particles in Suspension

When insoluble particles are added in an aqueous solution it is likely that the particles may become charged. Ionisation of the particles is one way the particles can become charged, the extent of which is dependent upon the pH of the liquid and the pKa of the particles. The second way in which the particles can become charged involves the adsorption of ions onto the surface of the particles when there are electrolytes present in the aqueous vehicle. It is this adsorption of ions onto the surface of the particles which results in an 'electrical double layer' being formed which can be modified by using electrolytes and surface active agents in a suspension to improve the stability of the formulation (Kayes, 1977).

Figure 1.7 displays the formation of the electrical double layer after the adsorption of cations onto the surface of the particle in the suspension. This leads to a positive charge on the particle which is referred to as the Nearnst Potential (Willmott et al 2010). This positive

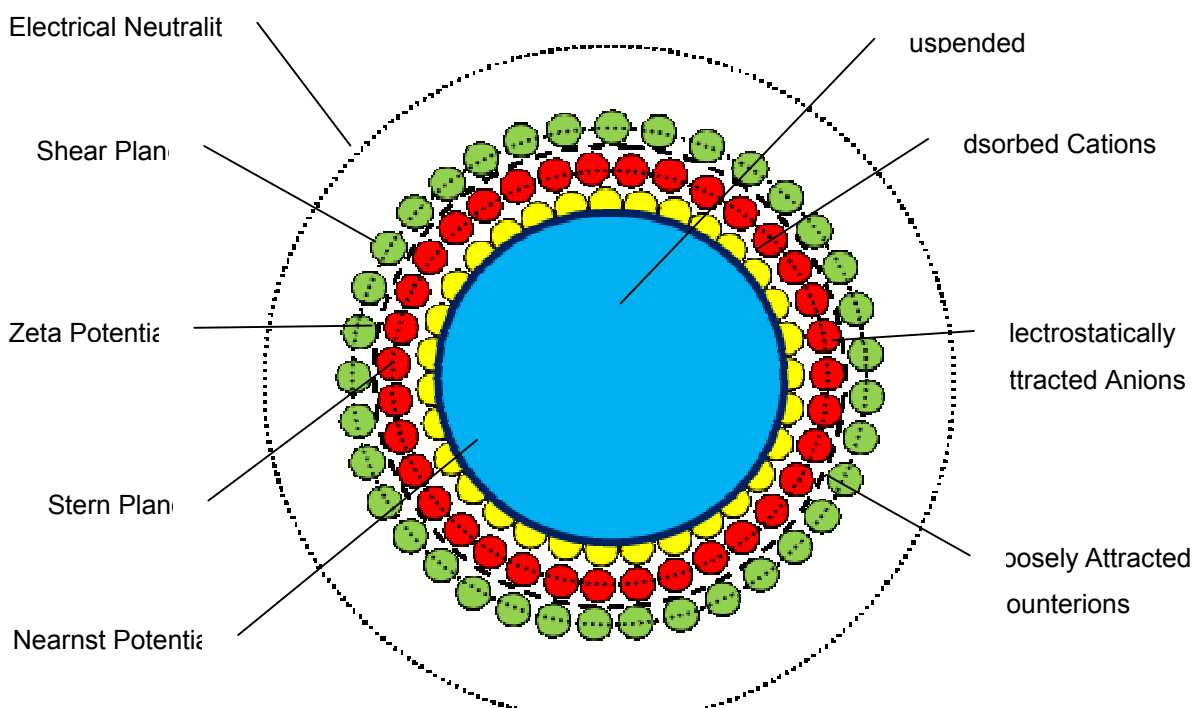


Figure 1.7. Diagrammatic Representation of the electrical double layer formed around particles in suspension.

charge electrostatically attracts the negatively charged anions which are present in the vehicle. This combination of particle, cations and anions make up the first part of the double layer with the presence of the anions acting to repel the approach of any further anions. The charge at the outer edge of this first layer is known as the Stern potential which falls at the Stern plane which runs through the centre of the anion layer. In most cases the charge at the Stern plane is lower than the Nearnst potential although there are exceptions to this rule. The second layer of the electrical double layer is the Shear plane which is formed from hydrated counterions that are loosely attracted to the particle and the charge at this level is referred to as the Zeta potential (Lyklema and Duval 2005). As the distance from the particle increases, the charge decreases to a point where electrical neutrality is attained.

1.4.3.1.2. Effect of particle Separation on Particle Interaction

The distance between particles in a suspension has a dramatic impact on the interaction between the particles. This is described by the ‘DVLO’ theory put forward by Derjaguin, Landau, Verwey and Overbeek (Derjaguin and Landau 1941; Verwey and Overbeek 1948), wherein they suggested a formula for the energy of interaction;

$$V_t = V_a + V_r$$

V_t = The total energy of interaction

V_a = The energy of attraction

V_r = The energy of repulsion

The attractive forces are London dispersion forces (LDF) and van de Waals forces. The magnitude of these forces decreases inversely upon increasing the distance between the particles. The repulsive forces are a result of the previously described electrical double layer with the distance at which the forces of repulsion acts being equal to the distance between the Shear Plane and the particle surface. These forces of repulsion are active at much closer distances than are observed for the LDF/van de Waals forces.

There are three levels of interaction which can be observed depending upon the separation of the particles. These are termed the primary minimum, the primary maximum and the secondary minimum (Figure 1.8).

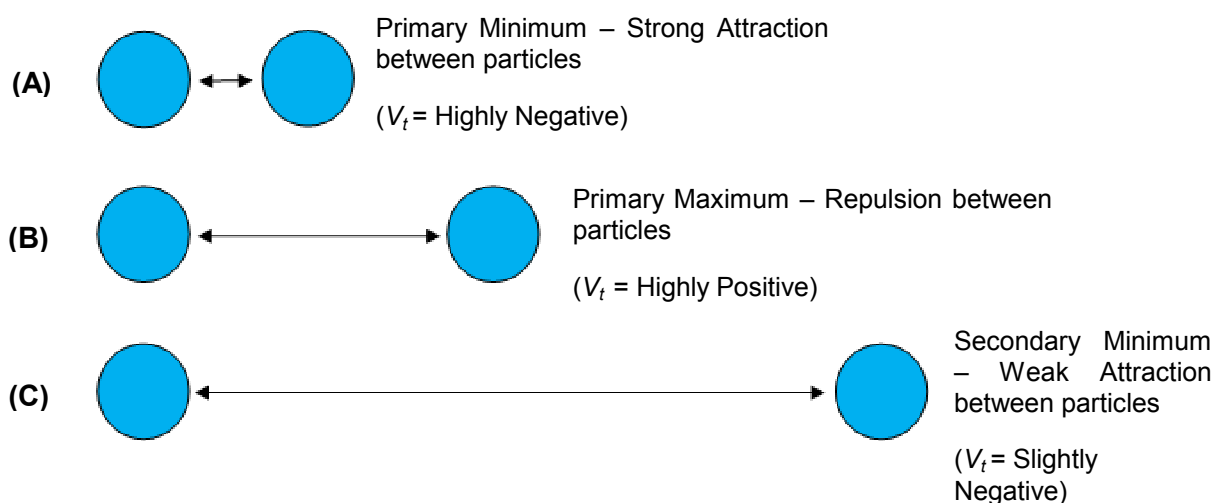


Figure 1.8. Schematic representation of the three possible levels of particle interaction when in suspension. **(A)** Particles interacting at the primary minimum will experience strong attractive forces and will coagulate irreversibly. **(B)** Particles existing at the primary maximum will experience forces of repulsion. **(C)** Particles at the secondary minimum will experience weak forces of interaction much lower than the attractive forces seen at the primary minimum and the particles will interact reversibly forming floccules in the process of flocculation resulting in a more stable suspension.

In suspensions where sedimentation is observed, it is common to manipulate the particles so that they interact in the secondary minimum. This is so that the floccules that are formed can be easily re-dispersed into the suspension as the interaction between the particles is weak and easily broken upon shaking. The use of electrolytes and surface active agents induces and controls flocculation in pharmaceutical suspensions by modifying the zeta potential and in doing so achieving a balance between the attractive and repulsive forces acting on the particles (Strand et al., 2003).

1.4.3.1.3. Electrolytes

In an effort to stabilise suspensions the rate at which the particles or floccules sediment can be controlled by the careful control of the electrolyte concentration. The concentration of electrolytes present in a formulation can be modified to control the zeta potential. Their addition reduces the zeta potential at the shear plane which leads to a reduction in the repulsive forces between particles. Careful manipulation of this allows for the closer interaction of the particles in the suspension. Reducing the zeta potential to a point at which the particles can interact at the secondary minimum allows for reversible aggregation which prevents caking upon sedimentation and allows for the redistribution of the particles in the suspension. It is necessary to produce a range of formulations containing varying

concentrations and assess the amount of sedimentation and the degree of flocculation at each concentration. The formulation which displays the largest degree of flocculation will be the most stable system. Highly flocculated systems are more stable than formulations where flocculation is low as the floccules sediment out into a larger volume than the individual particles which pack closer together. This reduces the compression of the sediment and thereby prevents caking (Figure 1.9) (Midmore and Hunter, 1988; Lippincot *et al*, 2005).

1.4.3.1.4 Surface Active Agents

Surface active agents can be included for use in suspensions for two main reasons; they can effect flocculation and they can also affect the wettability of the drug particles. Surface active agents affect the degree of flocculation observed in suspensions in a similar way as described for electrolytes. Both ionic and non-ionic surfactants can be used. However, non-ionic surfactants are routinely used in liquid oral suspensions as ionic surfactants have higher toxicity. Surfactants are normally used in low concentrations which vary depending upon the surfactants and the particles present (Schwartz and Perry, 1949).

Surface active agents are also employed to improve the wettability of drug particles in suspension which reduce the contact angle of the insoluble drug particles with the aqueous vehicle in which they are suspended. Due to the hydrophobic nature of insoluble drugs an aqueous vehicle in which they are suspended may resist the formation of a layer around the

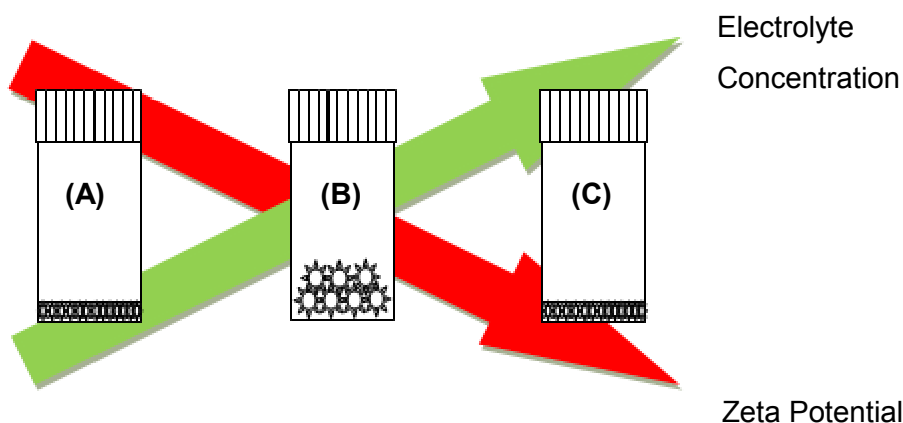


Figure 1.9. Diagrammatic representation of the effect of changing electrolyte concentration. **(A)** The electrolyte concentration is low allowing for a high zeta potential resulting in caking of the particles. **(B)** Sample illustrates a balance between electrolyte concentration and zeta potential which results in flocculation and a larger sedimentation volume. **(C)** Sample displays caking which results from the electrolyte concentration being too great and the zeta potential falling too low.

particles which results in poor wetting. In order to achieve maximum wettability the angle at which the liquid meets the solid particles surface needs to be low. The contact angle (θ) is defined in terms of the tensions between three phases, these being: (1) Solid/Vapour (γ_{sv}), (2) Liquid/Vapour (γ_{lv}), and (3) Solid/Liquid (γ_{sl}).

Young's equation is used to describe Wettability;

$$\gamma_{lv} \cos \theta = \gamma_{sv} - \gamma_{sl}$$

Decreasing the interfacial tensions in the Liquid/Vapour and the Solid/Liquid will lead to a reduction in the contact angle. This is attained by the addition of surfactants into the formulation which adsorb at the Liquid/Vapour and the Solid/Liquid interfaces reducing the tension (Guo *et al*, 2005, Stamkulov *et al*, 2009).

Poorly wetted drug particles have a tendency to clump together in an attempt to stabilise the suspension by lowering the Gibb's free energy. Sufficiently wetted particles aid the production of homogenous suspensions and this is essential for ensuring uniformity in dosage.

1.4.3.1.5. Hydrophilic Polymers

Hydrophilic polymers improve the stability of a suspension via steric repulsion. This occurs as the hydrophilic polymers adsorb to the surface of the particles in the suspension. However as the hydrophilic polymers are large molecules they often have long sections not absorbed to the particle surface and these sections extend into the vehicle which results in controlling flocculation and enhancing the stability of the system (Kellaway and Najib, 1981).

The second function of hydrophilic polymers is to modify the flow properties of the suspension, achieved by increasing the vehicle viscosity with increasing hydrophilic polymer concentration. This is useful for prolonging the suspension of particles but can at times in the same way make it more difficult to re-suspend any particles which do sediment. To get the best results from the addition of hydrophilic polymers, the ideal properties for a suspensions flow profile are pseudoplastic or shear thinning. These are non-Newtonian liquids for which the rate of shear is not proportional to the shear stress exerted (Figure 1.10) (Jones 2008). This is particularly useful as the relatively high viscosity under low shear conditions (such as during storage) slows the sedimentation process, and the relatively low viscosity under high shear conditions (such as shaking or pouring) allows for the easy re-dispersion of any sediment and also the easy dispensation of the medication (Figure 1.11) (Cross 1965).

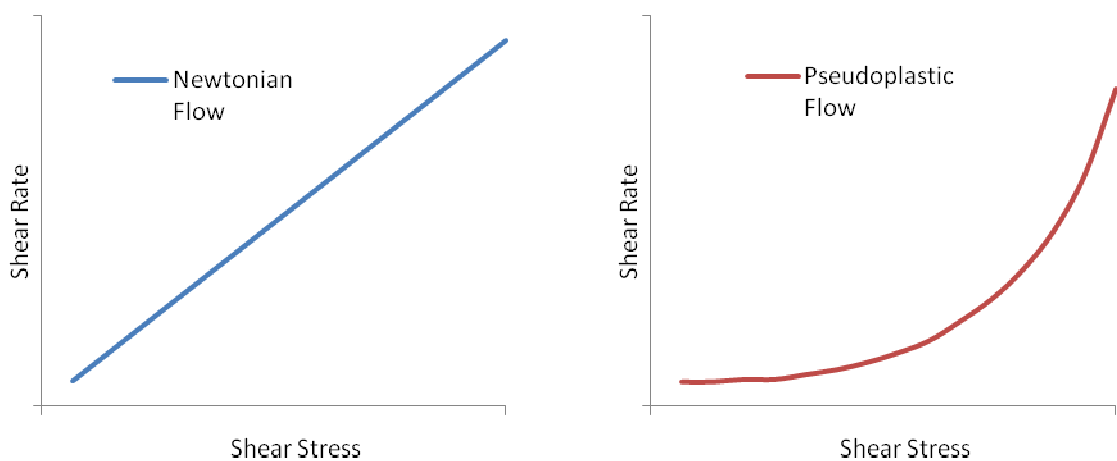


Figure 1.10. Comparison of the response in shear rate with increasing shear stress for Newtonian flow and pseudoplastic flow.



Figure 1.11. Typical plot of viscosity against shear rate for a pseudoplastic liquid. Increasing the shear rate causes a decrease in viscosity.

1.4.3.1.6. Nanoparticles

Nanoparticles are defined as submicron ($<1\mu\text{m}$) colloidal particles, of which there are monolithic nanoparticles (nanospheres) and nanocapsules. With regards to the former, the drug is able to be absorbed, dissolved, or dispersed throughout the matrix. With regards to the latter, the drug is confined to an aqueous space or oily core surrounded by the polymeric shell-like wall. This polymeric coating provides a dual action of API protection and regulated release, with the latter being mainly influenced by polymer-to-drug ratio, and molecular weight and composition of the polymer (Prabha and Labhasetwar, 2004)

This drug delivery system is particularly important for sensitive API's that are to be delivered orally, such as hydrophobic or acid labile drug molecules. Significant advancement has been made in using polymeric nanoparticles for gene therapy towards breast cancer cells, resulting in anti-proliferative effects (Prabha and Labhasetwar, 2004b).

1.5. Excipients for Inclusion in all Oral Liquid Formulations

The formulation of solutions and even more so for suspensions requires the use of several excipients. It is important that all ingredients in the formulations are chemically compatible to ensure the stability of a formulation. In addition to the previously mentioned solubilising agents, there is a need for inclusion of preservatives to protect against microbial contamination and in the majority of cases antioxidants are included to protect the API from oxidising agents.

1.5.1. Preservatives

The preservatives for inclusion in oral liquid formulations should be effective over a broad spectrum in order to prevent contamination as a result of bacterial (gram negative and gram positive) and fungal infection. They must also however be harmless to the patients and remain active and stable for the life of the product. There are a multitude of preservatives available for use with some of the most commonly used including benzoic acid, ascorbic acid and the paraben group of preservatives (Bean, 1972).

There are many factors in liquid formulations which can have an effect on the efficacy of the preservatives included in the formulation. The first determinant is the concentration of preservative included in the formulation. Below the minimum inhibitory concentration (MIC) the preservative will not be sufficiently effective to fully protect the formulation from

contamination. Other factors which can be of incidence on the efficacy of the preservatives include: pH of the system, presence of micelles, and the presence of hydrophilic polymers (Gallardo *et al*, 1991).

The pH of a system determines whether a compound will be present in its ionised or unionised form. In some cases only the unionised form of a preservative displays antimicrobial activity. As a result increased antimicrobial activity will be seen in acidic formulations, an example of such a preservative is benzoic acid. There are other preservatives which are less pH dependent such as parabens (pH range of around 4-8).

Micelles can impact preservative activity if the preservative displays hydrophobic properties, where this is the case the preservative can pass into the oil phase of the micelle leaving concentrations of preservative remaining dissolved in solution which may fall below the MIC. When micelles and hydrophobic preservatives are used in conjunction, it is important for the concentration of the preservative to be greater than intended for use, thus ensuring the concentration of the preservative present in the solution remains above the MIC (Jones 2008).

Hydrophilic polymers have been shown to interact with the preservative dissolved in solution via chemical reactions which reduces the availability of preservative. Electrostatic interactions between the hydrophilic polymers and the preservatives may also render the two incompatible (Kurrup *et al*, 1995).

1.5.2. Chemical stabilisers

Chemical stabilisers are substances which inhibit the reaction between two or more molecules of interest. Some of the common stabilisers used in the pharmaceutical industry include: antioxidants, sequestrants (inactivate traces of metal that would otherwise act as catalysts), emulsifiers and surfactants, and ultraviolet stabilisers.

Table 1.2. Classification of antioxidants.

Class	Description	Example
True antioxidants	Block chain reactions by reacting with free radicals	Butylated hydroxyanisole, butylated hydroxytoluene, tert-butyl-hydroquinone, 4-hydroxymethyl-2,6-di-tert-butylphenol, gallin acid, propyl gallate
Reducing agent	Reducing agents have a lower redox potential than the drug or excipient they are protecting	Ascorbic acid, thioglycolic acid, ascorbyl palmitate, sulphites, thioglycerol
Synergistic	Enhance the affects of antioxidants	EDTA, Lecithin,

Antioxidants are included in pharmaceutical preparations to protect the API when there is the possibility of oxidative degradation. Antioxidants are typically either compounds that inhibit free radical induced decomposition or they are redox systems, which exhibit higher oxidative potential than the drug they are protecting. They work to protect the drug by being oxidised in preference of the drug itself. Antioxidant concentration decreases markedly between production and the end of the shelf life of a formulation as the antioxidant is used up over time. Antioxidants are used in low concentrations and can be combined with chelating agents which provide added protection (Shah *et al*, 2010).

Oxidation can be defined as a chemical reaction involving the transfer of electrons/hydrogen from one substance to an oxidising agent, usually resulting in the formation of free radicals. It is these free radicals that are the most damaging to biological cells. Table 1.2 highlights the classification of antioxidants into three distinct groups: (1) true antioxidants, (2) reducing agents, and (3) antioxidant synergists. The latter group normally have limited antioxidant properties themselves, but enhance the actions of the true antioxidants by reacting with metal ions that catalyse oxidation.

1.6. Development of a Palatable Formulation

As children are less likely to be willing to take unpleasant tasting medications that an adult may deem acceptable, and as such the production of palatable formulation is also a necessity. This is particularly important when formulating solutions than suspensions, as the bitter taste of many API's is fully prevalent once the API is solubilised, where as in a suspension the bitter taste can be somewhat masked by the suspending agent. There are many methods of taste masking.

The inclusion of taste enhancers such as concentrates, fruit juices and sweetening agents are widely used but are limited in their capacity in taste masking very bitter drugs. Another approach is to coat the drug particles with agents which are not pharmaceutically active for example Eudragit, PEG and ethyl cellulose. These coatings prevent the interaction of the bitter tasting drug particles with the taste receptors in the mouth and thereby mask the bitter taste. It is important that the coating of the drug particles does not limit the bioavailability of the drug. Complexation of the drug molecule with a host molecule is another method by which the bitter taste of a drug can be masked, in this way the whole drug molecule or part of the molecule is contained within a host molecule (for example cyclodextrin), and in a similar way to the coating procedure prevents the interaction of the drug with the taste receptors. Yet another widely used approach involves the production of solid insoluble poly-electrolytes which have a high molecular weight known as ion exchange resins. The inclusion of a bitter tasting drug into a solid dispersion, liposomes or emulsions or alternatively the combination of the drug with amino acids are four further methods for taste masking, with the formation of pro-drugs or salts of the drug being two methods of improving palatability via chemical modification (Ayenew *et al* 2009).

1.6.1. Sweeteners

The most commonly used sweetening agents included in pharmaceutical preparations are sucrose, liquid glucose, glycerol, sorbitol, saccharin sodium and aspartame. Increasingly artificial sweeteners are being used in formulations and in paediatric formulation the use of sugar is to be avoided. This is also the case for formulations intended for use in patients suffering from diabetes mellitus.

1.6.2. Flavourings

In the same manner that sweeteners are included to mask the taste of unpleasant tasting formulations, purpose made flavourings can be added. The flavour selected for use must be effective at masking the taste and in order to do this the flavours to choose from depend on the initial taste of the formulation. For example, when a formulation is unpleasant as the result of a salty taste then some of the best flavours to mask this include; butterscotch, apricot, peach, vanilla and mint. In the same way, a bitter taste is best masked with flavours such as; cherry, mint and anise. Formulations which are overly sweet are best improved by including vanilla or fruit and berry flavours while sour tasting formulations are best masked using the citrus flavours and raspberry.

In most cases a combination of more than one flavouring agent coupled with a sweetening agent will produce the most palatable formulation and excipients with the roll of enhancing the flavours present are often included. Flavour adjuncts (such as menthol) are at times also included and these have the effect of reducing the sensitivity of the taste buds at the same time as adding to the flavour of the formulation.

1.7. Rational and aim of the project

Among the existing dosage preparations available on the pharmaceutical market, the oral route remains the preferred choice with better patient compliance. However the lipophilic nature of most API's enables them to effectively cross the lipophilic mucosal barrier to the site of action. Thus the current and mainstay for oral delivery remains to be solid dosage forms, as they can be applied to the vast number of hydrophobic API's on the market. However, these formulations have their disadvantages as they are relatively large and bulky, thus are difficult to administer to children and those patients who have suffered a stroke, motor neurone disease and advance Alzheimer's (resulting in dysphagia). Accordingly, the current research aims to investigate the role of formulation excipients in the development of oral liquid preparations (longer shelf life) with various API's, and use this knowledge to achieve further advances in the formulation field, particularly as drugs come to the end of their patent life.

The research strategy had been rationalised as follows:

- To develop a stable solution of captopril at 1 mg.mL^{-1} and 5 mg.mL^{-1} dosages by preventing the degradation product captopril disulphide, and to investigate the implications of the stabilising affects of HP- β -CD.
- To investigate the influence of salts and generally recognised as safe (GRAS) listed solubilising excipients on the solubilisation of gliclazide, in order to prepare an 8 mg.mL^{-1} and 16 mg.mL^{-1} formulation.
- To investigate the solubilising and stabilising properties of cyclodextrin (HP- β -CD) in the development a 1 mg.mL^{-1} melatonin formulation.
- To overcome the extreme bitterness of L-arginine and prepare an acceptable palatable 100 mg.mL^{-1} formulation with an optimised calibration validation protocol.
- To investigate the preservative efficacy of the oral liquid formulations prepared in chapters 2-5.
- To investigate the applications of nanoparticulate delivery for the acid labile drug lansoprazole, and the influence of polymer composition and ratio of the efficiency of drug loading.

The preparation of oral liquid formulations has three major advantages; firstly liquid preparations provide a practical solution for patients who have difficulty swallowing (dysphagia). This target group includes; geriatrics, paediatrics, and those hospitalised who suffer from a variety of disorders limiting their motor movements (such as stroke, parkinson's disease etc.). Secondly, as pharmaceutical drugs reach the end of their patents, the reformulation of the drug into a new dosage form enables the pharmaceutical companies to extend the patent life and ultimately their market exclusivity. Thirdly, oral delivery systems do not require strict sterile conditions and are thus less expensive to manufacture.

CHAPTER 2

Formulation development of an oral solution of
captopril

CHAPTER 2

Formulation development of an oral solution of captopril

2.1. Introduction

2.1.1. Angiotensin Converting Enzyme (ACE)

Angiotensin I-converting enzyme (ACE), a dipeptidyl carboxypeptidase is a transmembrane zinc metallopeptidase, which not only plays a vital role in cardiovascular homeostasis but also displays a physiological role in blood-pressure and metabolism of salt and water, via its actions on angiotensin I and bradykinin (Mayer and Meyer, 2000; Hattori *et al*, 2000). The metalloprotease acts by using a zinc atom for catalysis of the inactive decapeptide angiotensin I to the potent vasoconstrictor octapeptide angiotensin II. This action is carried out by the cleavage of the carboxy-terminal dipeptide.

As seen from figure 2.1, in order to reduce high blood pressure the angiotensin-converting enzyme can be inhibited at 2 distinctive points: the first is to inhibit the conversion of angiotensin I to angiotensin II in the endothelial tissues via ACE inhibitors. The second point of inhibition is by preventing further conversion of angiotensin II to angiotensin III in the adrenal gland by angiotensin receptor blockers (ARBs).

2.1.2. ACE Inhibitors

ACE inhibitors are competitive inhibitors of ACE, mimicking the structure of its substrate. There are a range of ACE inhibitors: sulphhydryl-containing agents such as captopril, dicarboxylate-containing agents including enalapril, ramipril, quinapril, perindopril, lisinopril (a lysine derivative of enalapril) and phosphonate-containing agents such as fosinopril. Captopril and lisinopril are active molecules. Others listed above are prodrugs that need to be converted to active metabolites (di-acids) to illicit a therapeutic response. The chemical structures of these ACE inhibitors are represented in figure 2.2. ACE inhibitors act by blocking the formation of angiotensin II and at the same time increasing the bradykinin level. This results in the reduction of vasoconstriction, sodium and water retention, resulting in increased vasodilation.



Figure 2.1. Angiotensin converting enzyme mechanism. (Source: Katzung *et al*, 2009, <http://www.accessmedicine.com>)

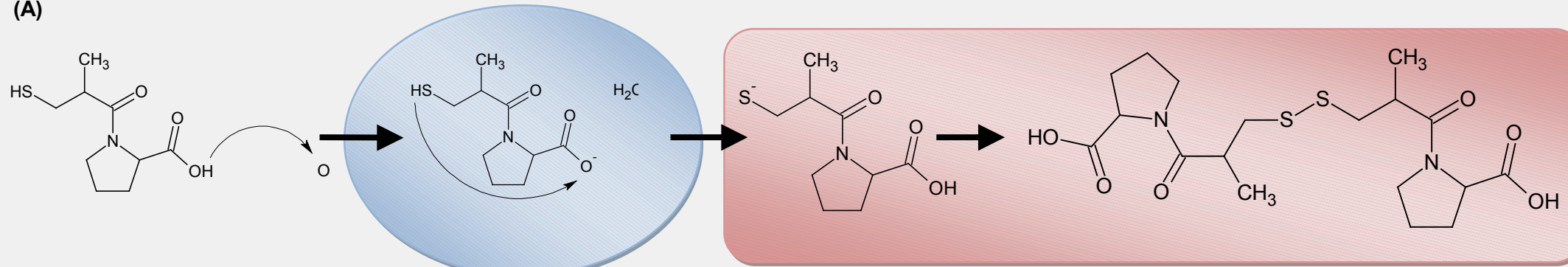


Figure 2.2. Chemical structures of ACE inhibitors currently on the pharmaceutical market.
(Structures taken from www.Drugbank.ca)

2.1.3. Captopril

Captopril is one of the potent hypotensive agents commonly prescribed to lower blood pressure. It is a white crystalline powder with a molecular weight of 217.3, freely soluble in water (160 mg.mL^{-1} at 25°C) and has a distinctive sulphide like odour. As a solid dosage form, captopril is marketed as Acepril®, Capoten®, and Ecopace®, which are available as 12.5, 25, and 50 mg tablets. Captopril is currently used for hypertension, heart failure and after care, as well as circulation problems associated with diabetes. One of the common physiological conditions prevalent in patients who have suffered from heart failure is dysphagia. Dysphagia is a medical condition where the patient experiences swallowing difficulties. To meet the patient needs, captopril is regularly prescribed as a liquid “special” with a shelf life of one month. The short shelf life of the liquid preparation is due to chemical instability of captopril via oxygen-facilitated first order free radical oxidation at its thiol group, yielding a major degradation product captopril disulphide (Figure 2.3). The mechanism is initiated by the hydrogen on the carboxylic group reacting with the free oxygen in solution creating an ionised carboxylic acid group ($-\text{COO}^-$). This in turn causes the thiol group ($-\text{SH}$) to donate its hydrogen atom to reform a carboxylic end group, resulting in an ionised sulphur atom ($-\text{S}^-$), which further reacts with another molecule of captopril undergoing the same chain reaction. The two captopril molecules dimerise to form the degradation product captopril disulphide (Kristensen *et al*, 2008). The rate of oxidation can however be reduced by a number of factors. Oxidation is pH-dependent and thus by reducing the pH of the system the stability of the system increases, with $\text{pH}<4$ achieving the greatest stability (Hillaert and Van den Bossche, 1999). Oxidation is also influenced by the presence of metal ions such as copper and iron. Research has also shown that captopril degradation may be inversely proportional to drug concentration, which is primarily due to the stoichiometry of the oxidation, as two moles of captopril is known to be lost for every half a mole of oxygen consumed (Connors *et al*, 1986).

(A)



(B)

Captopril
formulation
issues

Oxidation:

- Antioxidant/ chelating agent
- Antimicrobial activity
- Sweetening agent

Sulphide-like odour:

- Hydroxypropyl- β -cyclodextrin
- Peppermint oil

Figure 2.3. Schematic representation of the formulation issues associated with captopril degradation. (A) Degradation pathway of captopril: oxygen-facilitated, first order, free radical oxidation is initiated by the ionisation of the carboxylic group, which in turn ionises the thiol group, yielding the major degradation product captopril disulphide (B) captopril formulation issues required to be overcome in the study: prevention of the oxidation reaction and masking of the sulphide like odour of captopril.

2.1.3.1. “Specials” – current state of oral liquid captopril

Many drugs have been widely used as unlicensed oral liquid medicines that have been extemporaneously prepared in dispensaries in order to meet the needs of specific patient groups, such as paediatrics and geriatrics or those with swallowing difficulties.

Extemporaneous preparations are defined as formulations made to meet specific needs for the consumer without a license requirement. However the biggest disadvantage of extemporaneous preparations is the greater risk of adverse drug reactions as compared with the licensed medicines. These unlicensed medicines were commonly given to the most vulnerable patients in the community and in the hospitals and as such were unable to alert the medical staff to any adverse drug reactions they may have been experiencing. Research by Mulla and co-workers (2007) has shown that extemporaneous preparations of captopril had variable shelf life ranging from 7 -28 days, dosing inconsistencies and poor formulation harmonisation leading to potential toxicities. The research concluded that the inconsistencies in formulation raised serious issues over optimal dosing and its influence in paediatric cardiac surgical and interventional outcomes. Current formulations include simple solubilisation in water, syrups, and suspending agents. However the use of syrup as a vehicle for captopril was not recommended due to vulnerability to microbial contamination when diluted with other excipients. In addition, dilution results in an increased risk of the introduction of unwanted metal ions and thus catalysing drug degradation (Mulla et al, 2007)

2.1.4. Aims and objectives

The aim of the study was to formulate and stabilise captopril (max. 5 mg.mL⁻¹) in solution for oral delivery. This was to be achieved by overcoming two major obstacles; (1) preventing the initiation of the oxidation process and (2) overcoming sulphur-like smell (organoleptic properties) of captopril in solution (Figure 2.3B).

The various parameters tested to address these issues systematically included:

1. Influence of addition of antioxidant/chelating agent (EDTA-Na)
2. Influence of incorporation of antioxidant with preservative activity
3. Complex formation and stabilisation using HP-β-CD

2.2. Methods and materials

2.2.1. Materials

Captopril, glycerol, sodium metabisulphite, ethylenediaminetetraacetic acid disodium salt dihydrate (EDTA), hydroxypropyl- β -cyclodextrin (HP- β -CD), Pluronic F127 and potassium bromide were all purchased from Sigma. Deuterated dimethyl sulfoxide (DMSO-D₆) purchased from Goss Scientific Instrument Ltd (Cheshire, UK). Phosphoric acid and methanol were purchased from Fisher Scientific (UK).

2.2.2. Calibration validation

Calibration was carried out using a Dionex HPLC system comprising of a GP50 gradient pump, AS50 autosampler and a UVD170U detector (Dionex Corporation, USA). Samples were passed through a 5 μm C18 Gemini column (150 x 4.6 mm) (Phenomenex, USA). 25 mg of captopril was dissolved in 50 mL of water to obtain a stock concentration of 500 $\mu\text{g.mL}^{-1}$. Serial dilutions were then carried out to obtain concentrations of 400, 300, 200, 100, 50, and 25 $\mu\text{g.mL}^{-1}$. Using a mobile phase consisting of 0.1 % (v/v) phosphoric acid and methanol (72.5:27.5), 20 μL of each captopril concentration was injected into the Dionex HPLC and analysed at a wavelength of 220 nm. The retention time for captopril was 15 minutes. (Khan *et al*, 2000).

2.2.3. Formulation strategies

2.2.3.1. Captopril solubilisation

20 mg of captopril was solubilised in 20 mL water to produce a 1 mg.mL^{-1} formulation. The samples were stored in polyethylene terephthalate (PeT) (Neville and More Ltd, Southwater, England) bottles at 25 °C and 40 °C under 40 and 75 % humidity conditions respectively.

2.2.3.2. Addition of an antioxidant

20 mg of EDTA was added to 10 mL water under continuous stirring. Once fully dissolved 20 mg of captopril was added and stirred. The volume was then made up to 20 mL to produce a concentration of 1 mg.mL^{-1} . The samples were stored in PeT bottles at 5 °C, 25 °C (40 % humidity) and 40 °C (75 % humidity).

2.2.3.2.1. Addition of 0.1 % (w/v) sodium-metabisulphite

20 mg of EDTA and 20 mg of sodium-metabisulphite was added to 10 mL water under continuous stirring. Once fully dissolved, 20 mg of captopril was added and stirred magnetically. The volume was then made up to 20 mL to produce a concentration of 1 mg.mL⁻¹. The samples were stored in PeT bottles at 5 °C, 25 °C (40 % humidity) and 40 °C (75 % humidity).

2.2.3.2.2. Addition of 30 % (w/v) glycerol

20 mg of EDTA was added to 10 mL water under continuous stirring. Once fully dissolved 6 g of glycerol was added under continuous stirring to form a final concentration of 30 % (w/v). 20 mg of captopril was then added under continuous stirring until the drug had fully solubilised. The volume was then made up to 20 mL to produce a concentration of 1 mg.mL⁻¹. The samples were stored in PeT bottles at 5 °C, 25 °C (40 % humidity) and 40 °C (75 % humidity).

2.2.3.2.3. Addition of HP-β-CD

In 10 mL of water, 120 mg of HP-β-CD was dissolved under continuous stirring, to which 20 mg of captopril was then added. Once fully dissolved, 20 mg of EDTA was added under continuous stirring and the volume was then made up to 20 mL to produce a concentration of 1 mg.mL⁻¹. The samples were stored in PET bottles at 5 °C, 25 °C (40 % humidity) and 40 °C (75 % humidity).

2.2.3.3. 5mg.mL⁻¹ formulation of captopril

2.2.3.3.1. Addition of EDTA

20 mg of EDTA was added to 10 mL water under continuous stirring. Once fully dissolved 100 mg of captopril was added and stirred magnetically until fully solubilised. The volume was then made up to 20 mL to produce a 5 mg.mL⁻¹ concentration. The samples were stored in PeT bottles at 5 °C, 25 °C (40 % humidity) and 40 °C (75 % humidity).

2.2.3.3.2. Addition of HP-β-CD with EDTA

In 10 mL of water, 602 mg of HP-β-CD was dissolved under continuous stirring, to which 100 mg of captopril was then added. Once fully dissolved, 20 mg of EDTA was added under continuous stirring and the volume was made up to 20 mL to produce a 5 mg.mL⁻¹

concentration. The samples were stored in PeT bottles at 5 °C, 25 °C and 40 °C under 40 °C and 75 % humidity conditions respectively.

2.2.4. Microviscosity of glycerol

Viscosity of glycerol samples was measured using the automated micro viscometer (Anton Paar, Hertford, UK). Viscosity of a sample is based upon the falling ball principle in which the time taken for the ball to roll through transparent and opaque liquids is a measurement of the dynamic viscosity of the sample.

Various concentrations of glycerol ranging from 10 to 50 % (v/v) were prepared in distilled water, and transferred into the glass capillary tube to measure the dynamic viscosity using the rolling ball. The temperature was set at 25 °C for all of the samples and the density of water was calibrated to be 0.99700 g.cm⁻³.

2.2.5. Conductivity measurements

Conductometry was calculated using a conductivity meter 4310 (Jenway, Staffordshire, UK) ($K=1.08$ at 25 °C). In 50 mL of distilled water 250 mg of captopril was added and the conductivity was measured. To this increasing amounts of HP-β-CD was added and the reading for conductivity and potentiometry were recorded.

2.2.5.1. Calculation of association constant



The stability of the inclusion complex can be described by the association constant K:

$$K = \frac{C_{CD-D}}{(C_{CD,F}C_{D,F})}$$

$C_{CD,F}$ = Concentration of non-complexed cyclodextrin

$C_{D,F}$ = Concentration of non-complexed drug

C_{CD-D} = Concentration of the 1:1 complex

Thus using the above equation the association constant for this system can be calculated as follows:

Concentration of non-complexed Cyclodextrin = 4198 mg in 50 mL = 83.96 mg.mL⁻¹

Concentration of non-complexed drug = 5 mg.mL⁻¹

Concentration of 1:1 complex = 88.96 mg.mL⁻¹

Therefore using $K = C_{CD-D} / (C_{CD,F}C_{D,F})$

$$= 88.96 / (83.96 \times 5)$$

$$K = 1.79$$

2.2.5.2. Calculation of Molar conductivities

Definition of a molar conductivity is as follows:

$$\Lambda = \frac{\Lambda_{D,P} + \Lambda_{CD-D} KC_{CD,F}}{1 + KC_{CD,F}}$$

$\Lambda_{D,F}$ = Molar conductivity of non-complexed drug

Λ_{CD-D} = Molar conductivity of the 1:1 complex

$C_{CD,F}$ = Concentration of non-complexed cyclodextrin

$$K = 1.79$$

Thus by using the above equation the molar conductivity of a set added amount of cyclodextrin can be calculated:

Example:

Molar conductivity of non-complexed captopril ($\Lambda_{D,F}$) :

Conductivity reading of captopril	1457
Moles of captopril	0.023
= $\frac{1457}{0.023} = 63347$	

Molar conductivity of complexed drug with cyclodextrin (Λ_{CD-D}):

$$\frac{\text{Molar conductivity reading of complex}}{\text{Moles of cyclodextrin}} = \frac{1431}{0.25} = 5724$$

$$K = 1.79$$

The concentration of non-complexed cyclodextrin ($C_{CD,F}$) = 0.25, 0.50, 0.75 M etc.

Therefore for a 0.25 M HP β CD, which displayed a conductivity reading of 1431:

$$\Lambda = \frac{\Lambda_{D,P} + \Lambda_{CD-D} KC_{CD,F}}{1 + KC_{CD,F}}$$

$$\Lambda = \frac{63347 + 5724 \times (1.79 \times 0.25)}{1 + (1.79 \times 0.25)}$$

$$\underline{\text{Molar conductivity} = 45533 \text{ S.m}^2 \cdot \text{mol}^{-1}}$$

Analysis is conducted from the graph produced of molar conductivity versus concentration of HP- β -CD. A decrease in conductometry is due to complexation between the drug and the cyclodextrin and a plateau effect was seen when the drug was fully complexed with the cyclodextrin.

2.2.6. Freeze-drying protocol

5 mg.mL⁻¹ formulations of captopril with HP- β -CD were prepared (protocol 2.2.3.3.2.). The samples were placed into flat-bottom glass vials and frozen at -60 °C for 2 hours. The samples were then placed into an advantage 2.0 bench top freeze-dryer (VirTis, Suffolk, UK) in order to extract the water. The freeze-drying process involved primary drying for 48 hours at a shelf temperature of -40 °C followed by secondary drying for 10 hours at a shelf temperature of 20 °C at a vacuum of 50 mTorr.

2.2.7. Proton Nuclear Magnetic resonance Spectroscopy (H^1 -NMR)

The freeze-dried samples and individual ingredients of each formulation were dissolved in DMSO-D₆ at room temperature in 5 mm glass tubes. Approximately 2 mg of the sample was dissolved in 600 µL of DMSO-D₆. All NMR measurements were done with standard Bruker pulse sequences.

2.2.8. Differential Scanning Calorimetry (DSC)

Differential scanning calorimetry (DSC) (Perkin-Elmer, Wellesley, USA) was used to study glass transition temperatures (T_g) and melting points. Approximately 5 mg of sample was placed in a Perkin-Elmer aluminium pan, cooled to 10 °C using intra-cooler (2P Perkin-Elmer, Wellesley, USA) followed by heating to 240 °C at a rate of 200 °C·min⁻¹ with a nitrogen purge of 20 mL·min⁻¹. An empty aluminium pan was used as a reference.

The T_g and melting temperature (T_m) were then analysed using the Pyris Manager software. All of the measurements were carried out in triplicate with fresh samples being prepared for each DSC run. The DSC was calibrated for temperature and heat flow, prior to the samples being tested, using standard samples of indium (T_m 156.6 °C) and zinc.

2.2.9. Thermogravimetric analysis (TGA)

Thermal degradation of captopril was analysed using a TGA, which determines the dependence of the weight loss of a sample as a function of temperature. The system consisted of a Pyris 1 Thermogravimetric Analyzer (Perkin Elmer). The sample mass ranged from 2-5 mg and were heated from 20-300 °C at a rate of 10 °C·min⁻¹. The instrument self regulates the heating rate automatically in order to maintain a constant temperature during a given thermal event. All the studies were performed in triplicate.

2.2.10. Fourier Transform Infrared Spectroscopy (FTIR)

Characterisation of freeze-dried formulations was carried out with FTIR in order to investigate the interaction of the excipients and the drug. Freeze-dried samples of the formulations were prepared according to protocol 2.2.6. FTIR disks were prepared by adding the samples to potassium bromide at a ratio of 1:5 respectively. The mixed sample was then compacted by a mechanical press (Specac, Kent, UK) for 10 minutes at 8 tons to form a translucent pellet,

which was analysed using an IR200 spectrometer (Thermo Electron Corporation, UK) to determine the transmittance of each excipient.

2.2.11. pH

The pH of each sample was analysed using a Hydrus 500 (Fisherbrand, UK), calibrated at pH 4, 7 and 10.

2.3. Results and Discussion

2.3.1. Validation of Calibration Curve

HPLC method was developed and validated for the determination of captopril. At a wavelength of 220 nm, distilled water was used to solubilise captopril and analysed to generate a calibration curve. Results are presented in table 2.1.

2.3.1.1. Linearity

The linearity was evaluated by preparing the standard curve for captopril on three consecutive days. The peak area was plotted against captopril concentration and calibration response was assessed for variances. The resultant calibration curve was linear with a regression equation of $y=0.1905x$ ($R^2=0.9997$) (Figure 2.4).

2.3.1.2. Precision

In order to access the reproducibility of the calibration protocol, the method was carried out in triplicate over a period of 3 days for inter-day precision and in triplicate on the same day for intraday precision. The results showed that the method was reproducible with inter-day

Table 2.1. Summary of Calibration Validation of captopril.

Criteria	Validation
$Y=$	0.1905
R^2	0.9997
Intra-day Precision	110.3 %
Inter-day Presicion	109.1 %
Accuracy ($\pm SD$) 20 $\mu\text{g.mL}^{-1}$	97.2 (7.29)
Accuracy ($\pm SD$) 40 $\mu\text{g.mL}^{-1}$	94.68 (5.24)
Accuracy ($\pm SD$) 60 $\mu\text{g.mL}^{-1}$	97.73 (4.69)
LOD $\mu\text{g.mL}^{-1}$	4.33
LOQ $\mu\text{g.mL}^{-1}$	13.12

precision of 110.3 % and intra-day precision being 109.1 % (Table 2.1). The standard deviation of the regression equation was 0.002. Statistical data was compared using ANOVA with the resulting inter-day and intra-day precision being calculated to have a variance of $P>0.05$, suggesting no difference was seen between the calibration curves on the three days.

2.3.1.3. Accuracy

The accuracy of the developed method was determined from three concentrations of captopril in distilled water representing low, medium and high portions of the standard curve ($20, 40$ and $60 \mu\text{g.mL}^{-1}$). Accuracy of the three concentrations was in the range of 95-97 %.

2.3.1.4 Limit of detection (LOD) and limit of quantification (LOQ)

The limit of detection of an individual analytical procedure is the lowest amount of analyte in a sample which can be detected but not necessarily quantifiable as an exact value (EMEA, 1995). From the calibration range the LOD was calculated to be $30 \mu\text{g.mL}^{-1}$.

The limit of quantification of an individual analytical procedure is the lowest amount of analyte in a sample which can be quantitatively determined with accuracy and precision (EMEA, 1995). From the calibration range the LOQ was calculated to be $100 \mu\text{g.mL}^{-1}$.

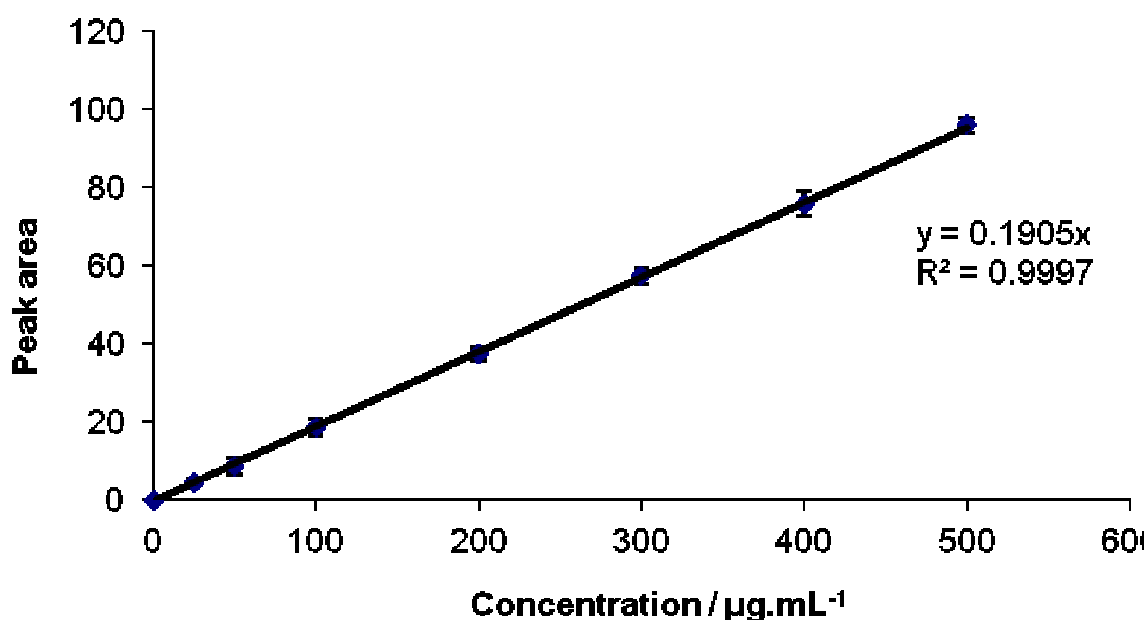


Figure 2.4. Graph of captopril calibration highlighting the linearity of the validation protocol (n=3).

2.3.2. Formulation development strategy

As outlined in figure 2.3, there were two main challenges in the development of oral liquid formulation of captopril: (1) prevention of oxidation and (2) the development of an odour free formulation (captopril has a distinct sulphur smell) (Mulla *et al*, 2010). To address these, the developmental work was divided into two phases. The first phase involved investigation of inclusion of antioxidants and chelating agents to minimise the process of degradation via oxidation. EDTA alone (chelating agent), EDTA along with glycerol (chelating action and preservative activity) and sodium metabisulphite (antioxidant and preservative) were investigated for their influence on captopril stability. This stage of the work was critical as reduction/prevention of oxidation also has a positive effect on reducing dimerisation of captopril (Figure 2.3). The second phase of developmental work was centred on enhancement of organoleptic properties of the formulation including taste, smell and appearance.

2.3.3. Approaches to reduce oxidation

2.3.3.1. *Influence of addition of antioxidant on the stability of captopril in solution*

EDTA is a chelating agent with a structural formula of $C_{10}H_{14}N_2Na_2O_8$ (Figure 2.5) and used as an antioxidant in concentrations between 0.005 to 0.1 % (w/v). In a study carried out by Berger-Gryllaki and co-workers (2007) a 1 mg.mL^{-1} formulation of captopril containing EDTA-sodium at 0.1 % (w/v) produced a stable formulation at 5 °C and room temperature with a shelf life of 2 years. EDTA acts by binding to metal ions by forming six bonds; two bonds are formed with nitrogen atoms in the amino groups and a further four bonds are formed at oxygen atoms in the carboxyl groups (Figure 2.5). These sites are able to initiate an oxidation reaction with free oxygen ions in water resulting in ionised sites for interaction of EDTA with the thiol group of captopril (Jurca and Vicas, 2010) thereby preventing the initiation of free radical oxidation of captopril.

Initial studies were focused on determining the influence of addition of EDTA on the stability of captopril. The formulation protocol comprised of inclusion of EDTA (0.1 % w/v) along with captopril (1 mg.mL^{-1}) in water and assessed for drug stability. All the formulations were stored at 5 °C, 25 °C (40 % humidity) and 40 °C (75 % humidity).

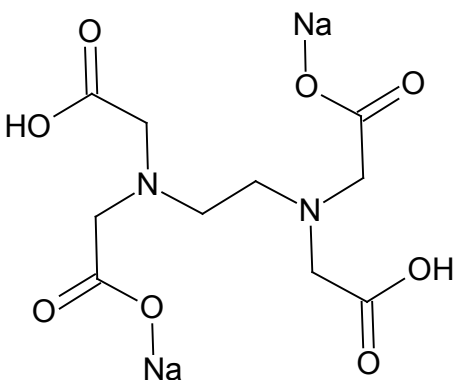


Figure 2.5. Structure of EDTA. Binding sites include: -O-Na, -COOH, and -NH.

The influence of addition of EDTA on the stability of captopril in solution is presented in figures 2.6 and 2.7. In the absence of EDTA, captopril stability was compromised within 30 days. The recovery of captopril decreased to $92.22 \pm 0.16\%$ at 25°C and $35.19 \pm 1.77\%$ at 40°C (Figure 2.6). The degradation of captopril was possibly a direct result of dimerisation initiated by partial deprotonation (17 %) of its carboxylic group ($\text{pKa} 3.7$) at pH 3.2, thereby acting as the driving force of proton donation from the thiol group to the deprotonated carboxylic group (Hillaert and Van den Bossche, 1999; Kristensen *et al*, 2008). In contrast, the addition of EDTA resulted in stable formulations with around 100 % drug recovery over a 12 month period at three temperatures including: 5°C , 25°C and 40°C (Figure 2.7). During the 12 month stability period, no change in pH was observed, with samples remaining stable at a pH range of 3.2-3.4 (Figure 2.8).

The improvement in captopril stability upon inclusion of EDTA can possibly be attributed to the influence of pH and the binding capabilities (chelating activity) of EDTA. The final pH of the formulation was around 3.2. Research by Kristensen and co-workers (2008) has shown that EDTA exists in its ionised state at low pH and exhibits improved chelation due to the presence of six charged groups in its structure ($\text{pKa}_1=0.0$, $\text{pKa}_2=1.5$, $\text{pKa}_3=2.0$ and $\text{pKa}_4=2.66$ all apply to the carboxyl protons; and $\text{pKa}_5=6.16$ and $\text{pKa}_6=10.24$ apply to the nitrogen protons) (Permyakov and Kretsinger, 2011). At pH 3.2, the deprotonated carboxyl groups of EDTA potentially bond with the ionised thiol groups of captopril preventing dimerisation (Figure 2.9).

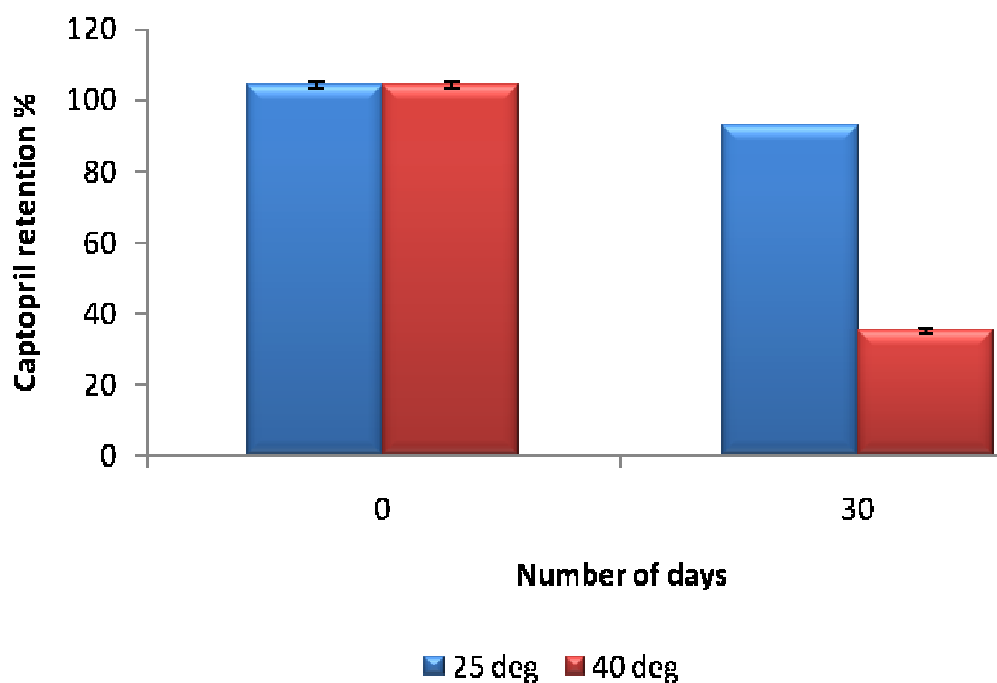


Figure 2.6. Stability of captopril in distilled water (1 mg.mL^{-1}) stored under 25°C (40 % humidity) and 40°C (75 % humidity) conditions. After 30 days storage, captopril retention was reduced to $92.99 \pm 0.07\%$ under 25°C conditions, with greater destabilisation of captopril occurring under 40°C conditions ($35.19 \pm 0.75\%$). (n=3)

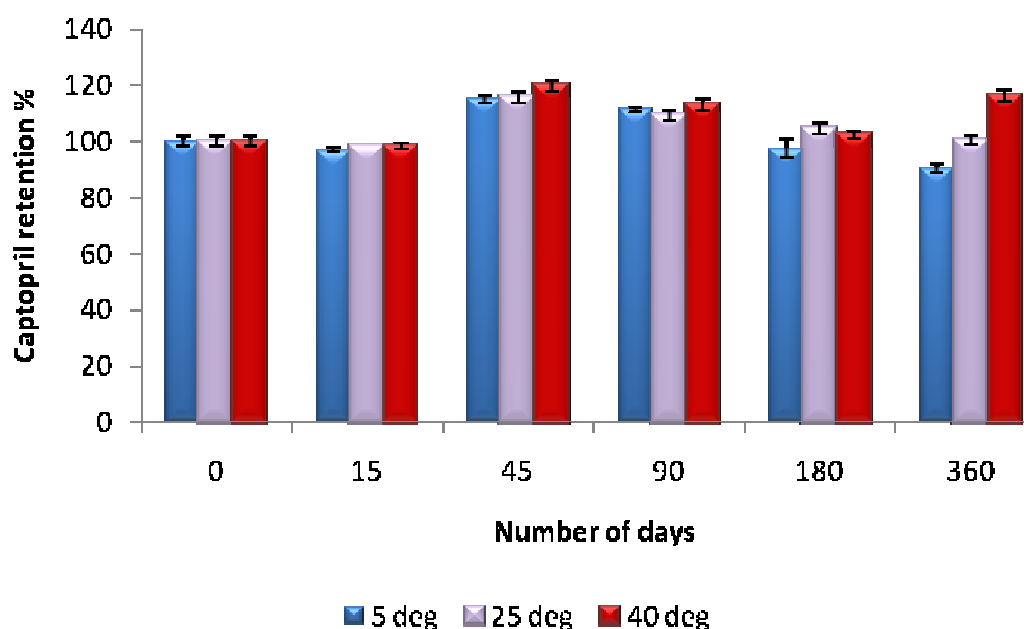


Figure 2.7. Stability of captopril with 0.1 % EDTA (1 mg.mL^{-1}) stored under 5°C , 25°C (40 % humidity) and 40°C (75 % humidity) conditions. After 12 months storage under 25°C and 40°C conditions, captopril retention remained stable at $100.49 \pm 1.61\%$ and $116.30 \pm 2.15\%$ respectively. (n=3)

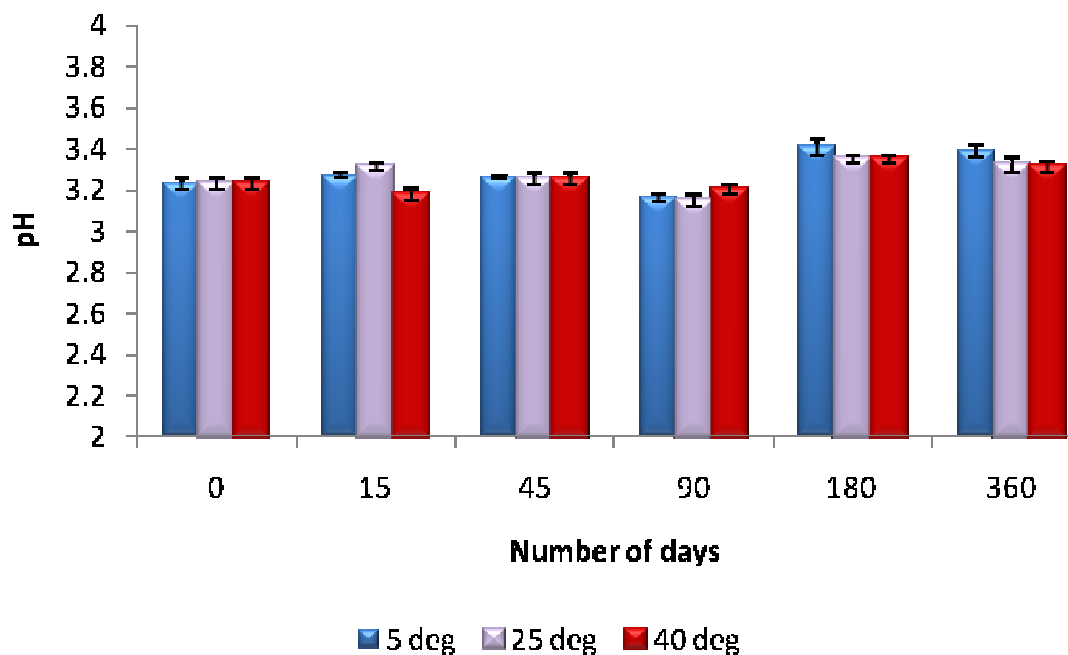


Figure 2.8. pH stability of captopril with 0.1 % EDTA (1 mg.mL^{-1}) stored under 5°C , 25°C (40 % humidity) and 40°C (75 % humidity) conditions. After 12 months storage, the captopril formulation remained stable in the pH range 3.2-3.4. Storage conditions had no effect on the pH stability. (n=3)

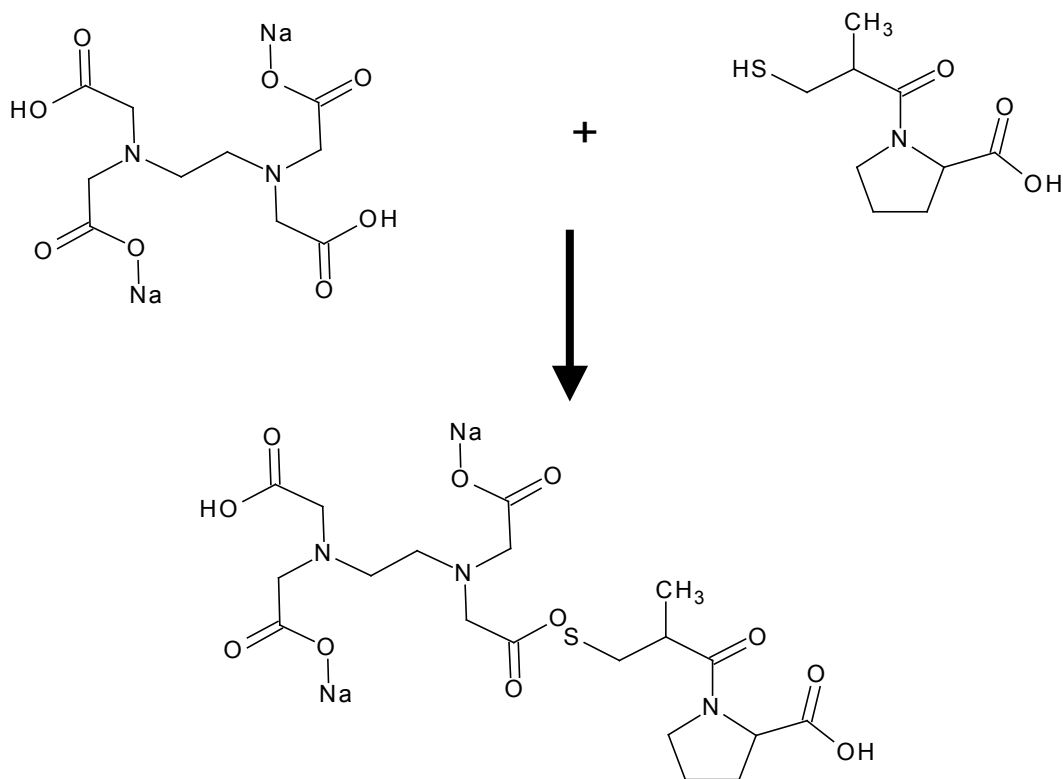


Figure 2.9. The chelation mechanism of EDTA with captopril. The protonated carboxyl group of EDTA binds to the ionised thiol group of captopril, thereby preventing captopril dimerisation.

To further assess the process of chelation and the binding ratios of captopril and EDTA, conductometry studies were performed (Figure 2.10). The conductance of a sample is related to the mobility of the charged particles with mobility of a complex being less than that of a free compound resulting in lowering of conductance. The experiments were performed on free captopril and its conductance was compared upon addition of EDTA. The results show that the addition of increasing concentration of EDTA from 0 to 0.6 M to a solution of captopril results in a linear decrease of conductance. Increase of EDTA concentration from 0.8 to 2 M further reduces the conductance of the solution but to a lower degree. The decrease in conductance of free captopril upon addition of increments of EDTA is possibly due to the formation of weak electrostatic association between the oppositely charged molecules. The molar binding ratio was determined by calculating the association complex (K , stability constant of the inclusion complex), the molar conductivity of non-complexed captopril ($\Lambda_{D,F}$) and the molar conductivity of the complexed drug with EDTA (Λ_{CD-D}). These calculations enabled the molar conductivity of captopril after each increment of EDTA (Λ) to be calculated (Section 2.2.5.1) and graphically plotted (Molar conductivity vs. number of moles of EDTA) (Cabaleiro-Laga *et al*, 2006).

Figure 2.10 showed that a 1:0.75 molar ratio between captopril and EDTA existed during complex formation. Based on the results from the assessment of stability of captopril upon

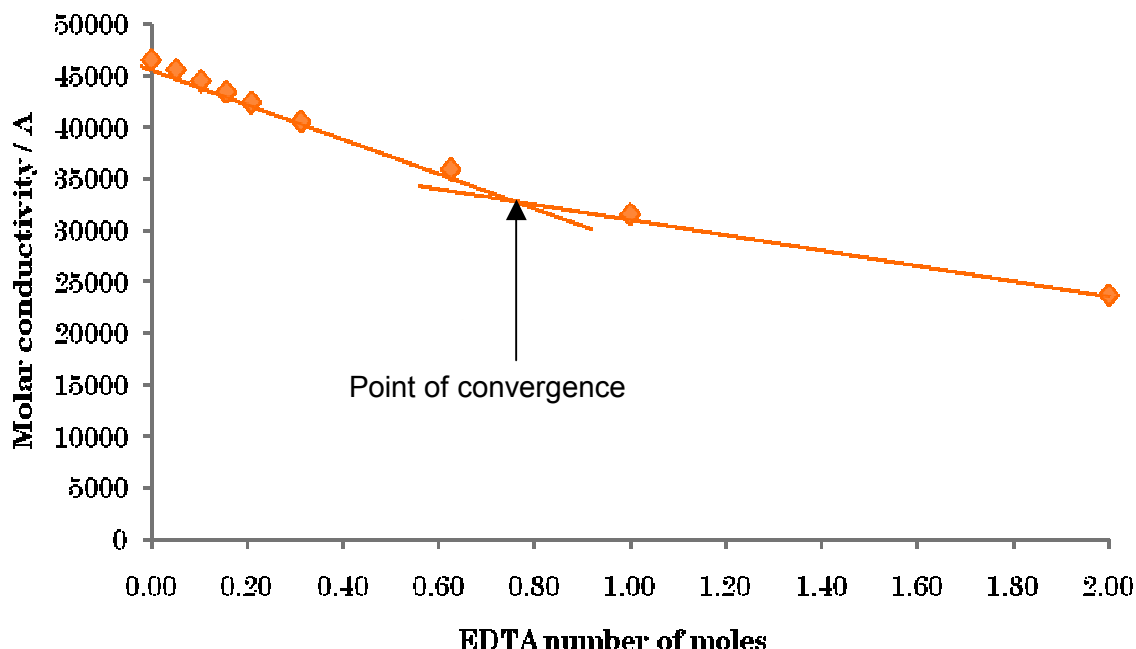


Figure 2.10. Conductometry of Captopril with increasing amounts of EDTA. The point of convergence indicated a molar ratio of 1:0.75 (captopril:EDTA). (n=3)

inclusion of EDTA, low pH and approximately 1:1 molar association between the two moieties, the stability offered by EDTA can be explained by the schematic presented in figure 2.9. The schematic can be further confirmed by results presented in section 2.3.4; investigating the influence of addition of cyclodextrins to further improve the taste and stability of the formulation.

2.3.3.2. Influence of EDTA and glycerol on the stability of captopril in solution

Glycerol has a chemical formula of $C_3H_8O_3$ and is widely used in the pharmaceutical industry for various applications depending on the type of formulations. In topical formulations, it is mainly used for its humectant and emollient properties, in creams and emulsions it is utilised for its solvent and co-solvent properties. In oral solutions glycerol is used primarily for its solvent, sweetening (0.6 times as sweet as sucrose) and viscosity-increasing and antimicrobial preservative properties (Rowe *et al*, 2006). As an alcohol, the preservative efficacy of glycerol increases with increasing concentration and would also have the added advantage of improving the taste of the formulation due to its sweetening properties (Scheler *et al*, 2010).

EDTA and glycerol were used in the formulation strategy to overcome two barriers for captopril: the first was stabilisation of captopril in solution, and the second was to preserve the drug from microbial activity with the added advantage of sweetening characteristics of glycerol.

The first stage of formulation with glycerol was to establish a concentration – viscosity profile to determine a suitable concentration that would not affect pourability significantly but at the same time would provide sufficient preservative efficacy. This was done by carrying out viscosity measurements of a range of concentrations of glycerol in distilled water. The results show that by increasing the concentration of glycerol from 10 to 30 % (w/v), the viscosity of the solution increased gradually (Figure 2.11). However further increase of glycerol concentration to 40 % (w/v) resulted in a significant increase in the viscosity of the solution to 18.04 ± 0.19 mPa.s. Above 50 % (w/v) the viscosity of the medium was too high to obtain any reading.

Further investigations were carried out using 30 % (w/v) glycerol. A six month stability profile of a 1 mg.mL⁻¹ formulation (captopril with 0.1 % (w/v) EDTA and 30 % (w/v) glycerol) stored under 5 °C, 25 °C (40 % humidity) and 40 °C (75 % humidity) conditions is presented in figure 2.12A. The results revealed that captopril was stable for 3 months at 5, 25, and 40 °C, with recovery values of 103.52 ± 0.65, 104.26 ± 0.15 and 96.19 ± 0.79 % respectively. After 6 months storage, formulations stored under 25 and 40 °C remained stable and above the 95 % acceptance limits, however a significant decrease in captopril retention was observed at 5 °C (92.42 ± 0.74 %). The pH of the formulation remained stable at pH 3.2-3.4 after 6 month's storage (Figure 2.12B).

The instability of the formulation at 5 °C can be explained by the amount of dissolved oxygen present in the enclosed container and its ability to initiate the oxygen facilitated first-order free radical dimerisation reaction of captopril. The law of oxygen dissociation involves the movement of oxygen content in the air dissolving across the air-water interface and into the medium. This is temperature dependant, with a reduction in temperature increasing the rate of oxygen movement across the air-water interface and a rise in temperature increasing medium resistance to the movement of oxygen across the air-water interface (Ibanez *et al*, 2007). In order to minimise the oxygen content within the storage containers, nitrogen-head capping was introduce (data not shown). However, the results indicated no significant

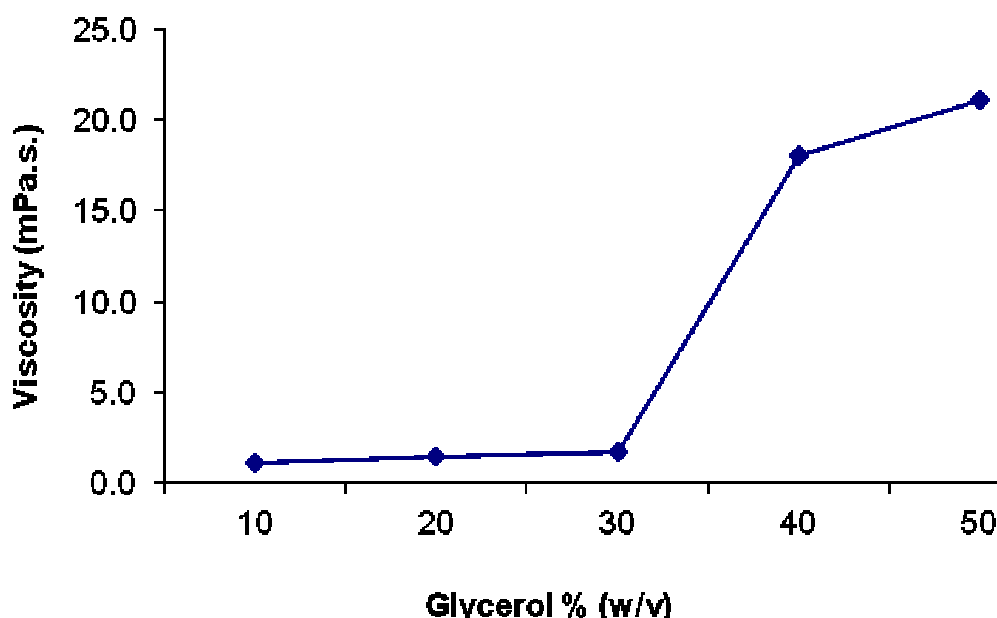


Figure 2.11. Viscosity of glycerol in distilled water with increasing concentrations of glycerol. Various concentrations of glycerol were transferred into glass capillary and viscosity was measure at an angle tilt of 30 ° at 25 °C. At glycerol concentrations above 30 % (w/v), the viscosity of the solution increased dramatically. (n=3)

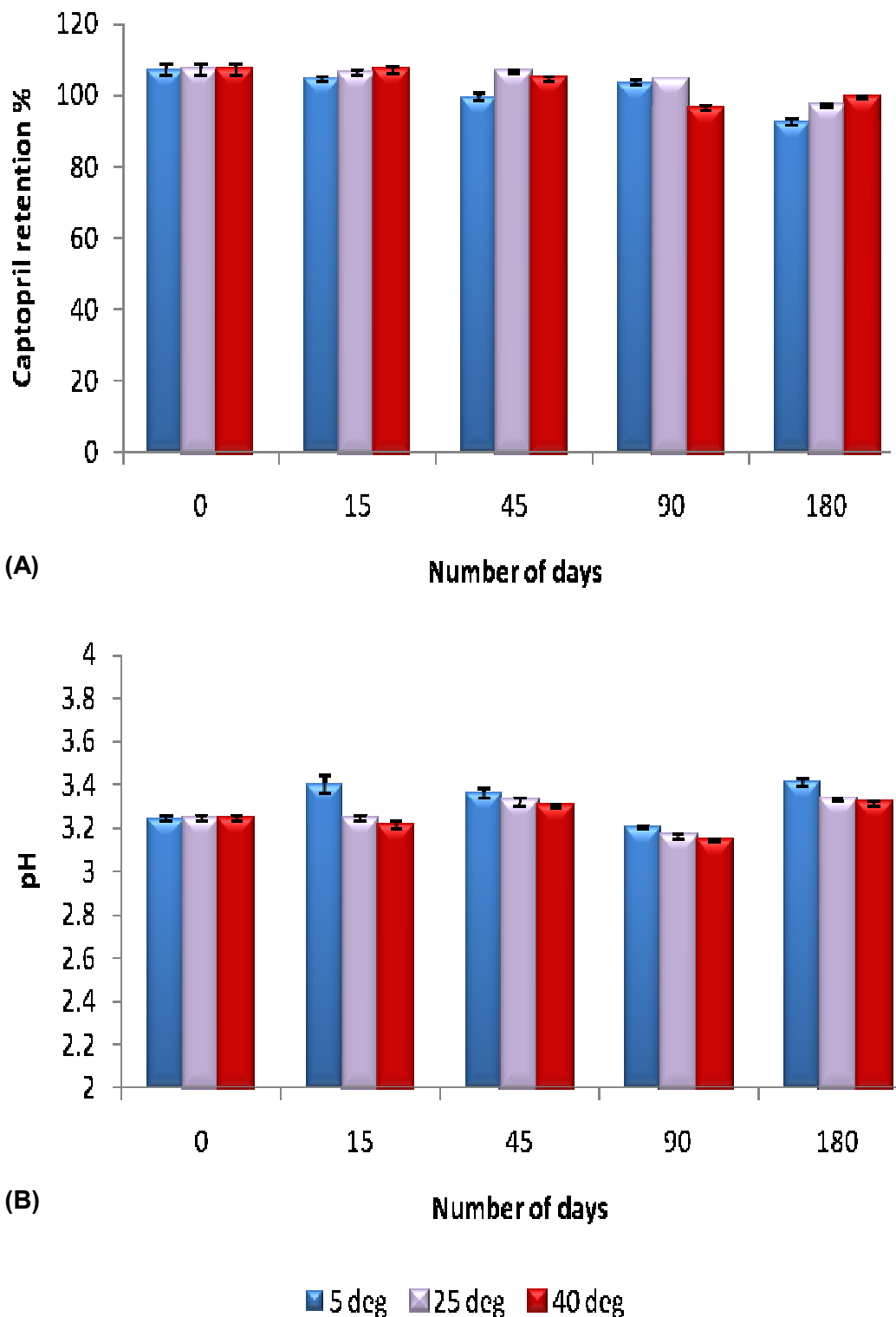


Figure 2.12. Six month stability profile of captopril with 30 % (w/v) glycerol (1 mg.mL^{-1}) stored under 5 °C, 25 °C (40 % humidity) and 40 °C (75 % humidity) conditions. **(A)** Captopril was found to be stable for 6 months at 25 and 40 °C; however formulations stored at 5 °C displayed a decrease in captopril retention ($92.42 \pm 0.74\%$). **(B)** Formulation was observed to be stable over the 6 month period (pH3.2-3.4). (n=3)



Figure 2.13. Schematic representation of the reaction mechanism of glycerol with captopril, forming the degradation product captopril disulphide. The hydroxyl groups of glycerol undergo a nucleophilic attack on the thiol group of captopril, initiating captopril dimerisation (Sam and Ho, 1998).

difference in captopril retention when compared to formulations stored in the absence of nitrogen-head capping.

The instability of captopril upon inclusion of glycerol within the formulation demonstrates that the presence of EDTA was insufficient as a chelating agent under 5 °C conditions for an extended period of time. Previous research by Sam and Ho (1998) has shown that the presence of linear sugar molecules destabilises captopril via a sugar-catalysed initiation of the degradation mechanism. The degradation mechanism involves a nucleophilic attack of the hydroxyl groups of glycerol on the thiol group of captopril which results in the formation of RS⁻ and subsequent dimerisation of captopril to captopril disulphide (Figure 2.13). Glycerol destabilises captopril in the presence of EDTA, indicating captopril has greater affinity to sugar molecules than to EDTA (Kristensen *et al*, 2008).

2.3.3.3. Influence of addition of sodium metabisulphite on captopril stability in solution

Sodium metabisulphite, has a chemical formula of Na₂S₂O₅ and exhibits dual functionality as an antimicrobial preservative and an antioxidant and is used at concentrations from 0.01 to 1.0 % (w/v) in oral pharmaceutical dosage forms.

Formulations comprising of 0.1 % (w/v) of sodium metabisulphite and captopril were prepared in water and assessed for chemical stability of the drug. The choice of sodium metabisulphite was based on previous literature which showed that the preservative efficacy of sodium metabisulphite rises with increase in acidity of the formulation (Rowe *et al*, 2006; Winfield *et al*, 2009).

The results showed that the formulations did not exhibit any chemical degradation when analysed on the day of preparation where nearly 100 % of captopril was recovered (Figure 2.14). However upon storage of the formulations at 25 °C and 40 °C for a period of 30 days,

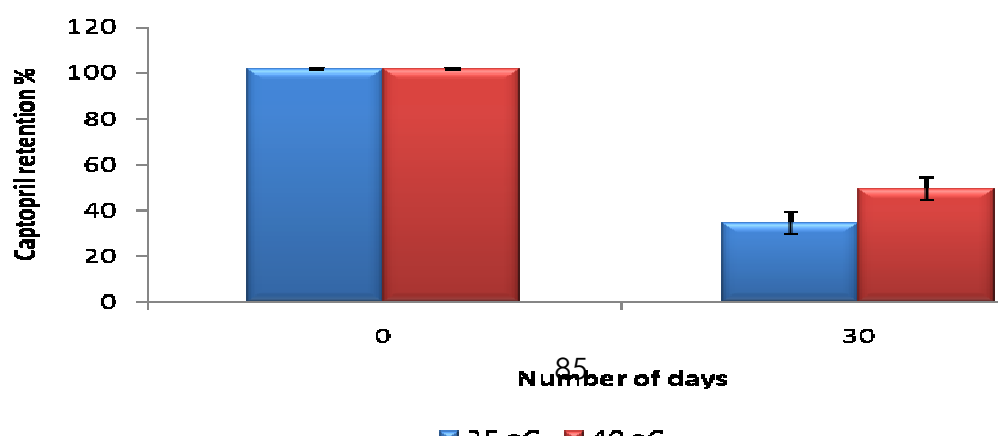


Figure 2.14. Stability of captopril in 0.1 % (w/v) sodium metabisulphite (1 mg.mL⁻¹) stored under 25 °C (40 % humidity) and 40 °C (75 % humidity) conditions. After 30 days, captopril retention was reduced to 34.34 + 2.07 and 36.82 + 2.14 % under 25 and 40 °C conditions respectively. (n=3)

the concentration of captopril was reduced to $34.34 \pm 2.07\%$ and $36.82 \pm 2.14\%$ respectively. The formulations had a pungent sulphide like odour with no changes in the colour or appearance (clear solution). The instability of captopril upon inclusion of sodium metabisulphite can potentially be attributed to oxygen facilitated first order free radical reaction. In water sodium meta-bisulphite is converted into its ionic state (Figure 2.15) which results in the formation of ionised oxygen atoms of sodium meta-bisulphite which possibly results in accelerating the process of dimerisation of captopril in solution (Figure 2.16). (Kristensen *et al*, 2008; Abu-Shandi and Redel, 2009). The oxidative dimerisation of captopril to a disulphide is a significant pharmaceutical obstacle to overcome.

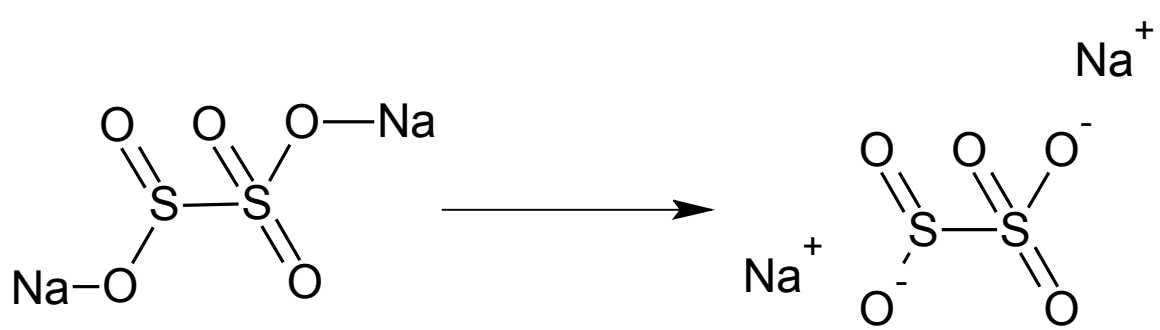


Figure 2.15. Schematic of sodium metabisulphite converted into its respective ions when placed in water.

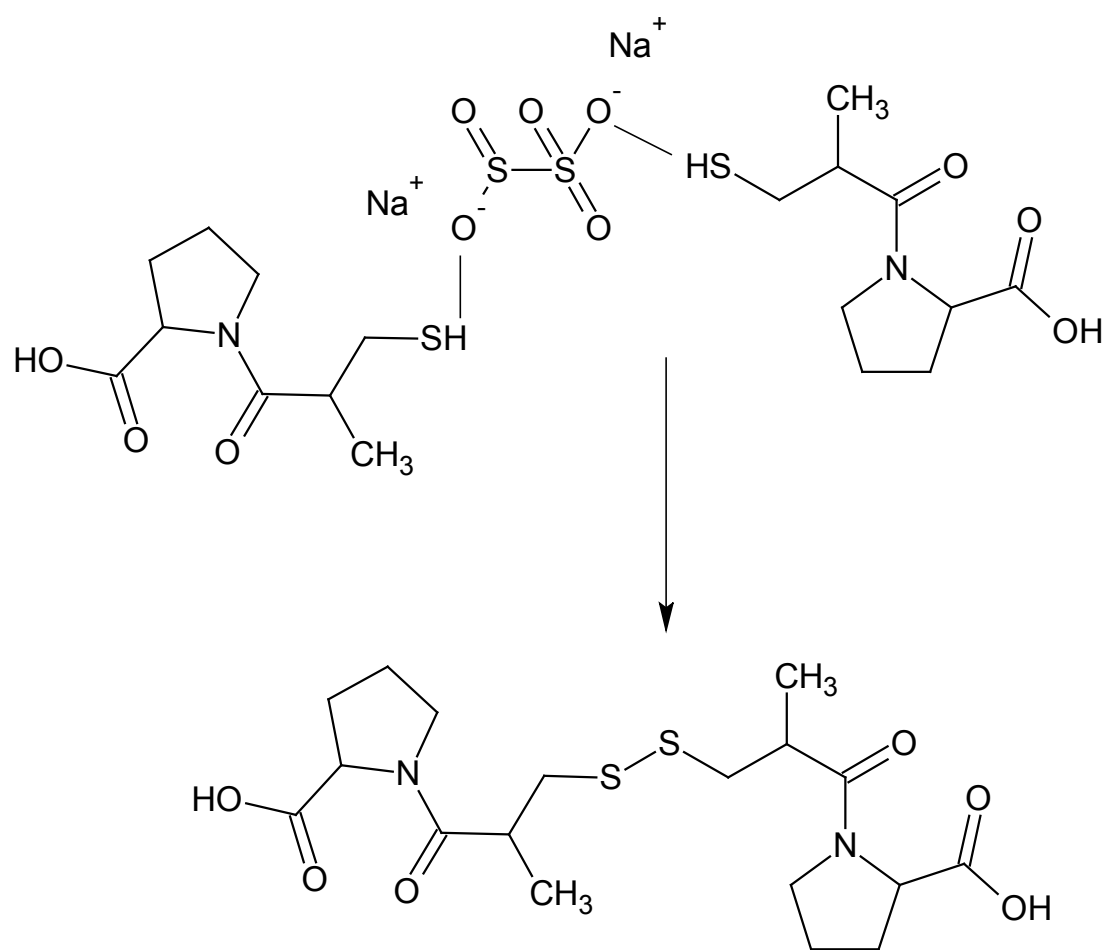


Figure 2.16. Schematic for the degradation pathway of captopril in the presence of sodium metabisulphite. The thiol group of captopril donates its hydrogen atom to the ionised $-\text{S}-\text{O}^-$ groups of sodium metabisulphite, initiating the dimerisation reaction.

2.3.4. Approaches to enhance the organoleptic properties of the formulation

2.3.4.1. Influence of HP- β -CD on captopril in solution

Cyclodextrins are effective drug delivery vehicles which are made up of sugar molecules bonded together in a ring. They are composed of five or more D-glucopyranoside units linked by 1-4 glycosidic bonds. The choice of cyclodextrins for inclusion into an oral liquid formulation is based on their binding constant and stability profile in the presence of a guest molecule. Extensive research has been carried out characterising and assessing safety profiles of cyclodextrins (Shabir and Mohammed, 2010). Cyclodextrins are widely used as taste masking as well as solubility enhancing agents.

Modified β -CD have the greatest potential in oral liquid formulation due to their larger cavity size, increased solubilising effects and reduced toxicity on the GI membrane. The formulation strategy for captopril included investigation of inclusion of HP- β -CD to prevent dimerisation with the eventual aim of reducing pungent like odour and improving the taste.

Preliminary investigations were focussed on determining the molar complexation of captopril using conductometry. Every ionisable analyte displays an electrical current in solution and it is the ability of maintaining this current in the presence of increasing concentrations of excipient which forms the basis of measurements for conductance. The point at which the slopes converge is an indication of the molar binding ratio in solution. The study involved measuring the conductivity of 1 M captopril in water with increasing increments of cyclodextrin. Using the calculations as described in section 2.2.5. (Cabaleiro-Laga *et al*, 2006), the mean molar conductivity was plotted (Table 2.2. and Figure 2.17). From the results a 1:1 molar ratio of captopril with HP- β -CD was determined, which was consistent with H¹-NMR analysis of the molecular interaction of their respective proton groups (Figures 2.18-2.20). Study of the physical mixture of captopril and HP- β -CD (Figure 2.20) revealed a reduced number of protons indicating an interaction of a 1:1 molar ratio.

Table 2.2. Conductometry calculations for captopril with increasing molar concentrations of HP- β -CD.

HP β CD Moles	Molar conductivity Captopril	Molar conductivity complex			Association constant x concentration of non-complexed CD KCCD,F	1 + KCDCD,F	Molar Conductivity					
		M	$\Delta\Lambda_{C,F}$	$\Delta\Lambda_{CD-C}$			Λ					
			1	2	3		1	2	3	Mean	SD	
0.00	41261		0	0	0	0	1	41261	41261	41261	41261	0.00
0.25	41261		3948	3944	3956	0.4475	1.4475	29725	29724	29728	29726	1.89
0.50	41261		1946	1944	1950	0.895	1.895	22693	22692	22695	22693	1.44
0.75	41261		1228	1227	1229	1.3425	2.3425	18318	18317	18319	18318	0.76
1.00	41261		909	911	910	1.79	2.79	15372	15373	15373	15373	0.64
1.25	41261		705	706	704	2.2375	3.2375	13232	13233	13231	13232	0.84
1.50	41261		573	572	575	2.685	3.685	11615	11614	11616	11615	0.97
1.75	41261		479	478	481	3.1325	4.1325	10347	10347	10349	10348	1.09
2.00	41261		408	408	409	3.58	4.58	9328	9327	9329	9328	0.60
2.50	41261		310	310	312	4.475	5.475	7790	7790	7791	7790	0.68
3.00	41261		246	245	247	5.37	6.37	6685	6684	6685	6685	0.74
3.50	41261		202	201	202	6.265	7.265	5853	5853	5854	5853	0.49
4.00	41261		168	168	169	7.16	8.16	5204	5204	5205	5204	0.44

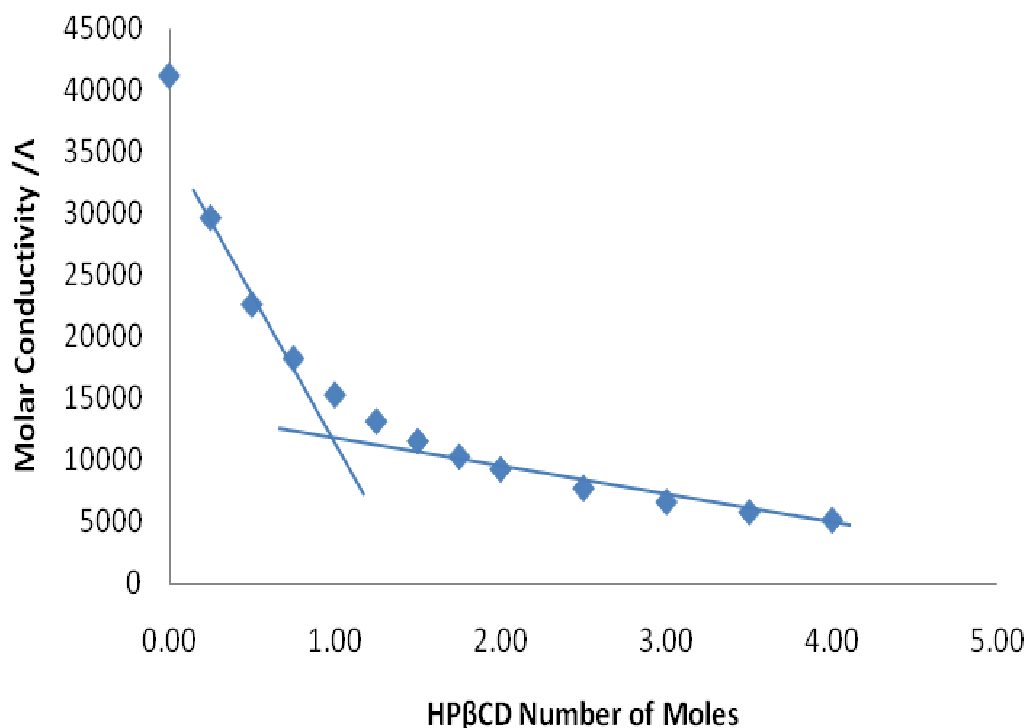


Figure 2.17. Investigations of the molar conductivities of captopril on the HP- β -CD molar concentrations. The point at which the slope changes is indicative of the binding and bulking of the molecules. Captopril and HP- β -CD achieved a 1:1 molar ratio. (n=3)

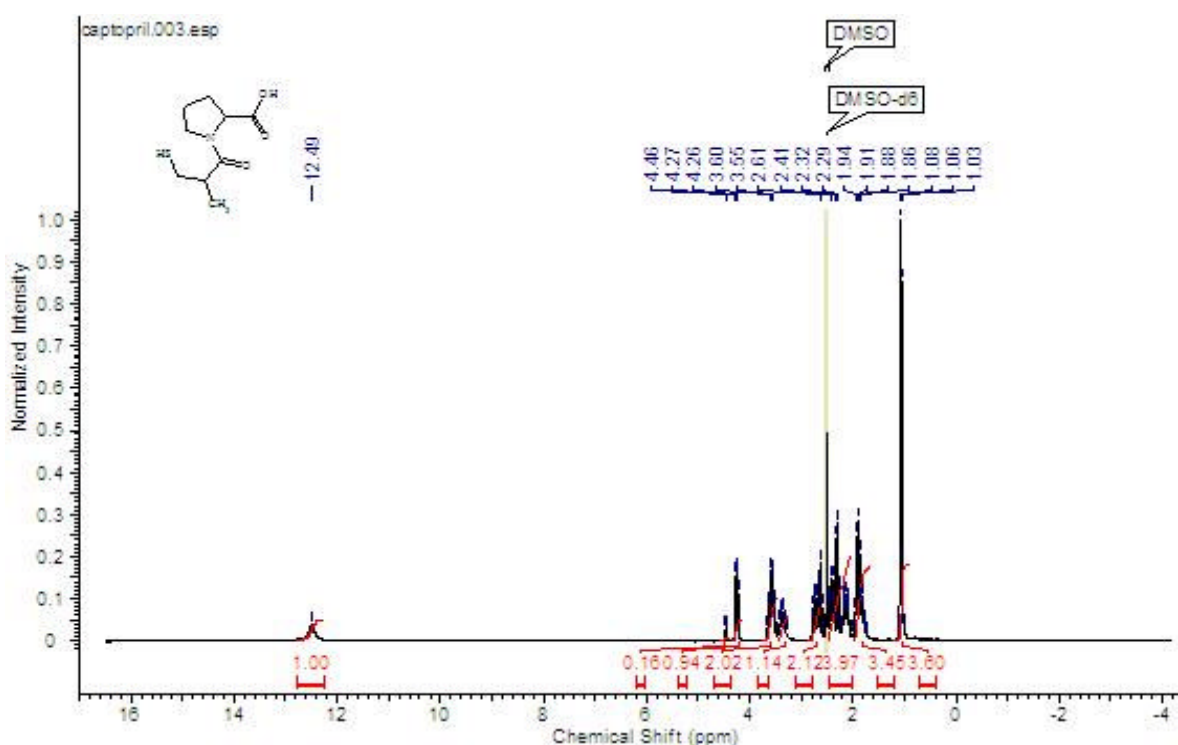


Figure 2.18. ^1H -NMR spectrum of captopril in DMSO-D₆, displaying 14 Hydrogen atoms.

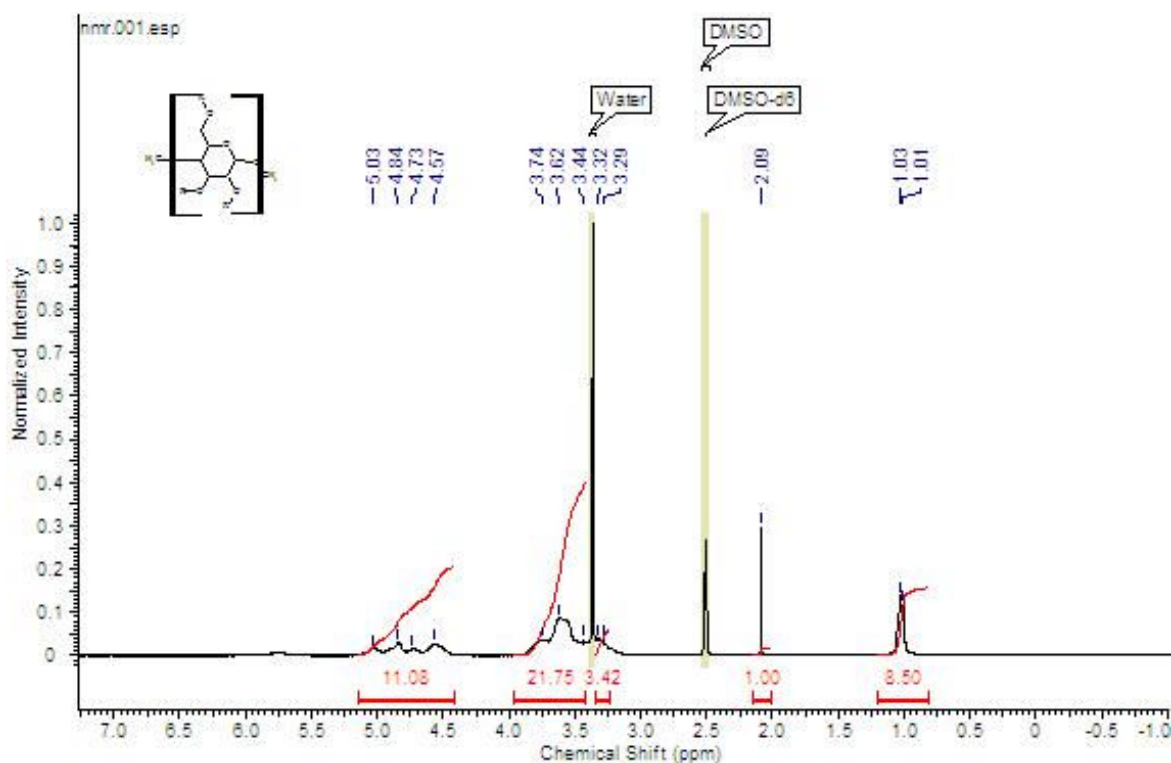


Figure 2.19. ^1H -NMR spectrum of HP- β -CD in DMSO- D_6 , displaying 43 Hydrogen atoms.

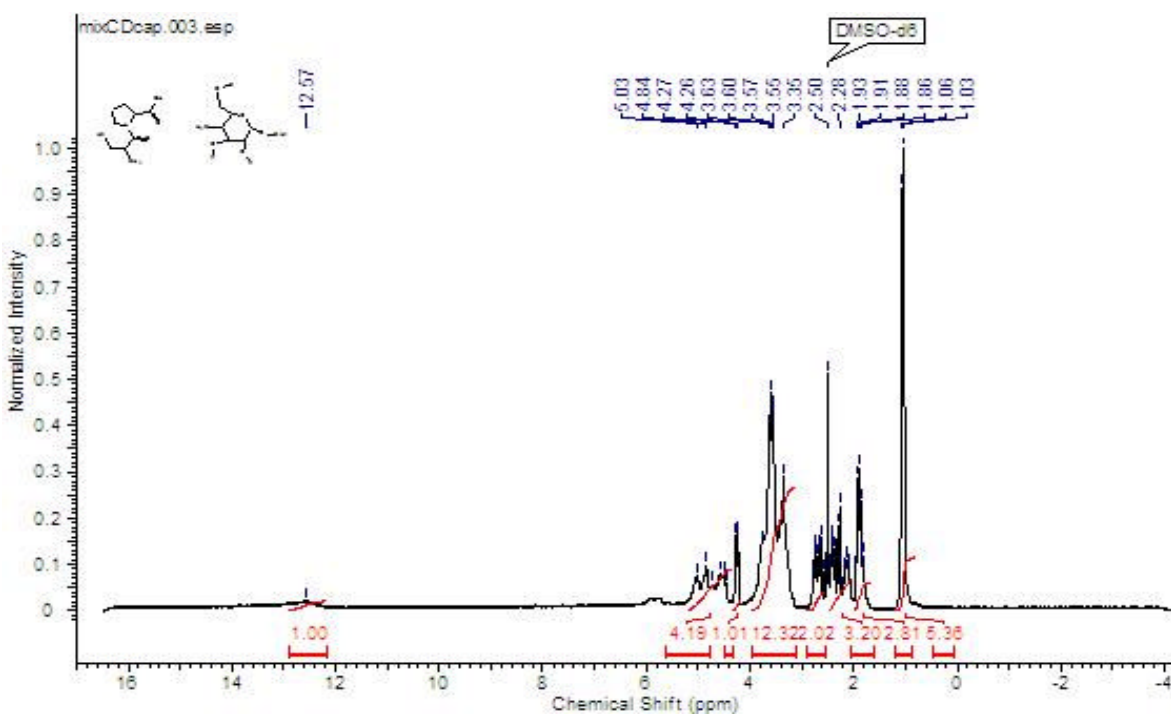


Figure 2.20. ^1H -NMR spectrum of captopril and HP- β -CD in DMSO- D_6 , displaying 31 Hydrogen atoms

Figure 2.21 show the stability profile of captopril (1 mg.mL^{-1}) with HP- β -CD (1:1 molar ratio), in the presence of 0.1 % (w/v) EDTA. After 12 months storage at 5 °C, 25 °C (40 % humidity) and 40 °C (75 % humidity), the formulation had greater than 95 % captopril recovery. In a parallel study, a 1 mg.mL^{-1} captopril-HP- β -CD (1:1 molar ratio) formulation in the absence of EDTA was prepared and stored at 25 and 40 °C conditions. The formulation was found to display a high degree of degradation after just 30 days with only 56.33 + 0.96 % and 52.10 + 0.27 % of captopril recovery when stored at 25 and 40 °C respectively (data not shown). These results can be explained by the non-convalent interaction of the cyclodextrin with its guest molecule (captopril), which possibly enables the cyclodextrin to continually associate and dissociate from its guest resulting in a dynamic ‘release-attach-release’ mechanism (Stella et al, 1999). In the absence of EDTA, captopril undergoes dimerisation when it dissociates from the cyclodextrin. However in the presence of EDTA the thiol group is protected from dimerisation as the captopril molecule associates and dissociates from the cyclodextrin, thereby maintaining 100 % captopril retention for a prolonged period.

In order to explain these findings, the interaction of the excipients was further investigated using analytical techniques such as FTIR and DSC.

2.3.4.2. Interaction of HP- β -CD with captopril and its influencing properties

FTIR and hyper-DSC (were used to understand the physicochemical interactions between EDTA, captopril and HP- β -CD).

To investigate the structural arrangement of EDTA-captopril-HP- β -CD complex, a 1 mg.mL^{-1} formulation was freeze-dried and analysed using FTIR. An infra-red spectrum produces molecular absorption and transmission of each sample through a unique molecular fingerprint. These absorption peaks correspond to the vibration frequencies exhibited by each of the bonds present in the compound. This process of physicochemical analysis has been widely used in the chemical industry to; identify unknown materials, determine the quality and consistency of a sample and the components in the mixture.

Table 2.3 and figures 2.22 highlight the specific band vibrations for captopril, EDTA, HP- β -CD. The fingerprint of captopril displayed absorption peaks for; the thiol group (-S-H) at 729 cm^{-1} , aromatic amine (-C-N) at 1346 cm^{-1} , aliphatic amine (-C-N) at 1123 cm^{-1} , ester at

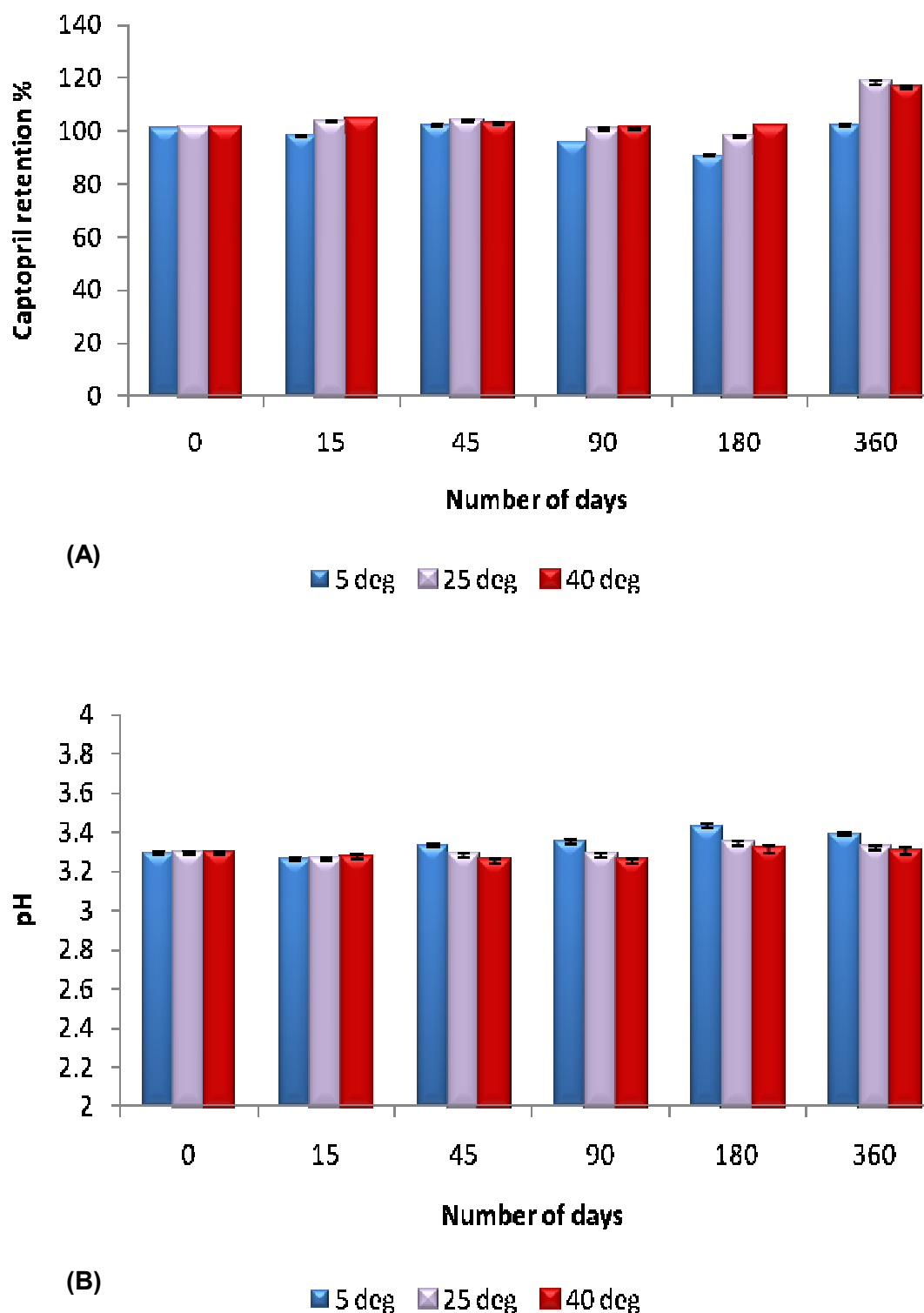


Figure 2.21. 12 months stability profile of captopril (1 mg.mL^{-1}) with 0.1 % EDTA and HP- β -CD stored under 5 °C, 25 °C (40 % humidity) and 40 °C (75 % humidity) conditions. (A) captopril was found to have >95 % stability. (B) Formulation was observed to be stable over the 12 month period (pH 3.2-3.4). (n=3)

1136 cm⁻¹, and the carboxylic group (-O-H at, 2980 cm⁻¹, -C=O at 1747 cm⁻¹, and -C-O at 1191 cm⁻¹). Interestingly it was found that the fingerprint for mixture comprising of EDTA-captopril-HP-β-CD did not reveal the absorption bands for carboxylic acid group and aromatic amine. The remainder of captopril's functional groups displayed a shift in transmittance, which was attributed to the re-arrangement of bond angles to compensate for partial insertion within the cyclodextrin cavity. The structure of captopril is composed of two parts: a halide and ester chain, and an aromatic side chain with a carboxylic acid side group (Figure 2.2). The FTIR results indicate partial insertion of captopril's aromatic side chain with the carboxylic acid side group into the cyclodextrins cavity via electrostatic interaction (Figure 2.23).

Table 2.3. Frequency of bond vibrations attributing to the captopril and HP-β-CD complex formulation.

Peak	Transmittance	Bond	Functional group	Donor
1	3274	O-H	Alcohol	HP-β-CD
2	2935	C-H	Alkane	HP-β-CD
3	1462	C-C	Aromatic	Mannitol
4	1351	C-H rock	Alkanes	Captopril
5	1261	C-N stretch	Aliphatic amines	EDTA
6	1087	C-O	Carboxylic acid	HP-β-CD
7	1022	C-N stretch	Aliphatic amine	Captopril
8	931	=C-H	Alkene	Mannitol
9	889	C-H	Aromatic	HP-β-CD
10	715	S-H	Halide	Captopril
11	624	C-S	Alkyl halide	Captopril

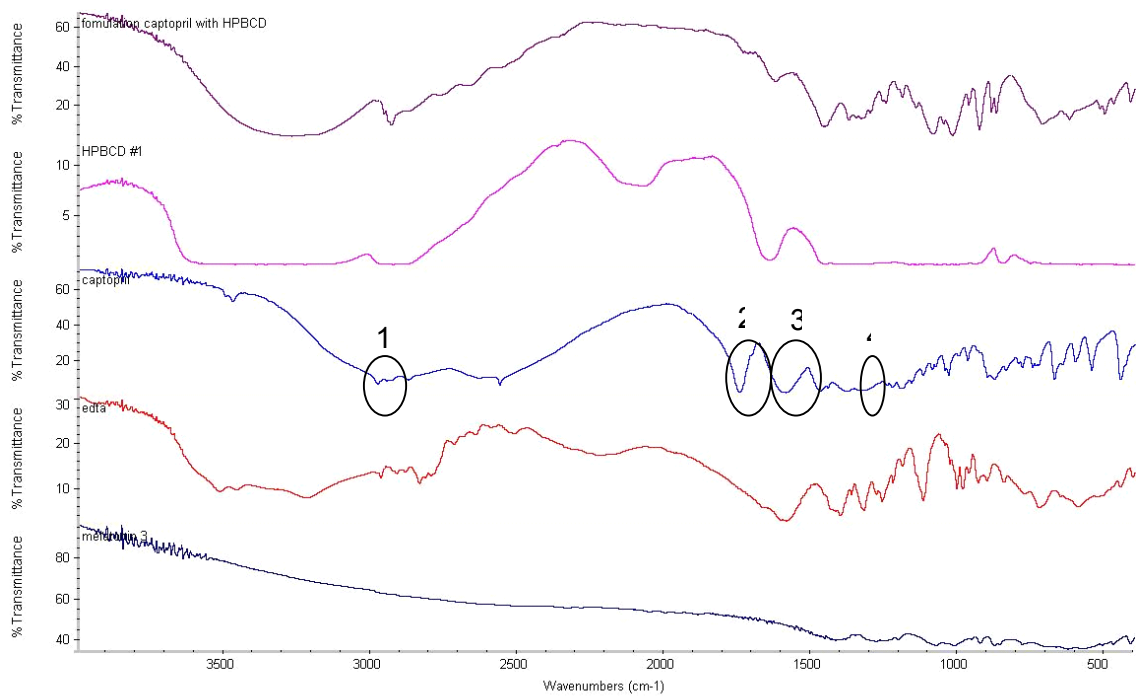


Figure 2.22. FTIR fingerprint absorption spectrum of captopril formulation with HP- β -CD and its excipients. In the captopril spectrum four points have been highlighted which are absent in the formulation spectrum; (1) O-H carboxylic acid group, (2) C=O carboxylic acid group, (3) C-C aromatic group, and (4) C-N aromatic amine.

DSC can be used to analyse the thermal properties of a substance. An increase in scan rate

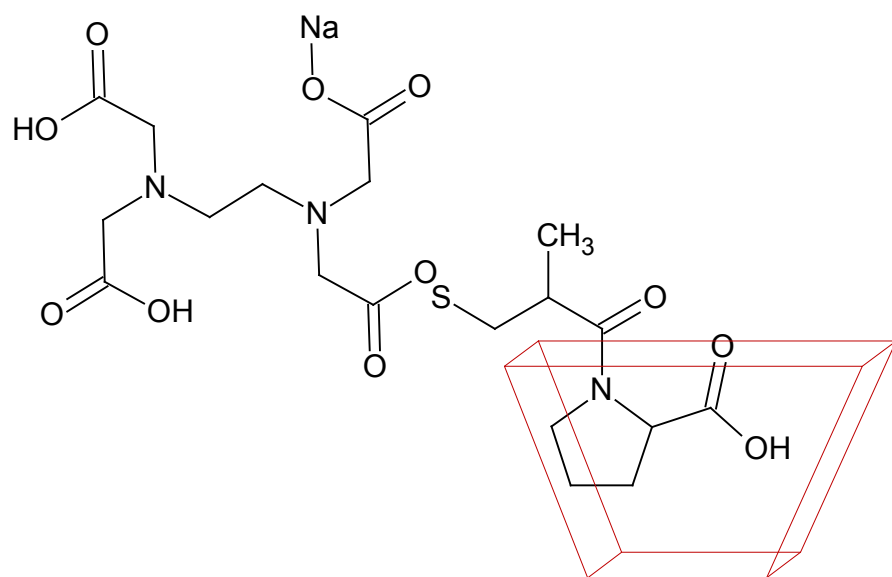


Figure 2.23. Schematic representation of the molecular arrangement of EDTA and HP- β -CD with captopril, predicted using FTIR.

to $200\text{ }^{\circ}\text{C}.\text{min}^{-1}$ allows for increased sensitivity of the thermal reactions/transitions. Thermal analysis technique can be used to further substantiate the interactions of captopril with HP- β -CD. The first stage of analysis was to identify the melting peaks for the individual components and to compare these against the thermal transitions obtained from the formulated samples. Captopril and EDTA have onset melting peaks of $103 \pm 0.25\text{ }^{\circ}\text{C}$ and $98.83 \pm 0.54\text{ }^{\circ}\text{C}$ respectively (Figure 2.24A). Interestingly, when captopril-EDTA complex was formed, the melting transition shifted to the left ($26.90 \pm 0.74\text{ }^{\circ}\text{C}$) (Figure 2.24B), resulting in less energy being required to break the forces of attraction between the constituents and causing a more disordered arrangement of constituents (Brown, 2001). Figure 2.25 showed that inclusion of the cyclodextrin significantly strengthened the thermal properties of the EDTA-captopril-HP- β -CD complex, as the thermal event of EDTA-captopril observed at $26.90 \pm 0.74\text{ }^{\circ}\text{C}$ was now absent (Figure 2.25B). Similar observations were made with captopril and various cyclodextrins by Ikeda and co-workers (2000). These finding further strengthen the structural arrangement of the EDTA-captopril-HP- β -CD complex displayed in figure 2.23.

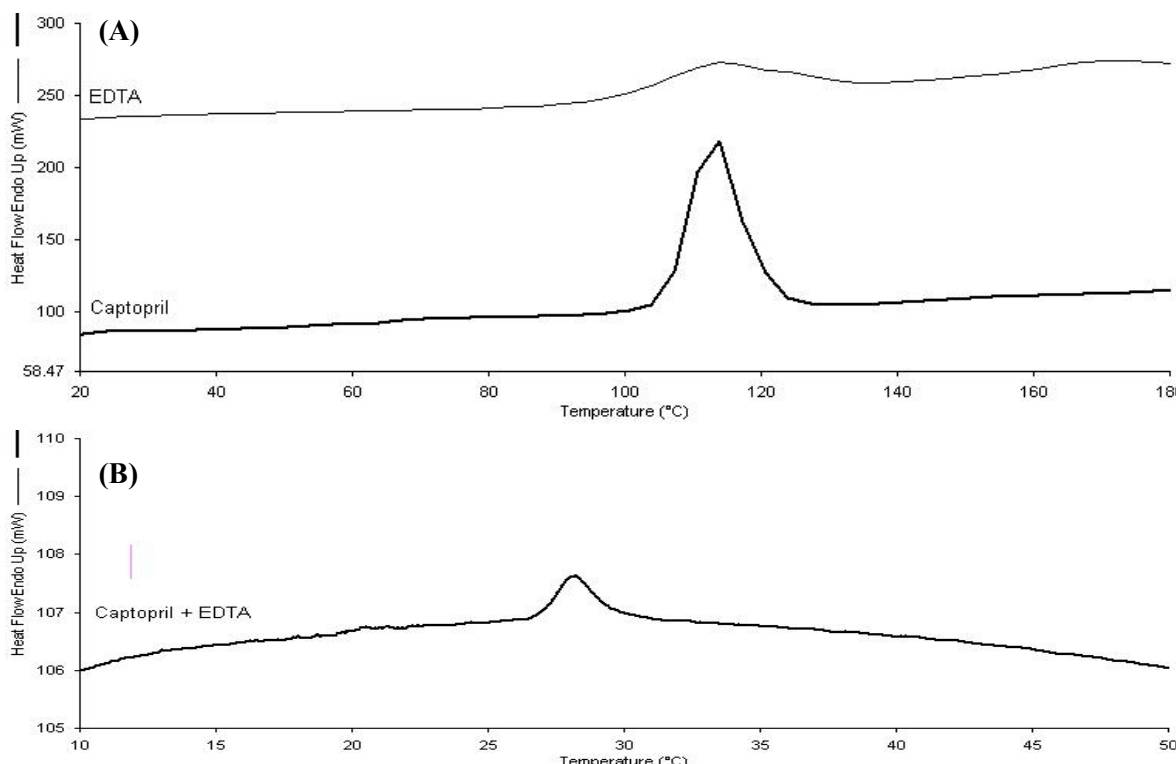


Figure 2.24. DSC thermogram of a 5 mg.mL^{-1} captopril formulation with 0.1 \% (w/v) EDTA. **(A)** Captopril and EDTA each displaying melting temperatures of $103 \pm 0.25\text{ }^{\circ}\text{C}$ and $98.83 \pm 0.54\text{ }^{\circ}\text{C}$ respectively, and **(B)** a 5 mg.mL^{-1} captopril formulation composed of 0.1 \% EDTA with a $26.90 \pm 0.74\text{ }^{\circ}\text{C}$ melting temperature.

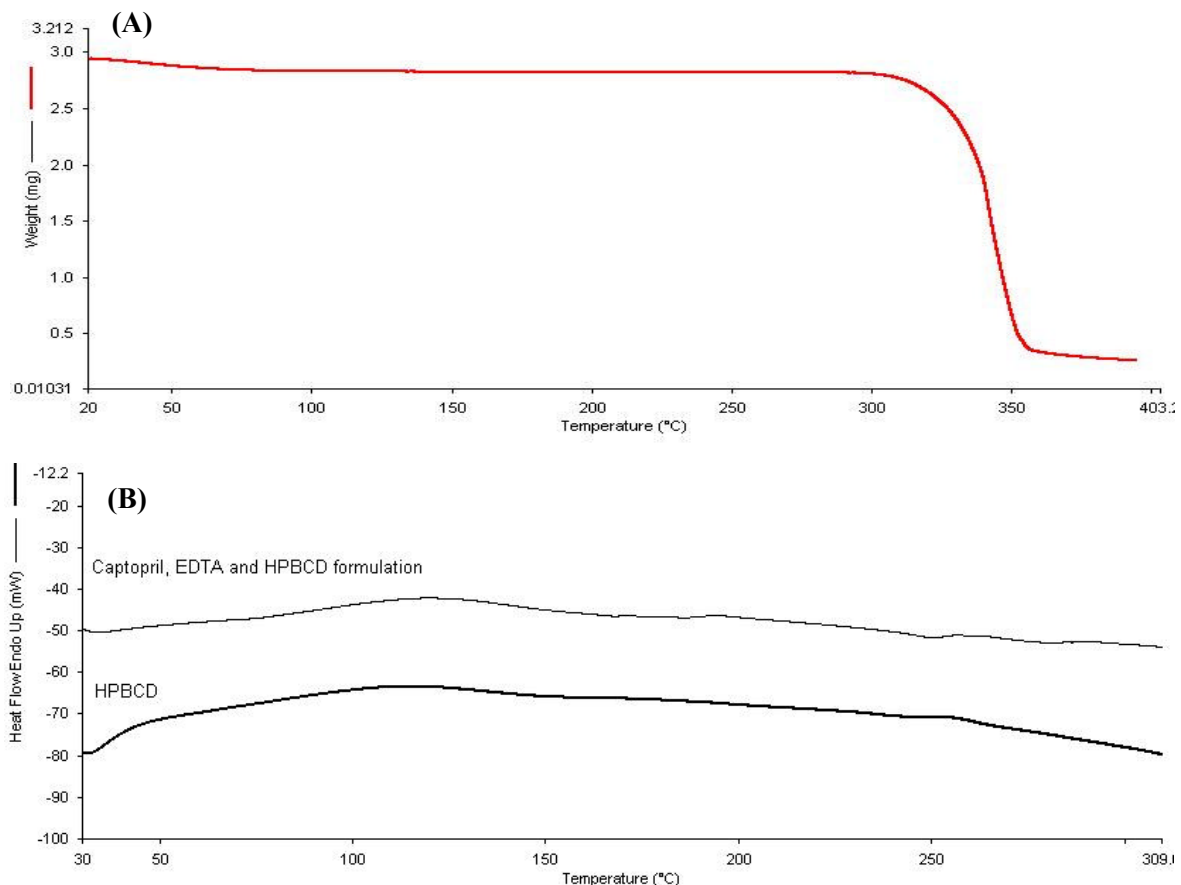


Figure 2.25. TGA and DSC Thermograms of a 5 mg.mL^{-1} captopril formulation composed of 0.1% (w/v) EDTA and HP- β -CD. (A) The TGA thermogram of HP- β -CD shows degradation occurring above 300°C . (B) DSC thermogram of EDTA-captopril-HP- β -CD complex shows no endothermic reaction occurring.

2.3.5. Influence of concentration of captopril and its affect on shelf life stability

Current captopril formulations on the market are available in dose sizes ranging from 12.5 to 50 mg. In order to minimise the frequency of dosing, the concentration of the EDTA-captopril and EDTA-captopril-HP- β -CD formulations prepared in this study were increased from 1 mg.mL^{-1} to 5 mg.mL^{-1} .

The stability of 5 mg.mL^{-1} EDTA-captopril formulations after 12 months storage at 5°C , 25°C (40 % humidity) and 40°C (75 % humidity) is presented in figure 2.26. The results revealed that formulations stored at 40°C had 100 % captopril retention after 6 months. In addition, samples stored for 12 months at 5°C and 25°C exhibited $94.76 \pm 9.03\%$ and $102.81 \pm 6.48\%$ captopril recovery respectively. These results were in accordance with work

carried out by Florey (1982), who suggested that by increasing the captopril concentration ultimately resulted in a reduction in its rate of degradation.

In a comparative study, figure 2.27 shows the stability of 5 mg.mL^{-1} EDTA-captopril-HP- β -CD formulation after 12 months storage at 5°C , 25°C (40 % humidity) and 40°C (75 % humidity) conditions. The results showed that the formulation was stable after 6 months storage at 40°C ($96.78 \pm 2.49\%$) and 25°C ($95.94 \pm 10.04\%$).

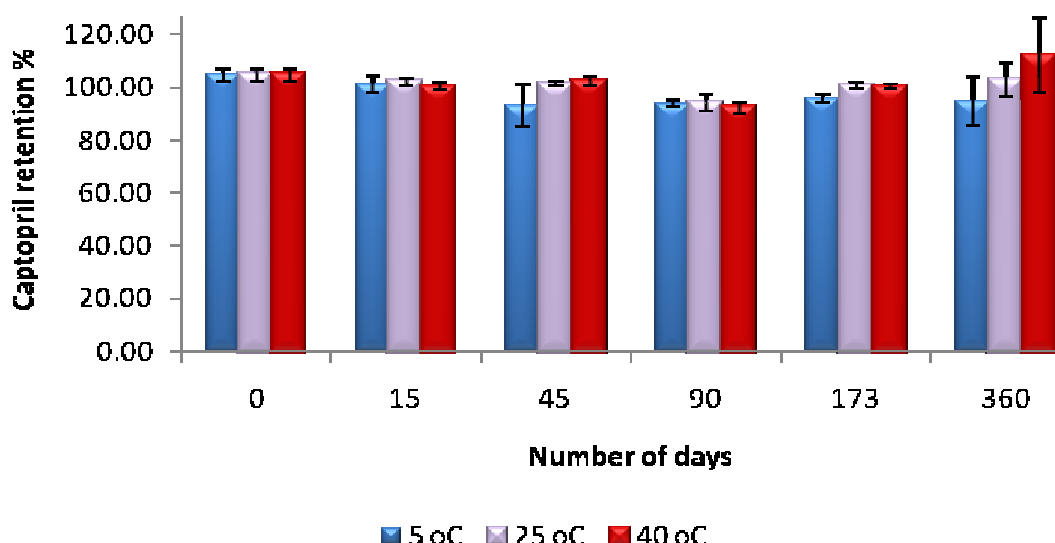


Figure 2.26. 12 month stability profile of captopril with 0.1 % (w/v) EDTA (5 mg.mL^{-1}) stored under 5°C , 25°C (40 % humidity), and 40°C (75 % humidity) conditions. The formulation achieved $> 95\%$ stability after 1 year storage. (n=3)

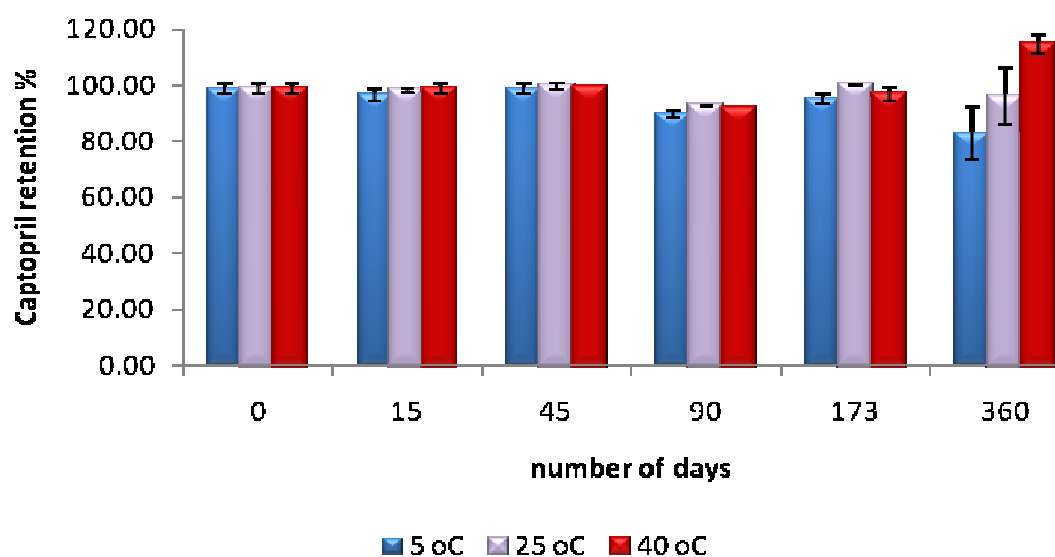


Figure 2.27. 12 month stability profile of captopril with 0.1 % (w/v) EDTA and HP- β -CD (5 mg.mL^{-1}) stored under 5°C , 25°C (40 % humidity), and 40°C (75 % humidity) conditions. Within 6 months storage at 40°C , the captopril formulation achieved $> 95\%$ retention. After 12 months storage at 5°C and 25°C captopril retention was analysed to be $82.99 \pm 9.22\%$ and $95.44 \pm 10.04\%$ respectively. (n=3)

2.4. Conclusion

The stability of captopril in solution was highly dependent upon the presence of EDTA as a chelating agent thus preventing dimerisation of captopril. Formulations consisting of 0.1 % (w/v) EDTA and captopril (1 mg.mL^{-1} and 5 mg.mL^{-1}) were stable for up to 1 year.

However EDTA was unable to prevent captopril dimerisation when in the presence of other excipients, such as sodium metabisulphite and 30 % (w/v) glycerol. Sodium meta-bisulphite was able to accelerate captopril degradation due to its ionic state when dissolved in water, whereas glycerol was able to initiate a sugar-catalysed degradation reaction of captopril.

HP- β -CD proved to be an excellent compatible stabiliser in the presence of EDTA, as well as being an odour neutraliser. 1 mg.mL^{-1} and 5 mg.mL^{-1} dosage forms of the EDTA-captopril-HP- β -CD complex were stable for 12 months with no change in the organoleptic properties. Further analysis into the chemical arrangement of the moieties showed EDTA to be bound to captopril at its thiol group, with the aromatic side chain and a carboxylic acid side group being bound to the cyclodextrin cavity, forming a rigid structure. This rigidity resulted in steric hindrance and thus a reduction in the sulphuric-like odour normally associated with captopril.

CHAPTER 3

Solubilisation and physicochemical analysis of
gliclazide

CHAPTER 3

Solubilisation and physicochemical analysis of gliclazide

3.1. Introduction

3.1.1. Gliclazide structure and mechanism of action

Sulphonylurea derivatives are a class of anti-diabetic drugs used in the management of Type 2 diabetes mellitus which include second generation drugs such as gliclazide and glipizide. Gliclazide is composed of a sulphonylurea backbone, consisting of a central S-phenylsulfonylurea structure with two unique side chain groups (Figure 3.1). However, it is the electronegative oxygen of the sulphonyl group in the structural backbone that dictates the acidity of the drug molecule resulting in a pKa of 5.8. The electronegative oxygen of the sulphonyl group and the acidic carbonyl groups have a tendency to withdraw electrons thereby creating a positive carbon atom. This results in the carbon atom attracting electrons from the nearby nitrogen groups and thus causing the hydrogen to be held less firmly (Alkhamis *et al*, 2003).

The mechanism by which gliclazide acts is by selectively binding to sulfonylurea receptors on the surface of the β -pancreatic cells causing the potassium ion channels to close, thereby

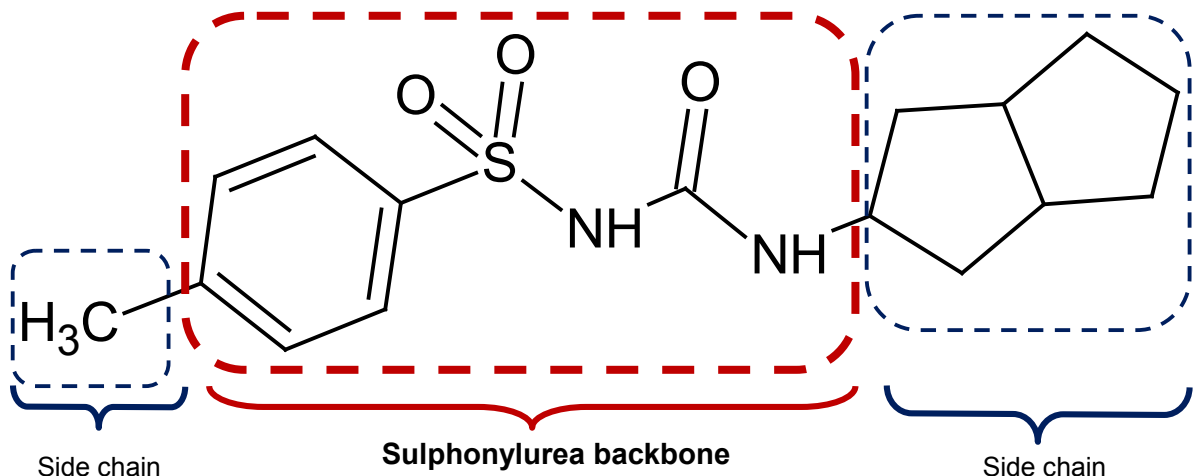


Figure 3.1. Chemical structure of gliclazide. The sulphonylurea backbone is highlighted in red, with the unique side groups of gliclazide highlighted in blue.

decreasing the efflux of potassium from the pancreatic cells which leads to the depolarization

of the cell. This action results in voltage dependent calcium ion channels to open increasing calcium influx. The calcium can then binds to and activates calmodulin, which in turn leads to exocytosis of insulin vesicles resulting in increased secretion of insulin (Campbell *et al*, 1991).

3.1.1. Gliclazide and its therapeutic affects

Gliclazide is a second-generation sulphonylurea oral hypoglycaemic drug with poor water solubility (55 mg.L^{-1}) (Varshosaz *et al*, 2008). This acidic drug has the added complication of low gastric fluid solubility and a lowered dissolution profile causing increasing inter-patient variability on drug bioavailability (Palmer and Brogden, 1993; Arias-Blanco *et al*, 1998).

The therapeutic effects of gliclazide include; the stimulation of insulin secretion by the pancreatic cells in patients diagnosed with non-insulin dependent diabetes mellitus (Davis *et al*, 2000; Hiremath *et al*, 2008), platelet aggregation and increased fibrinolysis (Kumar *et al*, 2011), low incidence of hypoglycaemia and low rate of secondary failure (Biswal *et al*, 2009). These therapeutic effects and good patient tolerability ensures that gliclazide remains one of the most important drug substances for the treatment of diabetes mellitus.

3.1.2. Current dosage forms

Current formulations in the pharmaceutical market include: Diamicron®, Diamicron modified release®, and Diaglyk® tablets. These are prescribed to adults in 40 to 80 mg dosage forms, with a maximum recommended single dose of 180 mg (BNF 2011). In children, ranging from 12 to 18 years, the prescribed dose is 20 mg daily, with a recommended maximum single dose of 160 mg (BNF for children 2011).

3.1.3. Aim

Previous work on the development of gliclazide formulations was focussed on increasing the bioavailability of gliclazide *in vivo* via the delivery of a tablet or soft capsule system (Hong *et al*, 1998; Varshosaz *et al*, 2008), or encapsulation with cyclodextrins (Shewale *et al*, 2008). However an oral liquid solution of gliclazide using simple solubilisation techniques has not yet been carried out.

Therefore the overall aim of the work was to establish a validated calibration protocol for the extraction and quantification of gliclazide using HPLC and to solubilise gliclazide in an oral liquid formulation without compromising the lipophilicity of the drug molecule.

The objectives included:

- Phase solubility studies involving amino acids (L-arginine and L-lysine), pluronic F127 and ethanol as potential solubilising agents for gliclazide
- Preparation and stabilisation of an oral liquid formulation with 8 mg.mL⁻¹ and 16 mg.mL⁻¹ dosages.
- Physicochemical analysis of the chemical interactions involved in the solubilisation of gliclazide using: DSC, FTIR and H¹-NMR.

3.2. Materials and Method

3.2.1. Materials

Acetonitrile (ACN), propan-2-ol and ethanol were purchased from Fisher Scientific (UK). L-arginine, L-lysine, pluronic F127, potassium bromide, monosodium glutamate, xylitol, butyl paraben, propyl paraben, HCl, sodium hydroxide, and sodium acetate were all purchased from Sigma Aldrich (UK). Gliclazide was purchased from Discovery Fine Chemicals (Bournemouth, UK). Deuterated water (D_2O) was purchased from Goss Scientific Instrument Ltd (Cheshire, UK).

3.2.2. Calibration Validation

Calibration was carried out using a dionex HPLC and a C18 Gemini column (150 x 4.6 mm). 15 mg of Gliclazide was dissolved in 15 mL of ACN to obtain a stock concentration of 1 mg.mL^{-1} . Serial dilutions were then carried out to obtain further 7 gliclazide concentrations in ACN (500, 250, 100, 50, 25, 5 and $0.5 \text{ \mu g.mL}^{-1}$). Using a mobile phase consisting of ACN and water (45:55), adjusted to pH 3 with phosphoric acid, 50 μL of each gliclazide concentration was injected in turn into HPLC and analysed at a wavelength of 220 nm and flow rate of 1 mL.min^{-1} . The retention time for gliclazide was 9 minutes (protocol modified from Rouini *et al*, 2003).

3.2.3. Phase solubility

In 10 mL of water set amounts of the solubiliser was added and fully dissolved within solution before excess amounts of gliclazide was added to this solution. After stirring for 20 minutes, 1 mL was taken and analysed on the HPLC in order to quantify the amount of gliclazide dissolved. Each analysis was carried out in triplicate.

3.2.3.1. Phase solubility with pH modification

In 10 mL of water, a set amount of solubiliser was added, to which sodium hydroxide or 0.1 M HCl was added to adjust the pH of the system. Excess amounts of gliclazide was then added and left to stir for 20 minutes, after which 1 mL of sample was extracted and analysed on the HPLC in order to quantify the amount of solubilised gliclazide. The studies were carried out in triplicate.

3.2.4. Oral liquid formulation of gliclazide

All excipients and their relative concentrations used within the formulations are GRAS listed and within the recommended guidelines.

3.2.4.1. *Solubilisation of gliclazide (8 mg.mL⁻¹) with L-arginine (7 mg.mL⁻¹)*

In 10 mL of water, 140 mg of L-arginine was dissolved to which 160 mg gliclazide was then added and magnetically stirred until the drug had fully dissolved. To this 40 mg of sodium acetate (0.2 % w/v) was added to decrease the bitterness of the solution and to act as a preservative, with 8 g of xylitol (40 % w/v) being added as a sweetener. Once these excipients had fully dissolved in solution, the preservatives were added: butyl paraben and propyl paraben, at 0.05 % and 0.02 % (w/v) respectively. 180 mg monosodium glutamate (0.9 % w/v) was added as a final excipient to enhance the taste of the formulation. The formulation was adjusted to 20 mL to produce a final concentration of 8 mg.mL⁻¹ of gliclazide. The final pH of the formulation was 8.47. The samples were prepared in triplicate and stored in amber coloured bottles at 5 °C, 25 °C (40 % humidity) and 40 °C (75 % humidity).

3.2.4.2. *Solubilisation of gliclazide (16 mg.mL⁻¹) with 5 % pluronic F127 (w/v) and 15 % ethanol (v/v).*

In 10 mL of water, 1 g of pluronic F127 (5 % w/v) was dissolved, after which 3 mL of ethanol (15 % v/v) was added. Once the solubilisers were mixed in solution, 8 g of xylitol (40 % w/v) was added as a sweetener and stirred magnetically until fully dissolved. 320 mg of gliclazide (16 mg.mL⁻¹) was then added and was left to stir until it was fully solubilised in solution. 180 mg of the taste enhancer monosodium glutamate (0.9 % w/v) was added, followed by propyl paraben and butyl paraben, at 0.02 and 0.05 % (w/v) respectively. The formulation was adjusted to 20 mL to produce a final dosage of 16 mg.mL⁻¹ of gliclazide, with the pH of the formulation being adjusted to 9 using 1 M sodium hydroxide. The samples were prepared in triplicate and stored in amber coloured bottles at 5 °C, 25 °C (40 % humidity) and 40 °C (75 % humidity).

3.2.5. Freeze-drying protocol

5 mg.mL⁻¹ formulations of gliclazide with L-arginine (Protocol 3.2.4.1) were prepared. The samples were placed into flat-bottom glass vials and frozen at -60 °C for 2 hours. The samples were then placed into an advantage 2.0 bench top freeze-dryer (VirTis, Suffolk, UK)

in order to fully extract the water. The freeze-drying process involved primary drying for 48 hours at a shelf temperature of -40 °C followed by secondary drying for 10 hours at a shelf temperature of 20 °C. Both the drying stages were carried out at a vacuum pressure of 50 mTorr. Samples were then stable enough to be stored at room temperature until further analysis of the samples was carried out.

3.2.6. Differential Scanning Calorimetry (DSC)

DSC (Perkin-Elmer, Wellesley, USA) was used to study T_g and melting points. Approximately 3 mg of sample was placed in a Perkin-Elmer aluminium pan, cooled to 10 °C using an intra-cooler (2P Perkin-Elmer, Wellesley, USA). The samples were heated to 300 °C at a scan rate of 200 °C·min⁻¹, with a nitrogen purge of 20 mL·min⁻¹. An empty aluminium pan was used as a reference.

The T_g and T_m were then analysed using the Pyris Manager software. All of the measurements were carried out in triplicate with fresh samples being prepared for each DSC run. The DSC was calibrated for temperature and heat flow prior to the samples being tested using standard samples of indium (T_m 156.6 °C) and zinc.

3.2.7. Thermogravimetric analysis (TGA)

Thermal degradation of glicazide was performed using TGA. The system consisted of a Pyris 1 Thermogravimetric Analyzer (Perkin Elmer). The sample masses ranged from 2-5 mg and were heated from 20-300 °C at a rate of 10 °C·min⁻¹ using dry nitrogen. All the studies were performed in triplicate.

3.2.8. Fourier Transform Infrared Spectroscopy (FTIR)

Characterisation of freeze-dried formulations was carried out with FTIR in order to investigate the interaction of the excipients and the drug. Freeze-dried samples of the formulations were prepared according to protocol 3.2.5. FTIR disks were prepared by adding the samples to potassium bromide at a ratio of 1:5 respectively. The mixed sample was then compacted by a mechanical press (Specac, Kent, UK) for 10 min at 8 tons to form a translucent pellet which was analysed using an IR200 spectrometer (Thermo Electron Corporation, UK) to determine the transmittance of each excipient.

3.2.9. Proton Nuclear Magnetic Resonance Spectroscopy (H^1 -NMR)

Approximately 2 mg of the freeze-dried samples and individual ingredients of each formulation were dissolved in 600 μ L D_2O at room temperature and placed in glass capillary vials. The sample vials were placed into the H^1 -NMR machine and analysed for the presence of hydrogen atoms using Bruker Advance DPX-250 NMR (at 250.1 MHz) and Bruker Topspin software.

3.2.10. pH

The pH of each sample was analysed using a Hydrus 500 (Fisherbrand, UK), calibrated at pH 4, 7 and 10.

3.3. Results and Discussion

3.3.1. Calibration Validation

A HPLC method was developed and validated for the determination of gliclazide. At a wavelength of 220 nm, ACN was used to solubilise gliclazide and analysed. Results are presented in table 3.1.

3.3.1.1 Linearity

The linearity of the HPLC method was evaluated by preparing the standard curve for gliclazide on three consecutive days. The peak area was plotted against the gliclazide concentration and the calibration response was assessed for variances. The results show that the Beer Lambert's law was obeyed in the range of 0.5-1000 µg.mL⁻¹ with the linear plot giving the regression equation of $y=0.9479x$ ($R^2=0.9996$) (Figure 3.2).

3.3.1.2 Precision

In order to assess the reproducibility of the calibration protocol, the calibration method was carried out in triplicate over a period of three days for interday precision, and in triplicate on

Table 3.1. Summary of calibration validation of gliclazide

Criteria	Validation
$Y=$	0.9479x
R^2	0.9996
Intra-day Precision	101.36 %
Inter-day Precision	102.55 %
Accuracy ($\pm SD$) 10 µg.mL⁻¹	92.62 (11.61) %
Accuracy ($\pm SD$) 100 µg.mL⁻¹	103.25 (8.77) %
Accuracy ($\pm SD$) 400 µg.mL⁻¹	104.02 (3.92) %
LOD µg.mL⁻¹	13.02
LOQ µg.mL⁻¹	39.46

the same day for intraday precision. The results showed that the calibration method was reproducible with inter-day precision being calculated to be 102.55 %, and the intra-day precision being calculated to be 101.36 %. Statistical data was compared using the ANOVA statistical test, with the resulting inter-day and intra-day precision calculated to have a variance of $P>0.05$.

3.3.1.3. Accuracy

The accuracy of the developed method was determined from three concentrations of gliclazide in ACN representing the low, medium and high portions of the standard curve (10, 100 and 400 $\mu\text{g.mL}^{-1}$). Accuracy of the three concentrations was in the range of 92.62-104.02 %.

3.3.1.4 Limit of detection (LOD) and limit of quantification (LOQ)

The LOD of an individual analytical procedure is the lowest amount of analyte in a sample which can be detected but not necessarily quantifiable as an exact value (EMEA, 1995). From the calibration range the LOD was calculated to be 13.02 $\mu\text{g.mL}^{-1}$.

The LOQ of an individual analytical procedure was the lowest amount of analyte in a sample which can be quantitatively determined with accuracy and precision. The LOQ was calculated to be 39.46 $\mu\text{g.mL}^{-1}$.

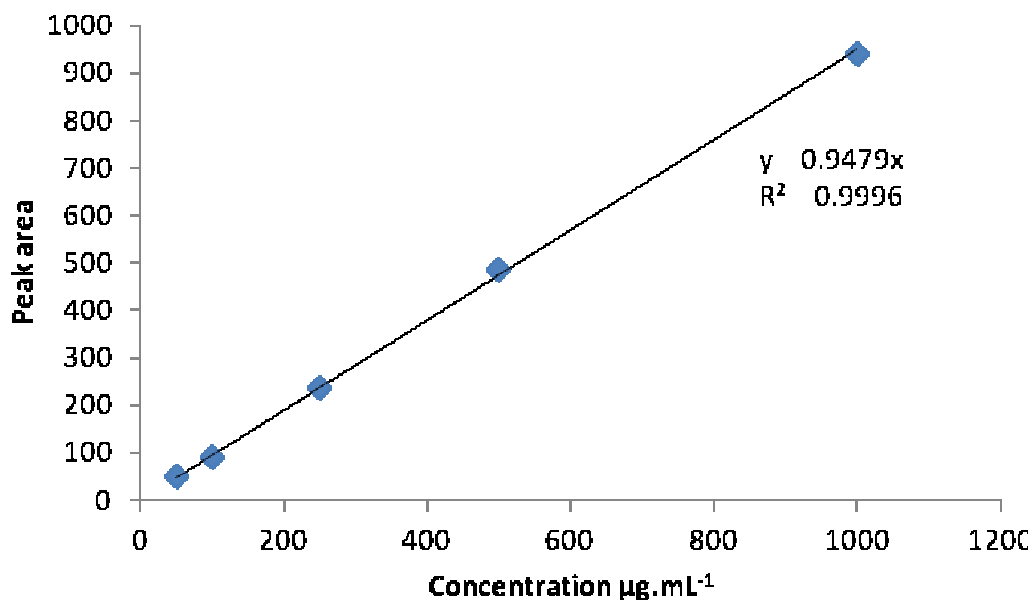


Figure 3.2. Calibration graph of gliclazide highlighting the linearity of the validation protocol.

3.3.2. Phase solubility

In order for the oral liquid formulation of gliclazide to be competitive with the solid dosage forms, a minimum concentration of 8 mg.mL^{-1} solution/suspension had to be formulated. However, hydrophobicity of gliclazide ($0.025 \pm 0.001 \text{ mg.mL}^{-1}$) is a major obstacle to be overcome in the formulation stage. The hydrophobicity of gliclazide has been attributed to the non-polar components in its structure, thereby preventing the molecule breaking into the lattice structure of water and being solubilised (Seedher and Bhatia, 2003).

Previously, extensive research had been carried out using cyclodextrins as complexing agents (Moyan *et al*, 1997; Ozkan *et al*, 2000) to overcome poor solubility, but did not result in high levels of solubilisations as needed for the development of a liquid dosage form which would be comparable to a solid dosage form in delivering a therapeutic dose. On the other hand, limited research has been carried out investigating the use of alternative solubilisers such as; amino acids (L-arginine and L-lysine), surfactants (pluronic F127), and ethanol. Therefore the first phase of the developmental work was concentrated on exploring the use of alternative solubilisers.

3.3.2.1. Solubilisation of gliclazide with amino acids.

The addition of gliclazide in water causes an acidifying affect, with the pH being reduced to 4.90 ± 0.01 in a $0.02 \pm 0.001 \text{ mg.mL}^{-1}$ gliclazide solution. Therefore basic amino acids were chosen as solubilising agents as suggested by previous research investigating salt formation (Tung *et al*, 1991). Amino acids are critical components that serve as the building blocks of life and make up the foundation of proteins. They not only have the added advantage of patient compliance at high concentrations, but also have no adverse affects in the presence of gliclazide or diabetes. Table 4.1 highlights the various amino acids available, with L-arginine and L-lysine being the most basic. Therefore L-arginine and L-lysine were studied for their solubilising efficacy in the presence of excess gliclazide.

3.3.2.1.1. L-arginine

Figure 3.3 displays the solubilisation of excess gliclazide with increasing concentrations of L-arginine ($10\text{-}200 \text{ mg.mL}^{-1}$). The results show that as the concentration of L-arginine increased from 10 to 25 mg.mL^{-1} , the concentration of gliclazide also increased linearly until maximum gliclazide solubility was achieved at $15.25 \pm 0.09 \text{ mg.mL}^{-1}$ in the presence of 25 mg.mL^{-1} L-arginine. The concentration of L-arginine was observed to have a direct affect

on the pH of the resultant solution, which was found to also increase in parallel with increasing L-arginine concentration (up to $\text{pH } 8.47 \pm 0.05$ with 25 mg.mL^{-1} L-arginine). Interestingly, further increase of L-arginine ($50\text{-}100 \text{ mg.mL}^{-1}$) showed that there was no increase in the solubility of gliclazide and the pH of the resultant solution was constant.

The solubilising properties of L-arginine can be attributed to the interaction of gliclazide with L-arginine through complex formation between the electronegative nitrogen groups of the amino acid and the acidic hydrogen of gliclazide (Grove *et al*, 2003). The stability of the complex was highly dependent on the pKa of the guanidinium group of L-arginine (pKa 12.48), which ensured a stable complex was formed. However, the decline in gliclazide concentrations at 200 mg.mL^{-1} L-arginine was possibly due to the hydrophobicity of the drug at specific pH environments. In order for a complex to be stable, pKa difference of the amino acid and the drug needs to be greater than 3 (Stahl and Wermuth, 2002). Gliclazide has a pKa of 5.8, attributed to the α -hydroxyl secondary amine group in its chemical structure (Figure 3.1) (Alkhamis *et al*, 2003; Shewale *et al*, 2008), thus at pH 9 the drug existed mainly in the unionised form (hydrophobic), thereby rendering the complex unstable.

3.3.2.1.2. L-lysine

Figure 3.4 shows the solubility of gliclazide with increasing L-lysine concentrations ($10\text{-}300 \text{ mg.mL}^{-1}$). It was observed that with the inclusion of 10 mg.mL^{-1} of L-lysine, gliclazide solubility increased to $5.31 \pm 1.88 \text{ mg.mL}^{-1}$, with gliclazide concentration increasing further as the concentration of L-lysine increased to 15 and 20 mg.mL^{-1} (7.47 ± 0.03 and $8.82 \pm 0.03 \text{ mg.mL}^{-1}$ respectively). Interestingly, the concentration of the drug in solution increased dramatically with 25 mg.mL^{-1} of L-lysine ($26.80 \pm 0.22 \text{ mg.mL}^{-1}$) followed by a plateau affect as the amino acid concentration was increased to 200 mg.mL^{-1} . A further slight increase in gliclazide solubility was observed ($29.74 \pm 0.32 \text{ mg.mL}^{-1}$) as the concentration of L-lysine was raised to 300 mg.mL^{-1} .

In order to observe the affect of pH against gliclazide solubility the pH of the solution was monitored with each additional increment of amino acid. It was found that in the presence of 10 mg.mL^{-1} of L-lysine the pH of the medium was slightly alkaline ($\text{pH } 8.32 \pm 0.01$), which increased in alkalinity as the concentration of L-lysine increased to 300 mg.mL^{-1} , exhibiting a final pH profile of 9.37 ± 0.01 (Figure 3.4). Thus as with the L-arginine phase solubility study gliclazide concentration increased with increasing pH until solubility plateau was observed at $\sim \text{pH } 8.6$.

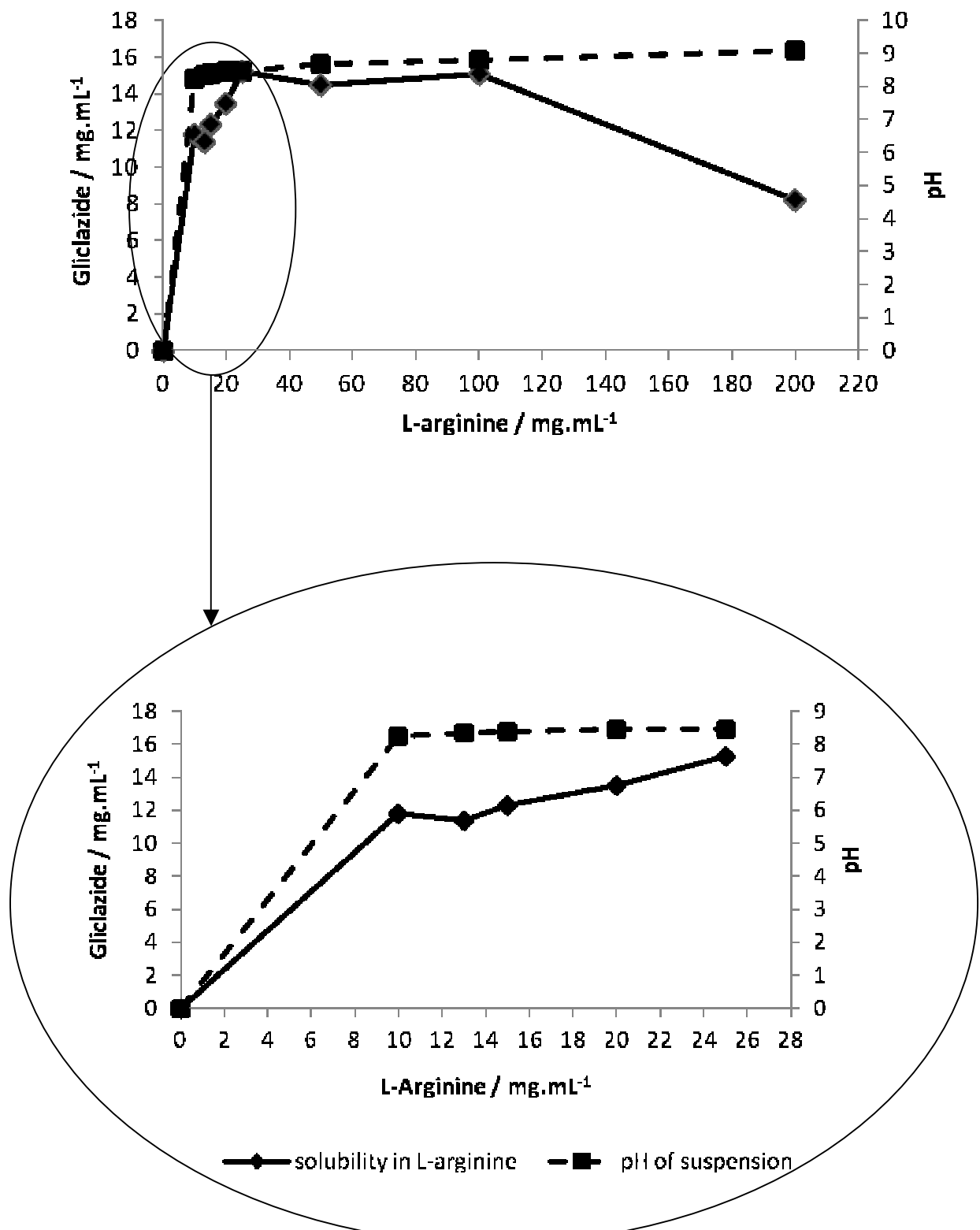


Figure 3.3. Phase solubility of gliclazide in L-arginine. At 25 mg.mL⁻¹ of the basic amino acid, a maximum of 15.25 ± 0.09 mg.mL⁻¹ gliclazide was solubilised in distilled water. The pH of the systems remained above pH 8. As the pH increased to pH 9, the amount of gliclazide solubilised decreased to 8.20 ± 0.20 mg.mL⁻¹. (n=3)

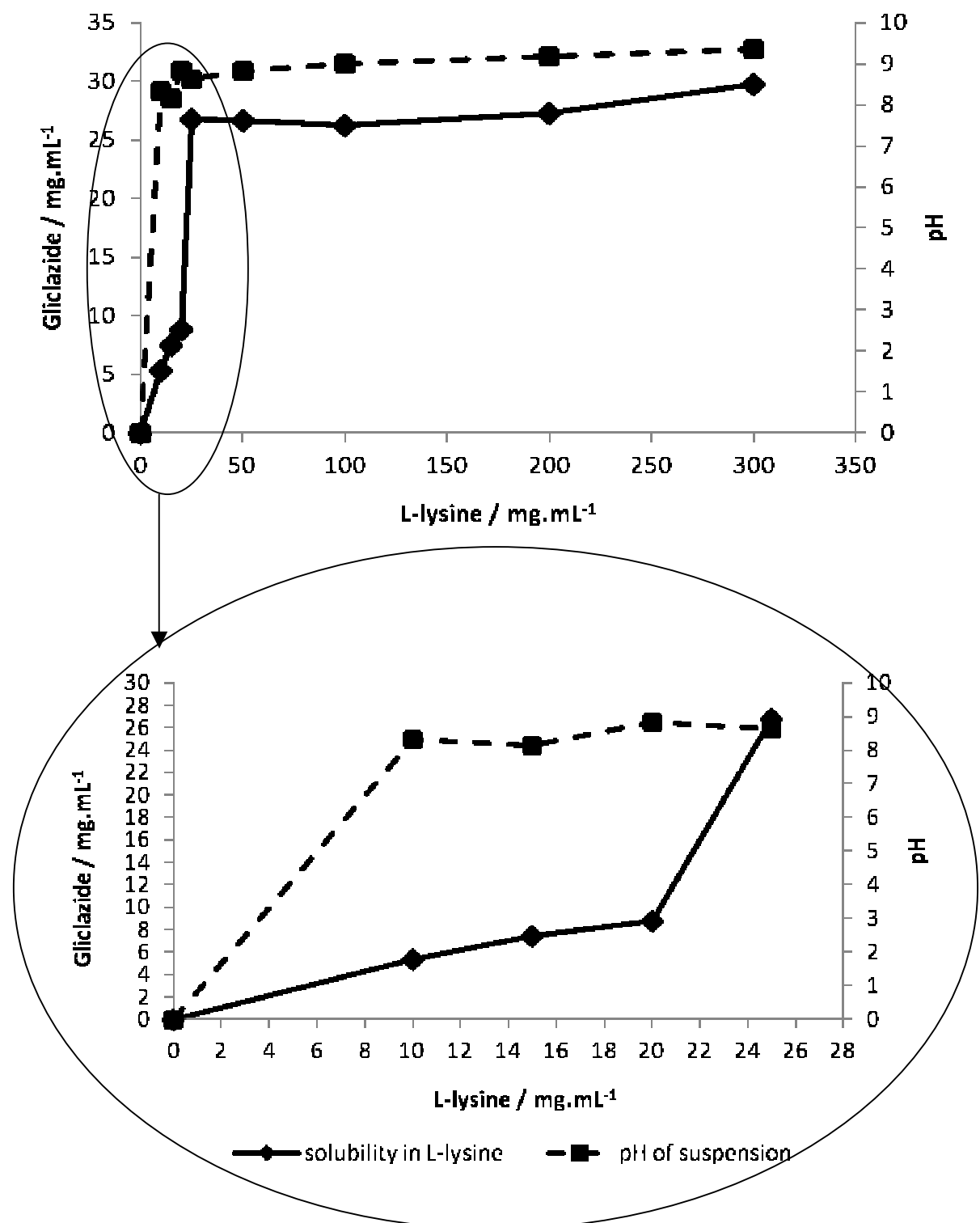


Figure 3.4. Phase solubility of gliclazide with increasing concentrations of L-lysine ($10\text{-}300 \text{ mg.mL}^{-1}$). At 25 mg.mL^{-1} of L-lysine a maximum of $26.80 \pm 0.22 \text{ mg.mL}^{-1}$ gliclazide was solubilised in water. The pH of the systems remained in the range of pH 8-9. However gliclazide remained unstable over time, as the drug precipitated out. (n=3)

Interestingly, in contrast to the L-arginine phase solubility study, L-lysine-gliclazide solution began salting out (was seen to precipitate out) after 24 hours. This salting out process was attributed to the pH of the medium being raised above the pH maximum of L-lysine in solution and thereby resulting in the salt to be converted to its free base with gliclazide returning to its solid state (Serajuddin, 2007). In order for the amino acid to act as a stable salt the pKa difference of the amino acid and the drug had to be greater than 3 (Stahl and Wermuth, 2002), thus the salting-out effect was attributed to the instabilities of L-lysine in the salt form. Table 3.2 compares the pKa of gliclazide against L-arginine and L-lysine, from which it can be concluded that the end groups in the amino acid chemical structures (pKa 3) displayed very different ionisable strengths. L-lysine had 3 pKa values of 2.20, 8.90 and 10.28 (Figure 3.5a) with L-arginine having 3 pKa values of 2.01, 9.04, and 12.48 (Figure 3.5b). It was found that the amine group of L-lysine was shown to display lower strength and stability than the guanidinium group of L-arginine and thus gliclazide formed a weaker salt complex with L-lysine which quickly precipitated.

Table 3.2. The calculated difference of gliclazide with L-lysine and L-arginine. Greater the difference in pKa, greater the stability of the complex.

	pKa ₁	pKa ₂	pKa ₃
L-Lysine	2.20	8.90	9.28
Difference with Gliclazide pKa 5.8	3.60	3.10	4.40
L-arginine	2.01	9.04	12.48
Difference with Gliclazide pKa 5.8	3.79	3.24	6.68

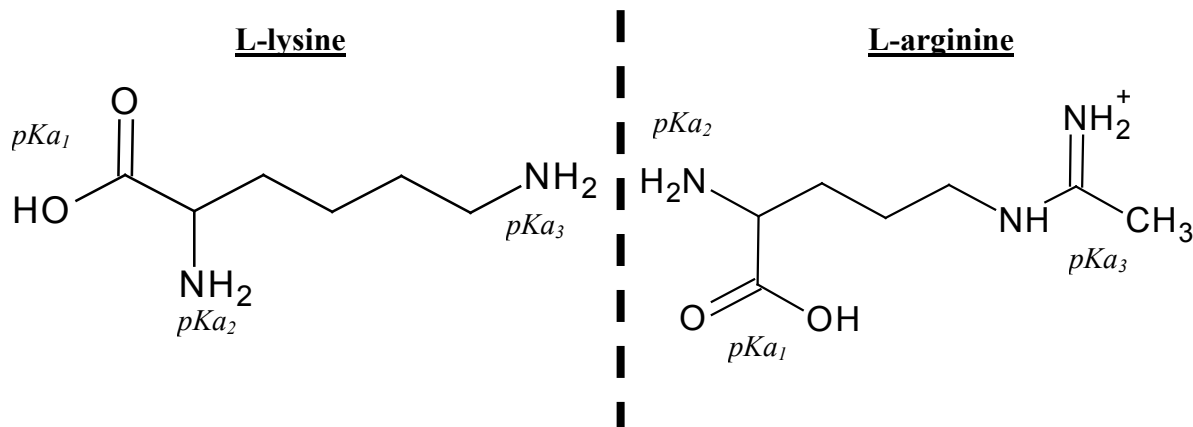


Figure 3.5. (A) Structure of L-lysine; containing an amine end group with a pKa₃ 9.28, and **(B)** structure of L-arginine, containing a guanidinium end group with a pKa₃ 12.48.

3.3.2.2. Solubilisation of gliclazide with Pluronic F127

Surfactants have been extensively used within the pharmaceutical field in the stabilisation of various vehicles used in the solubilisation of hydrophobic drugs (Rachmawati *et al*, 2008) or as solubilisers (Alkhamis *et al*, 2003). Surfactants are amphiphilic surface acting compounds that lower surface tension of a liquid. A surfactant can effectively act when it reaches its critical micelle concentration (CMC), which has been defined as the minimum concentration required of the surfactant to form a micelle in a given system. In this study the effect of CMC on the solubility of gliclazide was analysed with pluronic F127.

3.3.2.2.1. Influence of Pluronic F127 concentration

Figure 3.6 shows the affect of increasing the concentration of pluronic F127 (1-5 % w/v) in water on the solubilisation of gliclazide. It was observed that the concentration of solubilised gliclazide increased with increasing surfactant concentration, resulting in $0.073 \pm 0.000 \text{ mg.mL}^{-1}$ of gliclazide with 4 % (w/v) F127. Interestingly, by increasing the

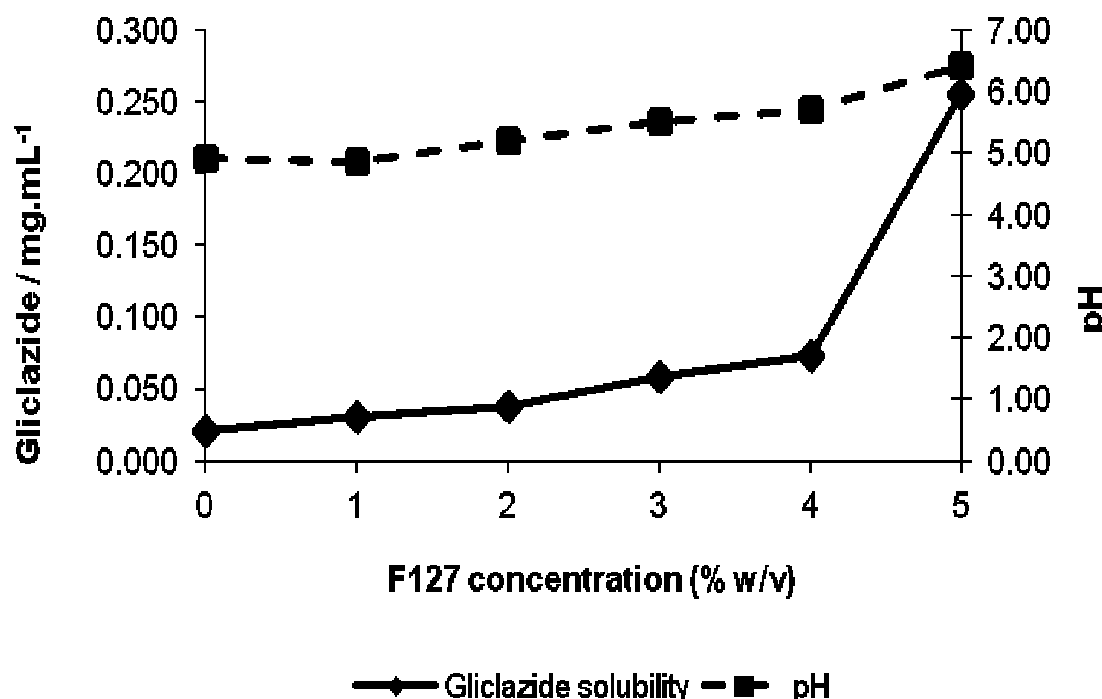


Figure 3.6. Phase solubility profile of gliclazide with increasing concentrations of surfactant F127, and its respective pH profile. CMC was achieved with 5 % (w/v) pluronic F127 increasing the gliclazide concentration to $0.256 \pm 0.001 \text{ mg.mL}^{-1}$. (n=3)

pluronic F127 concentration to 5 % (w/v), the amount of gliclazide solubilised in solution dramatically increased, achieving a concentration of $0.256 \pm 0.001 \text{ mg.mL}^{-1}$. This significant rise in gliclazide concentration marked the CMC point, thereby giving a CMC value of 50 g.L^{-1} .

The pH of the medium was closely monitored after each increment of surfactant. It was concluded that pluronic F127 exerted minimum affects on the pH of the solution, as the pH of the solution was seen to increase from $\text{pH } 4.90 \pm 0.01$ in the absence of surfactant, to $\text{pH } 6.41 \pm 0.02$ at the CMC (5 % w/v F127). However from the previous phase solubility study, it was understood that the concentration of solubilised drug increased when the pH of the medium was in the range of 6-8, hence the next stage was to analyse the influence of pH on the surfactant and its ability to solubilise gliclazide in water.

3.3.2.2.2. Influence of pH and pluronic F127 (5 % w/v)

Figure 3.7 displays the pH modification of a 5 % (w/v) F127 solution (pH 1.5, 4.0, 7.0, and 9.1) and its influence on the solubility of gliclazide. It was observed that under acidic conditions of pH 1.5 and 4.0, gliclazide concentration in solution increased to 0.237 ± 0.001 and $0.312 \pm 0.001 \text{ mg.mL}^{-1}$ respectively. By adjusting the pH of the system to pH 7.0, the concentration of gliclazide was observed to increase further until a maximum of $0.531 \pm 0.001 \text{ mg.mL}^{-1}$ was achieved. However, under more alkaline conditions (pH 9.1) the amount of gliclazide solubilised was significantly reduced to $0.513 \pm 0.01 \text{ mg.mL}^{-1}$ ($P<0.05$). Therefore it can be concluded that the influence of pH had the following affect: acidic to neutral conditions increased drug solubility, whereas alkaline conditions resulted in reducing drug solubility. This pattern indicates that the degree of drug ionisation has a decisive influence on the solubility of gliclazide at varying pH. The increase in gliclazide concentration was attributed to the protonation of the drug molecule resulting in a slightly more hydrophilic form, with the decline in gliclazide solubility being attributed to the pH exceeding the pKa of gliclazide, and thereby causing the drug molecule to become de-protonated (hydrophobic) (Shewale *et al*, 2008).

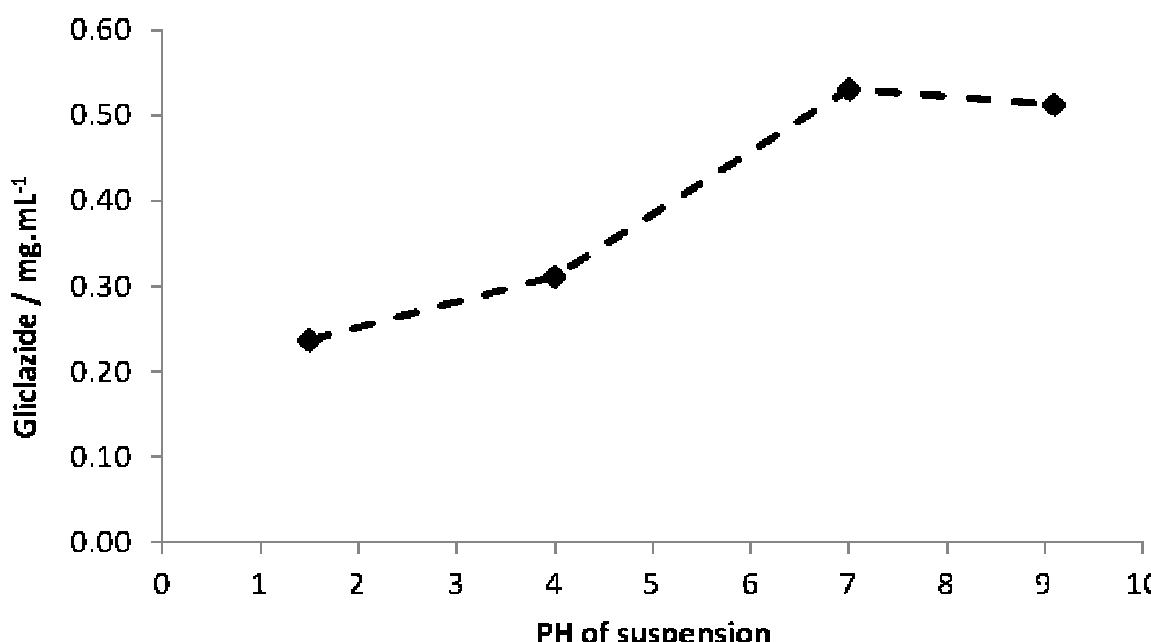


Figure 3.7. Phase solubility profile of gliclazide in 5 % F127 (CMC) at varying pH. Under acidic conditions, a maximum $0.312 \pm 0.001 \text{ mg.mL}^{-1}$ gliclazide was solubilised. At pH 7 the concentration of gliclazide increased to $0.531 \pm 0.001 \text{ mg.mL}^{-1}$, which was then seen to significantly decline as the pH was further increased to pH 9.1 ($0.513 \pm 0.01 \text{ mg.mL}^{-1}$) ($P<0.01$). ($n=3$)

3.3.2.2.3. Summary

Poloxamers (pluronic F127) are GRAS listed and FDA approved for consumption; however they cannot be metabolised by the body, and result in gel formation and reduced fluidity with increasing concentration (Rowe *et al*, 2006). Therefore a maximum of 5 % (w/v) pluronic F127 was used in the phase solubility study. It was observed that the CMC was reached with 5 % (w/v) surfactant, however the extent of drug solubilised after pH modification was considerably less in comparison with solubility studies carried out with L-arginine (0.531 ± 0.001 and $15.25 \pm 0.09 \text{ mg.mL}^{-1}$ respectively). This was attributed to L-arginine solubilising the drug through salt formation under slightly alkaline conditions (pH 8), whereas the solubilisation of gliclazide with pluronic F127 was highly dependent upon the degree of CMC. Thus at 5 % (w/v) pluronic F127, the concentration of micelles formed was too low for the minimum amount of gliclazide to be solubilised (8 mg.mL^{-1}).

Therefore in order to achieve an 8 mg.mL^{-1} oral liquid dosage form, the next phase of work involved the reduction in the medium's dielectric constant using a co-solvent system in the presence of pluronic F127 (5 % w/v) .

3.3.2.4. Solubilisation of gliclazide in a co-solvent system

A co-solvent, such as alcohol, is a water miscible organic solvent with two specific properties with regards to drug solubilisation: (1) the ability to reduce the dielectric constant of the medium (Chapter 5), resulting in a polar medium being altered into a non-polar medium, and thus allowing for greater solubility of poorly water-soluble substances; and (2) the ability to increase the chemical stability of the compound within this system.

Figure 3.8 demonstrates the effectiveness of using an ethanol based co-solvent system for the solubilisation of gliclazide in water. The concentration of ethanol was increased from 10–100 % (v/v), with the pH of the medium being closely monitored. It was observed that as the concentration of ethanol increased from 0 to 20 % (v/v), the amount of gliclazide solubilised remained consistent ($0.046 \pm 0.0001 \text{ mg.mL}^{-1}$). However as the concentration of ethanol was further increased to 40 % (v/v) a significant rise in drug concentration was observed ($0.11 \pm 0.001 \text{ mg.mL}^{-1}$, $P<0.05$). Interestingly, as the concentration of ethanol was doubled (80 % v/v) the amount of drug solubilised dramatically increased to $4.18 \pm 0.011 \text{ mg.mL}^{-1}$, with 100 % (v/v) ethanol achieving a $5.72 \pm 0.069 \text{ mg.mL}^{-1}$ gliclazide concentration.

The pH of the co-solvent system was not influenced by the concentration of ethanol or gliclazide, as the ethanol-gliclazide solution remained fairly constant at pH 5.45 ± 0.02 and pH 5.94 ± 0.01 (10 % and 100 % ethanol respectively, $P<0.05$).

The solubilising capabilities of an ethanol-water system (> 40 % v/v) was attributed to the octanol-water partition co-efficient ($\text{Log } P$) of the co-solvent and the polarity of the medium. The $\text{Log } P$ of the co-solvent which is also referred to as the hydrophobicity of the solvent, increases with increase in the concentration of ethanol which ultimately enhances the solubility of gliclazide (Seedher and Bhatia, 2003). Polarity of a medium can dictate the solubility of a compound in a given medium as solvents with reduced polarity have greater affinity for poorly soluble drugs (non-polar molecules). In a study carried out by Seedher and Bhatia (2003), the extent of solvent polarity was calculated as the dielectric constant. Water and ethanol have dielectric constants of 78.36ϵ and 24.3ϵ respectively, thus confirming that the polarity of water was greater than ethanol. Therefore, the dramatic increase in gliclazide concentration with 80 % (v/v) ethanol was attributed to a significant reduction in the polarity of the co-solvent system, enabling the solubilisation and formation of hydrogen bonds between the co-solvent and the hetero-atoms of gliclazide (nitrogen, oxygen and sulphur atoms).

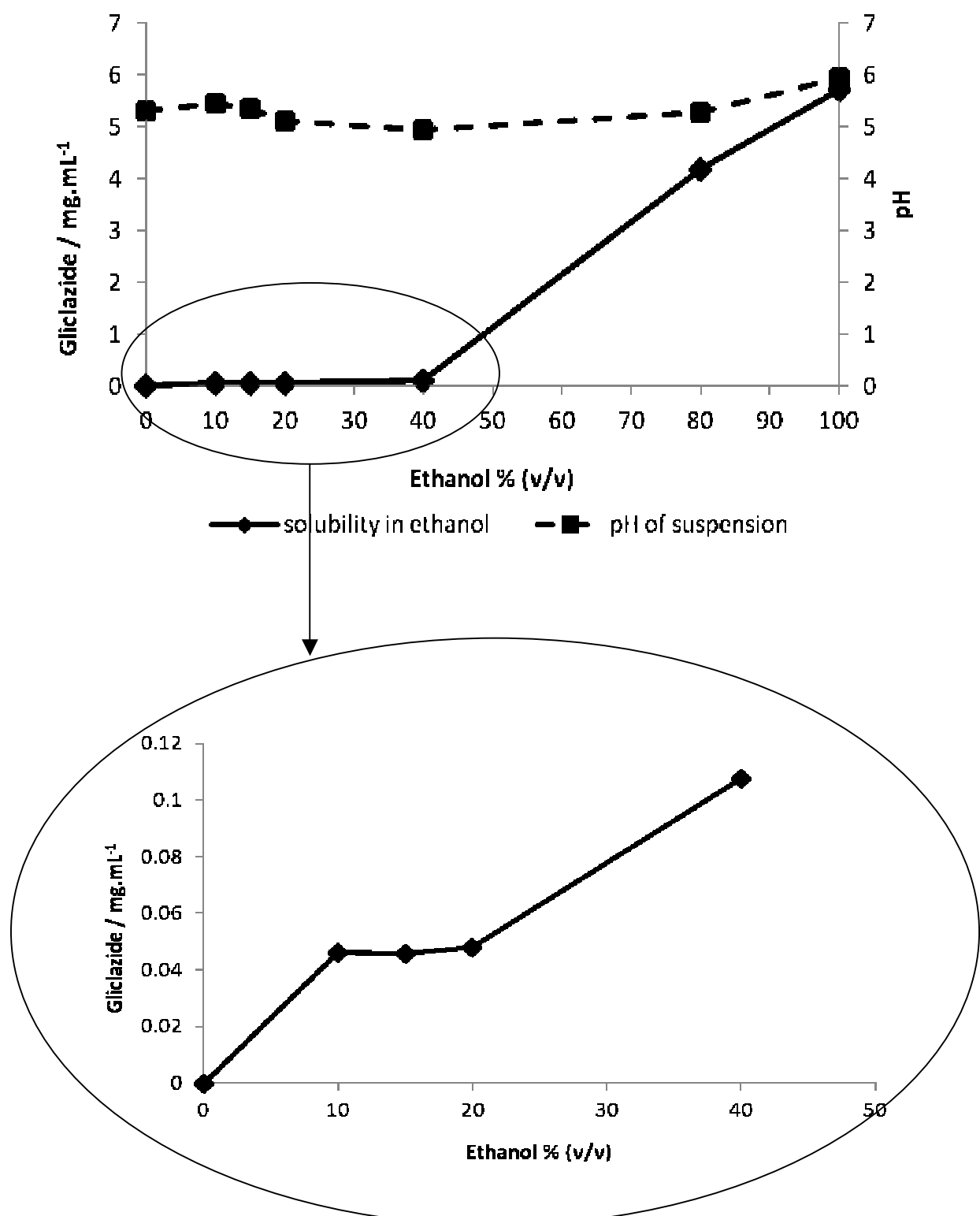


Figure 3.8. Phase solubility of gliclazide with increasing concentrations of ethanol as a co-solvent (10-100 % v/v). At 15 % (v/v) ethanol 0.046 ± 0.001 mg.mL⁻¹ gliclazide was solubilised in water, with increasing ethanol concentrations of 80 and 100 % achieving 4.18 ± 0.011 and 5.72 ± 0.69 mg.mL⁻¹ gliclazide respectively. The pH of the co-solvent system remained consistent at pH 5. (n=3)

3.3.2.4.1. Influence of pH and ethanol (15 % v/v)

Gliclazide has been shown to have increased solubility properties when the pH of the medium was in the range of 6-8 (Section 3.3.2.2.2.). However in the co-solvent system the pH did not exceed pH 5.94 ± 0.01 , therefore the influence of pH on gliclazide solubility in a 15 % (v/v) ethanol-water system was assessed. The maximum concentration of ethanol that is used in liquid preparations is between 15-20 %. Therefore a low concentration of ethanol (15 % v/v) was chosen for its antimicrobial preservative actions (≥ 10 % v/v) as well as to minimise the extent of a ‘burning taste’ associated with ethanol (Rowe *et al*, 2006).

Figure 3.9 shows that as the pH of the co-solvent became progressively alkaline the concentration of gliclazide rapidly increased from 0.494 ± 0.005 mg.mL $^{-1}$ at pH 7 to 19.22 ± 0.057 mg.mL $^{-1}$ (pH 8). Under extreme alkaline conditions (pH 11) a maximum drug concentration of 22.924 ± 0.071 mg.mL $^{-1}$ was achieved. As expected, under acidic conditions gliclazide remained relatively insoluble (0.04 ± 0.001 mg.mL $^{-1}$ at pH 4). These results were attributed to extent of ionisation (Section 3.3.2.2.2.) and the reduction of the dielectric constant, thus allowing greater amounts of gliclazide to be solubilised and stable under alkaline conditions.

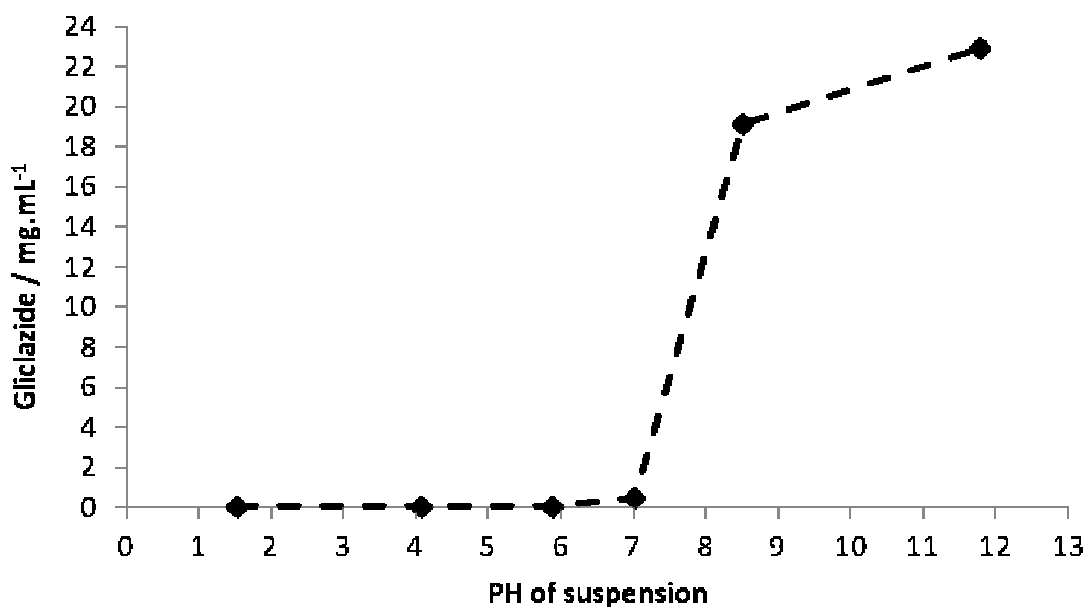


Figure 3.9. Influence of pH on the phase solubility of gliclazide in 15 % ethanol-water (v/v). Under acidic conditions, gliclazide remained relatively insoluble, however as the pH of the co-solvent system increased from pH 7 to pH 8, the concentration of gliclazide increased dramatically from 0.494 ± 0.005 to 19.22 ± 0.057 mg.mL $^{-1}$ respectively. (n=3)

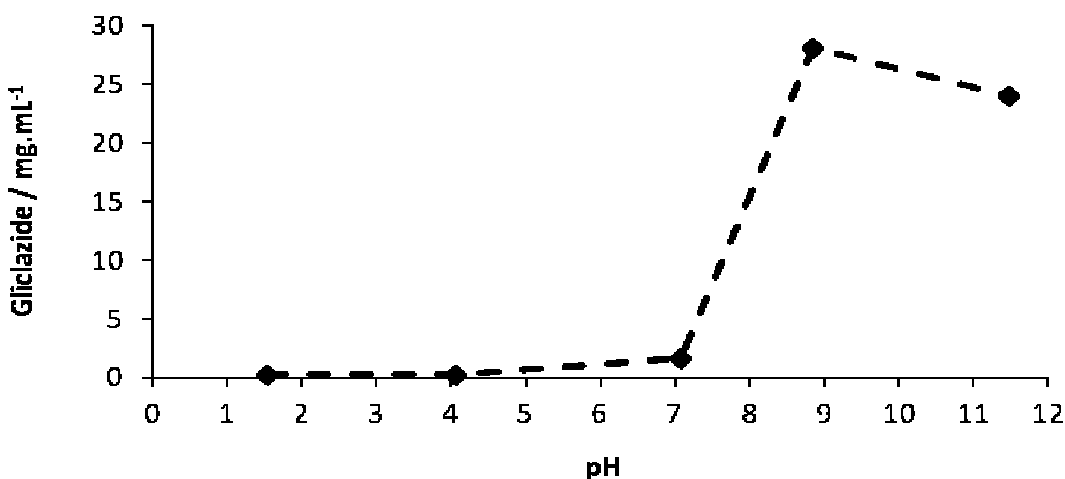


Figure 3.10. Influence of pH of the phase solubility diagram of gliclazide in 5% (w/v) F127 and 15 % ethanol-water (v/v). Under acidic conditions, gliclazide remained relatively insoluble, however as the pH of the co-solvent system increased from pH 7 to pH 8.84, the concentration of gliclazide increased dramatically from 1.615 ± 0.07 to 28.15 ± 0.1 mg.mL⁻¹ respectively. (n=3)

3.3.2.5. Solubilisation of gliclazide with 5 % (w/v) F127 and 15 % (v/v) ethanol-water

In order to effectively solubilise a hydrophobic drug, the phase solubility tests described above concluded the role of various parameters including pH, hydrophobic environment (CMC) and reduced polarity of the solution. Therefore a solubility study was conducted in which all 3 factors were analysed in parallel using a solution composed of pluronic F127 (5 % w/v) and ethanol (15 % v/v). Figure 3.10 shows the influence of pH on the solubility of gliclazide in a co-solvent-surfactant solution. As expected, under acidic conditions gliclazide remained fairly insoluble, with neutral (pH 7) and slightly alkaline (pH 8.84) conditions increasing the solubility of the drug considerably (1.615 ± 0.007 and 28.15 ± 0.1 mg.mL⁻¹ respectively).

3.3.2.6. Phase solubility summary

The solubility of a hydrophobic drug such as gliclazide has been shown to be governed by the following factors: pH, polarity of medium, salt formation, and CMC. Gliclazide is a weak acid with a pKa of 5.8 (Alkhamis *et al*, 2003) and was only partially ionised. By adjusting the pH of the medium to more alkaline conditions, the drug molecule is ionised to a greater

extent. Adjusting the composition of the medium, the polarity of the system reduced, resulting in conditions more suited to non-polar drugs.

3.3.3. Formulation and stability of an oral liquid solution of gliclazide

From the phase solubility studies it was concluded that using L-arginine and co-solvent-surfactant mixture as solubilisers were effective for formulating gliclazide at a dosing concentration of 8 mg.mL^{-1} and 16 mg.mL^{-1} . Formulations of gliclazide in solution were prepared as described in section 3.2.4. The samples were stored at different stability conditions as outlined in the ICH guidelines (5°C , 25°C (40 % humidity) and 40°C (75 % humidity)) and assessed for changes in organoleptic properties and chemical stability of the active ingredient.

3.3.3.1. Gliclazide (8 mg.mL^{-1}) oral liquid formulation in the presence of 7 mg.mL^{-1} L-arginine

Figure 3.11 highlights the stability profile of an 8 mg.mL^{-1} gliclazide oral liquid formulation, prepared with 7 mg.mL^{-1} L-arginine at pH 8. Analysis of gliclazide showed that the chemical stability profile of the active ingredient did not change during the entire duration of the study with drug retention remaining above the 95 % threshold. In addition, the pH of the formulations remained stable at pH 8 after being stored at different conditions over the 9 month period. Furthermore, the organoleptic properties of the formulation remained stable with no discolouration or odorous smell.

3.3.3.2. Gliclazide (16 mg.mL^{-1}) oral liquid formulation in the presence of 15 % (v/v) ethanol and 5 % (w/v) Pluronic F127

Figure 3.12 displays the stability profile of a 16 mg.mL^{-1} gliclazide oral liquid formulation prepared with 5 % (w/v) pluronic F127 and 15 % (v/v) ethanol, adjusted to pH 9. The pH of the formulations remained stable at pH 9 indicating the chemical stability of gliclazide remained stable for the duration of the study. Furthermore, analysis of gliclazide showed that the chemical stability profile of the active ingredient did not change during the entire duration of the study, with drug retention remaining above the 95 % threshold under 5°C , 25°C and 40°C conditions (97.45 ± 1.48 , 99.98 ± 0.75 and 101.61 ± 1.37 % respectively). The organoleptic properties were found to remain stable with no discolouration or unpleasant smell.

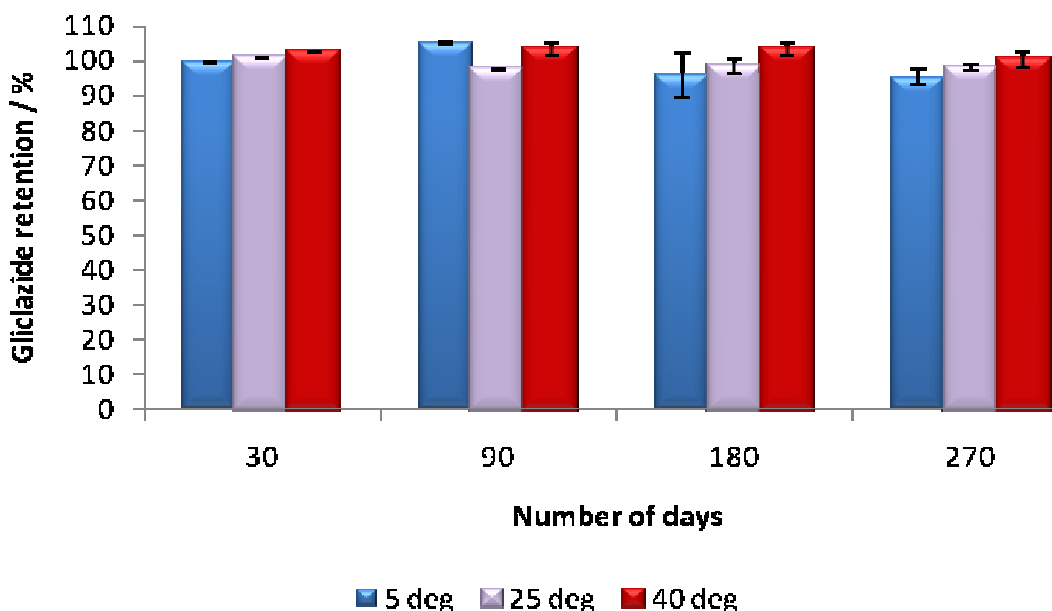


Figure 3.11. Nine month stability profile of 8 mg.mL^{-1} gliclazide with 7 mg.mL^{-1} L-arginine stored under 5°C , 25°C (40 % humidity) and 40°C (75 % humidity) conditions. The formulation was observed to have >95 % drug retention over the 9 month period. ($n=3$)

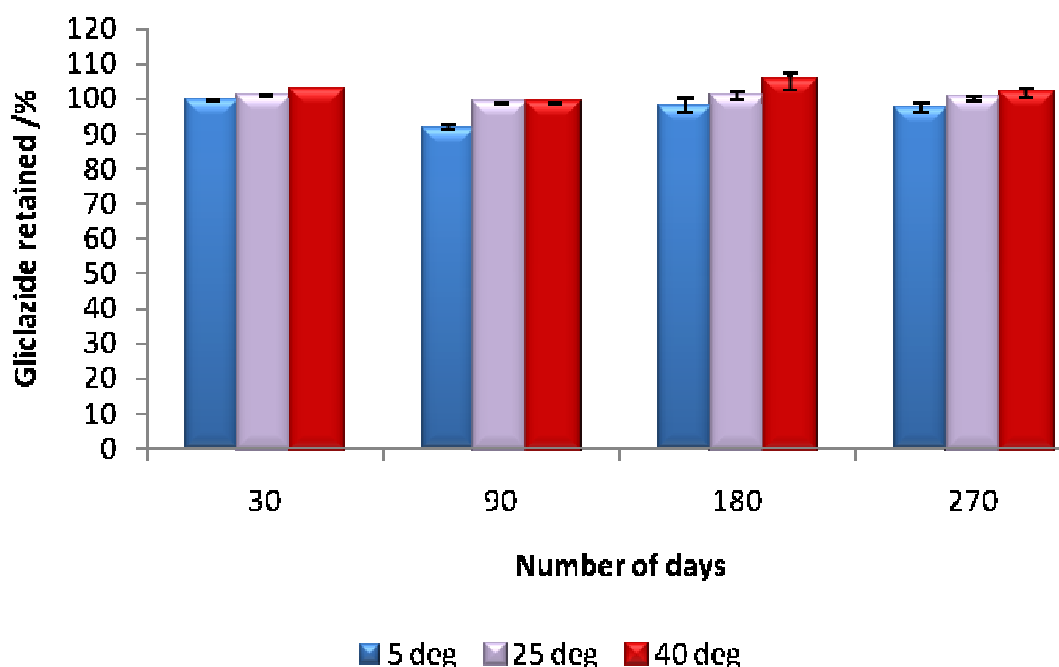


Figure 3.12. Nine month stability profile of 16 mg.mL^{-1} gliclazide with 5 % (w/v) pluronic F127 and 15 % (v/v) ethanol, stored under 5°C , 25°C (40 % humidity) and 40°C (75 % humidity) conditions. The formulation was observed to have >95 % drug retention over the 9 month period. ($n=3$)

3.3.4. Physicochemical analysis of gliclazide with L-arginine

In order to understand the solubilisation properties of L-arginine, a physicochemical analysis was carried out investigating the interactions between the active ingredient (gliclazide) and the amino acid. This involved understanding a number of interactions occurring within the system such as: thermodynamic interactions, which were assessed by using DSC; bond vibrations indicating formation of complexes which were assessed by using FTIR; and the presence/absence of hydrogen bond formation in the complexes (using H¹-NMR).

3.3.4.1. DSC

DSC analysis was carried out on freeze-dried samples of formulated gliclazide-L-arginine complex using hyper DSC. The advantage of using hyper DSC over conventional DSC was that it allowed for the suppression of kinetic events as well as increasing the strength of the signal allowing sensitivity towards low energy transitions. The DSC thermograms of individual excipients and freeze-dried gliclazide-L-arginine formulation are presented in figure 3.13. It was observed that at the beginning of each thermogram, an endothermic event occurred at ~25 °C. These thermal events were a result of mismatching in thermal properties between the sample and reference pan, thereby causing an unstable baseline. However once the sample pan and reference pan were rebalanced at the same temperature, the baseline was resumed (Brown, 2001). In order to ascertain a chemical interaction between gliclazide and L-arginine when in the solubilised form, the individual excipient of the formulation first had to be analysed to determine their melting points and any other distinctive thermal events. It was noted that xylitol displayed an onset melting point of 101.75 °C, and L-arginine had an onset melting peak at 108.41 °C, followed by a second melt at 145.65 °C, which was immediately followed by oxidation and degradation (Brown, 2001). Gliclazide displayed a single endothermic melt at 184.68 °C, which was followed by immediate degradation that was further confirmed using TGA. However, the presence of xylitol in the freeze-dried formulation potentially masked the thermal profiling of the various excipients including gliclazide and L-arginine, hindering further thermal analysis.

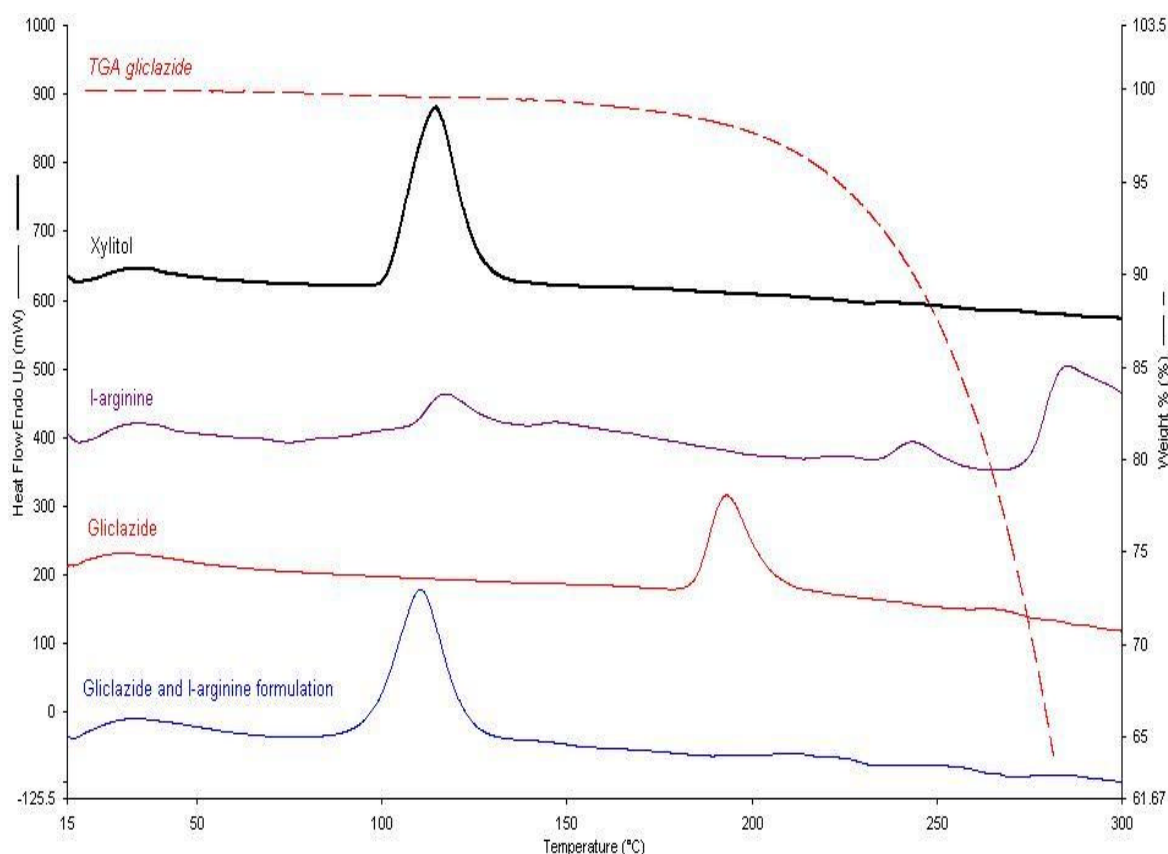


Figure 3.13. DSC overlay of xylitol, L-arginine, gliclazide, and gliclazide formulation with L-arginine after being freeze-dried, at a scan rate of $100\text{ }^{\circ}\text{C}.\text{min}^{-1}$.

To address this, a second study was carried out looking specifically at the interaction of gliclazide and L-arginine when in solution. A highly concentrated amount of gliclazide was dissolved in L-arginine solution before being analysed using DSC. It was observed that L-arginine in solution had an onset melt at $72.86\text{ }^{\circ}\text{C}$ (Figure 3.14), and when compared against the solubilisation of gliclazide, a Tg effect was observed occurring at $42.89\text{ }^{\circ}\text{C}$, followed by a melting peak at $76.25\text{ }^{\circ}\text{C}$. The Tg shows an abrupt change in positioning of the baseline, which was a direct result of the change in heat capacity of the sample as it changed from a glassy to a rubber-like state. The significant difference between the melts of L-arginine in solution and that of solubilised gliclazide (Table 3.3) ($P<0.05$), was a clear indication of intermolecular interactions between L-arginine and gliclazide.

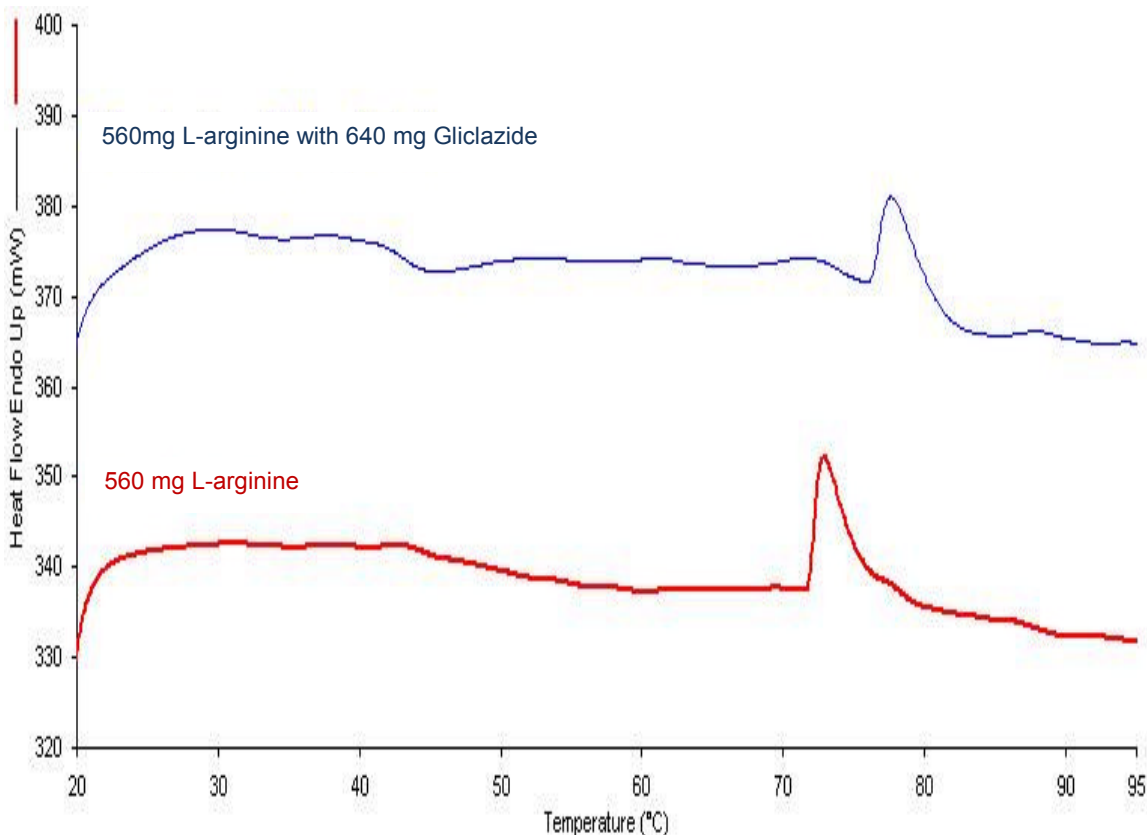


Figure 3.14. DSC of 40 µL L-arginine solution with dissolved gliclazide in comparison with 40 µL L-arginine solution, at a scan rate of 100 °C.min⁻¹.

Table 3.3. Summary of the thermokinetic changes occurring when solubilising gliclazide with L-arginine.

Excipient	Scan rate / °C.min⁻¹	Sample loading		Onset of T_m / °C	Enthalpy of transition / J.g⁻¹
		mg	µL		
Powder form:					
Xylitol	200	4		101.75	390.59
L-arginine	200	4		108.41	61.87
Gliclazide	200	4		184.68	137.25
In solution:					
560mg L-arginine	100		40	71.80	0.4815
560mg L-arginine with 640mg gliclazide	100		40	76.25	0.6965

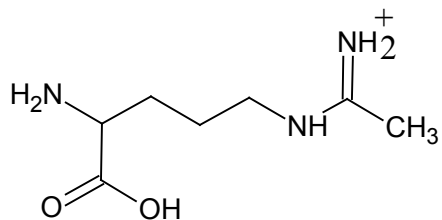
3.3.4.2. FTIR analysis

FTIR was therefore carried out in order to determine the interactions between gliclazide and L-lysine. FTIR analysis involves the interpretation of specific bond vibrations occurring at various wavelengths, with each compound displaying a specific fingerprint unique to its structure and its functional group.

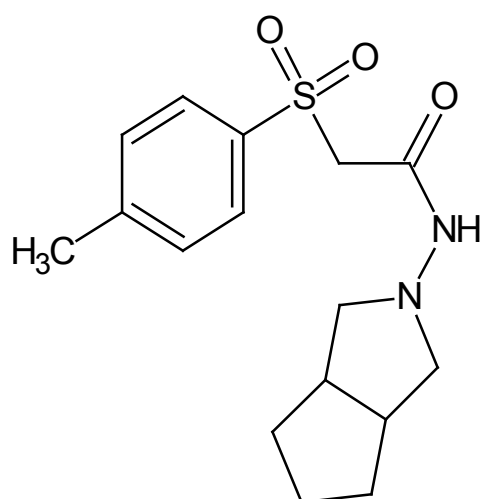
In order to effectively study bond vibrations, the excipients were first analysed to establish their true bonding vibrations relevant to their structural composition. The following was determined from their respective structures (Figure 3.15) and FTIR scans (Figure 3.16): L-arginine was composed of the carboxylic acids group, which have set vibrations at 3079, 2312, 1332 and 3079 cm⁻¹ for C=O, C-O and O-H functional groups respectively, as well as an amine group (C-N) (1008 cm⁻¹), and an imine group (C=N) (1685 cm⁻¹); gliclazide was composed of a double bonded aromatic (1896 cm⁻¹) and a single bonded cyclic chain (919 cm⁻¹), a sulphonamide group (S=O) (1348 and 1164 cm⁻¹), a ketone group (1710 cm⁻¹), and an amine functional group consisting of single bonded C-N (1087 cm⁻¹) and a single bonded N-H (3273 cm⁻¹) groups; monosodium glutamate was composed of the carboxylic acid group, which were observed to have set vibrations at 3409, 1307, 1687 cm⁻¹ for O-H, C-O, and C=O groups respectively, as well as an amine group (C-N) with a set bond vibration at 1094 and 1120 cm⁻¹; Sodium acetate was composed of a simple ethyl chain containing ester bond vibrations at 1641 cm⁻¹ (C-O) and 1412 cm⁻¹ (C=O), with a methyl end chain producing a specific bond vibration at 1020 cm⁻¹; xylitol consisted of a five-carbon alkane chain (2914 cm⁻¹) with alcohol end groups (3369 cm⁻¹ (O-H) and 1064 cm⁻¹ (C-O)); and finally the parabens were observed to have vibrational bonds for a double bonded C=C aromatic (1606 cm⁻¹) with an alcohol side chain (3270 cm⁻¹) on one side of the aromatic, and a carbonyl (C=O) (1679 cm⁻¹) and an ester group (C-O) (1167 cm⁻¹) followed by a propyl or butyl chain on the opposite end of the aromatic.

These specific bond vibrations were highlighted and extracted from the FTIR scans of the formulation, each bond vibration being designated as a donor group (excipient), with any alteration in bond vibration indicating possible intermolecular bonding between excipients. The aim was to highlight the cause of the solubility of gliclazide by labelling the bond vibrations of the formulated gliclazide-L-arginine complex and their respective donors. Once these vibrations were compiled (Table 3.4) absence of the single bonded N-H (3273 cm⁻¹) functional group was studied with the major groups of the other excipients being present and accounted for. This was indicative of hydrogen bonding between the amine group of

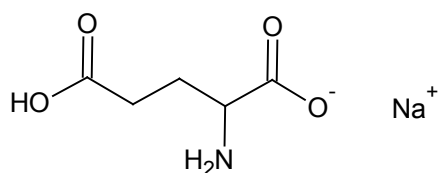
L-arginine



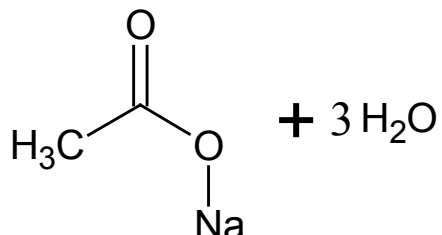
Gliclazide



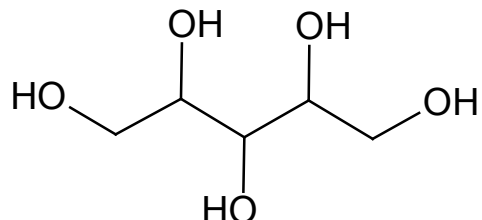
Monosodium glutamate



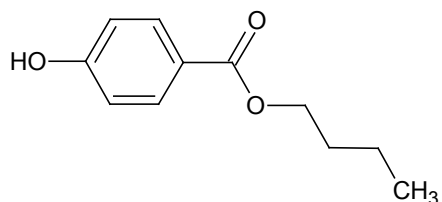
Sodium acetate



Xylitol



Butyl paraben



Propyl
paraben

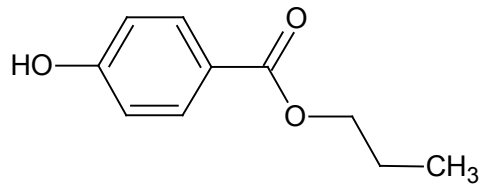


Figure 3.15. Respective chemical structures of the excipients used in the formulation of an oral liquid dosage form for gliclazide.

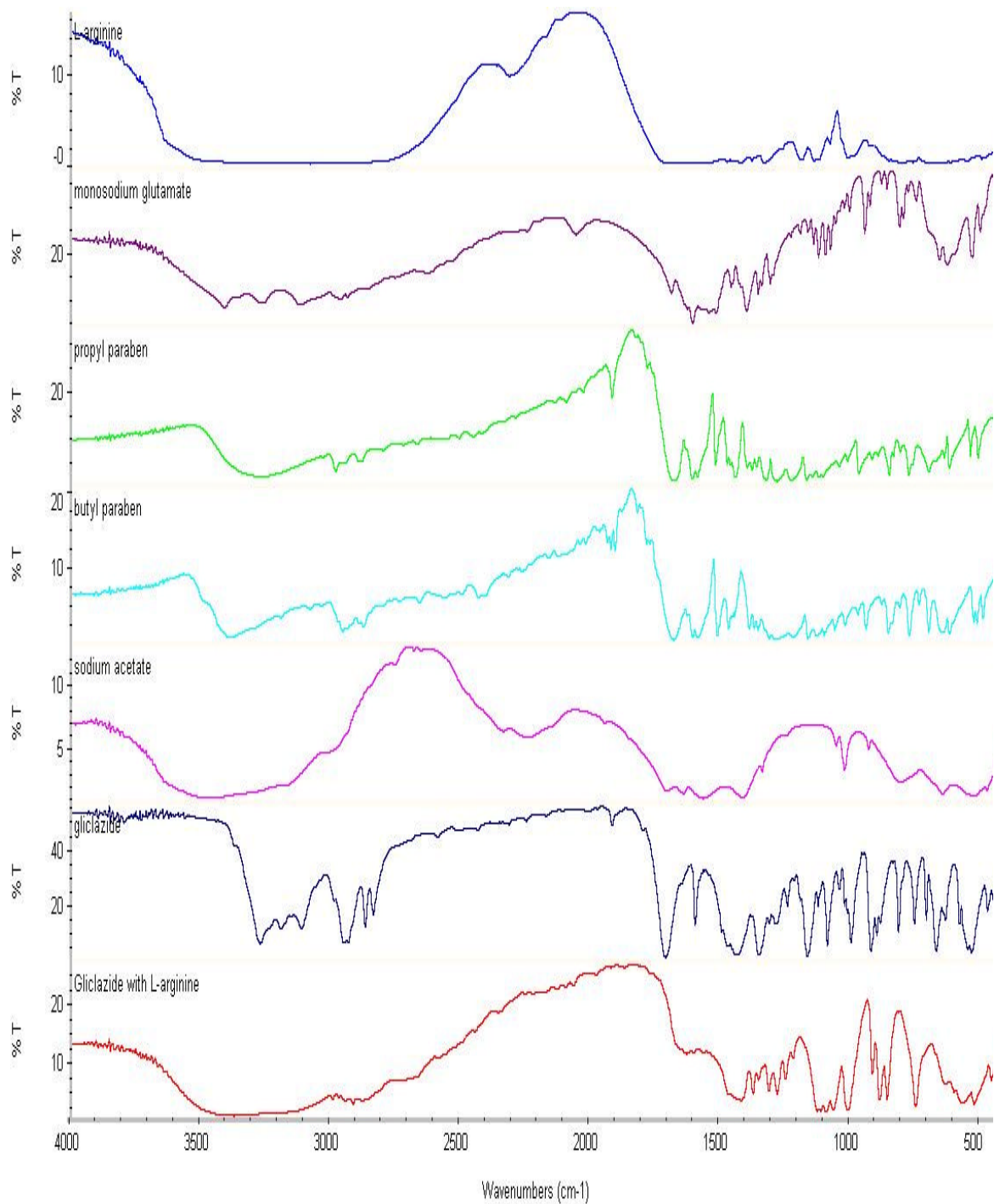


Figure 3.16. FTIR scans of the respective excipients used in the formulation of an oral liquid dosage form for gliclazide, with a comparative FTIR scan of the formulation.

Table 3.4. FTIR analysis of gliclazide in solution once formulated as an oral liquid dosage form, and its bond vibrations and their respective donors.

Peak	Wavenumber (cm ⁻¹)	Bond	Functional group	Donator
1	3327.	O-H	Alcohol	Xylitol
2	1419.50	C=O	Bend	Sodium acetate
3	2914.62	C=O	Carboxylic acid	L-arginine
4	1373.34	C-O	Carboxylic acid	L-arginine
5	1312.52	C-O	Carboxylic acid	Monosodium Glutamate
6	1280.08	C-O	Alkane	Parabens
7	1351.77	S=O	Sulfonamide	Gliclazide
8	1091.12	C-N	Amine	Monosodium Glutamate
9	1063.97	C-O	Alcohol	Xylitol
10	1007.32	C-N	Imine	L-arginine
11	913.28	C-H	Aromatic	Gliclazide
12	857.13	C-H	Stretch alcohol	Parabens

gliclazide and L-arginine. In order to fully understand the extent of the interaction H¹-NMR was carried out.

3.3.4.3. H¹-NMR

Proton nuclear magnetic resonance (H¹-NMR) spectroscopy can be defined as the absorptions and emission of electromagnetic radiation by the nuclei of hydrogen atoms when they are placed in a magnetic field (Field and Sternhell, 1989). The H¹-NMR spectrum can normally be represented as a graph of absorption intensity against the frequency of the radiation absorbed by the nuclei in the sample, with the intensity of the signal being proportional to the concentration of nuclei. This allows H¹-NMR to be a quantitative method of analysis, as the relative concentrations of components in the mixtures can be determined.

In the present study, L-arginine owed its hydrophilic properties to its highly polar molecular structure. D₂O was the solvent in which H¹-NMR could be performed was, as L-arginine was

soluble. Gliclazide was practically insoluble in D₂O, however when used in combination with L-arginine its solubility with the solvent increased, making D₂O a good candidate for H¹-NMR analysis. The choice of solvent also had an impact on the quality of H¹-NMR analysis, as each solvent gives rise to a different reference point and highlights and masks different functional groups. D₂O (heavy water) was known to be highly enriched in hydrogen isotope deuterium, however, the use of heavy water results in protons in the –OH groups being replaced with deuterium atoms. Deuterium has an even number of protons and neutrons in its nucleus, and thus does not show up in a proton NMR graph.

L-arginine has 16 protons in its structure, one of which is designated to an –OH group in its structure (Figure 3.17), this proton was therefore expected to be absent from the analytical H¹-NMR graphs, with ultimately only 15 protons emitting a signal. Gliclazide has no –OH groups and thus is expected to emit its full 22 protons.

From the H¹-NMR graphs, L-arginine was shown to display its 15 protons as expected (Figure 3.17), with the 1:1 molar ratio of L-arginine with gliclazide emitting the presence of only 35 protons (Figure 3.18). This reduction in protons is a quantitative conclusion of intermolecular bonding occurring between the compounds at a 1:1 ratio, thereby aiding in the increased polarity of the gliclazide molecular structure, and thereby enhancing its solubilising properties.

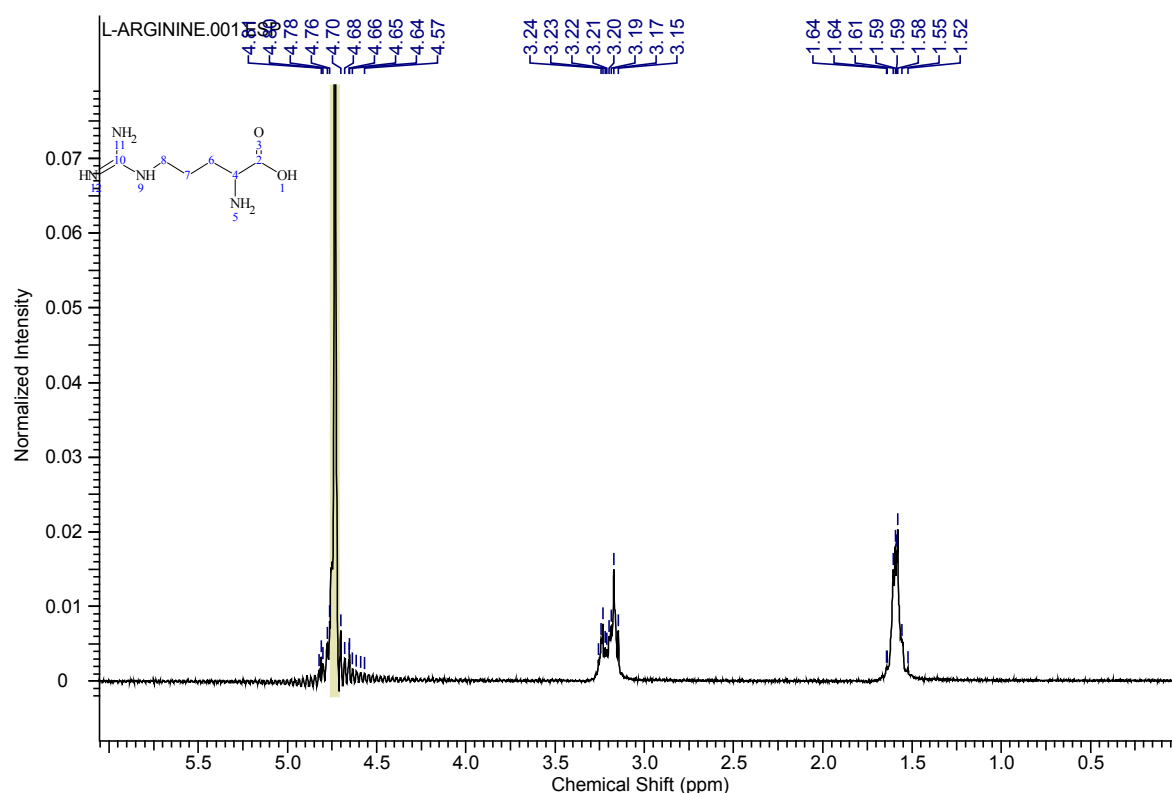


Figure 3.17. H^1 -NMR absorption graph for L-arginine using D_2O (reference at 4.77 ppm); 15 protons were detected. ($n=3$)

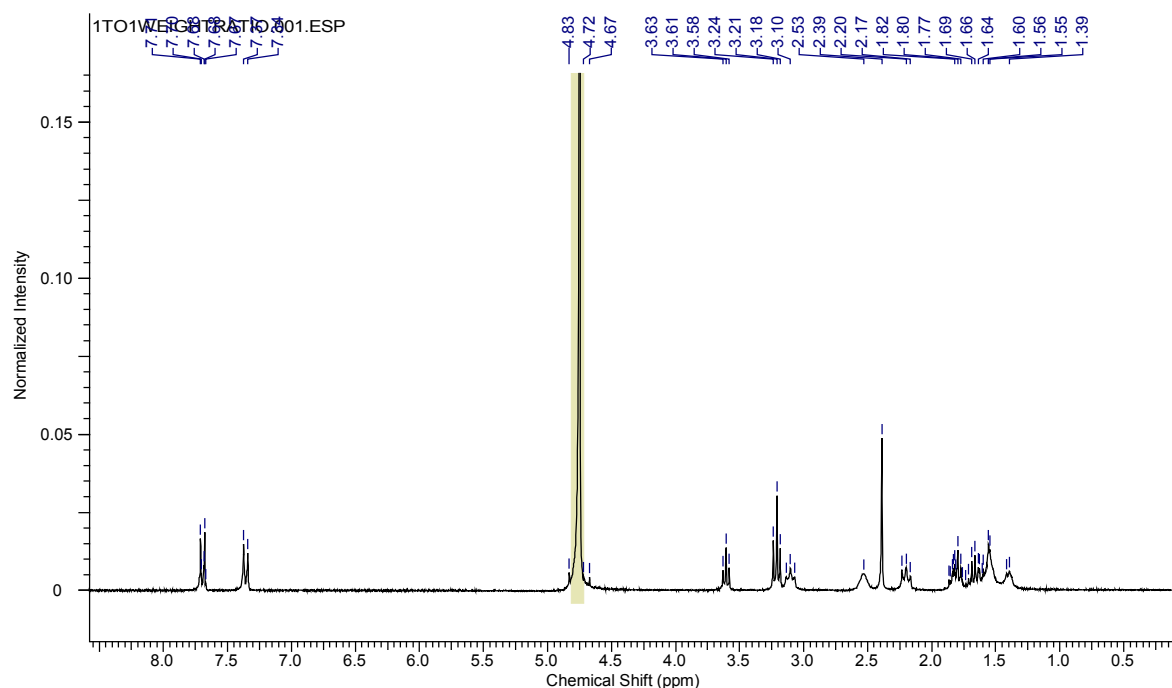


Figure 3.18. H^1 -NMR absorption graph for a 1:1 molar ratio mix of L-arginine with gliclazide using D_2O (reference at 4.77 ppm); 35 protons were detected. ($n=3$)

3.4. Conclusion

Enhancing the solubility profile of gliclazide was successfully carried out in two ways. The first formulation method involved the use of L-arginine, with no modification of the pH of the solution. The advantage of using the amino acid was that, as well as all of the excipients being GRAS listed and within the recommended guidelines, the formulation was within regulation to be potentially administered to paediatrics. The second formulation method involved the use of a co-solvent coupled with a surfactant; this formulation would be safe for use for adults as all excipients used within the formulation were GRAS listed and within the recommended dose range.

Both sets of formulations had chemical and organoleptic stability during the nine months storage under fridge (5 °C), room temperature (25 °C) and accelerated (40 °C) conditions.

CHAPTER 4

Optimisation of an extraction protocol and development of an oral liquid formulation for L-arginine

CHAPTER 4

Optimisation of an extraction protocol and development of an oral liquid formulation for L-arginine

4.1. Introduction and Aims

4.1.1. Amino Acids

Amino acids are one of the critical components that serve as building blocks of life and make up the foundation of proteins. The human body consists of 20 amino acids that are subdivided into 7 distinct groups (Table 4.1). Amino acids are made up of an amine group, carboxylic acid group and a side chain that varies between the different amino acids. There are twenty two different amino acids which are incorporated to form polypeptides/proteins and are referred to as standard amino acids. Of these, eight amino acids are classified as “essential” as they cannot be produced by the human body and are sourced from the diet.

Table 4.1. Summary of amino acids based on their difference in structure and physicochemical properties.

Group class	Amino acid
Aliphatic	Alanine (ala), Glycine (gly), Isoleucine (ile), Leucine (leu), Proline (pro) and valine (val)
Aromatic	Phenylalanine (phe), Tryptophan (trp), and Tyrosine (tyr)
Acidic	Aspartic acid (asp) and Glutamic acid (glu)
Basic	Arginine (arg), Histadine (his) and Lysine (lys)
Hydroxylic	Serine (ser) and Threonine (thr)
Sulphur-containing	Cysteine (cys) and Methionine (met)
Amidic (amide group-containing)	Asparagine (asn) and Glutamine (gln)

4.1.2. Arginine

4.1.2.1. Therapeutic effect of Arginine

Although arginine can be synthesised by the body, it does so in insufficient quantities, thereby requiring increased amounts to be absorbed through diet. This basic amino acid can be found in many food sources, including dairy products, meat, poultry and fish. It has a versatile role in the human body which includes; cell division, wound healing, immunity towards illness, production of nitric oxide causing relaxation of blood vessels, and most importantly removal of ammonia from the body in the urea cycle.

4.1.2.2. Structure and Metabolism

L-arginine consists of a 4-carbon aliphatic straight chain with the distal end of the chain being capped by a guanidinium group and the other by a carboxylic acid group. The amino acid has 3 pKa values; 2.01 (pK_a_1), 9.04 (pK_a_2) and 12.48 (pK_a_3) (Figure 4.2.). The pK_a of the guanidinium group ensures the cationic charge of L-arginine in most media regardless of the pH and therefore enables L-arginine to exert its basic chemical properties.

The metabolism of L-arginine (carried out by the enzyme arginase) breaks down the amino acid into its metabolites L-ornithine and urea.

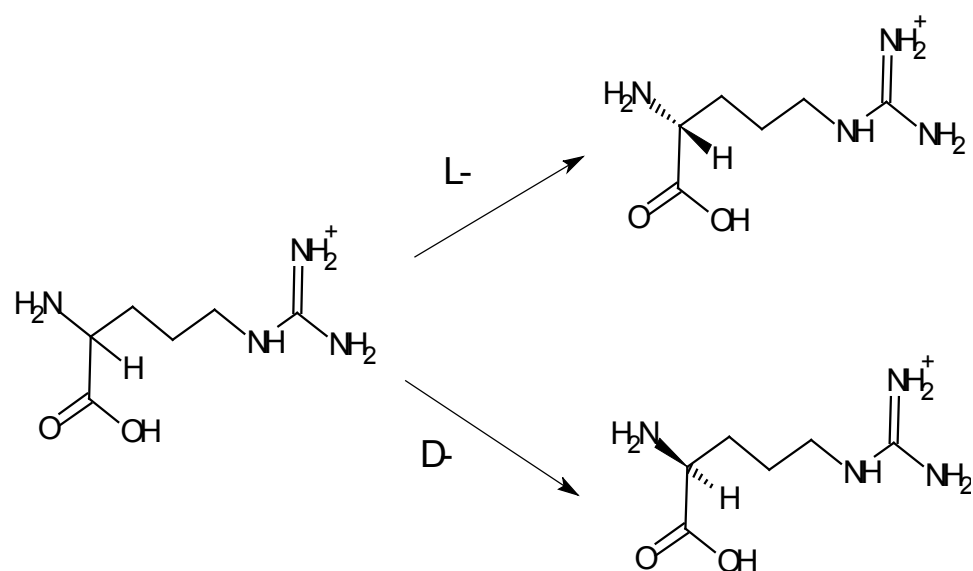


Figure 4.1. Chemical structures of Arginine and its stereo forms.

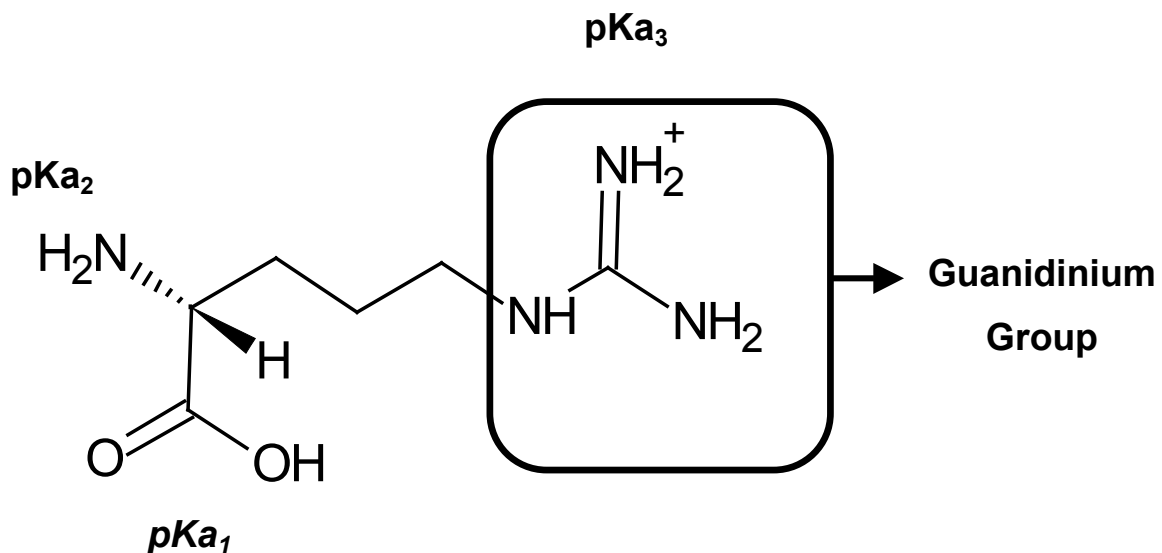


Figure 4.2. Chemical structure of L-arginine: 3-carbon aliphatic straight the distal end of which is capped by a guanidinium group.

Table 4.2. Urea Cycle disorders.

Urea Cycle Disorders	Definition
Hyperammonaemia in carbamylphosphate synthetase deficiency	Autosomal recessive metabolism disorder
Ornithine carbonyl transferase deficiency	Genetic disorder resulting in a mutated and ineffective form of the enzyme ornithine transcarbamylase
Hyperammonaemia in citrullinaemia	Autosomal recessive urea cycle
Arginosuccinic aciduria	Arginine succinase may be damaged or missing within the urea cycle, preventing the conversion of arginine succinate into arginine.

4.1.3. Aim

In the human body, arginine plays a central role in the urea cycle. Although it may not be an essential amino acid for adults, in infants the nutritional value is extremely vital, as the rate of synthesis of L-arginine in infants may not be fast enough to cover all of the requirements of the tissues.

Currently L-arginine is prescribed to patients who have urea cycle disorder (Table 4.2.) in 500 mg tablets or 100 mg.mL⁻¹ dosage forms, with currently no licensed oral liquid formulation present on the market.

In the developmental stages of drug formulation, the organoleptic properties are crucial in determining the acceptability of the drug formulation for the patient. The organoleptic properties include; smell, colour, appearance and taste. From the amino acids listed in table 4.1, the basic amino acids display a fairly bitter taste when in solution, particularly arginine which is extremely bitter in taste, and can be used in D- and L- stereochemical form (Figure 4.1).

The aim of the research presented in this chapter was to develop a stable oral liquid formulation of L- arginine. To achieve this, the work was divided into two phases:

- Phase 1: development of a validated calibration protocol for the quantification of L-arginine
- Phase 2: formulation of a chemically stable oral liquid preparation of L-arginine (100 mg.mL⁻¹) with improved shelf life

4.2. Materials and Method

4.2.1. Materials

L-Arginine, ninhydrin, tartaric acid, sodium benzoate, sorbitol, monosodium phosphate, disodium phosphate, phosphoric acid, and trifluoroacetic acid (TFA) were purchased from Sigma (UK). Raspberry concentrate was purchased from Flavex International Ltd. (Hertford, UK).

4.2.2. Method

4.2.2.1. Protocol for Ninhydrin-UV Calibration of L-arginine

4.2.2.1.1. Preparation of 1 M sodium phosphate

A 1 M stock solution of sodium phosphate was prepared by dissolving 5.723 g of monosodium phosphate and 7.425 g of disodium phosphate in 100 mL distilled water. 2.5 mL of this stock solution was added to 97.5 mL of distilled water under continuous stirring, to form a final concentration of 25 mmol.L⁻¹. The pH of this solution was then adjusted to pH 4.5 with phosphoric acid.

4.2.2.1.2. Preparation of stock solution of L-arginine

A 3 mg.mL⁻¹ concentration of L-arginine was produced by adding 30 mg of L-arginine to 10 mL of distilled water. By carrying out serial dilution, 1 mL of the 3 mg.mL⁻¹ stock solution was added to 10 ml distilled water, to produce a final concentration of 300 µg.mL⁻¹

4.2.2.1.3. Ninhydrin assay

The various stages for the development of calibration curve are outlined below:

1. Dilutions as listed in table 4.3 were prepared with samples being vortexed for 10 seconds after the addition of 25 mmol sodium phosphate buffer and addition of ninhydrin.
2. Samples were heated for 20 minutes at 80 °C in a pre-warmed water bath.

3. After 20 minutes, the samples were removed from the water bath and left to cool on the bench.
4. Each sample was diluted with 25 mmol.L⁻¹ sodium phosphate buffer at a ratio of 1:3 (sample:buffer ratio).
5. The samples were analysed using a UV spectrophotometry at a wavelength of 560 nm.

4.2.2.2. pH titrations using tartaric acid

A 100 mg.mL⁻¹ solution of L-arginine in distilled water was prepared, to which different concentrations of tartaric acid were added (w/v). Once the tartaric acid was fully dissolved, the pH of the solution was measured using a calibrated Hydrus 500 pH meter. The following tartaric concentrations (% w/v) were titrated and their pH measurements recorded: 0.1, 0.5, 1.0, 1.5, 2.0, 2.5, 3.0, 3.5, 3.6, 3.7, 3.75, 3.8, 4.0 % (w/V).

4.2.2.3. Oral liquid formulation recipe of L-arginine

To obtain a final concentration of 100 mg.mL⁻¹ of L-arginine, 5 g of the amino acid was dissolved in 42 mL of distilled water and left to stir for 5 minutes until the amino acid had fully

Table 4.3. Protocol for the preparation of L-arginine-ninhydrin solutions at various concentrations.

L-arginine concentration µg.mL ⁻¹	L-arginine stock (300 µg.mL ⁻¹) /mL	25 mmol.L ⁻¹ sodium phosphate buffer pH4.5 /mL	Ninhydrin /mL
30	0.20	1.80	1.00
36	0.24	1.76	1.00
45	0.30	1.70	1.00
54	0.36	1.64	VORTEX
60	0.40	1.60	VORTEX
66	0.44	1.56	VORTEX
75	0.50	1.50	VORTEX
Blank	0.00	2.00	1.00

solubilised. To reduce the pH of the solution, 2 g of tartaric acid (4 % w/v) was then added and left to stir until the acid had fully dissolved. A 0.5 % (w/v) concentration of the preservative, sodium benzoate (0.25 g) was then added under continuous stirring, followed by 250 µL of raspberry concentrate (0.5 % v/v), and 5 g of sorbitol (10 % w/v). The solution was kept under continuous stirring until all of the constituents had fully dissolved to reveal a clear solution. The volume of the solution was then adjusted to 50 mL and stored in amber coloured glass bottles at 5 °C, 25 °C (40 % humidity) and 40 °C (75 % humidity). Samples were prepared and stored in triplicate.

4.3. Results and Discussion

4.3.1. Optimisation of a calibration protocol for the detection and quantification of L-arginine in solution.

4.3.1.1. Preliminary investigations

The establishment of a validated calibration method to accurately quantify the presence of L-arginine in solution was essential. The primary hurdle in the development of an assay was the absence of a specific absorbance wavelength for L-arginine in the UV spectrum. Previous published protocols in the literature required multiple and complex stages of extraction and often relied on by product characterisation of arginine. The initial focus of our work was to further develop and optimise published analytical protocols with the aim of developing a simple and robust direct method.

One such method included utilising the fluorescence ability of L-arginine and its separation from human urine samples (Markowski et al, 2007) using a reverse phase HPLC system. For our investigation, this method was simplified on an isocratic HPLC system, with mobile phase comprising of di-sodium hydrogen phosphate buffer (pH 6.88), methanol and acetronitrile, at concentration ratios of 90:5:5 respectively which was pumped at a rate of $1\text{ mL}\cdot\text{min}^{-1}$ through a C18 column. Fluorometric detection was carried out at a maximum emission wavelength of 455 nm and at a maximum excitation wavelength of 338 nm. A $1\text{ mmol}\cdot\text{L}^{-1}$ stock solution of L-arginine was then prepared in methanol:water (1:1 v/v), with further diluted samples being prepared in water ($0.05\text{--}0.280\text{ mmol}\cdot\text{L}^{-1}$). As shown in figure 4.3, $20\text{ }\mu\text{L}$ of the prepared sample was injected and no separation of L-arginine from the diluents was observed even after 30 minutes. This was in contrast with the work carried out by Markowski and co-workers (2007), who detected a peak after 24 minutes. The criteria of the calibration protocol was to produce one that was simple and quick, by having a potential retention time of no longer than 1 hour as it would lead to lengthy analytical cycles.

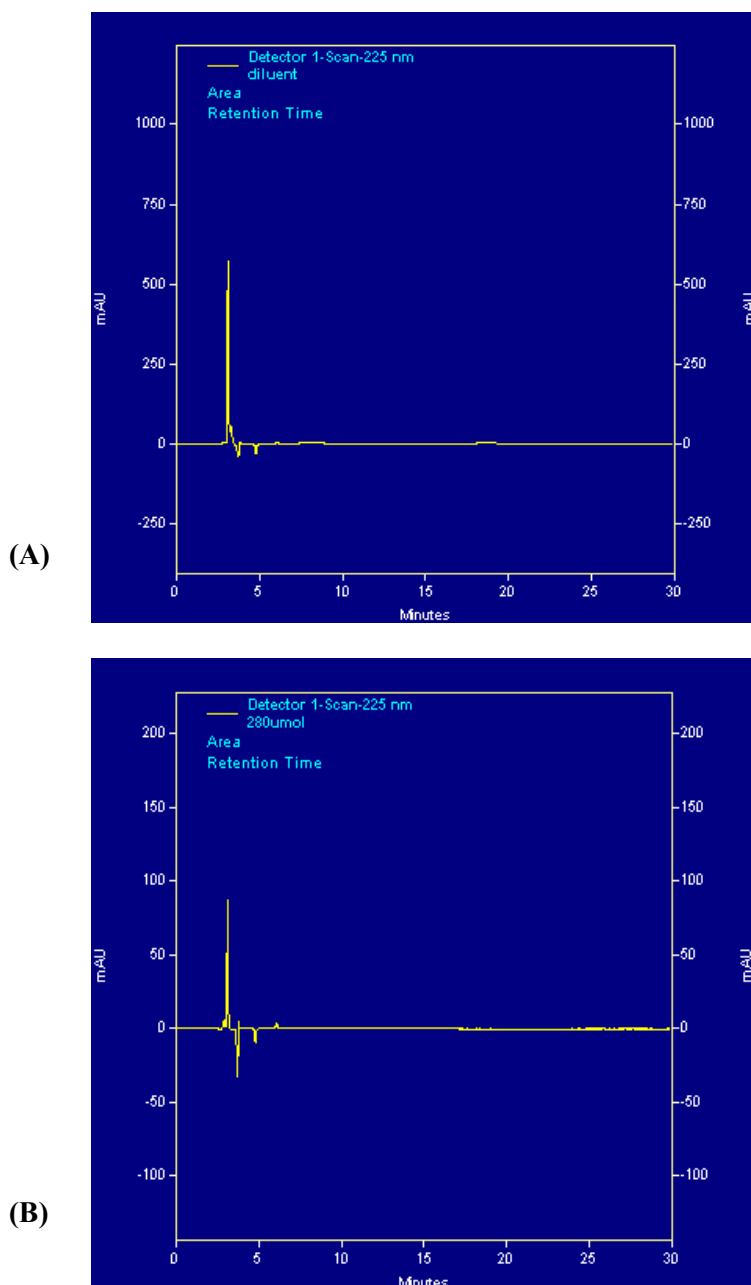


Figure 4.3. HPLC spectra of (A) methanol:water mix at a 1:1 ratio and (B) 0.28 mmol.L⁻¹ concentration of L-arginine. The spectra were very similar with no definite peak of L-arginine being detected after 30 mins.

In a separate study by Bi and Singh (1999), trifluoroacetic acid (TFA) was used in the separation of arginine from Arg⁸-vasopressin. TFA has been widely used in liquid chromatography as a buffering agent, allowing for the separation of organic compounds, particularly for the separation of peptides and small proteins, as well as enhancing the resolution of peptide separation and the presentation of the peaks (Huang et al, 2004). The protocol was modified by changing the pH of the control sample to 4.5, instead of 5 as used by Bi and Singh (1999). This was to ensure that the conditions of the calibration would be in an acceptable pH range to match the proposed L-arginine formulation in solution. The calibration protocol involved injection of 20 µL of a 25 mg.mL⁻¹ stock solution of L-arginine prepared in distilled water. C18 column (maintained at 35 °C) using an isocratic HPLC system at a flow rate of 1.5 mL.min⁻¹ was used at a wavelength of 220 nm (Bi and Singh, 1999), with the mobile phase consisting of 0.1 % TFA in water and methanol (70:30 v/v).

However L-arginine was not detected under these conditions (Figure 4.4). Due to non-specificity of L-arginine and its wavelength detection point, a diode-array was utilised to detect across larger ultra-violet spectrum. A protocol was adapted from Huang and co-workers (2004) in which a photo-diode array ranging from 200-300 nm had been used to analytically determine L-arginine and its mono- and dimethylated metabolites. Mobile phase consisting of water and ACN (90:10 v/v) containing 0.5 % TFA (v/v), was pumped through an isocratic HPLC setup at a flow rate of 0.2 mL.min⁻¹, with the diode array set between 200-400 nm. 5 µL samples of L-arginine, prepared from a stock solution of 1.0 mmol.L⁻¹ L-arginine in 0.1 mol.L⁻¹ HCl and serial dilutions carried out in water (5 – 120 µmol.L⁻¹), were injected into the HPLC. The expected retention time of L-arginine according to the Huang protocol (2004) was 3 minutes, however no clearly defined peak for L-arginine was detected (Figure 4.5). The concentration of L-arginine was further increased to 0.5 – 0.8 mmol.L⁻¹ but did not yield the desired results.

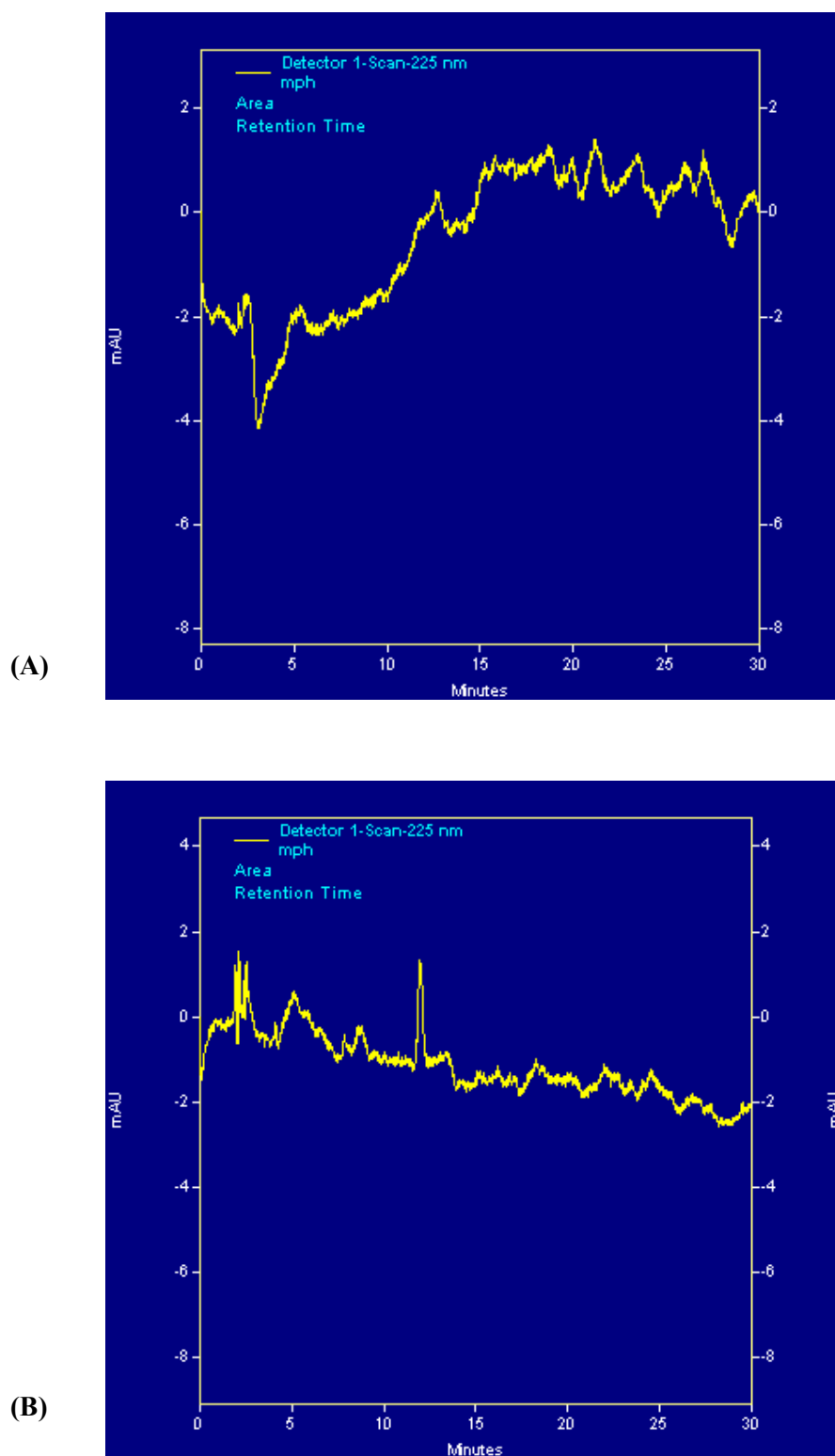


Figure 4.4. HPLC spectra for (A) Solvent front of the mobile phase consisting of 0.1 % TFA in water and methanol (70:30 v/v) and (B) 50 $\mu\text{g.mL}^{-1}$ sample of L-arginine. After 30 minutes, no definite solvent front or amino acid was detected. Both HPLC spectra displayed an unsteady baseline, which was attributed to the low sensitivity of the protocol (milli-absorbance unit did not exceed 2 mAU).

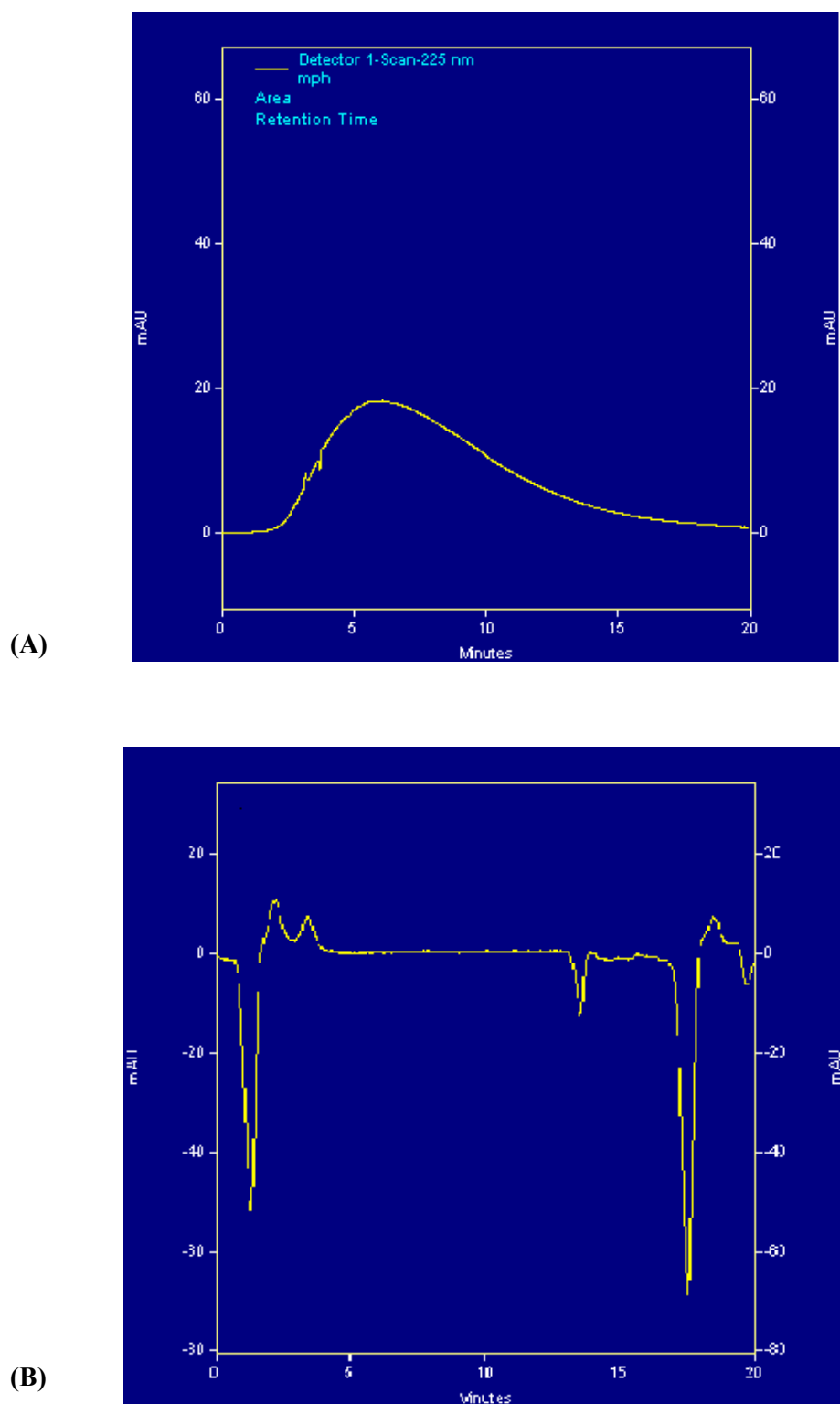


Figure 4.5. HPLC spectra for (A) solvent front of the mobile phase containing water and acetonitrile (90:10 v/v) with 0.5 % (v/v) TFA, and (B) 0.08 mmol.L⁻¹ L-arginine. The injection of 0.08 mmol.L⁻¹ resulted in an alteration in the detection of the solvent front, with no definite peak corresponding to L-arginine.

4.3.1.2. Development of Ninhydrin assay

The next strategy was to use a colorimetric derivatisation approach (second compound) that would undergo reaction with L-arginine and produce a UV detectable end product. Ninhydrin undergoes chemical reaction with amino acids in water to produce a distinct purple colour and has been used for the detection of peptides in a wide range of studies over a number of years, including: non-ionic surfactant vesicles and liposomes (Brewer *et al* 1995), bilosomes (Conacher *et al*, 2001), tissue samples (Starcher, 2001), and amino acid determination in polymer membranes (Zhu *et al*, 2002).

Using a modified protocol from Kowalcuk and co-workers (2007), concentrations (45-90 $\mu\text{g.mL}^{-1}$) of L-arginine were prepared in phosphate buffered saline at pH 9 and vortexed, after which 0.5 mL of ninhydrin was added to the mixture. The mixture was vortexed thoroughly before being heated at 80 °C for 20 minutes. The solution was then left to cool on the bench before adding 3 ml of propan-2-ol:water (1:1) to 1 ml of the ninhydrin mixture. After ensuring the solution had thoroughly mixed, the sample was analysed using a UV spectrophotometer at wavelength 404 nm (Figure 4.6). The blank used was a sample that had gone through

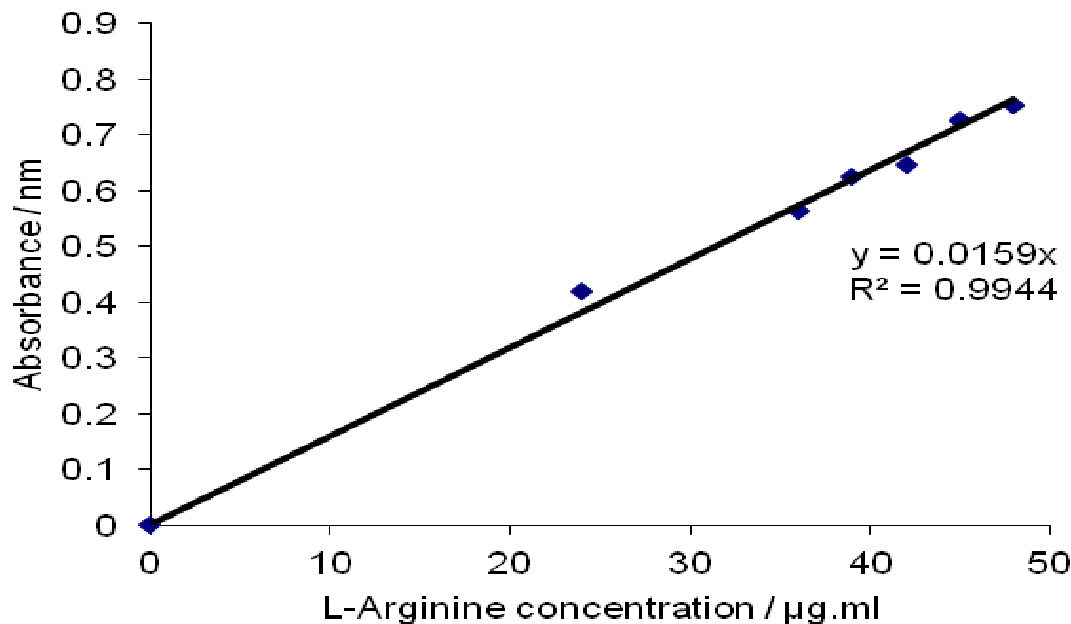


Figure 4.6. Calibration of L-arginine ($\lambda=404$ nm) using phosphate buffered saline at pH 9. A linear regression was achieved ($R^2=0.9944$), with intercept passing through the origin. (n=3)

the ninhydrin protocol without the addition of the amino acid. A linear regression line was obtained with intercept going through the origin ($R^2=0.9944$). The ninhydrin assay is widely used to study peptide hydrolysis into its constituent amino acids and can therefore be easily adapted to quantify individual amino acids. Firstly the phosphate buffered saline at pH 9 was omitted and replaced with a 25 mmol.L^{-1} sodium phosphate buffer (pH 4.5), with the pH of the buffer being more suited to the required pH of the ultimate formulation to be prepared in this study. Secondly, the ninhydrin volume was increased to 1 ml and was diluted with 3 ml of the buffer (pH 4.5). L-arginine was then added to ninhydrin at various concentrations ranging from $30\text{-}75 \mu\text{g.mL}^{-1}$ (Table 4.2), producing a calibration graph with a y-intercept of 0.363 nm (Figure 4.6). Ninhydrin has two distinct lambda max absorbancies, 404 nm and 560 nm (Meyer, 1957). As seen from figure 4.7, a higher peak area was displayed at 560 nm suggesting a stronger absorption band for L-arginine. The ninhydrin assay described was ultimately modified using a wavelength of 560 nm which produced a calibration curve with the y-intercept near zero ($R^2=0.9852$) (Figure 4.8). A calibration validation could now be carried out using this simplified method for L-arginine quantification using UV spectroscopy.

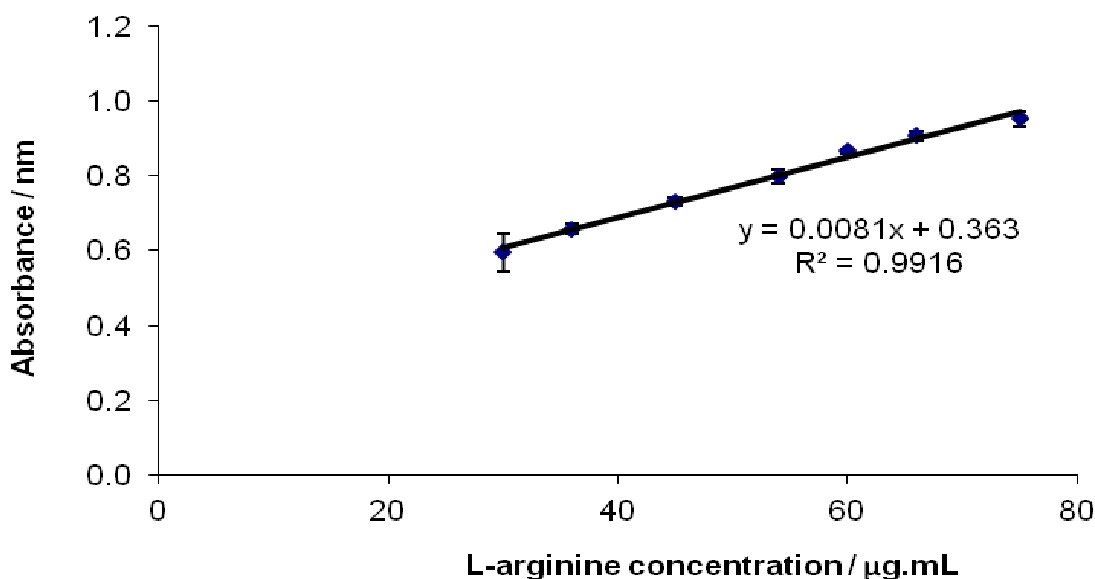


Figure 4.7. Calibration of L-arginine ($\lambda=404 \text{ nm}$) using a modified ninhydrin assay with 25 mmol.L^{-1} sodium phosphate buffer at pH 4.5. A linear regression line was achieved ($R^2=0.9916$), with a y-intercept of 0.363 nm. (n=3)

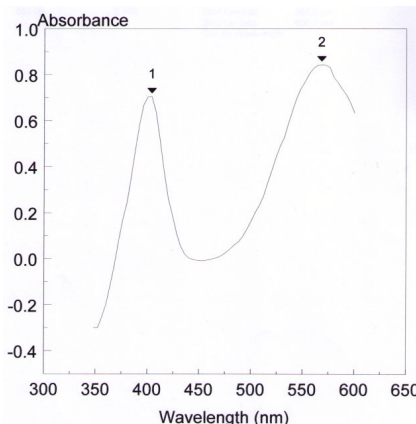


Figure 4.8. Lambda max of L-arginine solution after being treated with the modified ninhydrin assay. Two distinctive Lambda max were determined at 404 nm and 560 nm.

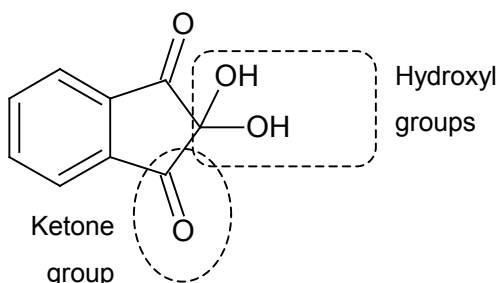


Figure 4.9. Chemical structure of ninhydrin ($C_9H_6O_4$), displaying its main functional groups; ketone and hydroxyl groups.

4.3.1.3. Ninhydrin mechanism

Ninhydrin (2,2-dihydroxy-1,3-indanedione), a white crystalline powder, has a melting range of 240–245 °C, and is soluble in water and alcohols (Wu *et al*, 2005). The exposure to high temperatures in solution (100 °C) causes the compound to display a distinct red colour. Ninhydrin has been widely used for the analytical determination of free amino groups and carboxylic groups in proteins and peptides due to its ability to change colour in the presence of an amino acid from a distinct red to Ruhemann's purple. Ninhydrin is composed of a carbonyl compound with reactive ketone groups (proton accepting) and hydroxyl groups (Figure 4.9). It is the deprotonation of these hydroxyl groups that initiates the formation of Ruhemann's purple, illustrated by the mechanism in figure 4.10. The reaction mechanism takes place in three stages: (1) reduction of ninhydrin to form hydrindantin and a water molecule; (2) the oxidative deamination, hydrolysis and decarboxylic reactions of L-arginine, catalysed by the water molecule, finally producing its degradative products which include aldehyde, carbon dioxide and ammonia; and (3) direct combination of hydrindantin, ninhydrin and ammonia to form Ruhemann's purple (MacFadyen and Fowler, 1950). The final product is detected with UV at a maximum absorbance of 560 nm.

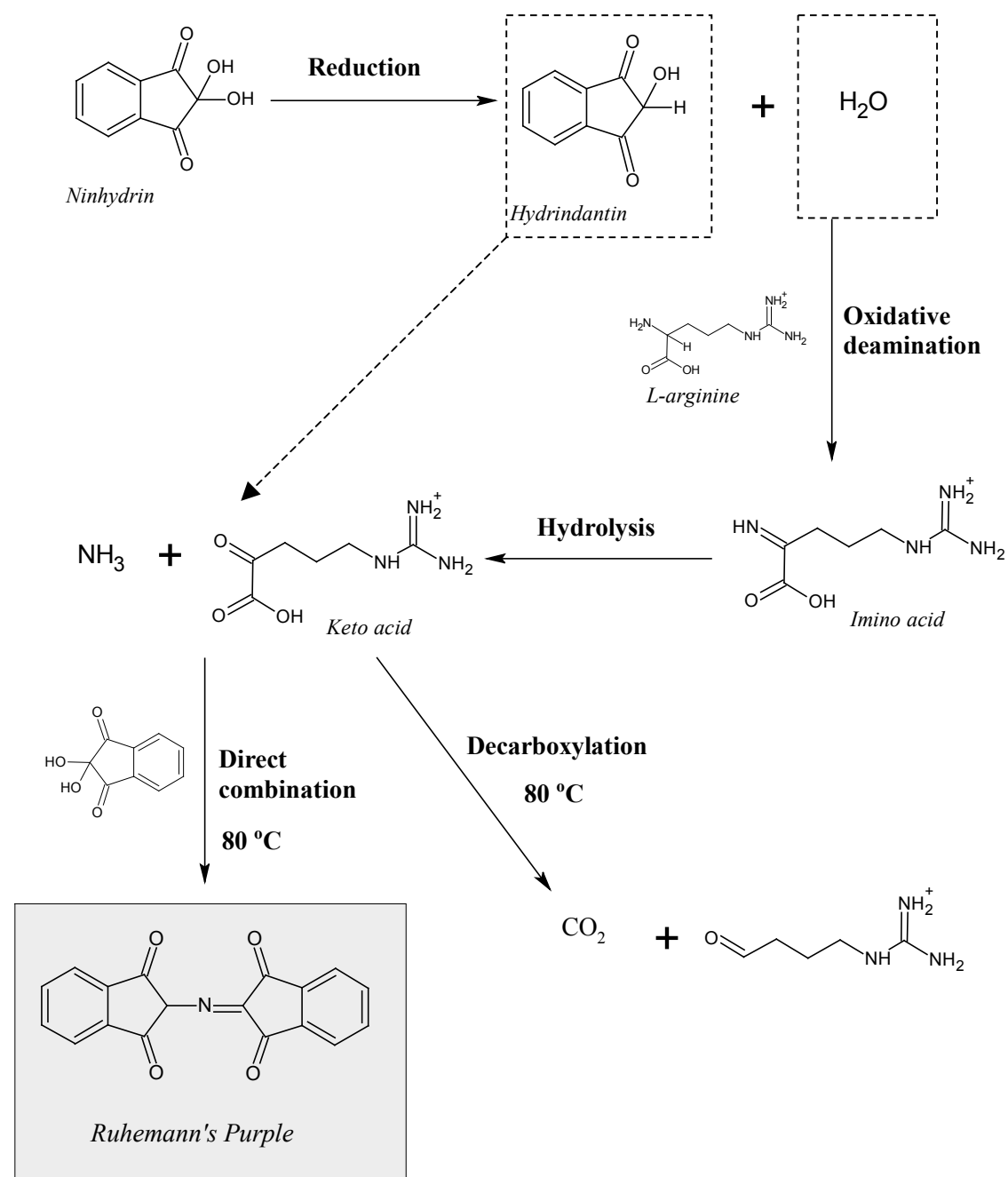


Figure 4.10. Mechanism of L-arginine and ninhydrin in the production of Ruhemann's purple. Ninhydrin is reduced to hydrindantin with the formation of water. This initiates the oxidative deamination reaction of L-arginine into an imino acid, with subsequent hydrolysis producing a keto acid and an ammonia molecule. When exposed to heat (80 °C) the keto acid undergoes further decarboxylation to form the degradation products of L-arginine (carbon dioxide and an aldehyde). Simultaneously, hydrindantin condenses with ammonia and ninhydrin to produce the intense blue-purple pigment known as Ruhemann's purple. (Modified from MacFadyen and Fowler, 1950; Wu et al, 2005)

4.3.2. Calibration Validation using a modified ninhydrin assay

An in-direct, simplified UV spectroscopy method was developed and validated for the determination of L-arginine (Table 4.3), at a wavelength of 560 nm, using ninhydrin to quantify L-arginine. Results are presented in table 4.4.

4.3.2.1. Linearity

The linearity of the UV spectroscopy method was evaluated by preparing the standard curve for L-arginine on three consecutive days. The peak area was plotted against the concentration and the calibration response was assessed for variances. The results showed that the Beer Lambert's law was obeyed in the range of 30-75 $\mu\text{g.mL}^{-1}$ with the linear plot giving the regression equation of $y=0.0107x$ ($R^2=0.9852$), which is represented in figure 4.11.

4.3.2.2. Precision

In order to assess the reproducibility of the calibration protocol, the calibration method was carried out in triplicate over a period of three days for interday precision, and in triplicate on the same day for intraday precision. It was concluded that the calibration method was

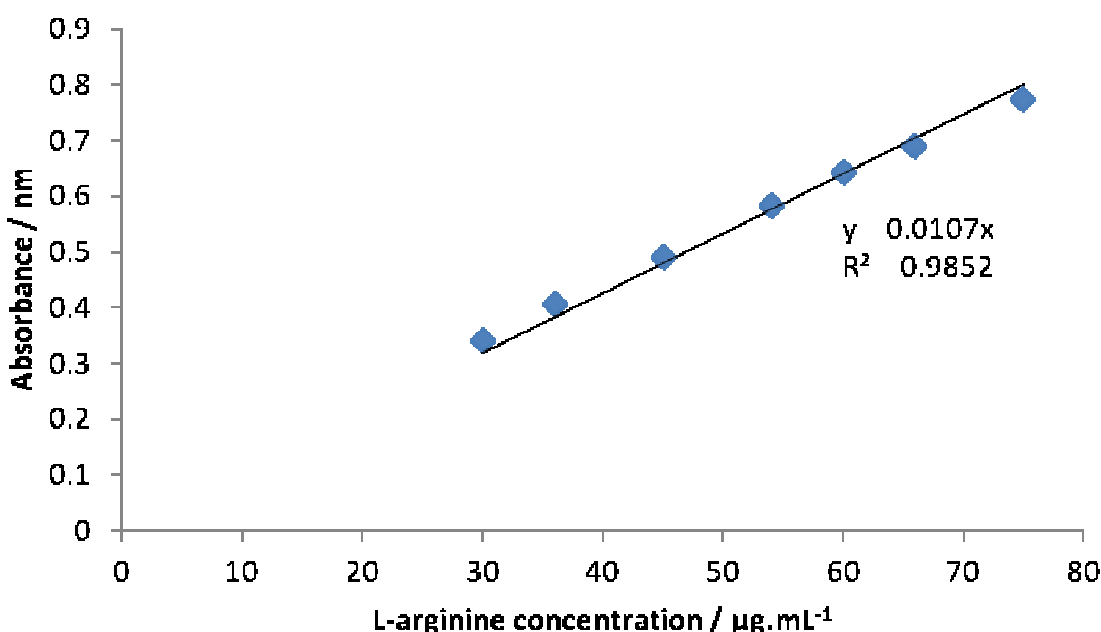


Figure 4.11. Calibration of L-arginine ($\lambda=560\text{nm}$) using a modified ninhydrin assay with 25 mmol.L^{-1} sodium phosphate buffer at pH 4.5. A linear regression line was achieved ($R^2=0.9852$), giving a regression equation of $y=0.0107x$. (n=3)

reproducible, with inter-day and intra-day precision being calculated to be 100 %. Data was analysed using ANOVA statistical test, with the resulting inter-day and intra-day precision being calculated to have a variance of $P>0.05$.

4.3.2.3. Accuracy

The accuracy of the developed method was determined from three concentrations of L-arginine in the ninhydrin protocol, representing the lower section of the standard curve (21, 27 and 33 $\mu\text{g.mL}^{-1}$). Accuracy of the three concentrations was in the range of 101-100 %.

4.3.2.4 Limit of detection (LOD) and limit of quantification (LOQ)

The LOD of an individual analytical procedure can be defined as the lowest amount of analyte in a sample which can be detected but not necessarily quantifiable as an exact value (EMEA, 1995). From the calibration range the LOD was calculated to be 0.112 $\mu\text{g.mL}^{-1}$.

The LOQ of an individual analytical procedure can be defined as the lowest amount of analyte in a sample which can be quantitatively determined with accuracy and precision. From the calibration range the LOQ was calculated as 0.34 $\mu\text{g.mL}^{-1}$.

Table 4.4. Summary of calibration validation of L-arginine.

Criteria	Validation
$Y=$	0.0107
R^2	0.9852
Intra-day Precision	100 %
Inter-day Presicion	100 %
Accuracy ($\pm SD$) 21 $\mu\text{g.mL}^{-1}$	101.00 (± 0.45)
Accuracy ($\pm SD$) 27 $\mu\text{g.mL}^{-1}$	100.03 (± 0.53)
Accuracy ($\pm SD$) 33 $\mu\text{g.mL}^{-1}$	100.90 (± 0.43)
LOD $\mu\text{g.mL}^{-1}$	0.112
LOQ $\mu\text{g.mL}^{-1}$	0.34

4.3.3. Optimisation of an oral liquid formulation for L-arginine: rational for taste masking

When formulating a pharmaceutical dosage form, the organoleptic properties chosen during the developmental stages are crucial in determining patient compliance. For oral liquid preparations these properties include; pleasant smell, smooth consistency, and most importantly a palatable taste (not too sour or too sweet). Taste consists of the following five basic qualities: sourness produced by hydrogen ions such as hydrochloric acid, acetic acid, and citric acid; saltiness produced by sodium chloride; sweetness produced by sugars; and bitterness produced by quinine, caffeine and magnesium chloride (umami) (Zheng and Keeney, 2006).

The hydrophilic properties of L-arginine enables large quantities of the drug to be solubilised in water (148.7 g.L^{-1}), resulting in increased ionised guanidinium groups to be present and subsequently increases the alkalinity of the solution (100 mg.mL^{-1} : L-arginine in water = pH 11). As the concentration of the guanidinium groups increases, the bitterness of the solution also increases. In order to prepare a formulation with palatable properties (by reducing the bitterness expressed by L-arginine), a pharmaceutical sweetener was added. Sorbitol ($\text{C}_6\text{H}_{14}\text{O}_6$) is a widely used excipient in liquid pharmaceutical preparations as a vehicle in sugar-free formulations and as a stabiliser for drug suspensions. It has a pleasant cooling sweet taste, with ~ 50-80 % sweetness as that of sucrose (Rowe *et al*, 2006). However, in the presence of L-arginine, by using the maximum sorbitol concentration (40 % w/v, Rowe *et al*, 2006), the addition of the sweetener was insufficient at reducing the bitterness of the formulation. Thus the formulations presented two major challenges: (1) the high alkalinity of the resultant solution provided a bitter taste; and (2) the absence of suitable preservatives that can function effectively under strong alkaline conditions (most work effectively in the more neutral and slightly acidic mediums).

4.3.3.1. Influence of Tartaric acid

Tartaric acid is used as an acidifying, flavouring and sequestering agent in pharmaceutical products, with a molecular formula of $\text{C}_4\text{H}_6\text{O}_6$ ($\text{pK}_{\text{a}_1} = 2.95$, $\text{pK}_{\text{a}_2} = 4.25$, $M_w = 150.09$) (Figure 4.12). It is a naturally occurring chemical found in plants (e.g. grapes and citrus fruits) and is commonly used as a sour-flavour additive in beverages, food products and pharmaceutical products. The next stage of the work was to improve the formulation of L-arginine by lowering the pH of the solution with the addition of tartaric acid. In order to

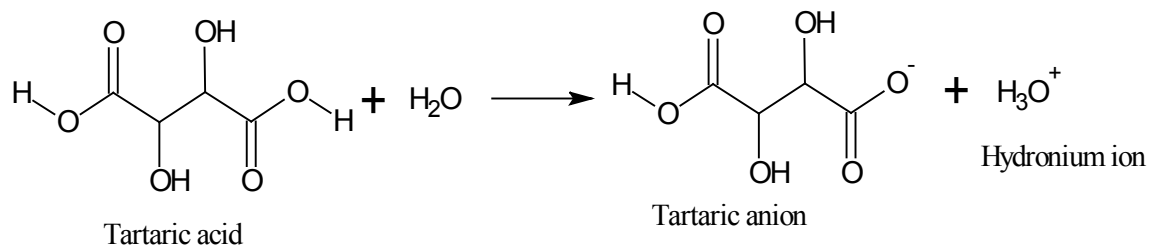


Figure 4.12. The mechanism of reaction of tartaric acid with water. The –OH reactive groups of tartaric acid enables proton donation to be carried out with water, forming hydronium ions.

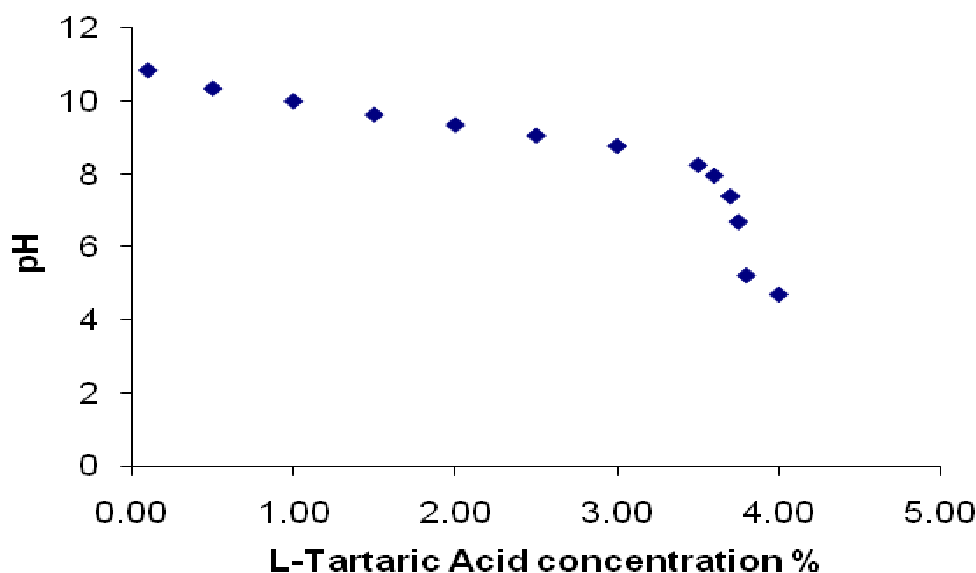


Figure 4.13. Influence of increasing concentrations of tartaric acid on the pH of L-arginine in solution. As the concentration of the acid increased, a decrease in pH was observed, with 4 % (w/v) tartaric acid reducing the pH of the solution to 4.7 ± 0.02 . (n=3)

determine the optimal concentration of tartaric acid, a titration experiment was set up to investigate the influence of addition of tartaric acid on pH of the solution containing L- arginine.

Figure 4.13 displays the titration of tartaric acid with 100 mg.mL⁻¹ L-arginine. The amino acid has very basic properties (pH 11 in the absence of tartaric acid), thus the titration was carried out to determine the relationship between concentration of tartaric acid and its ability to reduce the pH of the solution. The results show that as the concentration of tartaric increased from 0.1 to 4.0 % (w/v), a decrease in the pH of the solution was observed, reaching 4.70 ± 0.02 . This can be explained by the dissociation of tartaric acid in water into its

corresponding anion molecule and hydronium ion (Figure 4.12). pH is a measure of hydrogen ion concentration in a solution and as the number of hydrogen ion concentration increases, the acidity of the formulation increases. Therefore the reduction in pH by tartaric acid was a direct result of increased hydronium ions forming, thereby masking the basic properties and bitterness of L-arginine.

4.3.3.1. Formulation Optimisation

The addition of 4 % (w/v) tartaric acid produced a solution with low pH and an acceptable taste. The final formulation recipe comprising 100 mg.mL⁻¹ L-arginine is detailed in section 4.2.2.3. The alkalinity and bitterness of the formulation was reduced after the addition of 4% tartaric acid (w/v). The sweetness of the formulation was further increased by the addition of 40 % (w/v) sorbitol along with 0.5 % (v/v) raspberry concentrate, providing a pleasant odour. In order to ensure the formulation remained microbiologically stable throughout its shelf life, sodium benzoate (0.5 % w/v) was included as preservative. Sodium benzoate is an effective preservative and acts on the cell wall through a chemical reaction (Rowe *et al*, 2006). It was also found to have good chemical and organoleptic properties (colourless, odourless, effective in acidic mediums and readily soluble in water), thus making it compatible with the other excipients in the formulation.

4.3.4. Stability studies

Formulations of L-arginine in solution (100 mg.mL⁻¹) were prepared as described in section 4.2.2.3. The samples were stored at different stability conditions as outlined in the ICH guidelines (5 °C, 25 °C (40 % humidity) and 40 °C (75 % humidity)) and assessed for changes in organoleptic properties and chemical stability of the active ingredient.

Assessment of the organoleptic properties such as colour, smell and taste at the different conditions of storage showed that there was no significant difference in the formulations stored at 5 °C and at 25 °C (Table 4.5). All the formulation had pleasant raspberry fragrance with no changes in taste. However formulations stored under accelerated conditions (40 °C) changed colour after 30 days of storage. The intensity of colour change increased with the duration of storage, after 6 months storage the formulations changed from peach to a dark yellow colour and had an unacceptable taste. The change in colour can potentially be attributed to the degradation of raspberry concentrate at higher temperature and humidity conditions upon storage over a long duration.

Table 4.5. Stability study assessing organoleptic properties of the oral liquid formulation of L-arginine (100 mg.mL⁻¹). The formulations were stored at different storage conditions including 5 °C, 25 °C (40% humidity) and 40 °C (75% humidity).

Temperature °C	Number of days	Organoleptic properties		
		Colour	Smell	Taste
5	0	Light Peach	Raspberry	Sweet
	30	Light Peach	Raspberry	Sweet
	60	Light Peach	Raspberry	Sweet
	90	Light Peach	Raspberry	Sweet
	180	Light Peach	Raspberry	Sweet
	360	Light Peach	Raspberry	Sweet
25	0	Peach	Raspberry	Sweet
	30	Peach	Raspberry	Sweet
	60	Peach	Raspberry	Sweet
	90	Peach	Raspberry	Sweet
	180	Peach	Raspberry	Sweet
	360	Peach	Raspberry	Sweet
40	0	Light Peach	Raspberry	Sweet
	30	Peach	Raspberry	Sweet
	60	Dark Peach	Raspberry	Sweet
	90	Peach/Yellow	Raspberry	Sweet
	180	Dark Yellow	Burnt Raspberry	Less Sweet
	360	Dark Yellow	Burnt Raspberry	Less Sweet

Analysis of pH of the formulations stored at the different conditions over a 1 year period showed that there were no significant differences between pH variations (Figure 4.14) potentially suggesting that there were no chemical changes within the formulation. Furthermore analysis of L arginine showed that the chemical stability profile of the active ingredient did not change over the entire duration of the study (Figure 4.15). However, data from studies carried out at 5 and 25 °C provide a clearer indication of the stability profile as there were physical changes to the formulations stored under accelerated conditions.

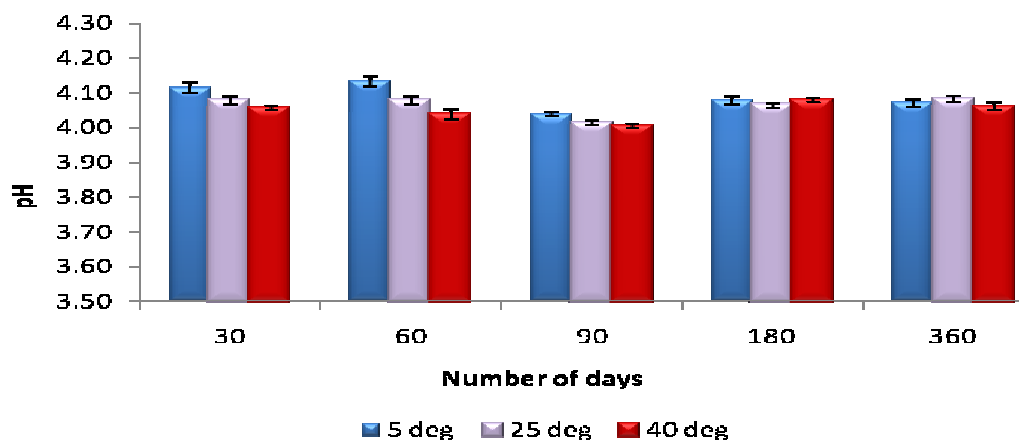


Figure 4.14. 12 months stability profile of 100 mg.mL^{-1} L-arginine with 4 % (w/v) tartaric acid and 0.5 % (v/v) raspberry concentrate stored under 5 °C, 25 °C (40 % humidity) and 40 °C (75 % humidity) conditions. Formulation was observed to be stable over the 12 month period (pH 4), with no significant difference between the time points ($P>0.05$). (n=3)

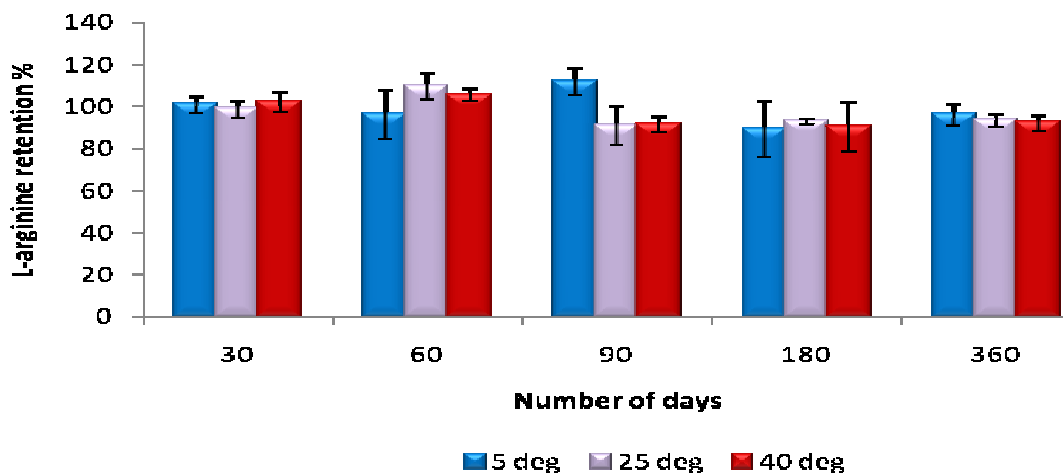


Figure 4.15. 12 months stability profile of 100 mg.mL^{-1} L-arginine with 4 % (w/v) tartaric acid and 0.5 % (v/v) raspberry concentrate stored under 5 °C, 25 °C (40 % humidity) and 40 °C (75 % humidity) conditions. The formulation was observed to have >90 % drug retention over the 12 month period. (n=3)

4.4. Conclusion

Extensive investigation of the analytical method resulted in the development of ninhydrin assay which was simple, reproducible and validated method for assessing the concentration of L arginine. The study resulted in the production of an oral liquid flavoured formulation of L-arginine with shelf life of one year as opposed to currently available extemporaneous preparations which have a short shelf life of 28 days (Hey, 2007).

CHAPTER 5

Solubilisation and formulation of melatonin as
a liquid oral dosage form

CHAPTER 5

Solubilisation and formulation of melatonin as a liquid oral dosage form

5.1. Introduction

5.1.1. Structure, biosynthesis and metabolism of melatonin

The pineal gland is a highly vascular neuroendocrine transducer located in the centre of the brain and is predominantly made up of two types of cells; (1) pinealocytes, which produce indolamines (melatonin) and peptides (arginine vasotocin), and (2) neuroglial cells (Amnon, 1997).

The indole structure is an aromatic heterocyclic organic compound consisting of a 6-membered benzene ring fused to a 5-membered nitrogen-containing pyrrole ring (Figure 4.1a). Indolamines are composed of aromatic indole attached to the essential amino acid L-tryptophan (Figure 4.1b). It is this indolamine that initiates the biosynthesis of melatonin in the pineal gland by a four-step pathway. The process is initiated by the conversion of the amino acid tryptophan into 5-hydroxytryptophan via the enzyme tryptophan 5-monooxygenase. Aromatic-1-amino acid decarboxylase then catalyses the hydroxynated form of tryptophan into 5-hydroxytryptamine (serotonin), which undergoes acetylation from

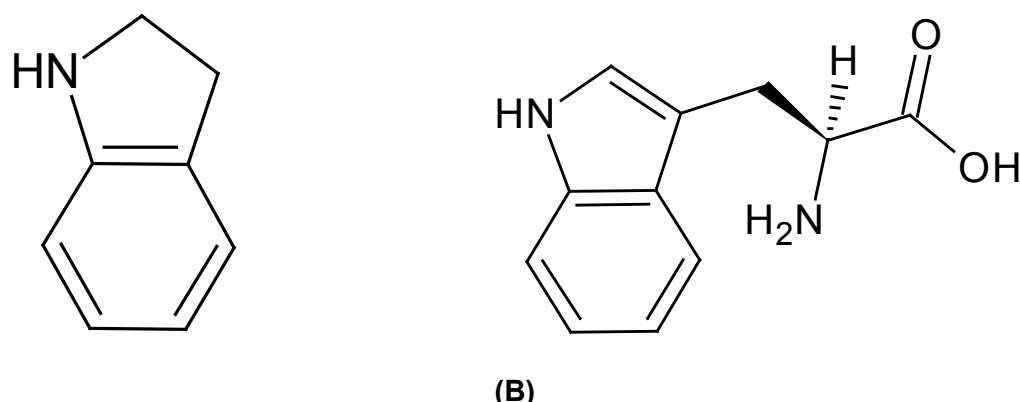


Figure 5.1. Chemical structures of (A) indole and (B) an indolamine (L-tryptophan). The indole is an aromatic heterocyclic organic compound composed of a 6-membered benzene ring fused to a 5-membered nitrogen-containing pyrrole ring. The indolamine is composed of the essential amino acid (L-tryptophan) fused to the indole structure.

arylalkylamine-*N*-acetyltransferase (AANAT) to form the precursor of melatonin: *N*-acetylserotonin. This precursor is then catalysed by the enzyme hydroxyindol-O-methyltransferase into melatonin (Figure 4.1) (Altun and Ugur-Altun, 2007).

Melatonin is metabolised in the liver, by hydroxylation to form 6-hydroxymelatonin, which is then conjugated to either sulphuric or glucuronic acid before being excreted in the urine (Amnon, 1997).

5.1.2. Melatonin and its therapeutic effects

Melatonin (*N*-acetyl-5-methoxytryptamine) is a melanophore containing indolamine hormone with poor water solubility ($100 \text{ }\mu\text{g.mL}^{-1}$) (Hardeland, 2006). It is secreted by the pineal gland during the dark phase of the day by simple diffusion with its lipophilic structure allowing it to passively diffuse across the cell membranes (Reiter, 1991; Cardinali and Pévet, 1998).

The physiological functions and therapeutic uses of melatonin include sleep and circadian entrainment (daily rhythm becomes susceptible to modulation by 24-hour environmental cycles), blood pressure regulation, temperature regulation, oncogenesis, retinal physiology, seasonal reproduction, ovarian physiology, immune function, induction of osteoblast differentiation, ageing process, as well as acting as a potent-free radical scavenger and a broad spectrum antioxidant (Haimore *et al*, 1994; Pieri *et al*, 1995; Amnon, 1997; Altun and Ugur-Altun, 2007; Rezzani *et al*, 2009).

5.1.3. Current dosage forms

The production of melatonin varies according to age, with children aged less than 3 months secreting very little melatonin from the pineal gland. In older infants, melatonin secretion increases and becomes circadian with the nocturnal concentration of melatonin achieving its peak in children aged 1-3 years. As the children grow older (>3 years old) the concentration of melatonin gradually begins to decline (Waldhauser *et al*, 1984; Amnon, 1997). Therefore insufficient production of melatonin can result in the need for supplementing it from an external source. Currently, melatonin dosage forms are supplied as modified release tablet (Circadin®) in 2 mg doses that can only be prescribed to adults over the age of 55 as a short-term treatment for insomnia.

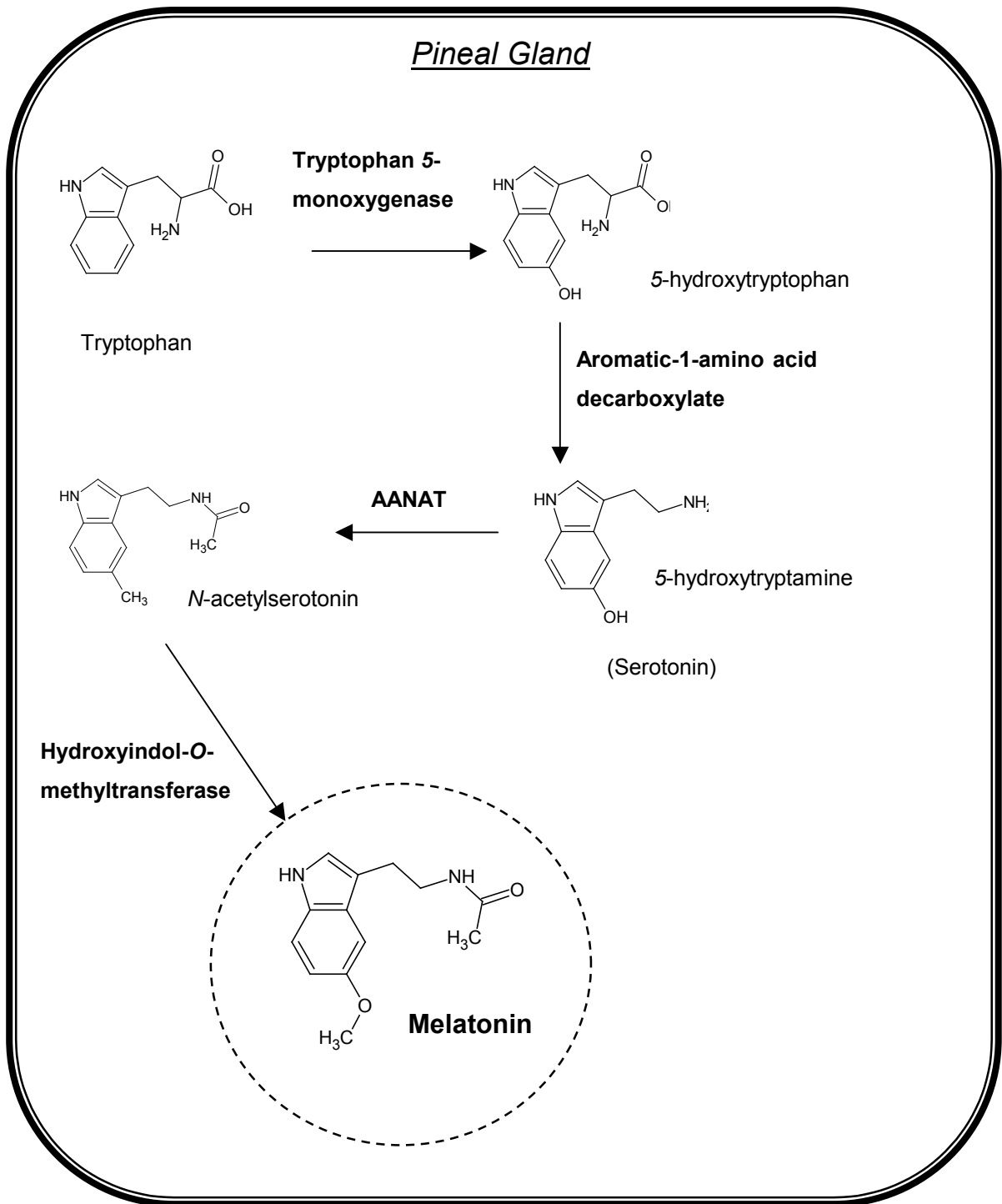


Figure 5.2. Four-step pathway synthesis of melatonin by the pineal gland. Tryptophan is converted to 5-hydroxytryptophan by the enzyme tryptophan hydroxylase, which is then decarboxylated to serotonin. The synthesis of melatonin from serotonin is catalysed by 2 enzymes (arylalkylamine-N-acetyltransferase (AANAT) and hydroxyindole-O-methyltransferase), which are mainly confined to the pineal gland (modified from Altun and Ugar-Altun, 2007).

5.1.4. Aim

Research into an alternative drug delivery method for melatonin has previously been carried out including the formulation of solid lipid nanoparticles (Rezzani et al, 2009), alginate beads (Lee and Min, 1996), lipospheres (Tursilli et al, 2006) and propylene glycol and HP- β -CD vehicles (Lee et al, 1997). However an oral liquid solution using simple solubilisation techniques which can be commercially translatable has not yet reached the pharmaceutical market.

The overall aim of the study was to establish a validated calibration protocol for the extraction and quantification of melatonin using HPLC and to solubilise melatonin in an oral liquid formulation without compromising the lipophilicity of the molecule and thus ensuring its diffusion across the cell layers.

The objectives included:

- Development of cyclodextrin based oral liquid formulation (1 mg.mL^{-1}) in the absence of conventional non-polar media, such as ethanol.
- Stabilisation of the liquid formulation from oxidation and degradation upon exposure to light

5.2. Materials and Method

5.2.1. Materials

Melatonin, HP- β -CD, sorbitol, tartaric acid, potassium sorbate, sodium acetate and EDTA were purchased from Sigma (UK). Methanol and ACN was purchased from Fisher Scientific (UK).

5.2.2. Method

5.2.2.1. Development of a calibration method for melatonin

Calibration was carried out using a dionex HPLC with a C18 Gemini column (150 x 4.6 mm) being heated to 45 °C using a column heater. 10 mg of melatonin was dissolved in 20 mL of methanol to obtain a stock concentration of 500 $\mu\text{g.mL}^{-1}$. Serial dilutions were then carried out to obtain further concentrations (250, 100, 50, 25, 10 and 5 $\mu\text{g.mL}^{-1}$). Using a mobile phase consisting of 75 mM sodium Acetate and ACN (84:16), 20 μL of each melatonin concentration was injected into the dionex HPLC and analysed at a wavelength of 275 nm. The retention time for melatonin was 20 minutes.

5.2.2.2. pH titration of tartaric acid

A 1 mg.mL^{-1} solution of melatonin in distilled water with HP- β -CD and 40 % (w/v) sorbitol was prepared, to which increasing increments of tartaric acid was added. Once the tartaric acid had fully dissolved, the pH of the solution was measured using a calibrated Hydrus 500 pH meter. The following tartaric concentrations (% w/v) were used and their pH measurements recorded: 0.1, 0.25, 0.5 and 1.00 % (w/v).

5.2.2.3. Oral liquid formulation recipe of melatonin

To solubilise melatonin, 0.6286 g of HP- β -CD was dissolved in 35 mL of water, to which 20 g sorbitol (40 % w/v) was then added and left to stir for 5 minutes until sorbitol had fully dissolved. The solution was then heated to 40 °C and 50 mg of melatonin solution was dissolved to achieve a 2:1 molar ratio of HP- β -CD with melatonin. To reduce the pH of the solution, 50 mg of tartaric acid (0.1 % w/v) was then added and left to stir until the acid had fully dissolved. A 0.2 % (w/v) concentration of the preservative, potassium sorbate (100 mg) was then added under continuous stirring, followed by 0.1 % of EDTA as an antioxidant (50 mg). The solution was kept under continuous stirring until all of the constituents had fully dissolved to obtain a clear solution. The volume of the solution was then adjusted to 50 mL and stored in amber coloured glass bottles at 5 °C, 25 °C (40 % humidity) and 40 °C (75 % humidity). Samples were prepared and stored in triplicate.

5.3. Results and discussion

5.3.1. Calibration Validation

A HPLC diode array calibration method initially described by Minami and co-workers (2009) was modified to produce a validated calibration protocol for the determination of melatonin in solution. At a detection wavelength of 275 nm, methanol was used to solubilise melatonin.

5.3.1.1. Linearity

The linearity of the HPLC method was evaluated by preparing the standard curve for melatonin on three consecutive days. The peak area was plotted against the concentration and the calibration response was assessed for variances. The results show that the data complied with the Beer Lambert's law in the concentration range investigated ($50\text{-}500 \mu\text{g.mL}^{-1}$) with the linear plot producing a regression equation of $y=0.3045x$ ($R^2=0.9954$) (Figure 5.3).

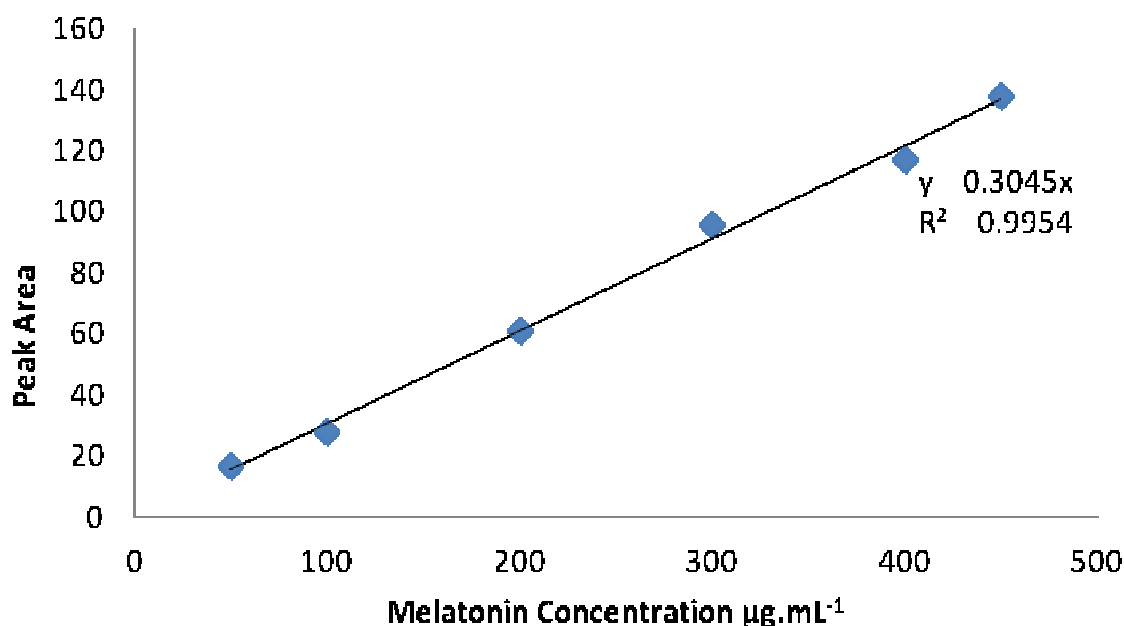


Figure 5.3. Graph of melatonin calibration highlighting the linearity of the validation protocol.

5.3.1.2. Precision

In order to access the reproducibility of the calibration protocol, the calibration method was carried out in triplicate over a period of three days for interday precision, and in triplicate on the same day for intraday precision. It was concluded that the calibration method was reproducible with inter-day precision of 100.42 % and the intra-day precision of 103.99 %. Statistical data was compared using ANOVA statistical test, with the resulting inter-day and intra-day precision being calculated to have a variance of P>0.05 (Table 5.1)

5.3.1.3. Accuracy

The accuracy of the developed method was determined from three concentrations of melatonin in distilled water representing low, medium and high concentrations of the standard curve (20, 60 and 150 $\mu\text{g.mL}^{-1}$). Accuracy of the three concentrations was in the range of 92.62-104.02 % (Table 5.1).

Table 5.1. Summary of calibration validation of melatonin

Criteria	Validation
$Y=$	0.3045x
R^2	0.9954
Intra-day Precision	103.99 %
Inter-day Precision	100.42 %
Accuracy ($\pm SD$) 20 $\mu\text{g.mL}^{-1}$	92.62 (11.61) %
Accuracy ($\pm SD$) 40 $\mu\text{g.mL}^{-1}$	103.25 (8.77) %
Accuracy ($\pm SD$) 60 $\mu\text{g.mL}^{-1}$	104.02 (3.92) %
LOD $\mu\text{g.mL}^{-1}$	0.83
LOQ $\mu\text{g.mL}^{-1}$	2.51

5.3.1.4. Limit of detection (LOD) and limit of quantification (LOQ)

The LOD of an individual analytical procedure is the lowest amount of analyte in a sample which can be detected but not necessarily quantifiable as an exact value (EMEA, 1995). From the calibration range the LOD was calculated as $0.83 \text{ } \mu\text{g.mL}^{-1}$.

The LOQ of an individual analytical procedure is the lowest amount of analyte in a sample which can be quantitatively determined with accuracy and precision. The LOQ is particularly determined for impurities and degradation products, and is a parameter of quantitative assays for low levels of compounds in sample matrices (EMEA, 1995). From the calibration range the LOQ was calculated as $2.51 \text{ } \mu\text{g.mL}^{-1}$.

5.3.2. Influence of polarity on the solubilisation of melatonin

The aim of the study was to produce an oral liquid preparation of melatonin (1 mg.mL^{-1}) using a single or combination of solubilising enhancers such as saccharides, alcohols, surfactants and pH. Previous research has shown that melatonin exhibits poor water solubility ($100 \text{ } \mu\text{g.mL}^{-1}$) under polar conditions, due to its lipophilic nature (Hardeland, 2006). The polarity of a molecule is dependent on the differences between the electro-negativity between the atoms in a compound and the asymmetry of its structure. The extent of polarity can dictate the physical properties of a medium including its aqueous solubility. For example, polar properties exhibited by water results from the uneven sharing of its electrons between oxygen and hydrogen atoms, with oxygen having greater electro-negativity than hydrogen. In contrast, non-polar mediums exhibit a uniform sharing of electrons between the carbon and hydrogen atoms in the molecular structure (e.g. methane), forming straight chains. In order for the lipophilic melatonin molecule to be solubilised in water, investigation was carried out in two phases: (1) development of inclusion complex of melatonin with HP- β -CD and (2) modification of polarity of water.

Phase 1

The use of cyclodextrins as solubilising agent has been widely explored in pharmaceutical research (Bertau and Jörg, 2004; Shabir and Mohammed, 2010). Cyclodextrins are cyclic saccharides that are characterised by strong intramolecular proton bridges making the overall structure of the cyclodextrin a rigid solvent cage for the inclusion molecule (Armstrong and DeMond, 1984). This enables the lipophilic molecule to bind in a reversible manner to the inner core of the cyclodextrin ‘cup’, solubilising and protecting the molecule from the

external aqueous medium. The addition of HP- β -CD in solution (2:1 ratio, cyclodextrin:melatonin respectively) temporarily enhanced the solubility of melatonin to 1 mg.mL⁻¹ but resulted in drug precipitation upon storage after 2 hours.

Phase 2

In order to prevent precipitation of the drug, the next strategy was to reduce the rigidity of the cyclodextrin and polarity of the medium (Bertau and Jörg, 2004). The modification of polarity causes a shift between the undissociated and dissociated states, resulting in solubilisation in non-polar and polar mediums respectively and thus controlling the extent of solubilisation for hydrophobic molecules. Polarity can be measured by the dielectric constant which measures the solvents ability to reduce the field charge of the electric field surrounding a charged particle. Polar media such as water have a dielectric constant of greater than 50 whereas semi-polar and non polar media exhibit lower values in the range of 20-50 and 1-20 respectively. The reduction in polarity supports the preferred media conditions for melatonin, as a hydrophobic drug can easily solubilise in a less polar medium.

Hence an alternative co-solvency method was used to solubilise melatonin in which two compounds of different polarities were mixed to form a system of optimum polarity (semi-polar). The 2 components of the semi-polar system included cyclodextrin-water complex (compound 1) and sorbitol (compound 2). Inclusion of sorbitol within the medium has a dual effect. It enhances the organoleptic properties of the formulation as a sweetener and reduces the polarity of the medium due to its alcohol based properties, as pure sorbitol has a dielectric constant of 35.5 (Ramakrishnan and Prud'homme, 2000). In our study it was observed that an increase in sorbitol concentration in the CD-water mixture resulted in an increase in stable solubilised melatonin. Furthermore, in the study carried out by Ramakrishnan and Prud'homme (2000) they observed that heating sorbitol above 50 °C reduced the dielectric constant of the medium from polar to non-polar region which in turn significantly increased the solubility of non-polar compounds. By applying this method to the present study, melatonin at a concentration of 1 mg.mL⁻¹ was fully dissolved and stabilised in HP- β -CD, 40 % (w/v) sorbitol and water mixture after being heated to 50 °C. This application of heat in the solubilisation protocol potentially caused a further reduction in the dielectric constant of the medium resulting in an increase in the net free energy charge and resulting in stronger attraction forces between the drug and HP- β -CD and sorbitol.

5.3.3. Organoleptic optimisation of melatonin in solution (1 mg.mL^{-1})

In order to formulate a 1 mg.mL^{-1} melatonin in water, the following excipients were added; HP- β -CD (2:1 ratio of cyclodextrin: melatonin), 40 % (w/v) sorbitol, potassium sorbate (preservative) and EDTA (antioxidant and chelating agent). Although the resultant solution was clear with no unpleasant odour, the formulation had a bitter taste despite the inclusion of sorbitol as a sweetener. From the study carried out in Chapter 4, it was concluded that pH can have an underlying affect on the taste of the formulation with alkaline solutions exhibiting increased bitterness.

The pH of melatonin formulation was alkaline ($\text{pH } 10.11 \pm 0.01$) which was attributed to the addition of potassium sorbate and EDTA. Figure 5.4 demonstrates the influence of these excipients on the pH of the melatonin formulation. In the absence of pH modification (0 % w/v tartaric acid) an increase in pH was observed with the addition of potassium sorbate (pH 7.18 ± 0.02) which further increased with the addition of EDTA (pH 10.11 ± 0.01). In order to acidify the formulation, increments of tartaric acid (0.1-1 % w/v) were added, followed by

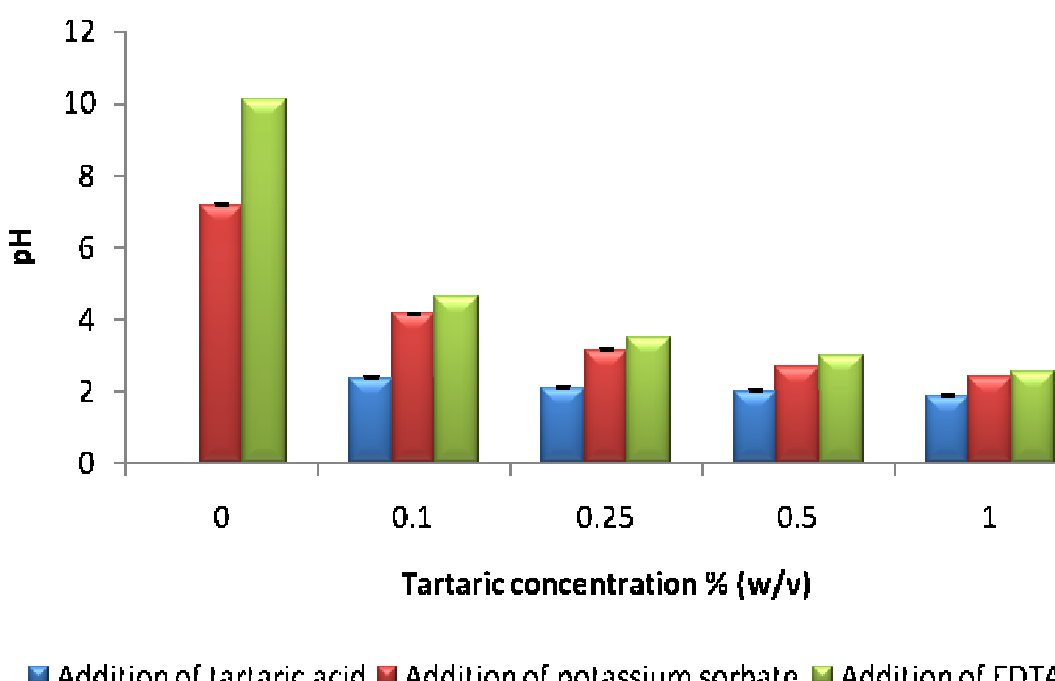


Figure 5.4. Influence of tartaric acid, and the subsequent addition of a preservative (potassium sorbate) and an antioxidant (EDTA), on the pH of the melatonin formulation (1 mg.mL^{-1}). In the absence of tartaric acid, the addition of potassium sorbate and EDTA caused a rise in pH (pH 10.11 ± 0.01). The pH of the formulation containing potassium sorbate and EDTA was reduced to pH 4.63 ± 0.01 and 2.53 ± 0.01 in the presence of 0.1 and 1.0 % w/v tartaric acid respectively. (n=3)

potassium sorbate and EDTA. It was found that with increasing tartaric acid concentration from 0.1 % to 1.0 % (w/v), the pH of the formulation decreased from pH 4.63 ± 0.01 to pH 2.53 ± 0.01 respectively. Under these acidic conditions the bitterness of the formulation had been eliminated, resulting in a taste-free formulation. Therefore, 0.1 % (w/v) tartaric acid was added to the melatonin formulation as it sufficiently reduced the pH of the formulation, while remaining within the acceptable limits for the preservative efficacy of potassium sorbate (pH<6).

5.3.4. Stability studies

Figure 5.5 demonstrates the stability of melatonin in solution (1 mg.mL^{-1}) after the inclusion of 0.1 % (w/v) tartaric acid. The formulation was prepared as outlined in section 5.2.2.3 and stored at 5°C , 25°C (40 % humidity) and 40°C (75 % humidity) for 12 months.

Interestingly samples stored under accelerated conditions (40°C , 75 % humidity) showed a reduction in melatonin retention after 3 months ($91.80 \pm 1.73\%$), with further reduction after 6 and 12 month analysis ($78.08 \pm 10.35\%$ and $62.22 \pm 0.84\%$ respectively). The reduction in melatonin concentration can potentially be attributed to three factors: (1) scavenging of hydroxide radicals ($\cdot\text{OH}$) (Bonnefont-Rousselot *et al*, 2011), (2) the formation of hydronium ions from tartaric acid (Figure 4.12), and (3) Le Chatelier's Principle.

The reaction of tartaric acid with water forms hydronium ions (H_3O^+) which combines with an electron and dissociates into a hydroxyl radical and hydrogen:



Le Chatelier's Principle states that if a dynamic equilibrium is disturbed by changing the conditions, then the position of the equilibrium moves to counteract this change. Thus at a storage temperature of 40°C the equilibrium of H_3O^+ potentially shifted to the right in order to lower the temperature by absorbing the extra heat. This forward reaction favoured the production of hydrogen and hydroxyl radicals, which were rapidly oxidised by melatonin to produce the oxidised form. Thus the oxidative degradation of melatonin was accelerated with increase in temperature.

A similar stability profile was observed in the melatonin formulations stored at 5 and 25°C (40 % humidity), but to a lesser degree. After 6 months storage, melatonin retention was reduced to 93.63 ± 1.12 and $94.17 \pm 4.37\%$ respectively, with a further decrease in

melatonin retention after 12 months ($88.40 \pm 4.38\%$ and $91.52 \pm 0.77\%$ respectively). It is possible that lower storage temperature slowed down the production of hydroxyl radicals, thereby preventing melatonin oxidation.

The organoleptic properties of melatonin remained stable with regard to taste and smell for formulations stored at 5 and 25 °C with formulations at 40 °C resulting in faint discolouration which intensified over time. The stability storage conditions had no influence on the pH of melatonin formulation, which remained stable for 12 months in the region of pH 4.5-4.65 (ANOVA, $P>0.05$) (Figure 5.6).

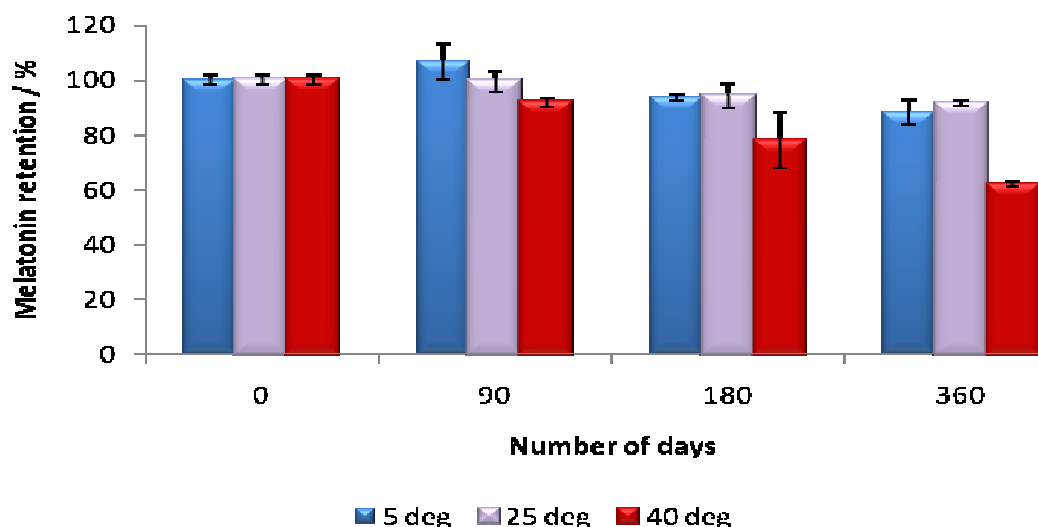


Figure 5.5. 12 months stability profile of 1 mg.mL^{-1} melatonin stored under 5 °C, 25 °C (40 % humidity) and 40 °C (75 % humidity) conditions. At 5 °C the formulation was observed to have >90 % drug retention for 6 months, with $91.52 \pm 0.77\%$ drug retention after 12 months storage at 25 °C. However, under accelerated conditions (40 °C), melatonin rapidly degraded: $91.80 \pm 1.73\%$ at 3 months to $62.22 \pm 0.84\%$ after 12 months storage. (n=3)

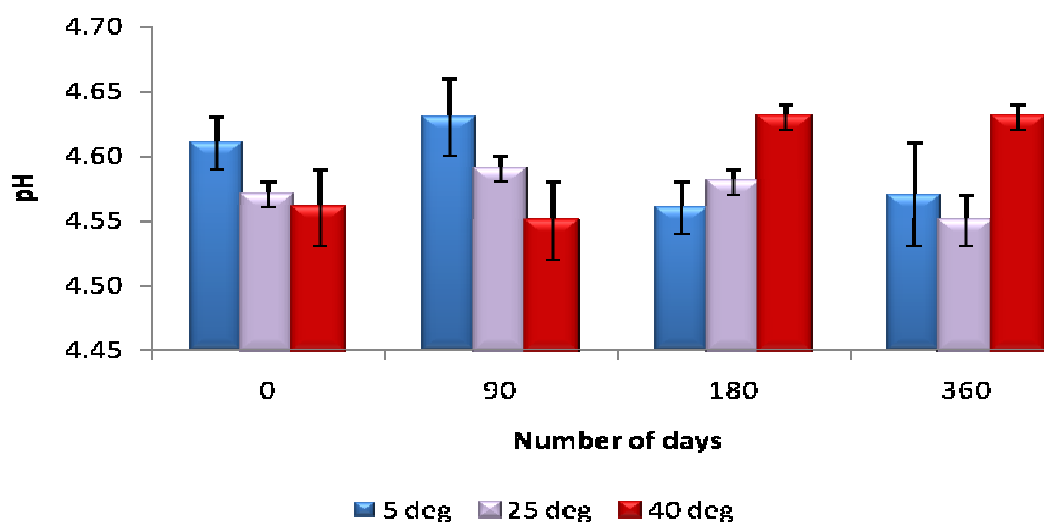


Figure 5.6. 12 months stability profile of 1 mg.mL^{-1} melatonin stored under 5 °C, 25 °C (40 % humidity) and 40 °C (75 % humidity) conditions. Formulation was observed to be stable over the 12 month period (pH 4.5-4.65), with no significant difference between the time points ($P>0.05$). (n=3)

5.4. Conclusion

In conclusion, hydrophobic melatonin was formulated as a 1 mg.mL^{-1} dosage form in water, without compromising its lipophilic properties which are essential for cellular transportation. The drug was solubilised using a dual approach: (1) encapsulating melatonin within the inner core of HP- β -CD and (2) reducing the polarity of water with the addition of sorbitol (20 % w/v).

The formulation remained stable for 6 months at 5 °C and for 12 months at 25 °C (>90 % drug retention). Under accelerated studies (40 °C), the formulation remained stable for 3 months (> 90 % melatonin retention), after which rapid degradation occurred.

CHAPTER 6

Preservative Efficacy Test (PET)

CHAPTER 6

Preservative Efficacy Test (PET)

6.1. Introduction

Investigation of microbial contamination of pharmaceutical products is vital to the pharmaceutical industry and the World Health Organisation, as it can become a major cause of product and economic losses, as well as deterioration in the patients' health or related side effects. The presence of large quantities of water in pharmaceutical drug preparation can make them susceptible to microbial growth, with microorganisms causing organoleptic alterations such as spoilage of product, unpleasant odour, and changes in the physical appearance (colour, turbidity, viscosity) as well as reduced therapeutic effect (Narang *et al*, 2009; Chorilli *et al*, 2011). In order to minimise the risk of spoilage by contaminants, preservatives are included within the formulation that kill low level of contaminants during the manufacturing process, storage and handling during frequent dosing (Narang *et al*, 2009). The chosen preservatives in a given formulation must therefore be stable for the shelf life of the formulation (Zani *et al*, 1997).

Pharmaceutical preservatives that have been listed as GRAS are used to reduce the likelihood of microbial growth in aqueous systems. Ideal preservative characteristics include broad spectrum of activity, active within the formulation at low concentration and effective within the pH range of the formulation.

In order to evaluate the effectiveness of the preservative within the pharmaceutical preparation, the BP and USP guidelines recommend a preservative efficacy test (PET) to be carried out. This challenge test involves the inoculation of microorganisms into the product, followed by the calculation of the loss of microbial viability over a period of 28 days. In accordance with BP and USP standards, the microbes that should be investigated include Gram-positive (*S.aureus*) bacteria, Gram-negative bacteria (*E.coli*, *P.aeruginosa*), mould (*A.niger*), and yeast (*C.albicans*).

The aim of the study was to evaluate the activity of the preservatives and the formulation on the microbes specified for the PET challenge.

6.2. Materials and Method

6.2.1. Materials

Tryptone soya agar, Sabroud dextrose agar, sodium chloride, polysorbate 80, tween 80, sodium bisulphite, sodium thiosulphate pentahydrate, thioglycollate, L-cysteine, and Lecithin were supplied by Sigma (UK).

6.2.2. Method

6.2.2.1. Preparation of neutraliser

In a 1 L sterile glass bottle the following ingredients were added to 500 mL distilled water, at a pH of 7: 60 mL tween 80, 12.5 mL sodium bisulphite (40 % w/v), 7.845 g sodium thiosulphate pentahydrate, 5 g thioglycollate, 1.5 g L-cysteine, and 2 g Lecithin. The mixture was then autoclaved and left to stir until all components had fully dissolved. The final volume was made up to 1 L with sterilised distilled water.

6.2.2.2. Preparation of the inoculum

All bacterial species were inoculated on Tryptone soya agar culture plates. Using the ‘streaking’ method, the surface of the agar was inoculated with *E. coli* ATCC 8739, and then placed in an incubation oven for 24 hours at 35 °C. This was repeated using *P. aeruginosa* ATCC 9027 and *S. aureus* ATCC 6538.

C. albicans ATCC 10231 was inoculated on Sabroud dextrose agar using the ‘streaking’ method and then placed in incubation cabinets for 48 hours at 25 °C.

A. niger ATCC 16404 was inoculated on Sabroud dextrose agar using the ‘streaking’ method and then placed in incubation cabinets for 1 week at 25 °C.

6.2.2.3. Harvesting bacteria and *C. albicans*

Using a sterile loop, colonies of the microbe were extracted from the surface of the culture plate and placed into 10 mL of suspending fluid A (9 g.L⁻¹ sodium chloride) in a sterile glass bottle to achieve a final concentration of 10⁸ CFU.mL⁻¹. The sample was vortexed to produce a suspension of microbial cells. The concentration of microbial cells present in the suspended fluid was analysed on UV spectrophotometer using an ‘in-house’ calibration table (Table 6.1).

6.2.2.4. Harvesting *A. niger*

Once sporulation was obtained, 10 mL of suspending fluid B (9 g.L⁻¹ sodium chloride with 0.5 g.L⁻¹ polysorbate 80) was pipette onto the surface of the colonised agar plate. A sterile spreader was used to gently release the spores, which were then pipetted into a sterile glass bottle and vortexed. To achieve a 10⁸ CFU.mL⁻¹ concentration, the spores were counted using a haemocytometer plate and the concentration was determined using the following equation:

$$\text{CFU.mL}^{-1} = \text{mean number of spores} \times \text{dilution factor} \times 10^4$$

The concentration of *A. niger* was then adjusted using suspending fluid B if required.

Table 6.1. ‘In-house’ calibration of known concentrations of bacteria and *C. albicans*.

Micro-organism	Absorbance	Concentration (CFU.mL ⁻¹)
<i>Absorbance at 570 nm</i>		
<i>S. aureus</i>	0.30	5x10 ⁸
<i>E. coli</i>	0.45	5x10 ⁸
<i>P. aeruginosa</i>	0.70	8x10 ⁸
<i>Absorbance at 420 nm</i>		
<i>C. albicans</i>	2.03	2x10 ⁸

6.2.2.5. Inoculation of pharmaceutical preparation

10 mL of the following preparations were prepared and stored in sterile amber glass bottles; captopril formulations with EDTA (Section 2.2.3.3.1) and EDTA-HP β CD (Section 2.2.3.3.2), gliclazide with L-arginine (Section 3.2.4.1.) and pluronic F127-ethanol (15 % v/v) (Section 3.2.4.2.) L-arginine (Section 4.2.2.3.), and melatonin (Section 5.2.2.3.). Each of these formulations was prepared in triplicate for the individual microbes to be tested.

For the inoculation of *E. coli*, 100 μ L of the microbial cell suspension (10^8 CFU.mL $^{-1}$) was added to each of the formulation vials to achieve a final microbial concentration of 10^6 CFU.mL $^{-1}$. The samples were vortexed and sealed, and then placed in an incubator for 28 days. Samples were taken after 7, 14, and 28 days. This procedure was repeated for the other microorganisms.

6.2.2.6. Preservative efficacy test

All of the samples were vortexed prior to microbial analysis. 1 mL of the inoculated sample was placed into a sterile vial containing 9 mL of neutraliser and vortexed. 1 mL of this sample was then plated on to either Tryptone soya agar for bacteria or Sabroud dextrose agar for fungi using the ‘pour-plate’ method, and stored accordingly (protocol 6.2.2.2.).

The preservative efficacy of the preservatives in each formulation against bacteria and *C. albicans* was assessed by counting the number of colonies formed on the agar plates.

The preservative efficacy against *A. niger* was assessed by adding 10 mL of suspending fluid B onto the surface of the colonised agar plate. A sterile spreader was used to gently release the spores, which were then pipette into a sterile glass bottle and vortexed. The sample was analysed using a haemocytometer plate.

6.3. Results and discussion

6.3.1. Preservative activity against Bacteria

6.3.1.1. Structure of bacteria

Bacteria are composed of a large group of unicellular, prokaryotic microorganisms that are able to produce spores in the dormant form that are potentially able to further contaminate surfaces upon contact. There are two main classes of bacteria, Gram-positive and Gram-negative, which can be fundamentally differentiated by their outer cell wall compositions. The internal structure of the bacteria is similar in both types.

A structural representation of the bacteria cell is illustrated in figure 6.1, from which the differences between the Gram-positive and Gram-negative bacterial structures can be clearly depicted. The general structure of the bacteria consists of a cell wall, cytoplasmic membrane and cytoplasm (Figure 6.1a). The cell wall surrounds the inner cytoplasmic membrane providing structural support and rigidity to the cell, as well as protecting the cytoplasmic membrane from rupture due to high osmotic pressure (Russell and Chopra, 1996). In order for preservatives to have bacteriostatic (inhibit bacterial growth) or bactericidal (cause bacterial death) properties, the compounds must first cross the bacterial cell wall.

The outer cell wall of Gram-negative bacteria is composed of a phospholipid layer protected by an outer layer of lipopolysaccharides (LPS). Imbedded within this outer membrane are transport proteins and porins which are utilised by the bacteria in the regulation of movement of substances into and out of the cell. This outer membrane has a structural resemblance to the cytoplasmic membrane, a structural feature unique to only Gram-negative bacteria. The inner cell wall is composed of a thin layer of peptidoglycan, a disaccharide polymer that is able to contribute to the mechanical stability of the cell walls. The medium between the outer membrane and the peptidoglycan consists of periplasm (Figure 6.1b).

In Gram-positive bacteria the inner cell wall is composed of secondary wall polymers (teichoic acids), polysaccharides, proteins and lipocarbohydrates that are covalently cross-linked with peptidoglycan. The composition of the outer membrane is similar to the inner membrane and so there is no periplasm. Additional surface appendages (pili, capsules, flagellae) are able to attach themselves to the cell wall initiating pathogenesis of bacterial

Examples

E. coli

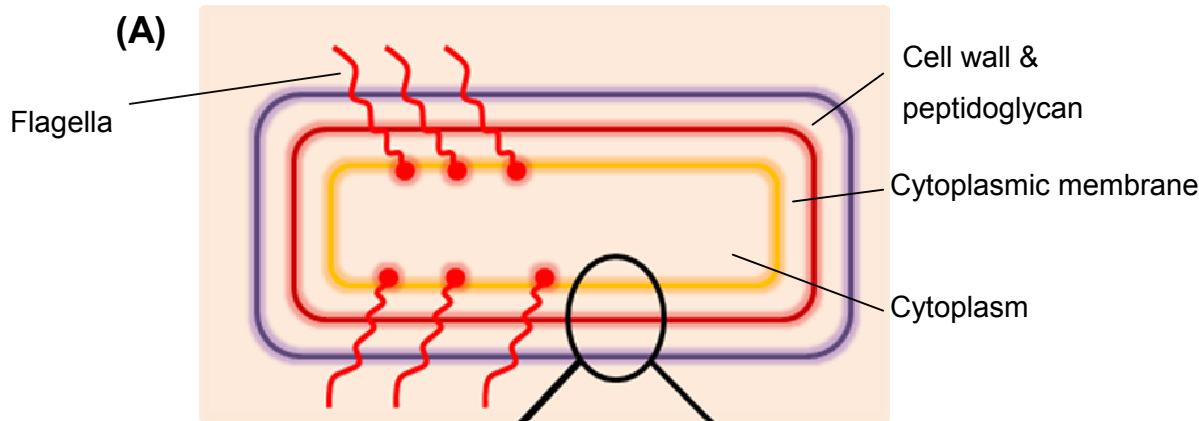
P. aeruginosa

Gram-negative

Outer wall membrane

Periplasm & peptidoglyca

Inner wall membrane



Example

S. aureus

Gram-positive

Outer wall membrane

Cell wall & peptidoglycan

Inner wall membrane

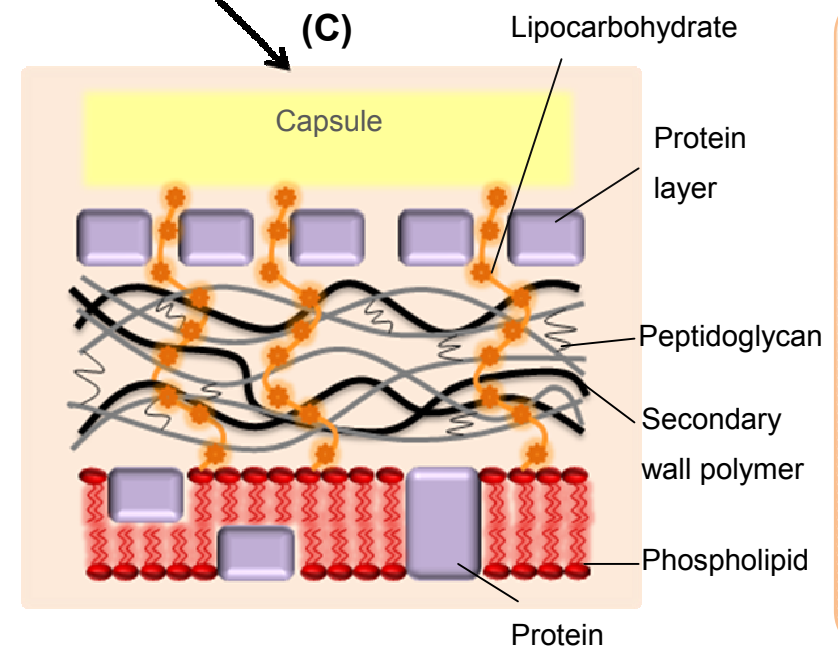
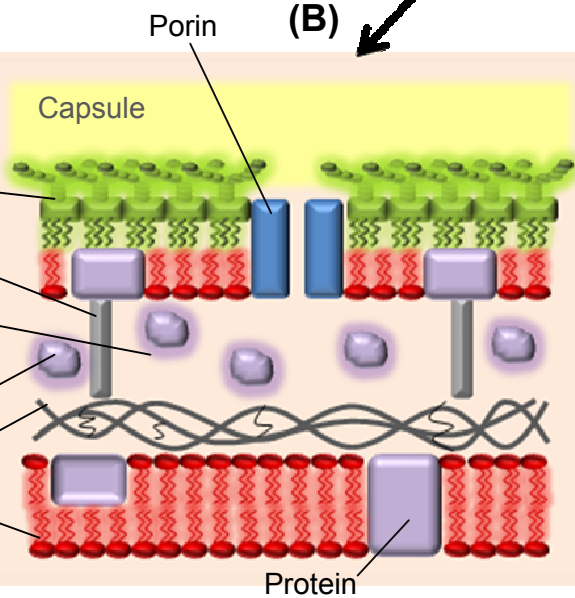


Figure 6.1. Schematic representations of (A) Bacterial cell, (B) Gram-negative bacteria cell, and (C) Gram-positive bacteria cell. (Modified from Russel and Chopra, 1996).

infections (Figure 6.1c). It is the structure of the outer membrane that makes Gram-positive bacteria more susceptible to biocides than Gram-negative bacteria.

In order for preservatives to be effective as biocides they must be able to transport themselves through the bacteria cell wall or be able to apply direct action on the components of the cell wall, thus destabilising the cell and causing the cell to burst and release its cytoplasmic contents. Table 6.2 highlights the 5 main factors influencing the activity of preservatives, which include: time of exposure, temperature, concentration, pH, and the type of micro-organism (Russell and Chopra, 1996).

Table 6.2. Summary of factors enhancing preservative efficacy

Factors affecting preservative activity	Discussed
Time of exposure	Increasing exposure time increases the extent of bacterial cells death.
Temperature	Increasing temperature increases the chemical activity of most preservatives.
Concentration	By increasing the preservative action the rate of bacterial inactivation increases. The rate of inactivation varies from preservative to preservative.
pH	Changes in pH cause alterations on the bacterial cell wall. For example an increase in pH causes the bacterial cell to display a more anionic surface charge.
Type of micro-organism	Order of bacterial sensitivity: Spores > acid-fast bacteria > Gram-negative > Gram positive

6.3.1.2. Self-preserving formulations

Self-preserving is defined as having preservative actions in the absence of preservative agents, with the conditions of the formulations being sufficient to be bactericidal and bacteriostatic. These conditions include; low or high pH, low osmotic pressure (available water (a_w)), multifunctional excipients with antimicrobial properties (alcohols, sweeteners, chelating agents) and a combination affect of these (synergy effects).

The captopril formulations described in Chapter 2 (Section 2.2.3.3.) were hypothesised to be a self-preserving formulation, as they contained no specific preservative. The two formulations taken forward in this study consisted of EDTA and captopril solubilised in water (Formula 1), and EDTA, captopril, and HP β CD solubilised in water (Formula 2), with the pH of the final solutions being acidic (pH 3.4). In order to understand the self-preserved actions of these formulations it was first necessary to highlight the physical and chemical stresses that could be induced on bacterial cells such as acidic environment, low a_w , chelating agents, surface acting agents, free fatty acids and nutrient depletion (starvation). All of these factors cause cellular injury to the microbial cell, either by altering the membrane permeability, altering its enzyme function, degrading the ribosomes enclosed within the cytoplasm, or by increasing the microbial cells sensitivity towards selective agents.

6.3.1.2.1. Preservation efficacy using acidic medium

Bacteria (Gram-positive and Gram-negative) require specific conditions for optimum growth; these include ambient temperatures, good nutrient supply, but most importantly a neutral pH environment (pH 7). By altering any one of these conditions (such as lowering of temperature), the rate and extent of bacterial growth reduces until a dormant phase is reached. On the other hand, upon altering the pH to more extreme conditions, the micro-organisms spend greater amount of energy to maintain the pH and ionic strength gradients across the cytoplasmic membrane, eventually leading to cell lysis (Miller, 1969) or a disruption of the cellular membrane causing cytoplasmic leakage (Kabara and Orth, 1997).

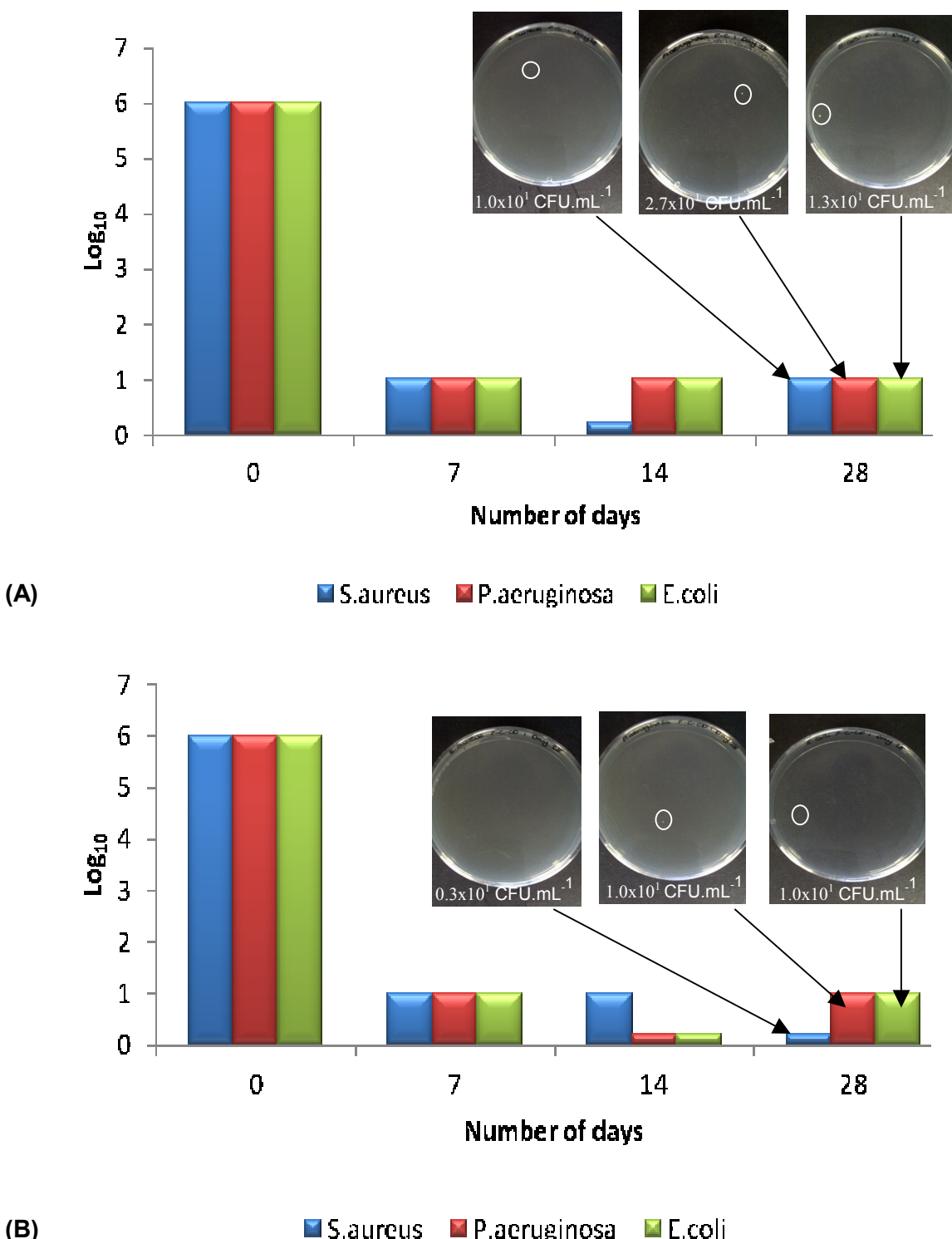


Figure 6.2. Preservative efficacy of captopril formulations at pH 3.4 on Gram-negative and Gram-positive bacteria, after 28 days incubation under 25 °C (75 % humidity) conditions. (A) Captopril with 0.1 % (w/v) EDTA, and (B) Captopril with 0.1 % (w/v) EDTA and HP β CD. Both formulations exhibited a log reduction of 5 after 7 days, with further inhibition after 28 days inoculation. (n=3)

The pH of the captopril self-preserving formulations containing EDTA and EDTA-HP β CD was 3.4. Figure 6.2 highlights the effectiveness of these preservative-free formulations against both Gram-negative (*E. Coli* and *P. aeruginosa*) and Gram-positive bacteria (*S. aureus*). After 7 days incubation, the number of colony forming units (CFU.mL⁻¹) was observed to have declined by a log₁₀ reduction of 5. According to BP guidelines, a log₁₀ reduction of 3 must be achieved for the formulations to pass the preservative efficacy test. After 28 days incubation no further increase in bacterial colony re-growth was observed. These observations were observed to be consistent for both formulations 1 and 2, both of which were acidic in nature and contained EDTA (chelating agent) (Figure 6.2).

6.3.1.2.2. Preservative efficacy using chelating agents on Gram-negative bacteria.

The acidity of the captopril formulations possibly provided optimum conditions for the preservative efficacy of EDTA. Under acidic pH conditions (< pH 3), EDTA is fully ionised and is able to complex with and inactivate metal ions present in the medium (Kristensen *et al*, 2008). The chelating agents are anionic in nature, and thus are able to act by binding to cationic alkaline earth and heavy metal ions, such as copper, manganese and phosphate (Kabara and Orth, 1997). Gram-negative bacteria contain divalent cations (Figure 6.3a) on the outer cell wall, thus have greater sensitivity towards chelating agents than Gram-positive bacteria.

EDTA is a chelating agent that has been GRAS listed, is inexpensive and is effective in small quantities. Most importantly it was reported to have preservative efficacy against Gram-negative bacteria in 1958 by Mac Gregor and Elliker. The chelating agent acts by having a lysis affect on the outer cell wall of the Gram-negative bacteria, thereby increasing the permeability (permeabiliser) of the outer membrane. As seen from figure 6.3a the outer membrane of Gram-negative is maintained by a number of structural bodies, such as hydrophobic lipopolysaccharide (LPS)-LPS and LPS-protein interactions and divalent cations (Mg²⁺) which stabilise the strong anionic charges of the oligosaccharide chain of the LPS molecule. In the presence of EDTA, the chelating agent is able to bind to these cations (Figure 6.3b), destabilising the outer membrane by releasing the LPS molecules and exposing the non-polar phospholipids attached to the inner membrane below (Figure 6.3c). The phospholipids are composed of two parts; hydrophilic heads and hydrophobic tails. Upon their exposure, the phospholipids are forced to quickly realign themselves to form a hydrophobic core, resulting in the cell wall folding upon itself causing partial solubility and

permeability of the cell wall, exposing the cytoplasmic contents beneath. This partial permeability of the cell wall allows for the movement of intracellular solutes out of the cell (Figure 6.3d), ultimately causing cell lysis. It can therefore be hypothesized that EDTA acts as a preservative agent by increasing cell permeability.

6.3.1.2.3. Conclusion.

The preservative-free captopril formulations 1 and 2 inhibited the growth of Gram-negative and Gram-positive bacteria cells eventually leading to cell lysis. The Gram-negative bacteria were attacked using a synergistic effect of chelating agent with acidic medium, whereas the Gram-positive bacteria were predominantly affected by the acidic pH of the medium in the formulations. Although EDTA was able to act as an antimicrobial, it can also act in synergy with other commonly used pharmaceutical preservatives (such as potassium sorbate) enhancing their preservative action.

6.3.1.3. Synergistic effect of EDTA with potassium sorbate

EDTA was used as an antioxidant and as an enhancer of the antimicrobial properties of potassium sorbate in the melatonin formulation (Section 5.2.2.3.). The formulation was prepared at pH 4.5 to maximise the antibacterial and antifungal properties of potassium sorbate, as the preservative had minimal antimicrobial properties above pH 6 (Rowe *et al*, 2006). At pH 4.5 potassium sorbate, although mainly in the undissociated form ($pK_a = 4.74$), was expected to remain effective in inhibiting bacterial growth (Beales, 2004).

The effect of potassium sorbate on the inhibition of Gram-negative and Gram-positive bacteria is presented in figure 6.4 and table 6.3. After 7 days incubation with *S. aureus*, *P. aeruginosa* and *E. coli*, melatonin formulation exhibited strong antibacterial properties with the number of viable microorganisms being reduced by a \log_{10} reduction of 5. After 28 days *S. aureus* and *E. coli* growth was completely inhibited. The inhibition of the Gram-negative and Gram-positive bacteria was possibly associated with the synergistic effect of EDTA, potassium sorbate and acidic pH. EDTA possibly influenced the permeability of the cell wall of gram-negative bacteria (as described in Figure 6.3), allowing for the movement of potassium sorbate into the bacterial cell to initiate bactericidal properties. The Gram-positive bacterium (*S. aureus*) was inhibited by the synergistic effect of acidic pH of the medium (pH 4.5) acting on the cell wall, modification of internal pH of the cell as potassium sorbate transgressed through the cell wall into the cytoplasm (Figure 6.5).

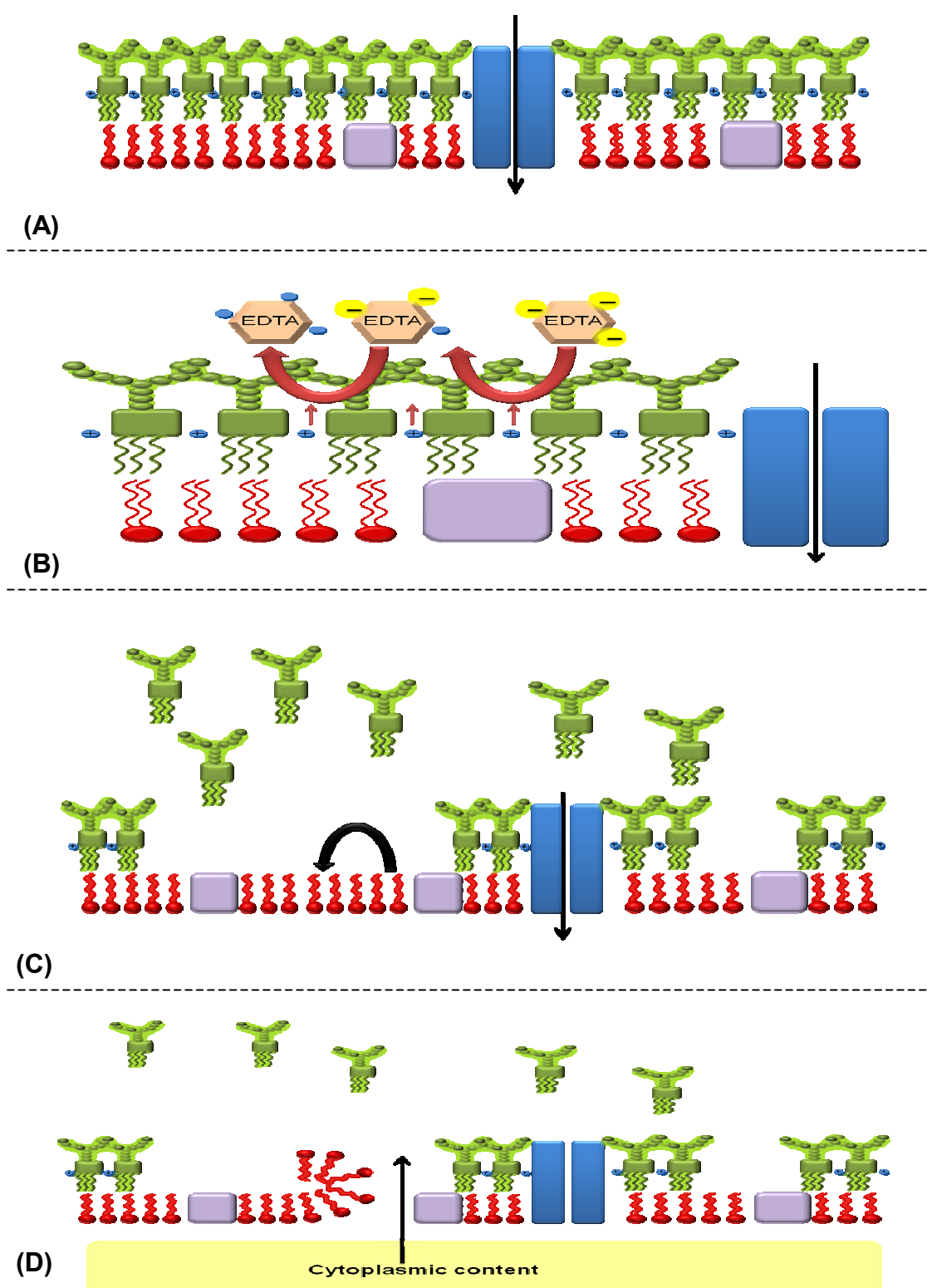


Figure 6.3. Schematic representation of the affect of EDTA on a Gram-negative bacteria cell wall. (A) Gram-negative bacteria cell wall, (B) EDTA removes the divalent cations binding the LPS to the cell wall, (C) LPS are detached from the cell wall exposing the phospholipid layer, (D) Partial permeability of the cell wall causes cytoplasmic contents to leak out of the cell, resulting in cell lysis.

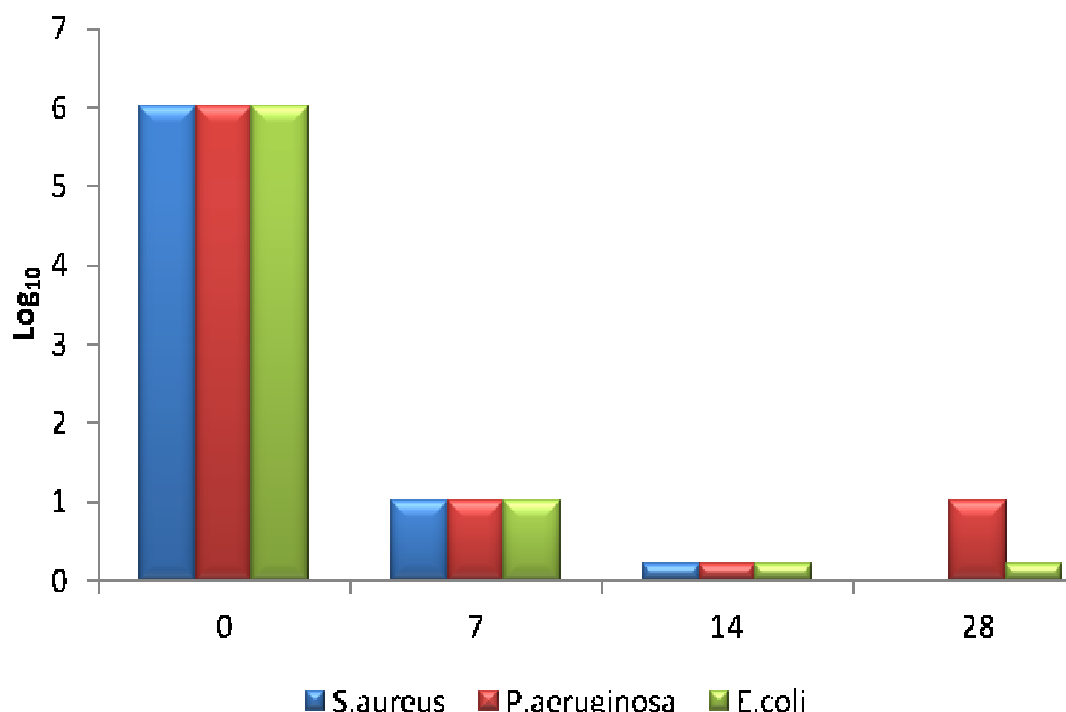
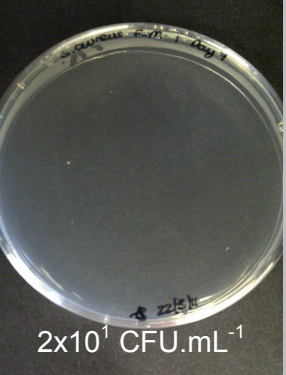
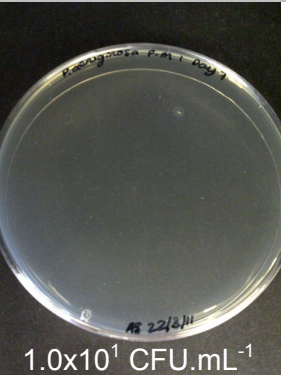
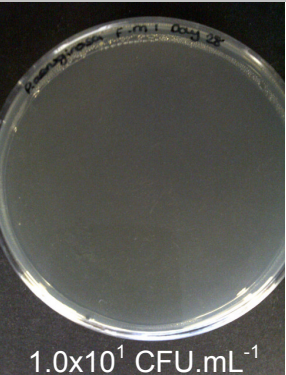
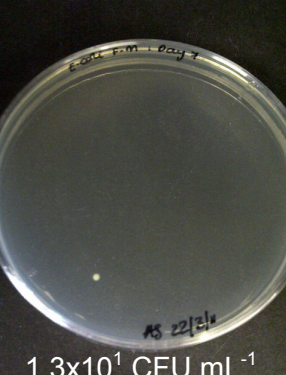
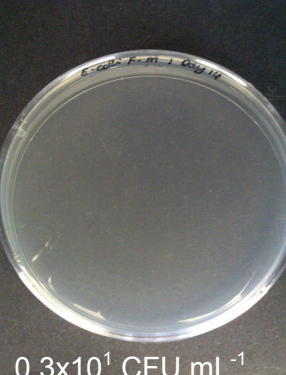
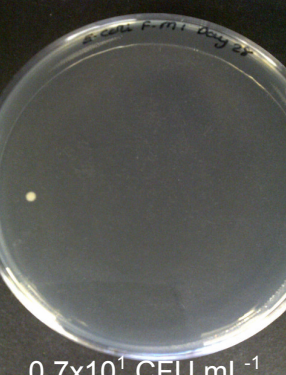


Figure 6.4. Preservative efficacy of potassium sorbate in the melatonin formulation against Gram-positive (*S. aureus*) and Gram-negative (*P. aeruginosa* and *E. coli*) bacteria. After 28 days there was complete inhibition of *S. aureus* and *E. coli*. The number of viable *P. aeruginosa* colonies observed a log₁₀ reduction of 5. (n=3)

Table 6.3. Tryptone soya agar plates cultured with bacteria after inoculation with potassium sorbate in the melatonin pharmaceutical preparation. Samples were cultured on days 7, 14 and 28. The preservative was found to be effective in inhibiting Gram-positive and Gram-negative bacteria growth in the oral liquid formulation. (n=3)

Bacteria	Day 7	Day 14	Day 28
<i>S. aureus</i>	 2x10 ¹ CFU.mL ⁻¹	 0.3x10 ¹ CFU.mL ⁻¹	 Complete
<i>P. aeruginosa</i>	 1.0x10 ¹ CFU.mL ⁻¹	 0.3x10 ¹ CFU.mL ⁻¹	 1.0x10 ¹ CFU.mL ⁻¹
<i>E. coli</i>	 1.3x10 ¹ CFU.mL ⁻¹	 0.3x10 ¹ CFU.mL ⁻¹	 0.7x10 ¹ CFU.mL ⁻¹

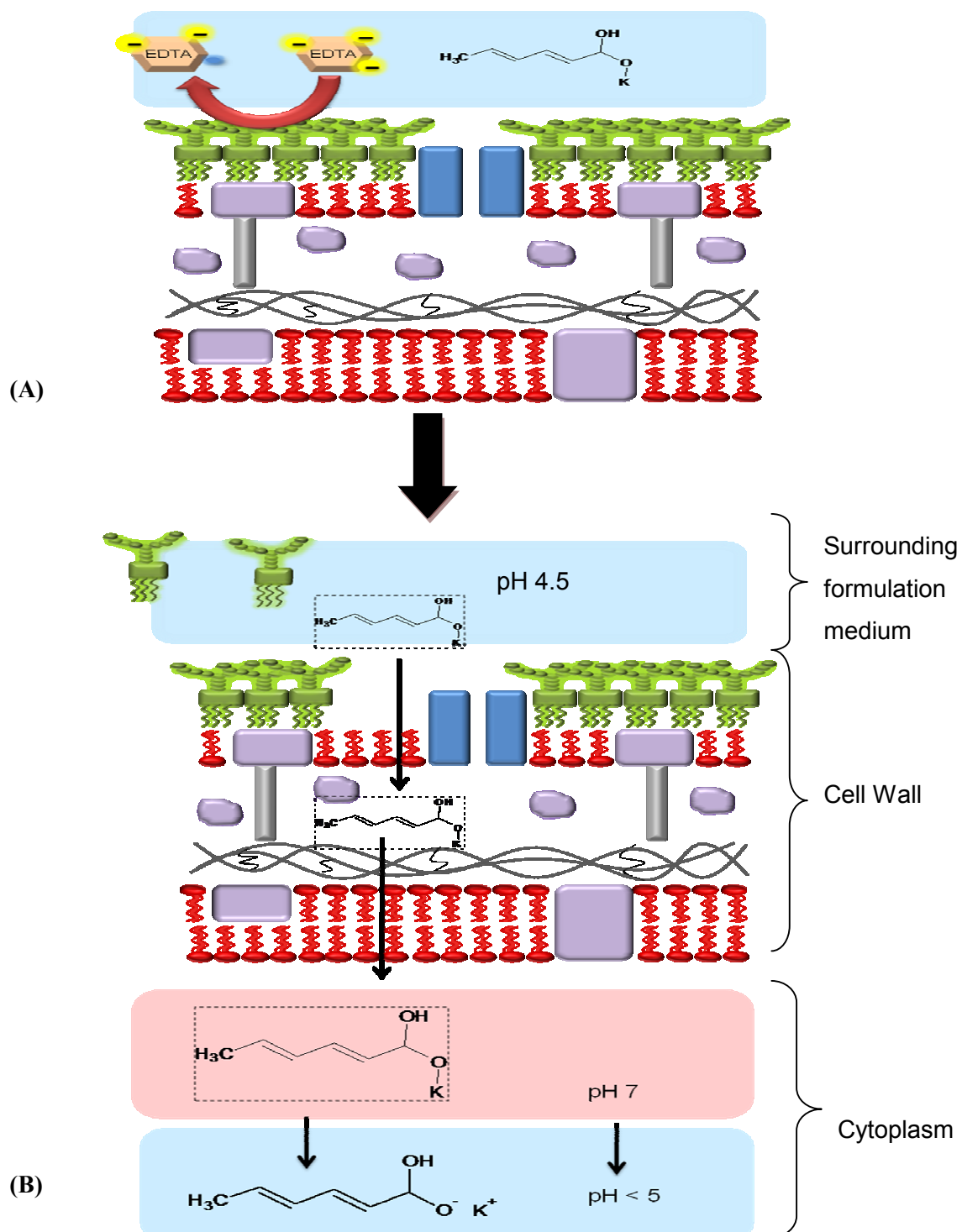


Figure 6.5. A schematic representation of the antimicrobial mechanism of potassium sorbate ($\text{C}_6\text{H}_9\text{O}_2\text{K}$) in the presence of EDTA on a Gram-negative cell. (A) The reaction is initiated by EDTA removing the divalent cations binding the LPS to the cell wall. (B) The exposed LPS layer enables potassium to migrate through the outer membrane, into the periplasm and peptidoglycan, and through the inner membrane into the cytoplasm. The neutral pH of the cytoplasm dissociates potassium sorbate into sorbic acid and K^+ . As the concentration of sorbic acid increases in the cytoplasm, the internal pH of the cell decreases until cellular activity is inhibited (modified from Beales, 2004).

6.3.1.4. Preservative affects of sodium benzoate

Sodium benzoate was used as a preservative agent in the L-arginine formulation that was prepared at pH 4 with 40 % (w/v) sorbitol (Section 4.2.2.3). Figure 6.6 and table 6.4 highlights the preservative efficacy of sodium benzoate against Gram-negative and Gram-positive bacteria. It was observed that after 7 days inoculation with the microorganisms, the number of viable cells of *E. coli* was 10^2 CFU.mL⁻¹ thereby exhibiting a \log_{10} reduction of 4, with *S. aureus* and *P. aeruginosa* exhibiting a \log_{10} reduction of 5. After 28 days no further growth of bacterium was observed, with sodium benzoate achieving complete inhibition of *S.aureus*.

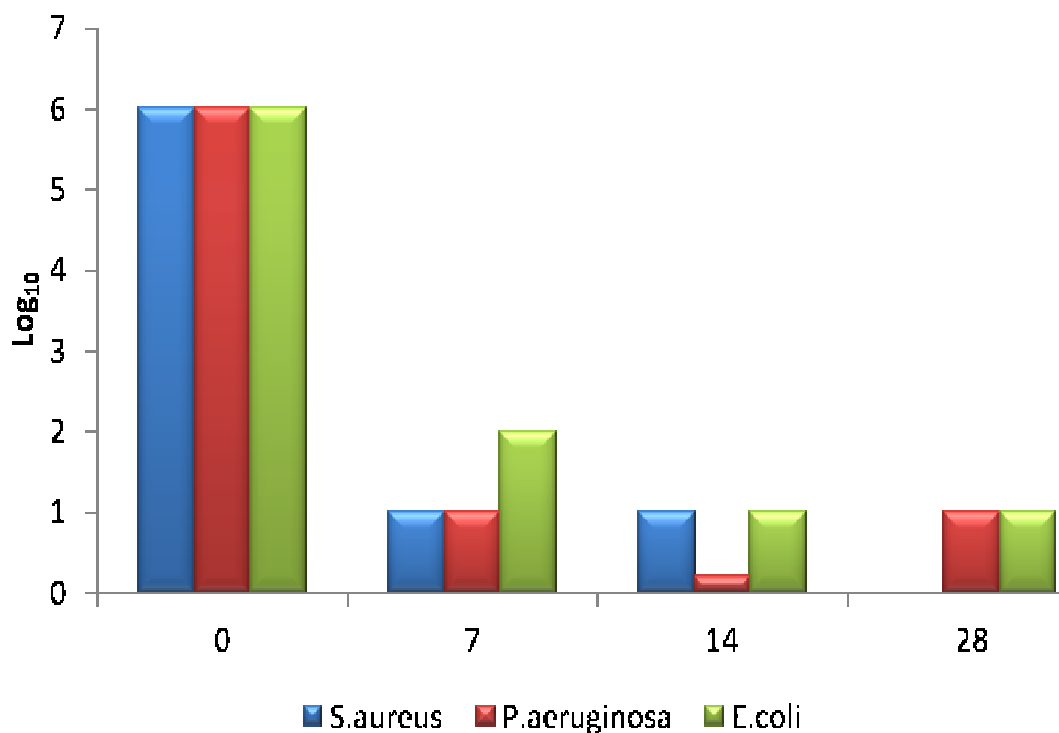
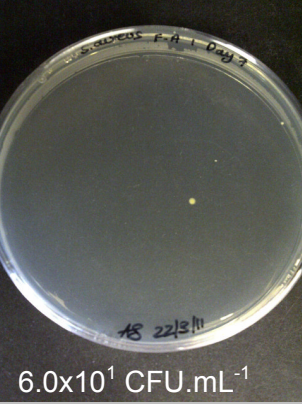
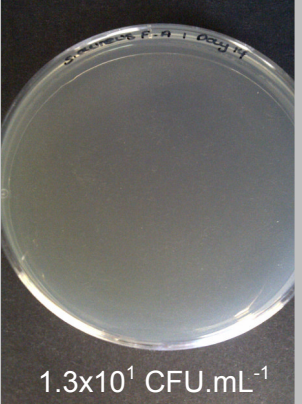
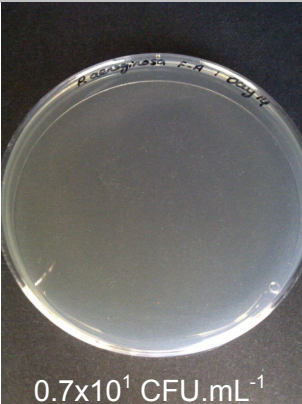
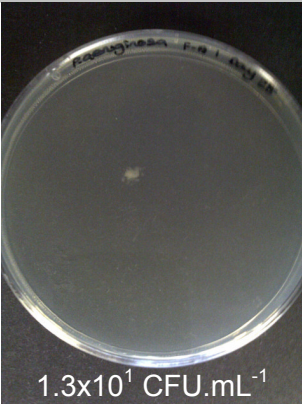
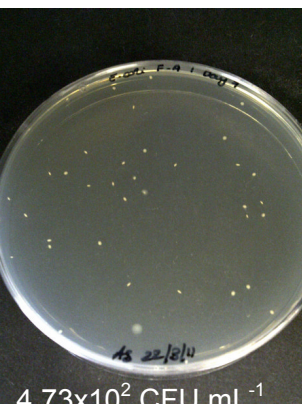
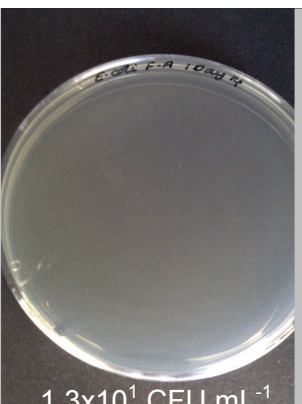
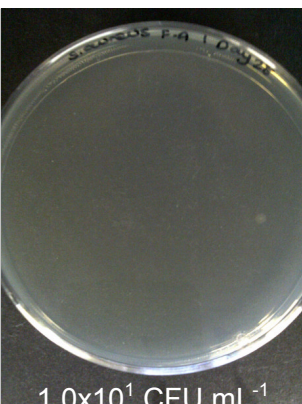


Figure 6.6. Preservative efficacy of sodium benzoate in the L-arginine formulation against Gram-positive (*S. aureus*) and Gram-negative (*P. aeruginosa* and *E. coli*) bacteria. A gradual inhibition of *E. coli* was observed, with a microbial concentration of 2×10^2 CFU.mL⁻¹ present after 7 days inoculation, decreasing to 1×10^1 CFU.mL⁻¹ after 28 days inoculation. *P. aeruginosa* was observed to have 10^1 CFU.mL⁻¹ remaining, with there being complete inhibition of *S. aureus* after 28 days inoculation. (n=3)

Table 6.4. Tryptone soya agar plates cultured with bacteria after inoculation with sodium benzoate in the L-arginine pharmaceutical preparation. Samples were cultured on days 7, 14 and 28. The preservative was found to be effective in inhibiting Gram-positive and Gram-negative bacteria growth in the oral liquid formulation. (n=3)

Bacteria	Day 7	Day 14	Day 28
<i>S. aureus</i>	 A tryptone soya agar plate with bacterial colonies. Handwritten text on the plate reads "S. aureus F-A 1 Day 7" and "AS 22/3/11". Below the plate, the CFU value is given as $6.0 \times 10^1 \text{ CFU.mL}^{-1}$.	 A tryptone soya agar plate with bacterial colonies. Handwritten text on the plate reads "S. aureus F-A 1 Day 14" and "AS 22/3/11". Below the plate, the CFU value is given as $1.3 \times 10^1 \text{ CFU.mL}^{-1}$.	 A tryptone soya agar plate showing no visible bacterial growth. Handwritten text on the plate reads "S. aureus F-A 1 Day 28" and "AS 22/3/11". The text "Complete inhibition" is written below the plate.
<i>P. aeruginosa</i>	 A tryptone soya agar plate with bacterial colonies. Handwritten text on the plate reads "P. aeruginosa F-A 1 Day 7" and "AS 22/3/11". Below the plate, the CFU value is given as $2.0 \times 10^1 \text{ CFU.mL}^{-1}$.	 A tryptone soya agar plate with bacterial colonies. Handwritten text on the plate reads "P. aeruginosa F-A 1 Day 14" and "AS 22/3/11". Below the plate, the CFU value is given as $0.7 \times 10^1 \text{ CFU.mL}^{-1}$.	 A tryptone soya agar plate with bacterial colonies. Handwritten text on the plate reads "P. aeruginosa F-A 1 Day 28" and "AS 22/3/11". Below the plate, the CFU value is given as $1.3 \times 10^1 \text{ CFU.mL}^{-1}$.
<i>E. coli</i>	 A tryptone soya agar plate with bacterial colonies. Handwritten text on the plate reads "E. coli F-A 1 Day 7" and "AS 22/3/11". Below the plate, the CFU value is given as $4.73 \times 10^2 \text{ CFU.mL}^{-1}$.	 A tryptone soya agar plate with bacterial colonies. Handwritten text on the plate reads "E. coli F-A 1 Day 14" and "AS 22/3/11". Below the plate, the CFU value is given as $1.3 \times 10^1 \text{ CFU.mL}^{-1}$.	 A tryptone soya agar plate with bacterial colonies. Handwritten text on the plate reads "E. coli F-A 1 Day 28" and "AS 22/3/11". Below the plate, the CFU value is given as $1.0 \times 10^1 \text{ CFU.mL}^{-1}$.

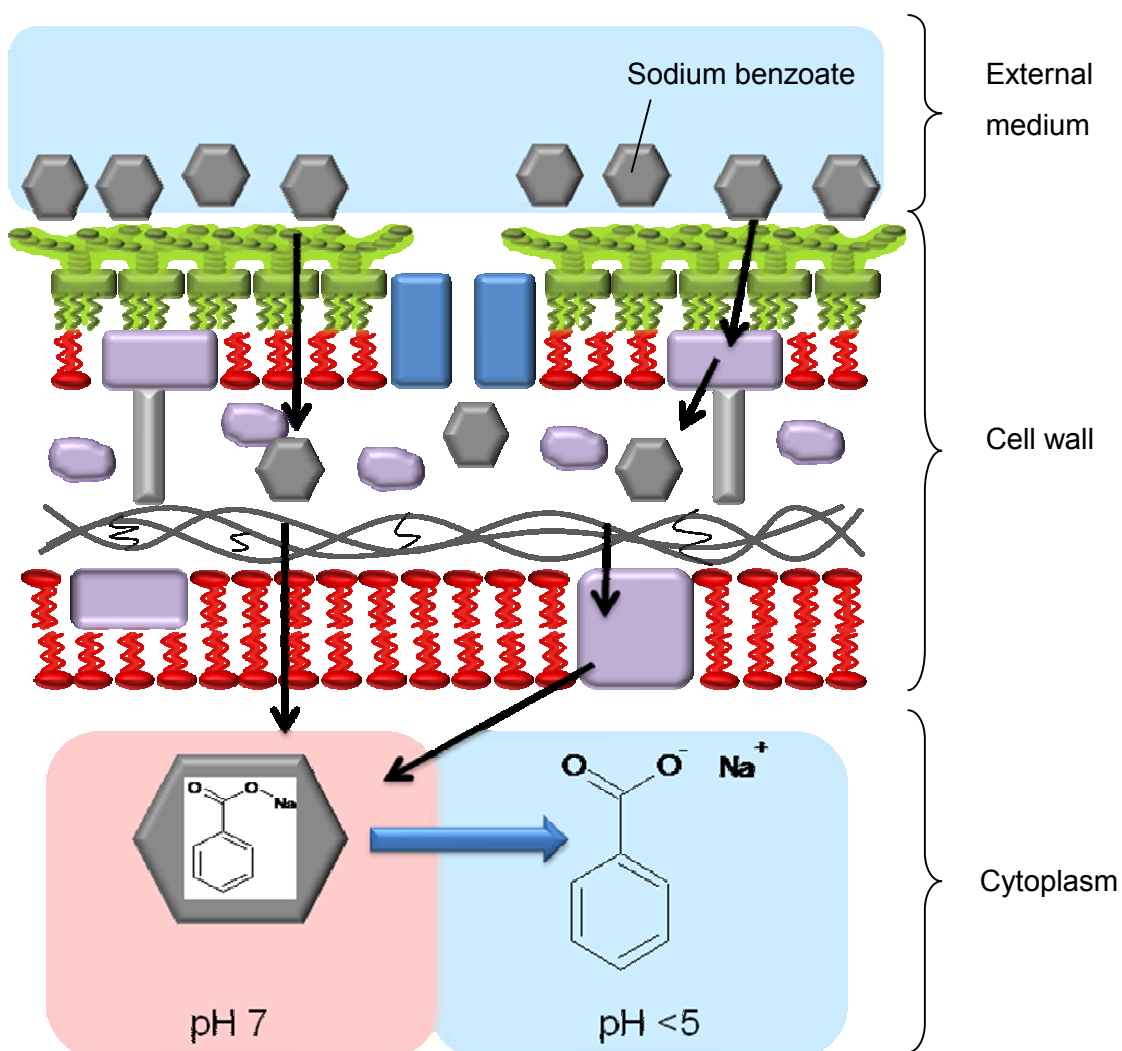


Figure 6.7. A schematic representation of the antimicrobial mechanism of sodium benzoate on the Gram-negative cell. The accumulation of sodium benzoate on the surface of the bacterial cell wall causes an influx of the preservative into the cell (modified from Chen et al, 1996).

Figure 6.7. demonstrates the bactericidal actions of sodium benzoate on the bacterial cell. Under acidic conditions (pH 2-5), sodium benzoate remains mainly in the undissociated form with high lipid solubility (Rowe *et al*, 2006). This lipophilic nature of sodium benzoate enables it to accumulate on the surface of the bacterial cell and is transported across the phospholipid layer of the cell wall (Chen *et al*, 1996). Once the preservative enters the cytoplasm of the bacterial cell (pH 7), the change in pH causes sodium benzoate to dissociate into benzoic acid and its sodium proton. As the concentration of benzoic acid increases within the cytoplasm of the cell, the intracellular pH increases in acidity causing inhibition of bacterial cellular activity (Krebs *et al*, 1983).

6.3.1.5. Preservative affects of parabens

In Chapter 3, two protocols were established in solubilising Gliclazide in water. The first method was based on using L-arginine (Section 3.2.4.1) and the second included Pluronic F127 and 15 % (v/v) ethanol (Section 3.2.4.2). Both formulations displayed alkaline pH profiles of pH 8 and pH 9 respectively, which were ideal conditions for propyl- and butyl-parabens to exert their antibacterial effects. Parabens are alkyl esters of *p*-hydroxybenzoic acid with broad antimicrobial properties, particularly against yeast and moulds, and are relatively stable over the pH range (Nguyen *et al*, 2005).

Figure 6.8 highlights the preservative efficacy of the parabens against Gram-positive and Gram-negative bacteria. After 7 days of inoculation with the microorganisms, the number of viable bacterial cells was reduced to 1.0×10^1 , 6.3×10^1 , and 1.7×10^1 CFU.mL⁻¹, for *E. coli*, *S. aureus*, and *P. aeruginosa* respectively. After 28 days inoculation, *E. coli* and *S. aureus* exhibited further reduced growth with the number of viable bacterial cells being reduced to 0.7×10^1 and 0.3×10^1 CFU.mL⁻¹ respectively. No further inhibition of *P. aeruginosa* was observed after 28 days inoculation (Table 6.5).

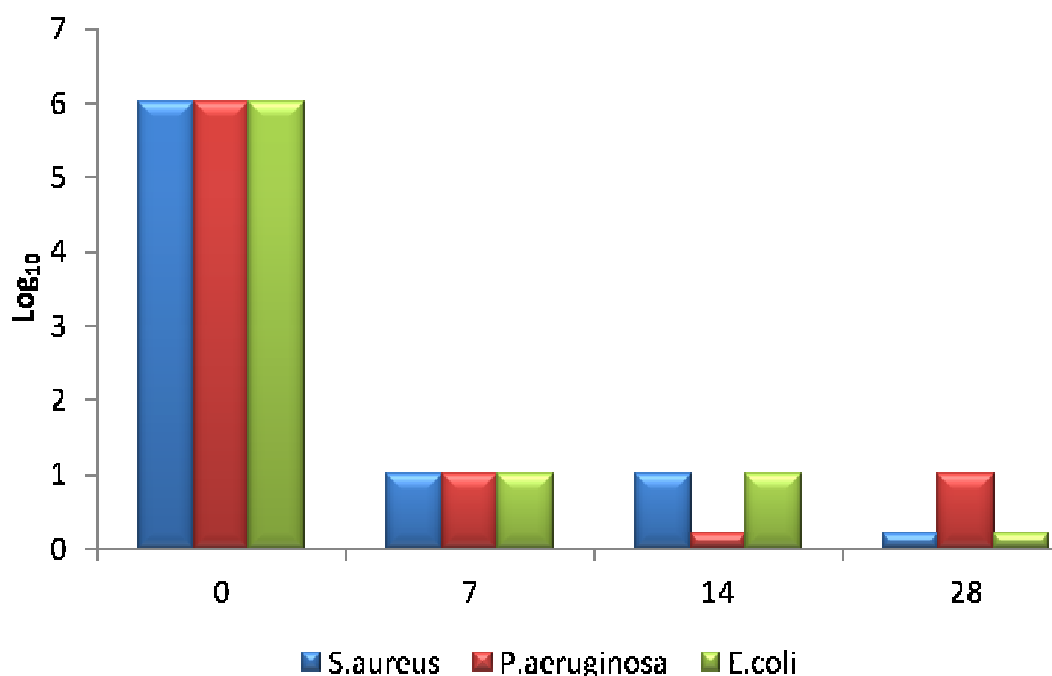


Figure 6.8. Preservative efficacy of propyl- and butyl- paraben in the Gliclazide formulation containing L-arginine against Gram-positive (*S. aureus*) and Gram-negative (*P. aeruginosa* and *E. coli*) bacteria. After 7 days inoculation the number of viable cells was reduced by a log of 5, which was maintained or further reduced by day 28. (n=3)

Table 6.5. Tryptone soya agar plates cultured with bacteria after inoculation with parabens in the Gliclazide-L-arginine pharmaceutical preparation. Samples were cultured on days 7, 14 and 28. The preservative was found to be effective in inhibiting Gram-positive and Gram-negative bacteria growth in the oral liquid formulation. (n=3)

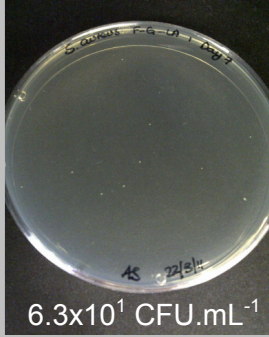
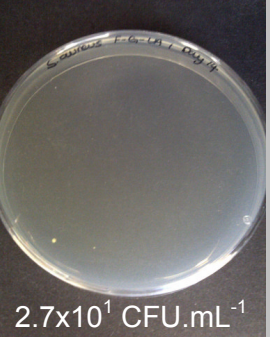
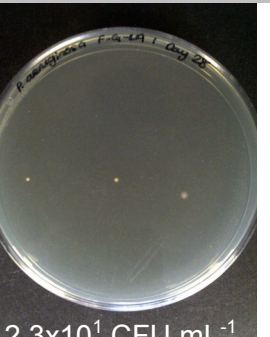
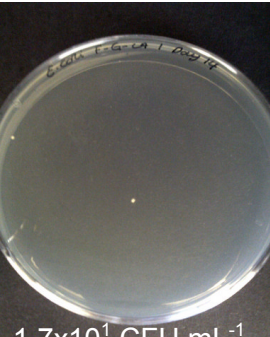
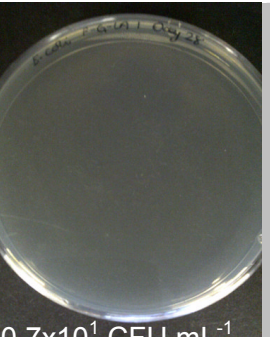
Bacteria	Day 7	Day 14	Day 28
<i>S. aureus</i>	 6.3x10 ¹ CFU.mL ⁻¹	 2.7x10 ¹ CFU.mL ⁻¹	 0.3x10 ¹ CFU.mL ⁻¹
<i>P. aeruginosa</i>	 1.7x10 ¹ CFU.mL ⁻¹	 0.7x10 ¹ CFU.mL ⁻¹	 2.3x10 ¹ CFU.mL ⁻¹
<i>E. coli</i>	 1.0x10 ¹ CFU.mL ⁻¹	 1.7x10 ¹ CFU.mL ⁻¹	 0.7x10 ¹ CFU.mL ⁻¹

Figure 6.9 and table 6.6 show similar preservative efficacy of the parabens against Gram-positive and Gram-negative bacteria when prepared in the Gliclazide formulation containing pluronic F127 and 15 % (v/v) Ethanol. After 7 days inoculation with the microorganisms, the number of viable bacterial cells was reduced to 0.7×10^1 , 0.7×10^1 , and 1.7×10^1 CFU.mL⁻¹, for *E. coli*, *S. aureus*, and *P. aeruginosa* respectively. After 28 days, no further growth of inhibition of *E. coli* and *P. aeruginosa* was observed, whereas *S. aureus* exhibited complete inhibition.

The bactericidal actions of the Gliclazide formulations were initiated by parabens which work in synergy to cause damage to the cytoplasmic membrane and thus inducing intracellular leakage through the cell wall (Furr and Russell, 1972; Soni *et al*, 2001; Nguyen *et al* 2005). Although the main antibacterial properties of the parabens involves their inhibitory effect on oxygen consumption and most oxidative enzymes, the exact mechanism by which this occurs remains relatively unknown (Soni *et al*, 2001).

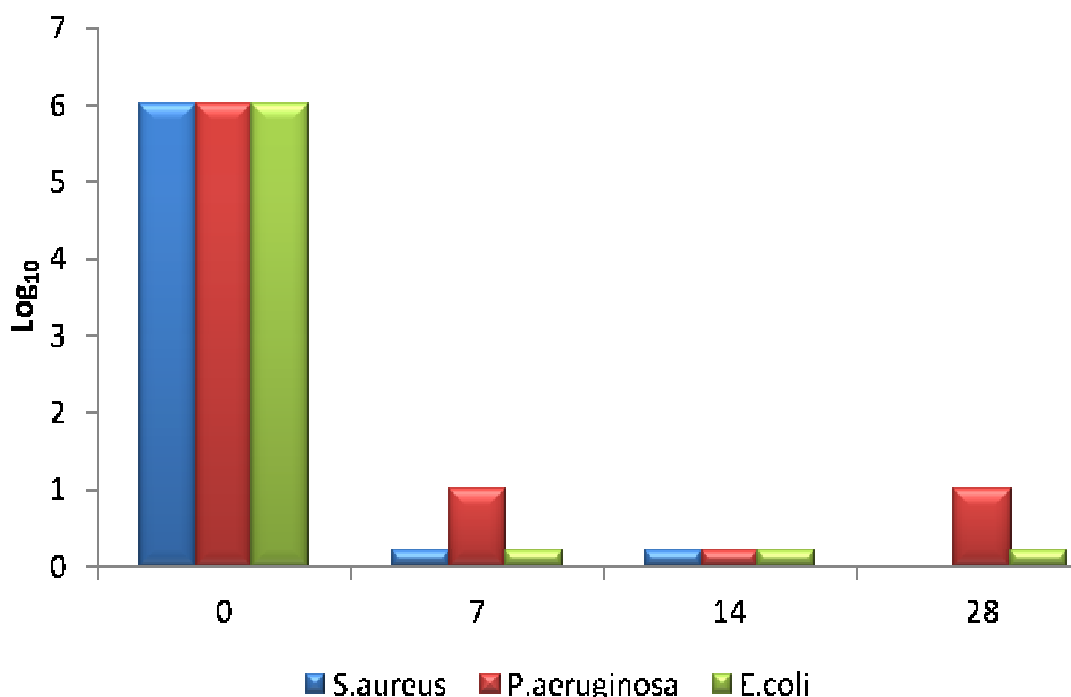
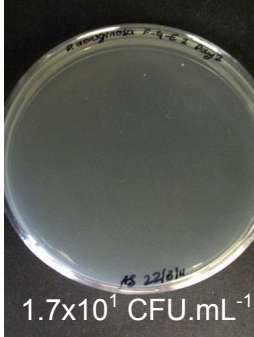
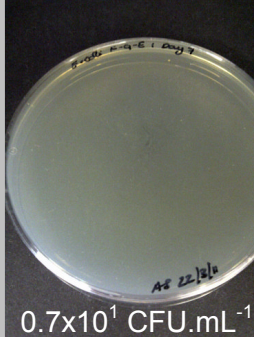


Figure 6.9. Preservative efficacy of propyl- and butyl- paraben in the Gliclazide formulation containing Pluronic F127 and ethanol (15 % v/v) against Gram-positive (*S. aureus*) and Gram-negative (*P. aeruginosa* and *E. coli*) bacteria. Complete inhibition of *S. aureus* was achieved after 28 days, with the number of viable Gram-negative cells being reduced by a \log_{10} of 5. (n=3)

Table 6.6. Tryptone soya agar plates cultured with bacteria after inoculation with parabens in the gliclazide-ethanol (15 % v/v) pharmaceutical preparation. Samples were cultured on days 7, 14 and 28. The preservative was found to be effective in inhibiting Gram-positive and Gram-negative bacteria growth in the oral liquid formulation. (n=3)

Bacteria	Day 7	Day 14	Day 28
<i>S. aureus</i>	 0.7x10 ¹ CFU.mL ⁻¹	 0.3x10 ¹ CFU.mL ⁻¹	 Complete
<i>P. aeruginosa</i>	 1.7x10 ¹ CFU.mL ⁻¹	 0.3x10 ¹ CFU.mL ⁻¹	 1.7x10 ¹ CFU.mL ⁻¹
<i>E. coli</i>	 0.7x10 ¹ CFU.mL ⁻¹	 0.7x10 ¹ CFU.mL ⁻¹	 0.7x10 ¹ CFU.mL ⁻¹

6.3.2. Preservative activity against Fungi

6.3.2.1. Fungi structure and classification

In contrast to bacterial cells (prokaryotic), fungi cells are eukaryotic in structure containing complex structures such as; mitochondria, golgi apparatus, microtubules and a nucleus enclosing the cellular DNA (Murray *et al*, 2002). Their cell wall is structurally different from the bacterial cell wall and comprises of an outer layer of mannoproteins forming a matrix with β -glucan and chitin, and an inner phospholipid membrane containing trans-membrane proteins (plasmalemma) (Figure 6.10). It is this outer cell wall that further differentiates fungal cell from mammalian cells (also eukaryotic cells).

Fungi are classified into three types based on their morphology; (1) threadlike tubular filaments (hypha), (2) group of hyphae (mycelium), and (3) single cell units reproducing by budding (yeast). However the morphology of fungi cannot be fixed as some fungal species (e.g. *C. albicans*) are dimorphic and opportunistic, and thus are able to exist in mycelium or yeast morphology depending on the growth conditions (Rose and Barron, 1983; Murray *et al*, 2002).

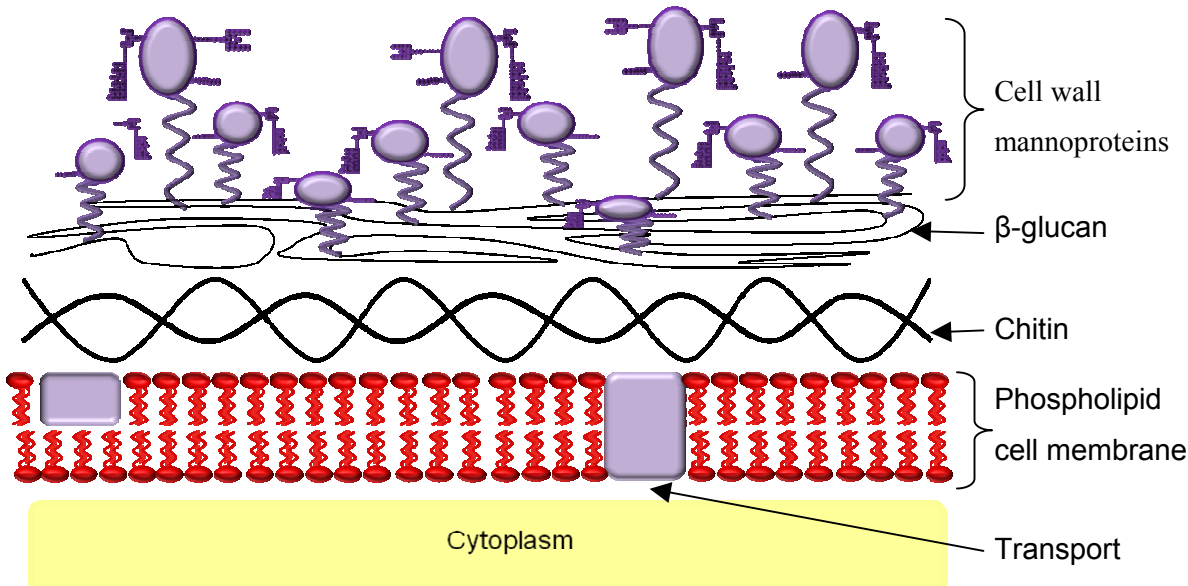


Figure 6.10. A schematic representation of a eukaryotic cell wall. The outer cell wall provides adhesion molecules and is composed of mannoproteins stabilised by β -glucan and chitin, with the inner cell wall composed of a phospholipid membrane regulating the transport of substances into the cell through transport proteins. (Modified from Grubb *et al*, 2008)

6.3.2.2. Preservative efficacy against *C. albicans*

C. albicans is an opportunistic fungi found on human mucosal surfaces, existing in the yeast form when placed in acidic-to-neutral conditions. (Grubb *et al*, 2008 and Bamford *et al*, 2009). Therefore oral pharmaceutical formulations stored in multi-dose containers must have sufficient antifungal properties to prevent proliferation.

Figure 6.11 highlights the antifungal efficacy of preservative-free captopril formulations (Section 2.2.3.3) against *C. albicans*. In the absence of a preservative, after 7 days the number of viable microbes was reduced to 10^4 CFU.mL⁻¹, achieving a \log_{10} reduction of 2. After 28 days no increases or reduction in the number of *C. albicans* was observed for either of the captopril formulations (Table 6.7). In contrast to bacterial cells, the growth of *C. albicans* decreases with increasing environmental pH conditions, with optimum microbial growth occurring at pH 6 (Faergemann *et al*, 2000). The initial decrease in microbial growth seen in figure 6.11 was attributed to the microbe being more sensitive to environmental change at the beginning of its growth. Thus as the yeast cells attempt to replicate by budding, the newly formed cells consequently lyse (Aboellil and Al-Tuwaijri, 2010).

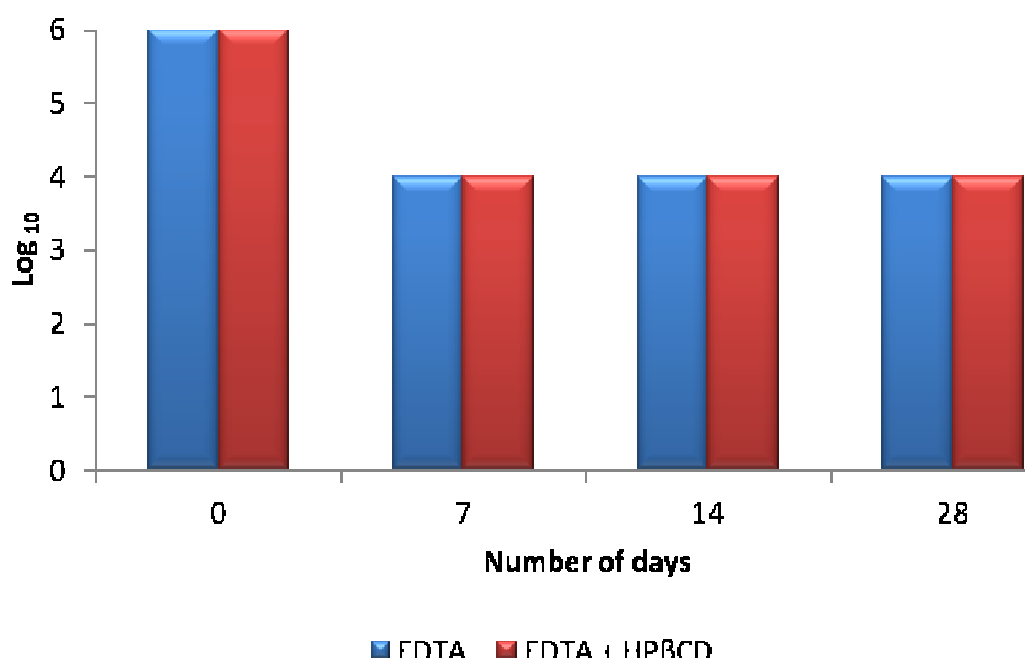


Figure 6.11. Preservative efficacy of captopril formulations containing EDTA (formulation 1) and EDTA with HPβCD (formulation 2) against *C. albicans*. After 7 days, the growth of the yeast has been reduced by a 10^2 CFU.mL⁻¹, with no further reduction or increase in the number of viable microbes being observed after 28 days. (n=3)

The preservative affect of potassium sorbate, sodium benzoate and parabens on the microbial growth of *C. albicans* is illustrated in figure 6.12 and table 6.8. After 7 days inoculation with the yeast, the number of viable microbial cells was reduced to 1×10^4 CFU.mL $^{-1}$ by potassium sorbate and sodium benzoate. After 28 days, the number of viable microbial cells was further reduced to 1.3×10^1 CFU.mL $^{-1}$ (potassium sorbate) and 6.33×10^2 CFU.mL $^{-1}$ (sodium benzoate), thus achieving a preservative efficacy by a log₁₀ reduction of 5 and 4 respectively. The inhibition of yeast was associated to the ability of the preservatives to transgress through *C. albicans* cell wall and into the cytoplasm. The neutral pH of the cytoplasmic fluid initiates the reaction of the undissociated form of the preservatives into their respective dissociated forms, thereby increasing toxicity and inhibiting cell growth (Beales, 2004).

Table 6.7. Sabroud dextrose agar plates cultured with *C. albicans* after inoculation with preservative-free captopril formulations. Samples were cultured on days 7, 14 and 28. The formulations were found to be ineffective in inhibiting the yeast despite the acidic pH of the pharmaceutical preparations. (n=3)

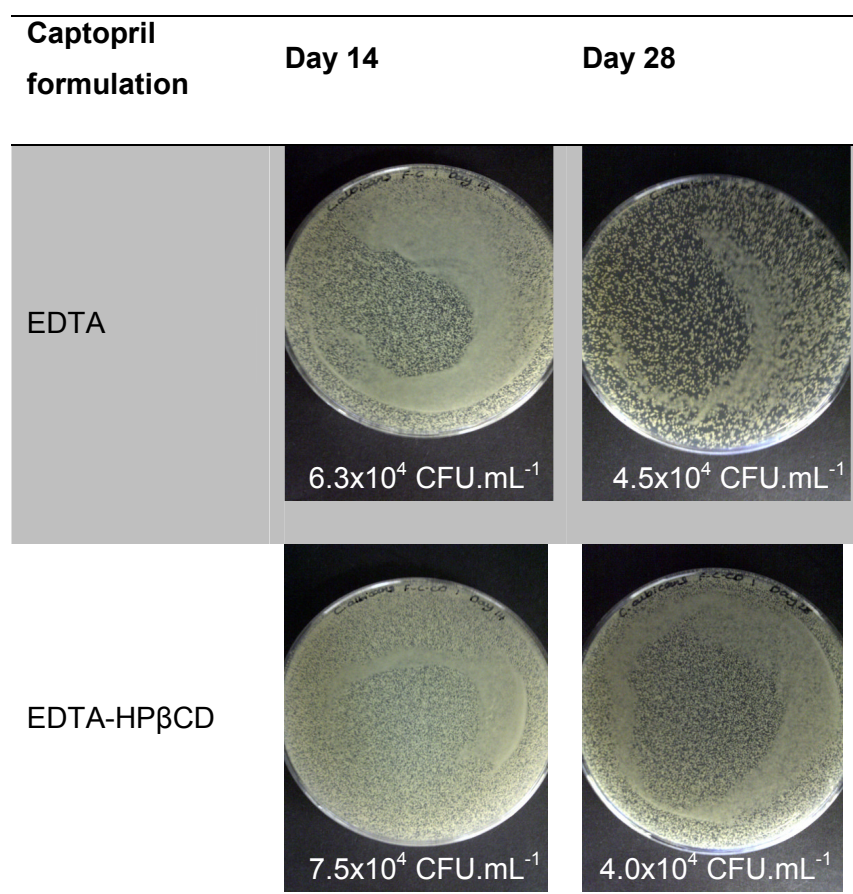


Figure 6.12 and table 6.8 displays the biocidal properties of gliclazide formulations against *C. albicans*, with the parabens working in synergy with the alkaline pH of the formulations (pH 8-9). Within 7 days of inoculation, the parabens (gliclazide-ethanol formulation, pH 9) had completely destroyed the yeast cells, with no re-growth occurring within the 28 day test period. In the absence of ethanol (gliclazide-L-arginine formulation, pH 8), parabens possibly had an inhibitory affect on the oxidative enzymes within the cytoplasm (Soni *et al*, 2001) thereby causing cell death and a reduction in the number of viable cells by 10^5 CFU.mL^{-1} at day 7, with almost complete inhibition occurring by day 28 ($0.3 \times 10^1 \text{ CFU.mL}^{-1}$). The latter formulation exhibited slightly slower biocidal affects which was attributed to the lowered alkaline environment in comparison to the former formulation. It was known that inhibition of *C. albicans* increased with increasing pH above 6 (Faergemann *et al*, 2000).

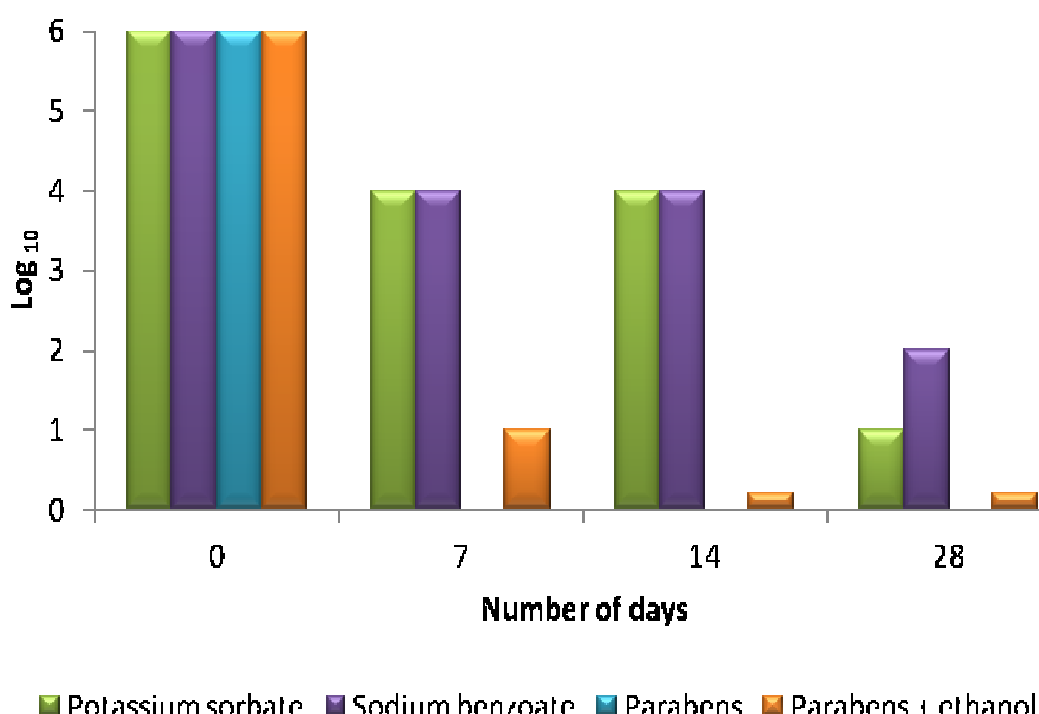
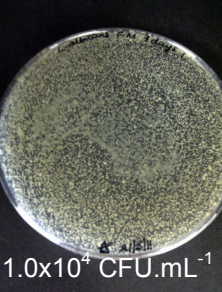
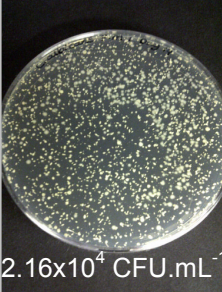
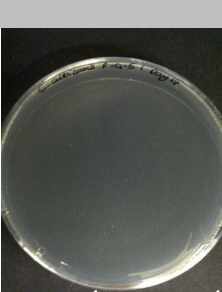
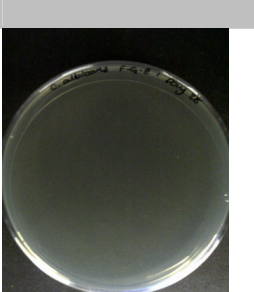


Figure 6.12. Preservative efficacy of; potassium sorbate (melatonin formulation), sodium benzoate (L-arginine formulation), parabens (gliclazide-L-arginine formulation) and parabens with ethanol (gliclazide-ethanol formulation) against *C. albicans*. After 7 days inoculation, potassium sorbate and sodium benzoate achieve a microbial reduction of 10^2 CFU.mL^{-1} , with the number of viable cell decreasing to 10^1 and 10^2 CFU.mL^{-1} by day 28. The parabens exhibited excellent biocidal properties against *C. albicans* with complete inhibition by day 14. (n=3)

Table 6.8. Sabroud dextrose agar plates cultured with *C. albicans* after inoculation with formulations containing; potassium sorbate, sodium benzoate, parabens, or parabens in the presence of ethanol (15 % v/v). Samples were cultured on days 7, 14 and 28. The formulations were found to be effective in inhibiting yeast cells. (n=3)

Preservatives	Day 7	Day 14	Day 28
Potassium sorbate	 1.0x10 ⁴ CFU.mL ⁻¹	 2.16x10 ⁴ CFU.mL ⁻¹	1.3x10 ¹ CFU.mL ⁻¹
Sodium benzoate	 1.0x10 ⁴ CFU.mL ⁻¹	 1.0x10 ⁴ CFU.mL ⁻¹	6.33x10 ² CFU.mL ⁻¹
Parabens	 Complete	 Complete	 Complete
Parabens in the presence of ethanol (15 % v/v)	 1.7x10 ¹ CFU.mL ⁻¹	 0.3x10 ¹ CFU.mL ⁻¹	 0.3x10 ¹ CFU.mL ⁻¹

6.3.2.3. Preservative efficacy against *A. niger*

A. niger is classified as a filamentous fungi with hyphal morphology. Its structure enables production of club-shaped cell (ascomycete) spores. These cells are rich in supply of a range of hydrolytic and oxidative enzymes that are susceptible to attack by antimicrobial agents (Baker, 2006). In the presence of antimicrobial preservatives, almost complete inhibition of *A. niger* was achieved within 7 days of inoculation (Figure 6.13 and Table 6.9). After 28 days inoculation, the parabens had effectively eliminated majority of the fungal cells, with the microbial cell count in the presence of potassium sorbate and sodium benzoate being reduced to 0.3×10^1 and 0.7×10^1 CFU.mL⁻¹ respectively, achieving a log₁₀ reduction of 5. The eradication of the microbial cells was possibly associated with the increase of β-glucan sensitivity to alkaline conditions (pH > 5) (Shenoy *et al.*, 1984), thereby being more susceptible to attack in the early stage of microbial growth. The parabens exhibited biocidal actions by inhibiting the oxidative enzymes and causes cell starvation and death (Soni *et al.*, 2001).

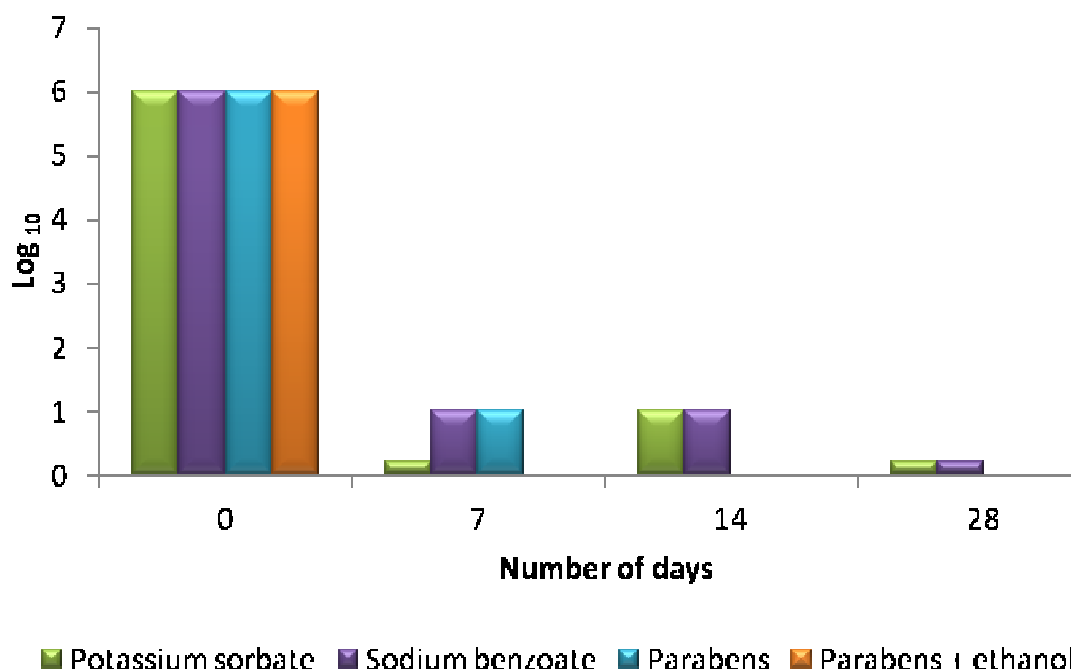
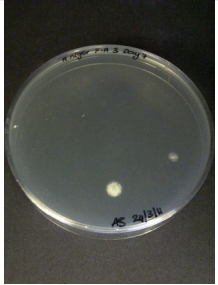
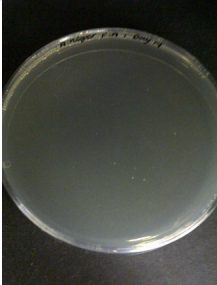
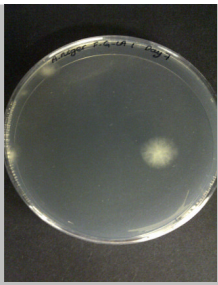
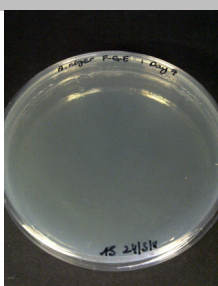
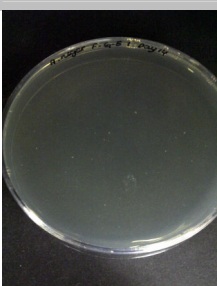


Figure 6.13. Inhibition of *A. niger* by preservative-containing formulations within 28 days of inoculation. The rich oxidative enzymes within the microbial cell allowed for the complete inhibition of *A. niger* within 7 days of inoculation. After 28 days, formulations containing parabens had eradicated the fungi, with the microbial cell count being reduced to 0.3×10^1 and 0.7×10^1 CFU.mL⁻¹ by potassium sorbate and sodium benzoate respectively. (n=3)

Table 6.9. Sabroud dextrose agar plates cultured with *A. niger* after inoculation with formulations containing; potassium sorbate, sodium benzoate, parabens, or parabens in the presence of ethanol (15 % v/v). Samples were cultured on days 7, 14 and 28. The formulations were found to be effective in inhibiting fungi cells. (n=3)

Preservative	Day 7	Day 14	Day 28
Potassium sorbate			
Sodium benzoate			
Parabens			
Parabens in the presence of ethanol (15 % v/v)			

6.4. Conclusion

The preservative efficacy test was aimed to challenge the efficacy of the antimicrobials when placed in a pharmaceutical preparation containing active constituents. This was essential with preparations being stored in multi-dose containers that were susceptible to microbial contamination. According to the BP (2009), the criteria of acceptance for oral preparations was a \log_{10} reduction of 3 and 1 for bacteria and fungi respectively, with no further increase in growth within 28 days of incubation. The study has shown that all the different formulations had sufficient preservative activity against both bacterial as well as fungal microbes.

CHAPTER 7

Solubilisation of a proton pump inhibitor
(lansoprazole) using nano-particulate delivery

Papers relating to this chapter

Shabir, A., AlHusban, F., Mohammed, A. (2011). Effects of ball-milling on PLGA polymer and its implication on lansoprazole-loaded nanoparticles. *Journal of Basic and Clinical Pharmacy*, 2(2): 71-82

CHAPTER 7

Solubilisation of a proton pump inhibitor (lansoprazole) using nano-particulate delivery

7.1. Introduction

7.1.1. Therapeutic effect of proton pump inhibitors (PPI's)

Proton pump inhibitors (PPI's) are a specialised class of anti-secretory drugs used to treat peptic ulcer, gastroesophageal reflux, dyspepsia, gastrinomas, Barrett's oesophagus and laryngopharyngeal reflux. They act by preventing the secretion of H⁺ ions into the gastric lumen and lowering acid production by blocking the gastric proton pump of the parietal cells (terminal stage in gastric secretion).

7.1.1.1. Structure, mechanism of action and metabolism of lansoprazole

Lansoprazole (PPI) is a substituted benzimidazole, [[[3-methyl-4-(2,2,2-trifluoroethoxy)-2-pyridyl] methyl] sulfinyl] benzimidazole (Figure 7.1), with a molecular weight of 369.37 and pKa 17.3. The molecule is relatively lipophilic with a water solubility profile of 0.97 mg.L⁻¹. This enables the molecule to readily cross the cell membranes into acidic intracellular compartments, resulting in protonation of the drug into its active form and allowing it to covalently and irreversibly bind to the gastric pump resulting in its deactivation.

Lansoprazole ultimately blocks the final step in acid production. This is carried out by suppressing the gastric acid secretion by specific inhibition of the (H⁺,K⁺)-ATPase enzyme system at the secretory surface of the gastric parietal cell (Wallmark *et al*, 1983). The extent of acid inhibition can be dose related and leads to inhibition of the basal and the stimulated gastric acid secretion, regardless of the stimulus.

Lansoprazole can be metabolised in two ways. The first is by S-mephenytoin 4 β -hydroxylase (CYP2C19) which converts lansoprazole to hydroxylansoprazole (Shirai *et al*, 2002). The second method involves partial conversion to lansoprazole sulphone by CYP3A4 followed by full metabolism to hydroxylansoprazole sulphone by CYP2C19 (Pearce *et al*, 1996). Both metabolised products are then excreted in the urine.

7.1.1.2. Current dosage forms

Currently lansoprazole is only marketed as a solid dosage form: Zoton® (FasTab®) and Lansoprazole (capsules), supplied as 15 and 30 mg doses. In the US however, lansoprazole is available as a delayed release capsule (Prevacid) and a delayed release orally disintegrating tablet (Solutab). However, aqueous preparations (liquid dosage forms) have as yet to be developed for the pharmaceutical market due to two major obstacles: (1) insolubility in water and (2) degradation rate increasing with decreasing pH.

7.1.2. Polymeric nanoparticle delivery

In order to overcome obstacles of poor water solubility and degradation in acidic media, polymeric particles provide a practical approach as their matrix provides a hydrophobic environment within which the drug molecule is protected from the harsh acidic conditions in the stomach. Therefore for the current study, polymeric nanoparticles were prepared using the solvent displacement technique, chosen for its simple manufacturing process and its success with high entrapment of poorly soluble drugs (Fessi *et al*, 1989; Quintanar-Guerrero, 1998; Barichello *et al*, 1999; Hans and Lowman, 2002). However the efficiency of entrapment was found to be dependent upon the compatibility between the drug and the polymer.

Polycaprolactone (PCL) and Polylactide-coglycolide (PLGA) (Figure 7.1) are hydrophobic biodegradable polymers that are approved by the FDA for human use (Faraji and Wipf, 2009). PCL has a semi-crystalline structure with its crystallinity decreasing with increasing molecular weight (Woodruff and Hutmacher, 2010). It was initially synthesised in the early 1930s (Van Natta *et al*, 1934). The polymer's numerous advantages have propelled its use within the biomedical field which include: good solubility, low melting point of 59-64 °C and a glass transition temperature of -60 °C enabling ease of preparation at relatively low temperatures, tailorabile degradation kinetics and mechanical properties capable of providing controlled release of the drug load from its matrix (Chandra and Rustgi, 1998; Okada, 2002; Nair and Laurencin, 2007). PLGA (a poly-lactide (50:50)) has an amorphous structure with a glass transition temperature of 55-50 °C.

Both polymers were chosen for their dual action purpose; (1) protection of lansoprazole against acid degradation and (2) regulation of the release rate of lansoprazole.

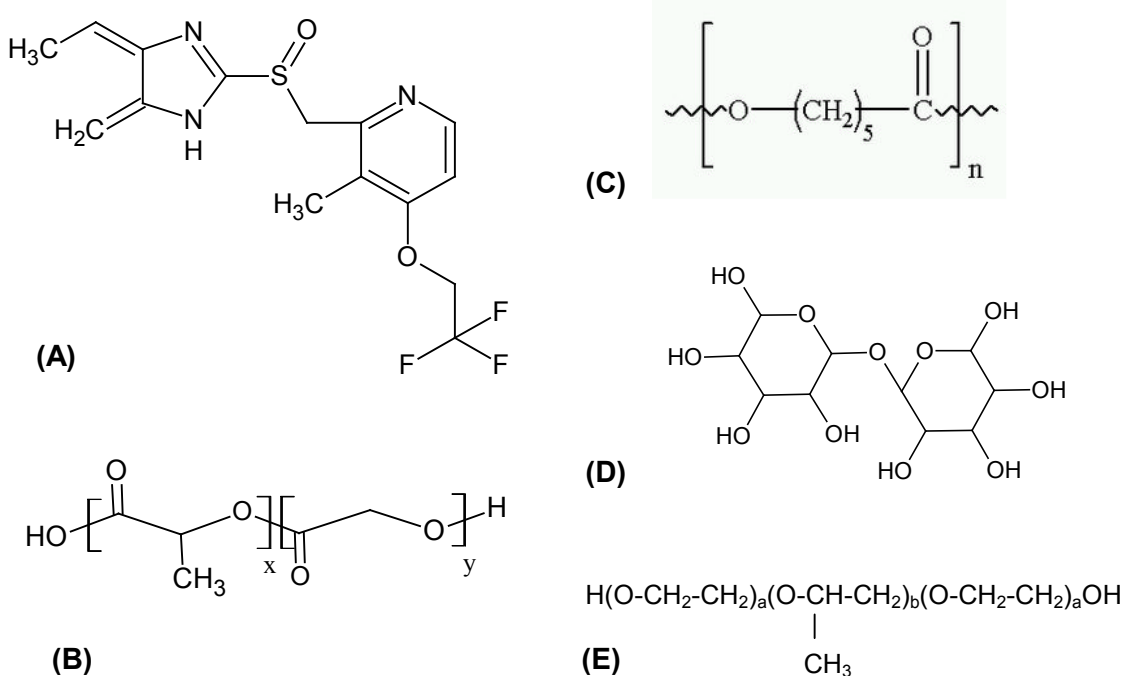


Figure 7.1. Chemical structures of: (A) lansoprazole and the monomer units of (B) PLGA (C) PCL, (D) Trehalose and (E) Pluronic F127.

7.1.2.1. Special consideration for nanoparticulates during formulation

After administration, the main parameters controlling the drug distribution, absorption and biological activity include: mean particle size, surface charge, and hydrophobicity of the biodegradable polymer (Gibaud *et al*, 1996). These nanoparticle characteristics are key determinates of nanoparticle interaction with the intestinal cell membrane and their penetration across the physiological drug barriers (Norris *et al*, 1998; Kumari *et al*, 2010). This was particularly important with regard to the hydrophobicity and particle size of the nanoparticles, as by reducing the hydrophobicity of the particle with the adsorption of poloxamines, the uptake of particles into the cells of the immune systems was also reduced, and thus enabling the nanoparticles to avoid elimination (Moghimi *et al*, 1994; Florence *et al*, 1995; Hillery and Florence, 1996; Davis and Illum, 1998). Similarly, a reduction in particle size results in an increase in the absorption of particles across the cell wall barrier and thus more particles are distributed more easily to distant sites and remain undetected by macrophages for a longer period of time.

With regard to oral delivery of nanoparticles, the composition of the particle must enable it to navigate pH gradients, have a protective membrane, pass through hydrophilic and hydrophobic domains, pass through opposing solubility and absorption regimes and survive various metabolic and transport proteins (Arayne *et al*, 2007).

7.1.3. Aim

Previous studies indicated that a variation in the polymer-drug ratio, molecular weight and composition of the polymer can modify the extent of release of the drug (Prabha and Labhasetwar, 2004b). The choice of polymer also influences the mechanism of internalisation and intracellular localisation (Murakami *et al*, 1999). Therefore the polymer chosen to form the colloidal matrix was extremely important not only for polymer-drug compatibility to ensure maximum loading but also to ensure maximum *in-vivo* effects at the targeted site of action. Therefore PCL and PLGA were chosen for their biodegradable and hydrophobic nature.

The overall aim of the study was to establish a validated calibration protocol for the extraction and quantification of lansoprazole using UV spectrophotometry and formulate nanoparticles loaded with a minimum dose of 1 mg.mL^{-1} that could potentially be effective *in-vivo*.

The objectives included:

- Preparation and characterisation of PCL and PLGA nanoparticles at varying polymer-drug ratios (5:1, 6:1 and 7:1) using the solvent displacement technique
- Comparison of the solvent displacement technique against emulsion diffusion technique using PCL nanoparticles at a varying polymer-drug ratios (5:1, 6:1 and 7:1)
- Influence of milled polymers on the characterisation of the nanoparticles
- Physical implications of milling on PCL and PLGA
- Physicochemical implications on the nanoparticles formed
- Drug release studies and the implication of milling the polymer on the drug release rate

7.2. Methods and Materials

7.2.1. Materials

Lansoprazole (assay $\geq 98\%$), polycaprolactone (PCL, Mw 115,000), poly (DL-lactide-co-glycolide) (PLGA, 50:50, Mw 5,000-15,000), phosphate buffered saline (PBS), pluronic F127. Trehalose, monobasic sodium phosphate, sodium hydroxide and sodium dodecylsulphate and HCl were all purchased from Sigma (U.K.). Tetrahydrofuran and acetone were purchased from Fisher Scientific (UK). Deuterated Dimethyl sulfoxide (DMSO-D₆) was purchased from Goss Scientific Instrument Ltd (Cheshire, UK).

7.2.2. Methods

7.2.2.1. Development of a calibration method for lansoprazole

Calibration was carried out using a JENWAY 6105 U.V/Vis spectrophotometer at a wavelength of 285 nm. 6 mg of lansoprazole was dissolved in 350 mL PBS to obtain a stock concentration of $17 \mu\text{g.mL}^{-1}$. Serial dilutions were then carried out to obtain further concentrations (3, 6, 9, 11, 13 and $15 \mu\text{g.mL}^{-1}$). Once the UV spectrophotometer had been set to zero using PBS, 2.5 mL of each lansoprazole concentration was analysed in disposable cuvettes.

7.2.2.2.1. Calibration validation protocol

Linearity

Linear regression was calculated by the least square regression method, with the standard curves being prepared on three different days. The calibration curves were obtained using six concentrations of reference standard solution for the spectrophotometric method (3, 6, 9, 11, 13, and $15 \mu\text{g.mL}^{-1}$).

Precision

The precision of the protocol was determined by immediate precision of the calibration protocol (intra-day), which was evaluated by assaying samples of set sample concentrations on the same day, and repeatability (inter-day), which was analysed by comparing the assays on three different days.

Accuracy

The accuracy was determined by assaying three known concentrations in triplicate. For the spectrophotometric method these concentrations were 5, 10 and 14 µg.mL⁻¹.

Limit of detection (LOD)

The LOD was calculated on the SD of the response and slope. The equation used is as follows:

$$\text{LOD} = \frac{3.3 \times \text{Mean SD of blank determination}}{\text{Slope of standard curve}}$$

Limit of quantification (LOQ)

The LOQ was calculated based on the SD of the response and slope using three calibration curves. The equation is as follows:

$$\text{LOQ} = \frac{10 \times \text{Mean SD of blank determination}}{\text{Slope of standard curve}}$$

7.2.2.2. Nanoparticle preparation using the solvent displacement technique

The polymer (PLGA or PCL) was dissolved in 10 mL of acetone, with slight heating, to which 10 mg of lansoprazole was added and left to stir until lansoprazole had fully dissolved. The amount of polymer added was varied to produce the following polymer-to-drug ratios: 5:1, 6:1 and 7:1. The organic solution formed was added drop-wise slowly into 0.25 % (w/v) Pluronic F127 solution in PBS, under magnetic stirring. The volume of nanosphere dispersion was then concentrated to 10 mL under reduced pressure. The final solution was then centrifuged at 3200 for 30 minutes or 20000 rpm for 1 hour (PLGA and PCL nanoparticles respectively), to allow for the separation of the non-encapsulated lansoprazole from the encapsulated nanoparticles. The supernatant formed was separated for lansoprazole analysis via UV and

the pellets were re-dispersed in distilled water to produce a final concentration of 1 mg.mL^{-1} of lansoprazole.

7.2.2.3. Nanoparticle preparation using the emulsion diffusion technique

PCL was dissolved in 5 mL of acetone, with slight heating, to which 10 mg of lansoprazole was added and left to stir until lansoprazole had fully dissolved. The amount of polymer added was varied to produce the following polymer-to-drug ratios: 5:1, 6:1 and 7:1. The organic solution formed was added drop-wise slowly into 0.25 % (w/v) Pluronic F127 solution in PBS under magnetic stirring. The nanoparticle solution was magnetically stirred for 3 minutes before being emulsified for 7 minutes with a high-speed homogeniser, after which 25 mL of water was added under moderate magnetic stirring for 3 minutes. This nanosphere solution was then centrifuged at 4,500 rpm for 1 hour to allow for the separation of the non-encapsulated lansoprazole. The supernatant formed was separated and the pellets were re-dispersed in 5 mL of distilled water to produce a final concentration of 1 mg.mL^{-1} of lansoprazole.

7.2.2.5. pH

The pH of each sample was analysed using a Hydrus 500 (Fisherbrand, UK), calibrated at pH 4, 7 and 10.

7.2.2.6. Particle sizing

Particle size of the nanoparticulate suspension was analysed using a Zetasizer (Brookhaven, U.K). 50 μL of sample was diluted in 2 mL of distilled water in a cuvette. Values reported are the mean \pm SD of 3 different batches of each formulation. For particle size analysis the polydispersity index was also measured. This is a measure of the width of distribution calculated from the SD of the distribution divided by the mean value.

7.2.2.7. Planetary-ball milling

PCL was initially mechanically milled by pestle and mortar as the sample must be less than 0.5 mm in diameter prior to planetary micromilling. Into each of the planetary mill chambers were placed 18 agate balls, to which 3 g of the polymer was placed on top. The lid was secured in place ensuring the white rim was also in place to help seal the lid down. The chambers were then screwed securely in place. PLGA and PCL polymers were milled using a planetary micromill (Pulveristte 7, Fritsch, Germany) for 1 hour at 200 rpm and 400 rpm.

7.2.2.8. Scanning electron microscopy (SEM)

SEM was performed on the milled and non-milled polymers and on PCL nanospheres. The samples were mounted onto standard specimen stubs using a double-sided adhesive tape and left to air dry for 24 hours. The stubs were then in turn loaded and fastened to a universal specimen holder and subjected to low-vacuum gold sputter before being subjected to SEM.

7.2.2.9. Micro-viscosity testing of PCL nanoparticles

Non-milled PCL lansoprazole-loaded nanoparticles prepared using the emulsion diffusion techniques were measured for their viscosity before and after homogenisation. This was carried out using the automated micro-viscometer (Anton-Paar, AMVn, Graz, Austria), which measures the viscosity of a sample by measuring the rolling ball time between a fixed distance along the 1.8 mm glass capillary tube. Temperature within the capillary tube was controlled to 25 °C.

7.2.2.10. Molecular weight analysis of milled polymers using gel permeation chromatography (GPC)

Using a PL-GPC 50 machine (A Varian, Inc. Company, by polymer laboratories), 3 mg of the milled polymer was dissolved in 1 mL of tetrahydrofuran, which was then injected into the GPC machine. Samples were analysed using the GPC/SEC software.

7.2.2.11. Wettability profiling

Contact angle measurements were made using the Wilhelmy-plate method in order to determine the wetting interaction between the polymer surface and distilled water. This was carried out using the QCT-100 programme in which the glass coverslip was coated with double-sided tape and dipped into the polymer ensuring both sides of the coverslip was thoroughly coated. Excess particles were dabbed off into a plastic tray. The coverslip was then hung on a balance and slowly lowered into a beaker containing distilled water at a rate of 0.2 mm.s⁻¹. The advancing, receding and hysteresis contact angles of the particles was then calculated using the QCT-100 software provided.

7.2.2.13. Freeze-drying preparation of nanoparticles

Nanoparticles were prepared using the solvent displacement technique. After re-hydration in distilled water, 1 % (w/v) trehalose was added to provide structural integrity and support during the freeze-drying process. The freeze-drying process involves primary drying for 48 hours at a shelf temperature of -40 °C followed by secondary drying for 10 hours at a shelf temperature of 20 °C. Both drying stages were carried out at a vacuum pressure of 50 mTorr.

7.2.2.14. Differential scanning calorimetry (DSC)

DSC (Perkin-Elmer, Wellesley, USA) was used to study the T_g and melting points. Approximately 5 mg of sample was placed in a Perkin-Elmer aluminium pan. The sample was cooled to 10 °C using the attached intra-cooler (2P Perkin-Elmer, Wellesley, USA) followed by heating to 240 °C at a rate of 10 °C·min⁻¹, with a nitrogen purge of 20 mL·min⁻¹. The samples consisted of Lansoprazole, PCL and PLGA in their original states, and after planetary-ball milling at 200 rpm for 1 hour, and various nanoparticle formulations after being freeze-dried. An empty aluminium pan was used as a reference.

The T_g and T_m were then analysed using the Pyris Manager software. All of the measurements were carried out in triplicate with fresh samples being prepared for each DSC run. The DSC was calibrated for temperature and heat flow, prior to the samples being tested using standard samples of indium (T_m 156.6 °C) and zinc.

7.2.2.15. Thermogravimetric Analysis (TGA)

Thermal degradation of Lansoprazole was performed using a TGA which determines the dependence of the weight loss of a sample as a function of temperature. The system consisted of a Pyris 1 Thermogravimetric Analyzer (Perkin Elmer). The sample masses ranged from 2-5 mg and were heated from 25-300 °C at a rate of 10 °C·min⁻¹ in a dry nitrogen atmosphere. The instrument regulated the heating rate automatically in order to maintain a constant temperature during a given thermal event.

7.2.2.16. Fourier Transform Infrared Spectroscopy (FTIR)

FTIR spectra of samples (lansoprazole, PLGA, milled PLGA, PCL, milled PCL, pluronic F127, and nanoparticle formulations) were obtained on an IR spectrophotometer (UK). The sample and freeze-dried nanoparticles (7.2.2.13.) were added to potassium bromide at a ratio of 1:5 (sample : potassium bromide) and thoroughly mixed which was then compacted

by a mechanical press for 5 minutes to form the translucent pellet used to determine the transmittance of each excipient.

7.2.2.17. Proton Nuclear Magnetic Resonance Spectroscopy (H^1 -NMR)

Lansoprazole-loaded nanoparticles (PCL/PLGA), physical mixture of PCL/PLGA and lansoprazole were dissolved in DMSO-D₆ solution at room temperature in 5 mm glass tubes. Approximately 2 mg of sample dissolved in 600 μ L of DMSO-D₆. All NMR measurements were done with standard Bruker pulse sequences.

7.2.2.18. In Vitro Release Studies

The release of lansoprazole from the nanoparticles was studied in the fasted state in accordance with the USP 31-standard, and non-fasted states in accordance with the BP standard. All dissolution vessels have been wrapped in foil to prevent photodegradation of lansoprazole as it was being released from the nanoparticles into the medium.

In vitro release was carried out in dissolution baths at 37 °C in various buffers according to the fasted and non-fasted state protocols.

7.2.2.18.1. Nanoparticle preparation

PCL and PLGA loaded nanoparticles were prepared according to the above protocol (7.2.2.2) at 20,000 rpm for 1 hour.

2.2.2.18.2. Fasted State

The buffer consisted of an acid stage containing 500 mL 0.1 M HCl at pH 3. The nanoparticles were placed in rotating baskets at 75 rpm for 1 hour in the acid solution. After which samples were placed into a 900 mL phosphate buffer at pH 6.8. The buffer consisted of monobasic sodium phosphate, sodium hydroxide (NaOH) and sodium dodecylsulphate (16.35 g, 7.05 g and 3 g respectively in 1 L of distilled water). The buffer was adjusted to pH 6.8 using 10 M NaOH. At set time points (5, 10, 15, 30, 45, 60, 90, 120, 180, 240, 360, 1440 and 2880 minutes) 5 mL samples of the release medium was withdrawn, following this 5 mL of fresh phosphate buffer was added to the dissolution baths in order to maintain sink conditions. The 5 mL samples of release medium were then assayed at 285 nm for drug recovery using the UV spectrophotometer. The drug release experiments were carried out in triplicate.

7.2.2.18.3. Non-Fasted State

The buffer consisted of an acid stage containing 500 mL phosphate buffer at pH 4.5, composed of 10 M sodium hydroxide and 0.05 M phosphate buffer (1:99 ml respectively). The nanoparticles were placed in rotating baskets at 75 rpm for 1 hour in the acid solution. After which samples were placed into a 900 mL phosphate buffer at pH 6.8. The buffer consisted of monobasic sodium phosphate, sodium hydroxide and sodium dodecylsulphate (16.35 g, 7.05 g and 3 g respectively in 1 L of distilled water). The buffer is adjusted to pH 7 using 10 M NaOH. At set time points (5, 10, 15, 30, 45, 60, 90, 120, 180, 240, 360, 1440 and 2880 minutes) 5 mL of the release medium is withdrawn and immediately replaced with fresh 5 mL phosphate buffer in order to maintain sink conditions. The samples taken from the release medium was then assayed at 285 nm for drug recovery using the UV spectrophotometer. The drug release experiments were carried out in triplicate.

7.2.2.19. Statistical analysis

Statistical analysis was carried out by analysis of variance (ANOVA) and the unpaired *t*-test, with the significant differences being judged as $P<0.05$.

7.3. Results

7.3.1. Calibration Validation

A UV spectrophotometer calibration was used to produce a validated calibration protocol for the in-direct determination of lansoprazole loaded within the nanoparticles. At a detection wavelength of 285 nm, the supernatant of the nanoparticles was dissolved in PBS to quantify the amount of lansoprazole un-bounded to the nanoparticles.

7.3.1.1 Linearity

The linearity of the UV method was evaluated by preparing the standard curve for lansoprazole on 3 consecutive days. The absorbance was plotted against the lansoprazole concentration and the calibration response was assessed for variances. The results show that the data complied with the Beer Lambert's law in the concentration range investigated ($3\text{-}17 \mu\text{g.mL}^{-1}$), with the linear plot producing a regression equation of $y=0.0319x$ ($R^2=0.9955$) (Figure 7.2).

7.3.1.2 Precision

In order to assess the reproducibility of the calibration protocol, the calibration method was carried out in triplicate over a period of 3 days for interday precision, and in triplicate on the

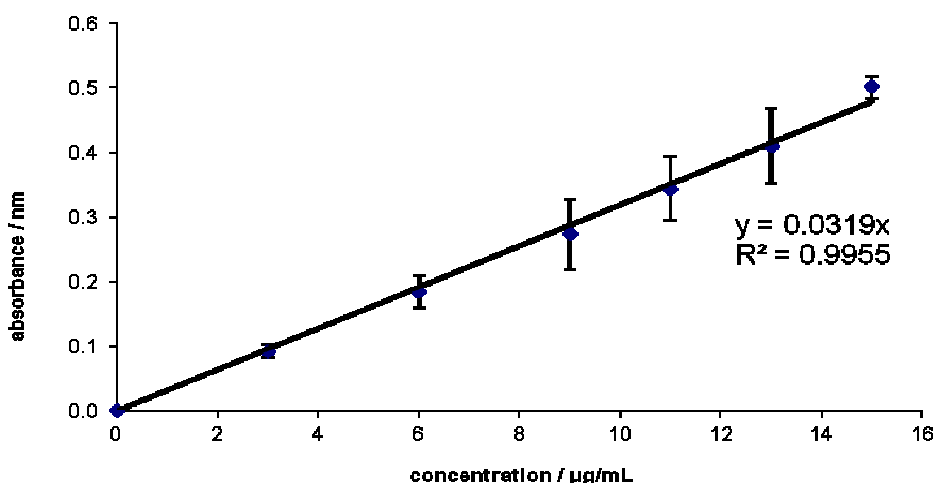


Figure 7.2. Graph of lansoprazole calibration highlighting the linearity of the validation protocol. ($n=3$)

same day for intraday precision. It was concluded that the calibration method was reproducible, with inter-day precision of 110.3 %, and the intra-day precision of 109.1 %. Statistical data was compared using ANOVA statistical test, with the resulting inter-day and intra-day precision being calculated to have a variance of P>0.05 (Table 7.1).

7.3.1.3. Accuracy

The accuracy of the developed method was determined from three concentrations of lansoprazole in PBS, representing the low, medium and high portions of the standard curve ($5, 10$ and $14 \mu\text{g.mL}^{-1}$). Accuracy of the three concentrations was in the range of 98.1-99.3 % (Table 7.1).

7.3.1.4 Limit of detection (LOD) and limit of quantification (LOQ)

The limit of detection of an individual analytical procedure is the lowest amount of analyte in a sample which can be detected but not necessarily quantifiable as an exact value (EMEA, 1995). From the calibration range the LOD was calculated as $0.321 \mu\text{g.mL}^{-1}$.

The limit of quantification of an individual analytical procedure is the lowest amount of analyte in a sample which can be quantitatively determined with accuracy and precision. From the calibration range the LOQ was calculated as $0.972 \mu\text{g.mL}^{-1}$.

Table 7.1. Calibration validation of lansoprazole using a UV spectrophotometer

Criteria	Validation	
Y =	0.0319 x	
R²	0.9955	
Intra-day Precision		109.1%
Inter-day Precision		110.3%
Accuracy ($\pm SD$): $5 \mu\text{g.mL}^{-1}$		99.2% ($\pm 0.96\%$)
Accuracy ($\pm SD$): $10 \mu\text{g.mL}^{-1}$		99.3% ($\pm 0.18\%$)
Accuracy ($\pm SD$): $14 \mu\text{g.mL}^{-1}$		98.1% ($\pm 0.59\%$)
LOD $\mu\text{g.mL}^{-1}$		0.321
LOQ $\mu\text{g.mL}^{-1}$		0.972

7.3.2. Influence of PCL and PLGA polymer ratio on nanoparticle preparation and characterisation using the solvent displacement technique

The influence of PCL concentration on nanoparticle characteristics is presented in table 7.2. In the absence of lansoprazole, the nanoparticle size was observed to increase as the polymer concentration increased (448.4 ± 16.6 to 538.5 ± 47.8 nm). These results were significantly larger in comparison to the lansoprazole-loaded nanoparticles ($P<0.05$), which also displayed a similar trend (increasing particle size with increasing polymer concentration). This increase in particle size was attributed to the lowered viscosity of the inner organic phase, preventing formation of polymer chain aggregates and ultimately forming smaller particles (Khandal *et al*, 2010). Both of these formulations (drug loaded and unloaded) were seen to exert anionic properties, which increased in strength with increasing polymer concentration. Interestingly, although an increase in PCL concentration resulted in larger particles being formed, the drug-loading efficiency of the particles decreased. As the polymer-drug ratio increased from 5:1 to 7:1, the drug entrapment efficiency decreased from 85.57 ± 1.80 to 76.21 ± 1.54 % respectively ($P<0.05$).

Table 7.2. Characterisation of PCL nanoparticles before and after lansoprazole loading. It was observed that an increase in polymer concentration resulted in larger nanoparticles being formed ranging in size from 448-538 nm in the absence of drug and 271-301 nm in the presence of lansoprazole. The polymer exerted anionic properties, which increased in strength with increasing PCL concentration. (n=3)

Polymer to drug ratio	Particle size (nm)	PI	Zeta potential (mV)	pH	Drug loading (%)
5:0	448.4 ± 16.6	0.01 ± 0.00	-16.19 ± 7.32	7.01 ± 0.04	-
6:0	478.3 ± 29.7	0.01 ± 0.00	-24.55 ± 3.08	7.07 ± 0.05	-
7:0	538.5 ± 47.83	0.14 ± 0.06	-30.10 ± 1.92	7.11 ± 0.02	-
5:1	271.8 ± 4.75	0.11 ± 0.01	-15.78 ± 4.00	7.09 ± 0.01	85.57 ± 1.80
6:1	285.1 ± 13.37	0.05 ± 0.01	-16.41 ± 0.20	7.11 ± 0.01	80.38 ± 0.66
7:1	301.2 ± 13.64	0.27 ± 0.01	-24.73 ± 5.35	7.53 ± 0.03	76.21 ± 1.54

The choice of polymer used to form the nanoparticle matrix had a drastic impact on the characteristics and drug-loading capabilities of the nanoparticles formed. This was clearly observed when the influence of PLGA on nanoparticle formation was investigated (Table 7.3). It was observed that in the absence of lansoprazole, the particles formed were above the nano-metric range, which increased significantly from 1146.3 ± 480.2 to 1508.4 ± 44.1 nm as the polymer concentration increased (5:0 to 7:0 polymer-drug ratio respectively) ($P<0.05$). However once the particles had been loaded with lansoprazole, the particle size was significantly reduced into the nano-metric range, ranging from 259.8 ± 17.41 to 292.5 ± 21.0 nm (5:1 to 7:1 polymer-drug ratio respectively). A slight increase in particle size was observed as the polymer concentration was increased ($P=0.044$). Interestingly the loading of polymer concentration had no impact on the entrapment efficiency of lansoprazole, which remained consistent at 80 %.

The characterisation differences observed between the PCL and PLGA nanoparticles can be explained by the structural folding nature of the polymers when in an aqueous environment. The flexibility of a polymer chain can be related to the length of its monomer backbone. PCL has a longer monomer backbone (-CH₂- groups) than PLGA (Figure 7.1), which hinders its ability to form a tight nanosphere construct, and hence resulting in PLGA nanoparticles being relatively smaller in size than PCL nanoparticles (Leroueil-Le Verger *et al*, 1998). The extent

Table 7.3. Characterisation of PLGA nanoparticles with and without lansoprazole loading. It was observed that an increase in polymer concentration resulted in significantly larger nanoparticles being formed ranging in size from 1146-1508 nm in the absence of drug, in comparison to nanoparticles prepared in the presence of lansoprazole (259-292 nm). The polymer exerted strong anionic properties, which increased in strength with increasing PLGA concentration. (n=3)

Polymer to drug ratio	Particle size (nm)	PI	Zeta potential (mV)	pH	Drug loading (%)
5:0	1146.3±480.2	0.27±0.01	-37.64±3.25	7.21±0.12	-
6:0	1286.5±93.4	0.25±0.04	-38.73±1.15	7.21±0.02	-
7:0	1508.4±44.1	0.30±0.15	-39.60±2.88	7.29±0.05	-
5:1	259.8±17.41	0.13±0.05	-25.89±3.22	6.10±0.25	80.55±0.64
6:1	272.0±1.56	0.12±0.04	-37.31±6.44	6.76±0.12	80.01±0.65
7:1	292.5±21.0	0.06±0.03	-37.64±4.65	7.11±0.05	80.49±0.54

of anionic charge exhibited by the nanoparticles was attributed to two factors: (1) the type of polymer used to form the particle and (2) the number of terminal carboxylic groups on the polymer being forced to protrude out of the particle matrix (Leroueil-Le Verger et al, 1998). It has been generally perceived that a higher energy barrier associated with a bigger particle charge forms a more stable suspension (Benita and Levy, 1993). For example a particle charge of -25 mV has greater electronegative properties enabling the particles to repel each other when in suspension, preventing aggregation upon ageing and thereby ensuring particle stability (Muller, 1991). From the results however (Table 7.2 and Table 7.3) it was observed that drug-loading caused a reduction in the extent of anionic charge exerted. This can be attributed to the rearrangement of the polymer chains in the particle matrix in order to accommodate for the drug into its hydrophobic core and possible surface adsorption of the drug.

Figure 7.3 and 7.4 show images of nanoparticles when in suspension (light microscope) and when exposed to SEM respectively. The former demonstrates that the nanoparticles were free of aggregation when still in aqueous suspension. However, when the particles were treated with trehalose for the freeze-drying protocol partial aggregation was observed. This

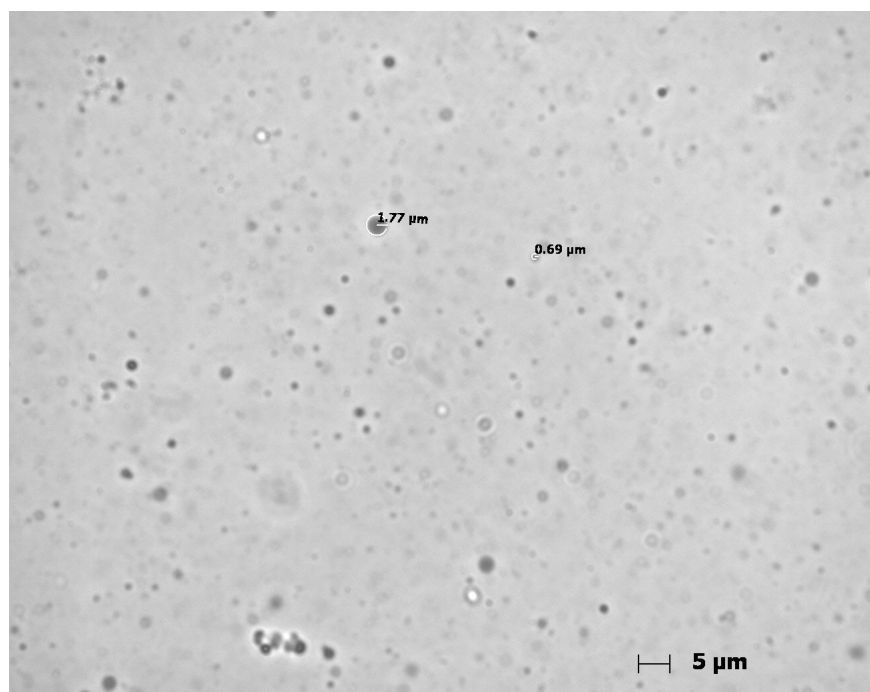


Figure 7.3. Light microscopy of PCL nanoparticles in suspension and viewed on a glass slide and coverslip at 100 x objection. The largest visible nanoparticle was observed to be $\sim 1.77\text{ }\mu\text{m}$.

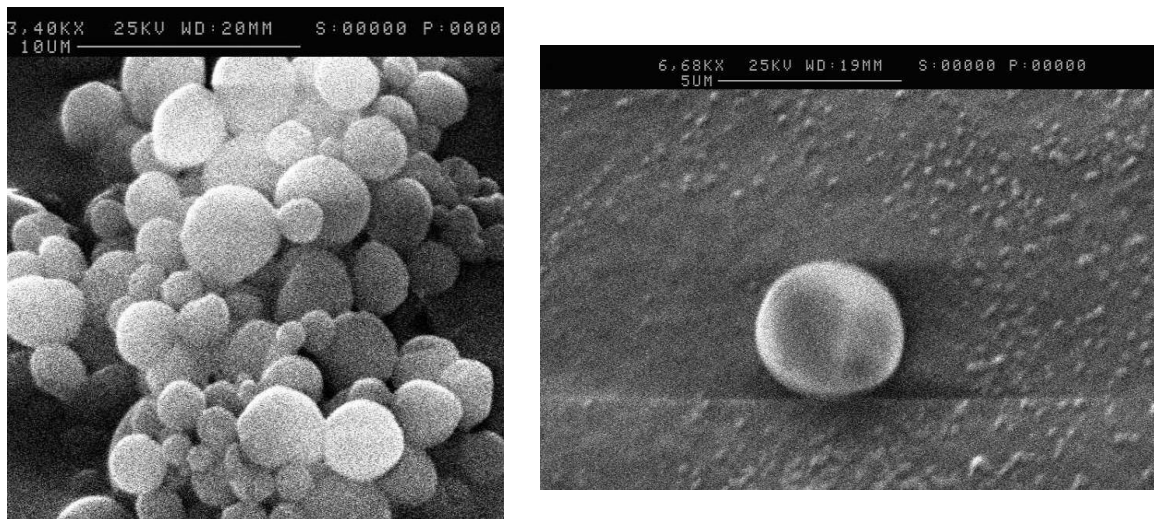


Figure 7.4. SEM profiling of PCL-coated nanoparticles after freeze-drying. The addition of trehalose caused a significant rise in the size of the particles, resulting in microparticles (1- 4 µm).

affect was attributed to the influence of stabilising agent trehalose, a non-reducing disaccharide that had been extensively used in the freeze-drying process of nanospheres, microspheres, solid- lipid nanoparticles (SLN) and liposomes (Saez *et al*, 2000; Abdelwahed *et al*, 2006; Lee *et al*, 2007). It was found that trehalose was able to bind to the surface of a liposomal particle through hydrogen bonding resulting in a significant increase in the size of the particle without distorting its structure (Christensen *et al*, 2007).

The type of polymer also had an influence on the efficiency of drug entrapment, which was attributed to two factors: (1) pH of the colloidal system and (2) chemical structure and flexibility of the polymer chains (Li and Zhao, 2003). Previous studies have shown that the pH of the colloidal suspension influences the extent of drug incorporation, with increased entrapment occurring when the pH of the colloidal system was below the pKa of the drug (Govender *et al*, 1999). The pKa of lansoprazole is 7.3 with the pH of the colloidal system being ~pH 7. Thus it can be concluded that the extent of drug loading was less influenced by pH and mostly influenced by the composition and flexibility of the polymer.

7.3.3. Influence of the mode of preparation of PCL nanoparticles: solvent displacement versus emulsion diffusion method

The solvent displacement technique resulted in a reduction in the loading efficiency of PCL nanoparticles. Therefore an alternative method was utilised to investigate the influence of nanoparticle preparation technique against drug loading, with the ultimate aim to increase the drug loading capabilities of PCL nanoparticles. The emulsion diffusion was chosen for its viscosity enhancing properties, which would aid the rate of diffusion of lansoprazole into the nanoparticle matrix.

7.3.3.1. Characterisation of lansoprazole loaded PCL nanoparticles

Table 7.4 demonstrates the influence of nanoparticle preparation techniques (solvent displacement vs. emulsion diffusion) on the characterisation of the lansoprazole loaded PCL nanoparticles. In the previous study with nanoparticles prepared using the solvent displacement technique, it was concluded that an increase in polymer load resulted in an increase in particle size and charge (Section 7.3.2). Nanoparticles prepared using the emulsion diffusion technique remained fairly consistent, with the polymer load having no influence over the particle characteristics (Table 7.4). Statistically no variation in particle size and particle charge was observed as the polymer-drug ratio was increased ($P>0.05$). At the 5:1, 6:1 and 7:1 polymer-drug ratios the nanoparticles measured 299.27 ± 2.46 , 293.53 ± 14.05 and 298.90 ± 13.90 nm respectively, and exerted strong anionic properties (-21.29 ± 4.06 , -24.10 ± 3.82 and -23.10 ± 4.55 mV respectively). Interestingly, by altering the method of nanoparticle preparation to the emulsion diffusion technique the drug loading efficiency increase significantly ($P<0.05$). Particles prepared at the 5:1 polymer-drug ratio had 91.06 ± 0.13 % entrapment efficiency. As the polymer load was increased to 6:1 (polymer-drug ratio) the entrapment efficiency was reduced to 88.46 ± 0.66 %, which remained consistent as the polymer load was increased further. This increase in drug-loading efficiency using the emulsion diffusion technique can be explained by the viscosity of the suspensions.

Table 7.4. Comparison of lansoprazole loaded PCL nanoparticles preparation techniques: solvent displacement vs. emulsion diffusion. The former method exhibited an increase in particle size and charge, and a reduction in drug loading, with increasing polymer concentration. The latter technique exhibited no significant change in particle size or charge as the polymer concentration increased. However, a higher drug loading was achieved in comparison to the solvent diffusion method, with the 5:1 polymer-drug ratio achieving 91.06 ± 0.13 % drug loading, this was reduced to 88.46 ± 0.66 % with a 6:1 polymer-drug ratio, with no significant increase with the 7:1 polymer-drug ratio. (n=3)

Nanoparticle preparation technique	Polymer to drug ratio	Particle size (nm)	PI	Zeta potential (mV)	pH	Drug loading (%)
Solvent displacement	5:1	271.8 \pm 4.75	0.11 \pm 0.01	-15.78 \pm 4.00	7.09 \pm 0.01	85.57 \pm 1.80
	6:1	285.1 \pm 13.37	0.05 \pm 0.01	-16.41 \pm 0.20	7.11 \pm 0.01	80.38 \pm 0.66
	7:1	301.2 \pm 13.64	0.27 \pm 0.01	-24.73 \pm 5.35	7.53 \pm 0.03	76.21 \pm 1.54
Emulsion diffusion	5:1	299.3 \pm 2.46	0.10 \pm 0.08	-21.29 \pm 4.06	6.88 \pm 0.35	91.06 \pm 0.13
	6:1	293.5 \pm 14.05	0.18 \pm 0.05	-24.10 \pm 3.82	6.84 \pm 0.36	88.46 \pm 0.66
	7:1	298.9 \pm 13.90	0.10 \pm 0.06	-23.10 \pm 4.55	7.19 \pm 0.06	88.15 \pm 1.03

7.3.3.2.1. Influence of viscosity

The characterisation of the nanoparticles has ascertained that the homogenisation of the organic solution during the formation of the nanoparticles not only ensures homogeneity of particle size but also increases the drug-loading efficiency. These findings can be attributed to the shear force of the homogeniser and to the viscosity of the nanoparticle solution formed.

The size of the nanoparticle formed was attributed to the macromolecular coiling capabilities of the polymer: by increasing the speed of rotation through homogenisation, the amount of time the polymer had to rearrange its hydrophobic chain into a protected shell (colloid/nanoparticle) was considerably reduced (Kwon *et al*, 2001). Therefore the shear force of the homogeniser effectively hindered large nanoparticle growth. This however had a marked affect on the viscosity of the organic solution. Figure 7.5 highlights the viscosity of the suspension being lowered after homogenisation. The greatest difference in viscosity was observed with the 5:1 polymer-drug ratio ($P<0.05$). Before homogenisation the particles had particle size of 271.8 ± 4.75 nm with a drug entrapment efficiency of 85.57 ± 1.80 %. This

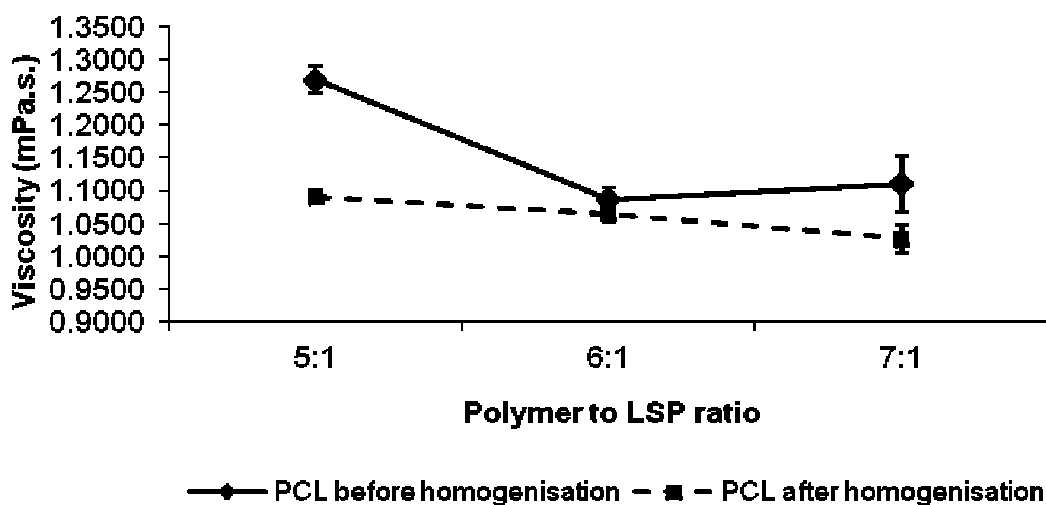


Figure 7.5. Viscosity measurements of PCL nanospheres before and after homogenisation. The homogenisation process significantly reduced the viscosity of the nanoparticle solution, with the greatest reduction being observed with 5:1 polymer-drug ratio. (n=3)

was significantly improved on by lowering the viscosity of the suspension to 1.0907 ± 0.01 mPa.s⁻¹ (299 ± 2.46 nm with 91.06 ± 0.13 % entrapment efficiency). In a suspension with less viscosity, the interfacial tension/resistance between two components (such as organic solution and nanoparticles) becomes weaker, thereby making it easier for the drug molecule to diffuse across the polymer outer shell into its hydrophobic core (from a high to a low concentration), and ultimately increasing the drug-loading efficiency of the PCL nanoparticle. These results therefore enforce viscosity to be a major factor in efficient drug loading.

7.3.3.2.1. Conclusion

In order to increase the drug load of a nanoparticle, the viscosity of the organic solution had to be reduced. This can normally be achieved by applying shear force in the method of nanoparticle preparation. However, this can result in the generation of heat which could cause degradation to heat-sensitive compounds. Since the aim of the study was to produce a simple nanoparticle protocol which ultimately would result in high loading efficiency with relatively small nanoparticles, an alternative method of preparation was to be investigated, such as planetary ball milling.

7.3.4. Planetary ball milling

Various studies have been reported where the loading and sizing on nanoparticles has been recorded using pre-formed polymers, however limited research has highlighted the implications of modifying the surface properties of the polymer prior to nanoparticle formation, and analysing its implications on its physical characteristics, drug loading and release profile. The major advantage of dry milling the polymer prior to nanoparticle formation involved the modification of polymer surface characteristics without the need for any chemical modification. Planetary ball milling can be used to reduce particle size and in turn alter the surface properties of materials by increasing the surface area, porosity and shape. Therefore the aim of the following study was to ascertain the implications of milling on the physical properties of the polymer and when prepared as a colloidal suspension.

7.3.4.1. Implications on physical properties of PCL and PLGA

7.3.4.1.1. Impact on molecular weight

The molecular weight of PCL and PLGA before and after milling was analysed using a GPC/SEC software, in order to ascertain the influence of milling on the physical properties of the polymers (Table 7.5). It was observed that the repeated mechanical impaction of the

Table 7.5. Influence of milling on the molecular weight of PCL and PLGA. Both polymers showed a significant increase in molecular weight after milling, with PCL displaying variation and inconsistency as the milling time was increased from 15 to 60 mins at 400 rpm. This was associated with the robustness of the polymer surface.

Polymer	Rotation (rpm)	speed	Duration (mins)	Molecular weight (Mw)
PLGA	-		-	8260
Milled PLGA	200		60	8356
PCL	-		-	14000
Milled PCL	200		60	60054
Milled PCL	400		15	35263
Milled PCL	400		30	30388
Milled PCL	400		45	37070
Milled PCL	400		60	29067

aggregate balls on the polymer surface caused a significant increase in the polymers molecular weight, particularly with regard to the milled PCL polymer. This can be associated with the scissoring, mass transfer and cross linking events in the polymer chain (Smith *et al*, 2001). The extent of which was dependent upon the surface structure of the polymer, as PCL had a tough surface which required greater energy to grind than the glassy structure of PLGA. Therefore although the molecular weight of PCL increased after milling, it displayed a variation and inconsistency as the milling time was increased from 15 to 60 minutes at 400 rpm.

7.3.4.1.2. Wettability studies: Impact on polymer hydrophobicity

Wettability is used to assess the hydrophobic and hydrophilic properties of materials. The compositions of the milled and non-milled polymers were analysed using Camtel QCT-100 tensiometer. This calculates the advancing and receding angle of the hydrophobicity of the polymer, with the difference between the two angles being used to calculate the hysteresis angle, the results of which are displayed in table 7.6. The contact angle is a quantitative

Table 7.6. Wettability profiling of PCL and PLGA before and after milling. Prior to planetary ball milling, both polymers exhibited hydrophobic properties with receding contact angles of $90.00 \pm 0.00^\circ$. After planetary ball milling, PCL retained its hydrophobicity (receding contact angle of $90.00 \pm 0.00^\circ$), however the receding angle for milled PLGA was not measurable, indicating incomplete wetting. (n=3)

Polymer	Rotation speed/ rpm (duration/ mins)	Advancing angle (\pm SD)	Receding angle (\pm SD)	Hysteresis
PCL	0	60.25 ± 14.93	90.00 ± 0.00	29.75
	200 (60 mins)	59.57 ± 10.58	90.00 ± 0.00	30.43
	400 (15 mins)	59.03 ± 11.36	90.00 ± 0.00	30.97
	400 (30 mins)	63.77 ± 1.65	90.00 ± 0.00	26.23
	400 (45 mins)	57.99 ± 4.82	90.00 ± 0.00	32.01
	400 (60 mins)	58.99 ± 11.91	90.00 ± 0.00	31.01
PLGA	0	67.17 ± 0.43	90.00 ± 0.00	22.83
	200 (60 mins)	51.71 ± 10.97	-	38.29

measure of the wetting of a solid by a liquid, with the contact angle of less than 90 ° indicating that the liquid wets the solid spontaneously (lower the contact angle greater the wetting of the solid). An angle of greater than 90 ° indicates that the solid has not wetted at all, and that it is hydrophobic in nature. Currently there are three methods to measure the wettability of a solid sample: Washburn method, Goniometry, and Tensiometry. For the purpose of this study, the latter method was employed using the Wilhelmy method, which allowed for fast and accurate measurements to be taken and was able to calculate the hysteresis of the two contact angles, an advantage over the Goniometry method.

Table 7.6 highlights the wetting profiles of PCL and PLGA and their relative milled versions. PCL was a hydrophobic polymer, as indicated by table 7.6 and figure 7.6a in which after complete immersion in distilled water, the advancing contact angle was 60.25 ± 14.93 °, and the receding angle was 90.00 ± 0.00 °. These results indicated that the polymer had not 'wetted' and was therefore hydrophobic. After the polymer had been milled for 1 hour at 200 rpm, the advancing contact angle was 59.57 ± 10.58 °, and the receding angle was 90.00 ± 0.00 °. As the rotational speed of the mill was increased to 400 rpm, the physical appearance of the polymer showed no significant change (Figure 7.6b), with the receding angle remaining consistent at 90.00 ± 0.00 °.

The SEM profiling of PCL highlighted in figure 7.6 showed that the milling process did not alter the physical appearance of the polymer; it only reduced the size of the polymer particles which retained their sheet-like appearance. This was attributed to the robustness of the polymer and its ability to withstand the heat generated in the planetary mill. Therefore it can be concluded that the hydrophobicity of the PCL was not influenced by the milling process.

Similarly, PLGA was a hydrophobic polymer, as shown by results in table 7.6 and figure 7.7a in which after complete immersion in distilled water, the advancing contact angle was 67.17 ± 0.43 °, and the receding angle was 90.00 ± 0.00 °. Interestingly however, after the polymer had been milled at 200 rpm for 1 hour, the advancing angle was 51.71 ± 0.91 ° with incomplete wetting during the receding angle (no angle was measurable), indicating the hydrophobicity of the polymer had been altered. This was further supported by the physical alteration of the PLGA polymer after milling (Figure 7.7). Prior to milling PLGA had a large smooth glassy appearance, however the milling process caused physical changes in the PLGA polymer. This resulted in the formation of smaller particles aggregated together to form a bigger globular structure, containing nano-pores/tubules.

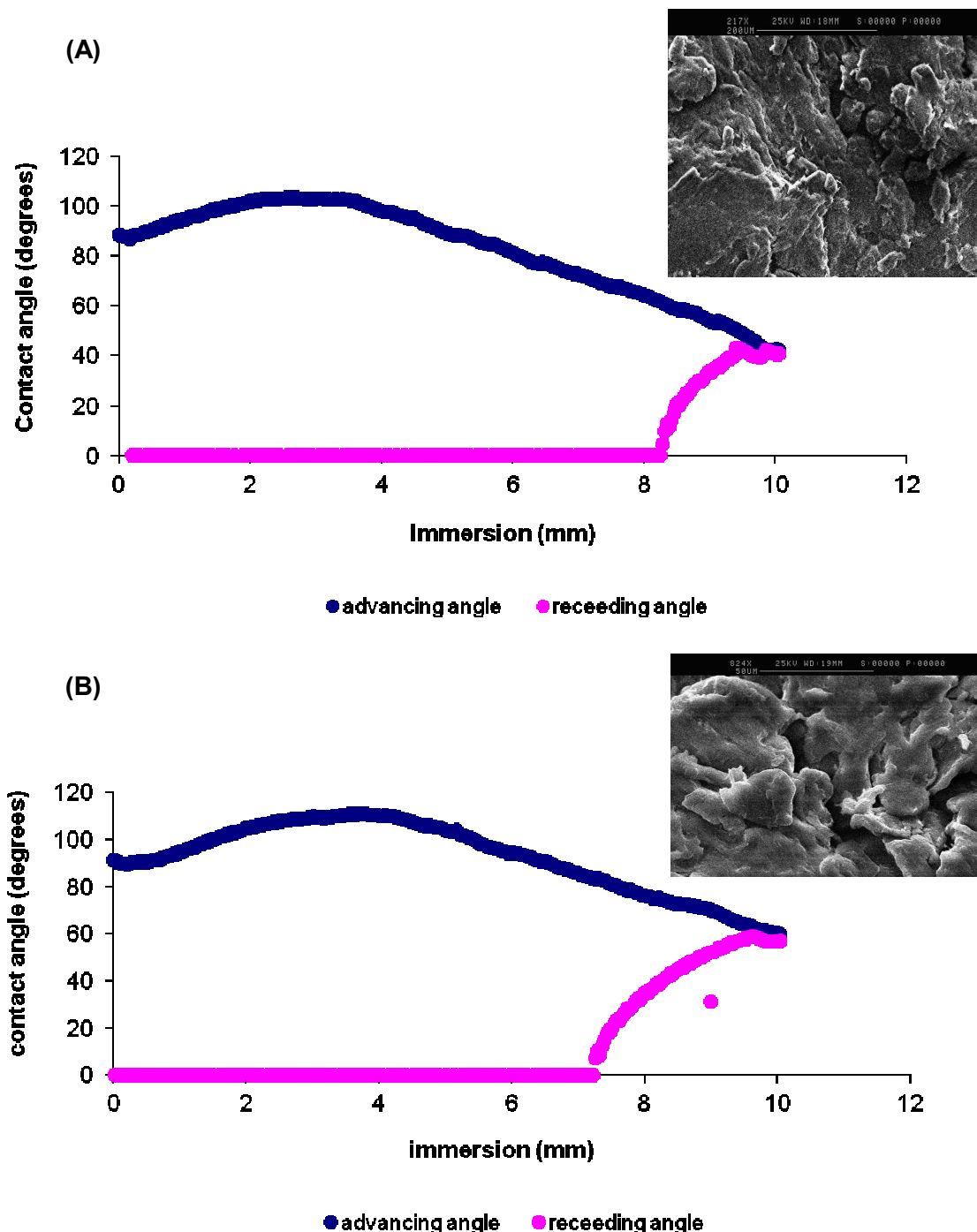


Figure 7.6. Wettability and SEM profiling of PCL (A) before and (B) after milling for 1 hour at 200 rpm. Prior to milling PCL had an advancing contact angle of $60.25 \pm 14.93^\circ$, and the receding angle was $90.00 \pm 0.00^\circ$, with SEM showing a smooth sheet-like structure. After milling, the physical appearance of the polymer did not change, the advancing contact angle was $59.57 \pm 10.58^\circ$, and the receding angle was $90.00 \pm 0.00^\circ$. Thus the milling process had no influence on the hydrophobicity of PCL. (n=3)

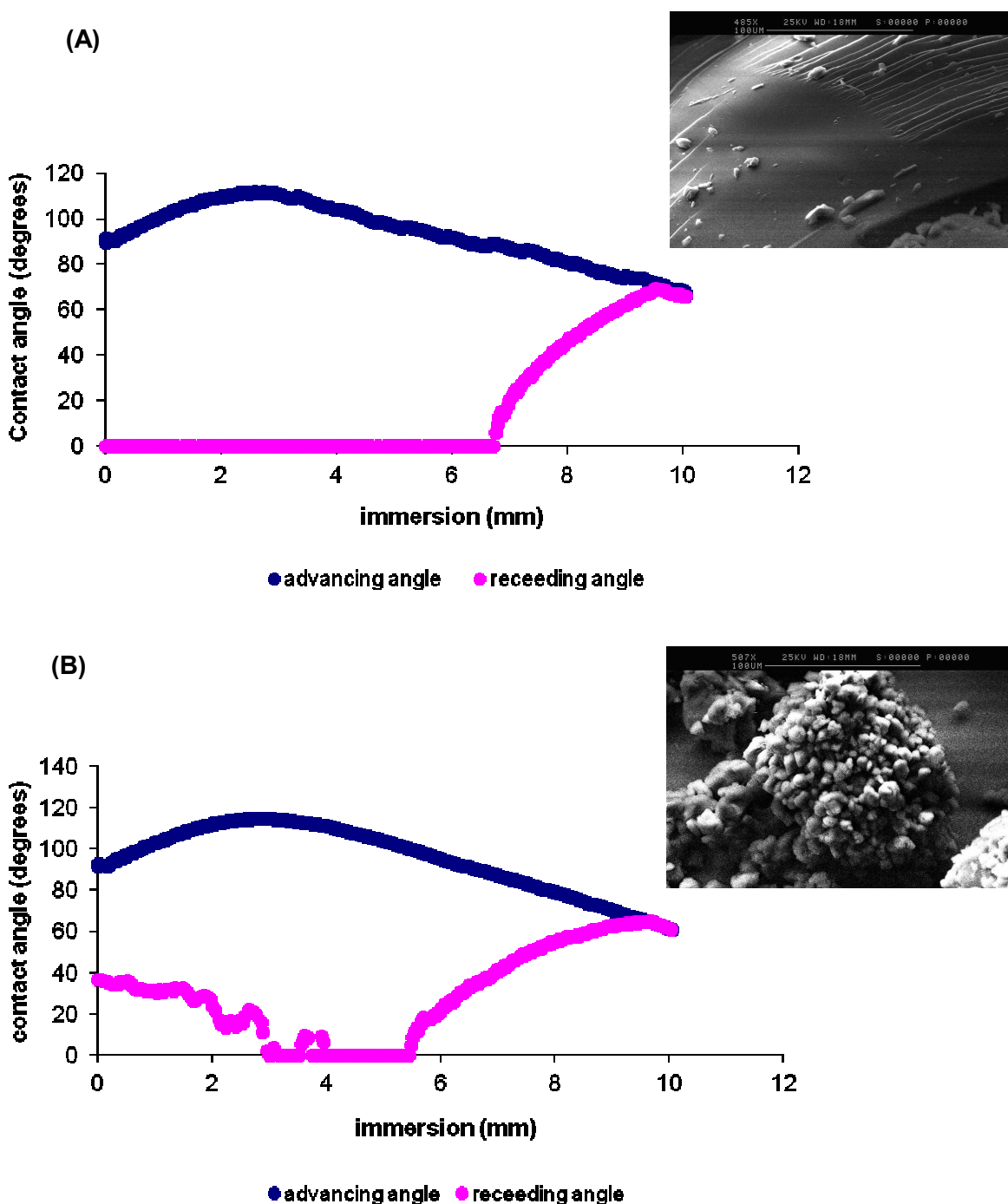


Figure 7.7. Wettability and SEM profiling of PLGA (A) before and (B) after milling for 1 hour at 200 rpm. Prior to milling PLGA has an advancing contact angle $67.17 \pm 0.43^\circ$, and the receding angle was $90.00 \pm 0.00^\circ$, with SEM showing a smooth glassy structure. The heat of generated during the milling process resulted in the polymer forming a multi-globular nano-porous structure. These nano-pores caused the hydrophobicity of PLGA to be reduced (advancing angle was $51.71 \pm 0.91^\circ$, with incomplete wetting during the receding angle (no angle was measurable). ($n=3$)

In the field of material science, research has shown that the application of milling results in the formation of amorphous phase and nano-porous structures within the surface, which further results in increased surface area (Oberlain, 1989; Chen *et al*, 1999). The formation of the nano-porous surface was attributed to the high energy impact that occurred when the surface of the material came into direct contact with the rotating balls in the planetary mill, thus resulting in the formation of the nano-pores due to the heat generated between the two surfaces. Therefore it can be concluded that the reduced hydrophobicity of milled PLGA displayed by the wettability studies was a direct result of water penetration into these nanopores.

7.3.4.1.3. Thermal analysis

DSC was carried out in order to establish the thermodynamics of the non-milled and milled PCL and PLGA polymers. The DSC technique involved measuring the effect of change in temperature on the heat flow in or out of the known sample compared with an inert reference pan. The heat flow can be defined as a function of the change in temperature and of the absolute temperature. Data was represented in the form of a thermal analysis curve, which depicts the change in heat flow against temperature, from which three main transitions can be detected: a T_m, crystallisation (solid to crystal transition), and a T_g. T_g occurs at the temperature at which the heat capacity reaches halfway between that of the liquid and glassy states.

Figure 7.8 shows the influence on milling PCL and PLGA on their relative T_m, which were seen to decrease significantly ($P<0.05$). Pure PCL has a T_m of 62 ± 0.05 °C which was reduced to 57 ± 0.07 °C once the polymer had been milled for 1 hour at 200 rpm. Similarly a reduction in T_m was observed for pure PLGA after being milled under the same conditions, from 33 ± 0.03 °C to 29 ± 0.06 °C respectively. This was attributed to the milling process weakening the polymer chain bonds through repetitive impaction, and ultimately resulting in less energy to break the polymer chains.

A parallel study was carried out looking at the milling process of the candidate drug alone (lansoprazole), in order to ascertain its stability and robustness under stress conditions. Figure 7.8 and 7.9 show that pure lansoprazole has a T_m of 180 ± 0.04 °C which was instantly followed by a sharp exothermic reaction (degradation) (Zhang *et al*, 2008). Surprisingly following planetary ball milling lansoprazole for 1 hour at 200 rpm, two thermodynamic responses occurred; the first was the expected reduction in T_m (reduced to 177 ± 0.03 °C), however the second was the unexpected formation of a T_g at 87 ± 0.06 °C.

T_g was indicative of the alteration of heat capacity as the drug matrix changed from a glass state to a rubber state (2nd order endothermic reaction). The T_g can be attributed to the repeating mechanical impaction on the structural properties of lansoprazole, with the degrees of T_g shift being influenced greatly by the duration and frequency of milling (Chieng *et al*, 2009; Corrigan and Li, 2009).

Therefore, planetary ball milling caused weakening of the chemical composition of the PCL and PLGA, resulting in a reduced T_m with no indication of any instability. In contrast, the mechanical impaction on lansoprazole caused a shift in its chemical state, in the form of a

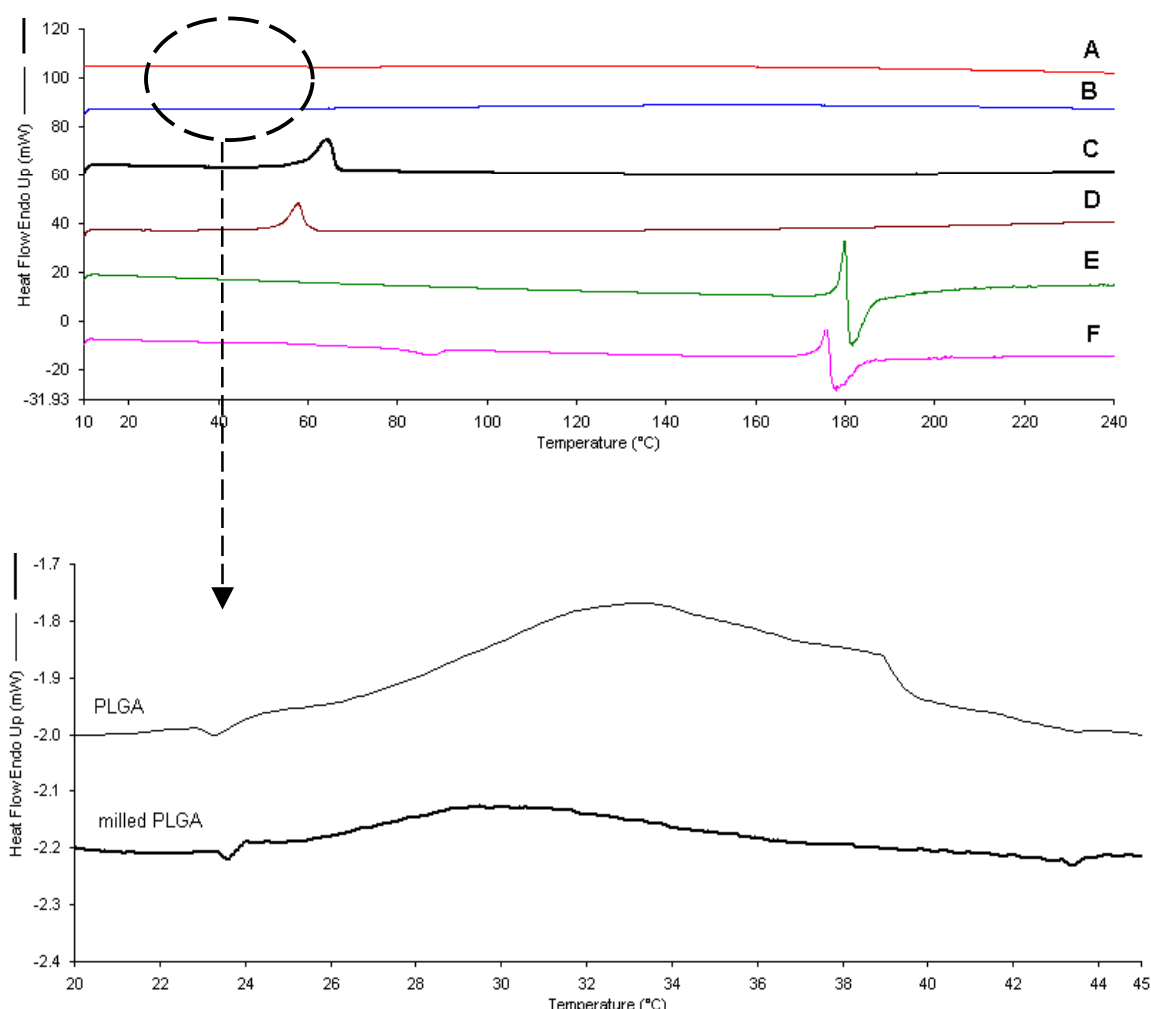


Figure 7.8. DSC thermographs of; (A) PLGA, (B) milled PLGA, (C) PCL, (D) milled PCL, (E) lansoprazole and (F) milled lansoprazole. The planetary ball milling of the pure components resulted in a reduction of their relative T_m . Pure PLGA and PCL have a T_m of 33 ± 0.03 °C and 62 ± 0.05 °C respectively, which were reduced after milling for 1 hour at 200 rpm (29 ± 0.06 °C and 57 ± 0.07 °C respectively). Pure lansoprazole has a T_m at 180 ± 0.04 °C with instant degradation occurring, interestingly the milled lansoprazole displayed a reduction in its T_m (177 ± 0.03 °C) and an additional T_g (87 ± 0.06 °C). (n=3)

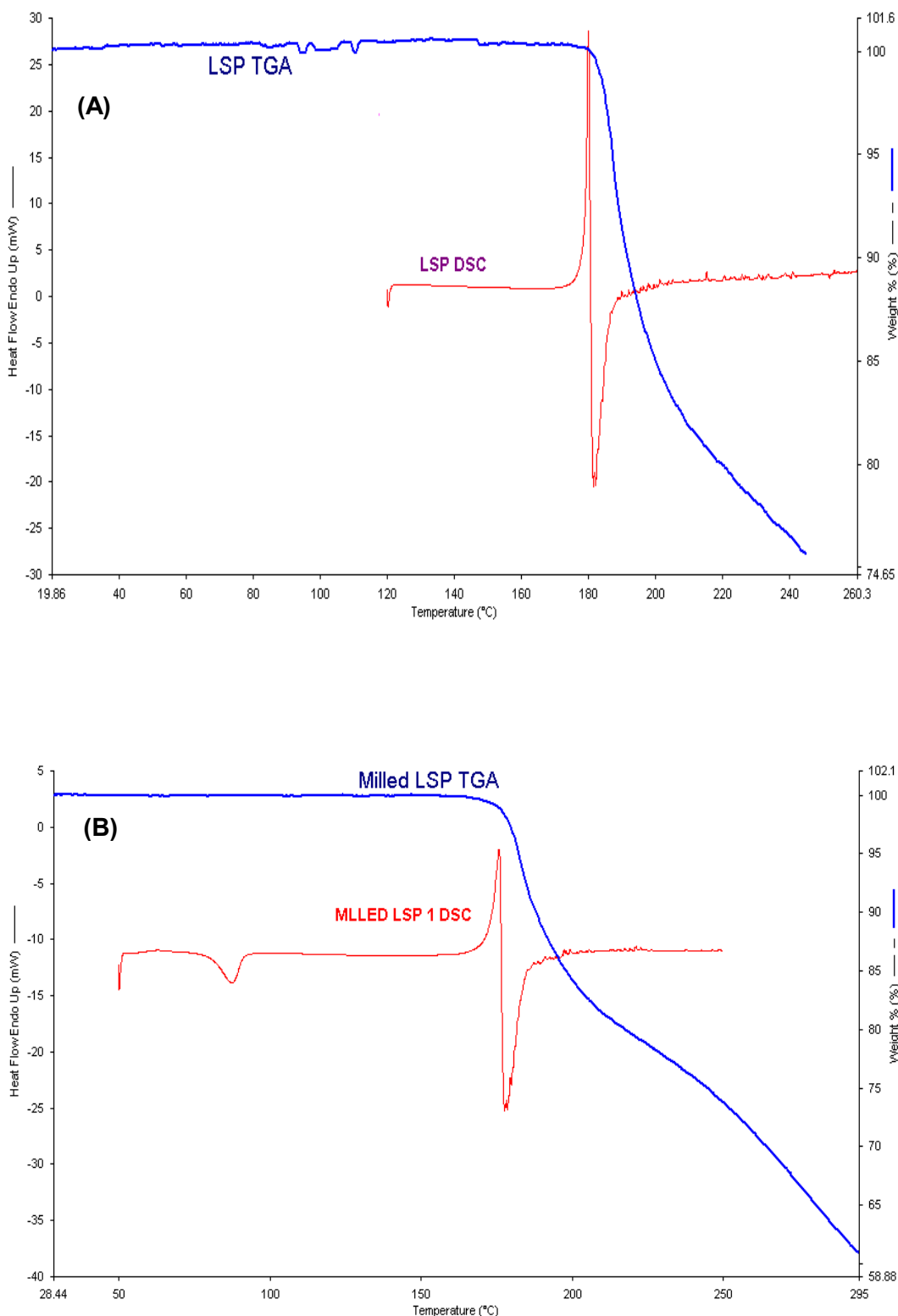


Figure 7.9. TGA and DSC thermographs of lansoprazole: **(A)** un-milled and **(B)** milled. Pure lansoprazole displays a T_m at 180 ± 0.04 °C followed by immediate degradation, supported by the TGA significant weight loss at 180 °C. Similarly the milled lansoprazole displays a similar profile at a reduced temperature (177 ± 0.03 °C), with its T_g (87 ± 0.06 °C) being displayed clearly. (n=3)

Tg. The aim of the study was to prepare a nanoparticle system for the safe delivery of lansoprazole to the patient; however these findings have highlighted that by milling the drug, lansoprazole would no longer be in its true thermodynamic form. Therefore the following study will concentrate on lansoprazole loaded nanoparticles being prepared from pre-milled polymers (200 rpm for 1 hour).

7.3.4.2. Influence of milled polymers on nanoparticle formation

Numerous studies have been carried out on milling of polymers in solution (wet milling) in order to reduce the particle drug size and control its release profile *in vitro* (Gubskaya *et al*, 1995; Annapragada *et al* 1996; and Villiers, 1996). However, no study has yet to look at the effects of milling on the polymer prior to drug encapsulation. Thus the aim of the study was to assess if milling the polymer prior to nanoparticle formation would result in a reduction in particle size and thus an increase in the polymer surface area and drug-loading efficiency. Lansoprazole loaded nanoparticles were therefore prepared with pre-milled PCL and PLGA polymers (200 rpm for 1 hour) using the solvent displacement technique and characterised for particle size, particle charge, and drug loading.

7.3.4.2.1. Milled PCL nanoparticles

The characterisation of lansoprazole loaded nanoparticles prepared using milled PCL is displayed in table 7.7. It was observed that the 5:1, 6:1 and 7:1 polymer-drug ratios formed 286.1 ± 7.92 , 275.9 ± 0.78 and 292.3 ± 7.71 nm nanoparticles respectively, which exhibited a

Table 7.7. Characterisation of nanoparticles prepared using milled PCL (200 rpm, 1 hour). As the polymer-drug ratio increased from 6:1 to 7:1, a significant increased in particle size was observed ($P<0.05$). Interestingly a significant rise in drug loading was observed as the polymer-drug ratio was increased from 5:1 to 6:1($P<0.05$), which remained stable when the polymer concentration was further increased to 7:1 ($P>0.05$). (n=3)

Polymer ratio	Particle size (nm)	PI	Zeta Potential (mV)	pH	LSP retention (%)
5:1	286.1 ± 7.92	0.06 ± 0.05	-16.11 ± 1.37	6.84 ± 0.13	79.97 ± 5.88
6:1	275.9 ± 0.78	0.05 ± 0.03	-15.94 ± 0.24	6.77 ± 0.24	90.70 ± 2.14
7:1	292.3 ± 7.71	0.06 ± 0.00	-16.61 ± 2.13	7.16 ± 0.03	91.87 ± 0.43

stable anionic charge (-16.11 ± 1.37 , -15.94 ± 0.24 and -16.61 ± 2.13 mV respectively). These findings were found to be significantly different to nanoparticles prepared from pure PCL ($P<0.05$), which were characterised to be greater in size and anionic charge (Table 7.2). In contrast to the nanoparticles prepared with non-milled PCL (Table 7.2) it was observed that an increase in polymer concentration resulted in an increase in drug loading, with nanoparticles prepared using the 6:1 polymer-drug ratio achieving a loading efficiency of 90.70 ± 2.14 %. Statistically this was a significant improvement on the non-milled PCL nanoparticles which previously achieved a maximum drug load of 85.57 ± 1.80 % (5:1 polymer-drug ratio).

7.3.4.2.2. Milled PLGA nanoparticles

The characterisation of lansoprazole loaded nanoparticles prepared using milled PLGA is presented in table 7.8. As the polymer-drug ratio increased from 5:1 to 7:1, a significant increase in the nanoparticle size (237.7 ± 7.44 to 267.6 ± 10.05 nm respectively) and particle charge was observed (-14.78 ± 4.53 to -30.60 ± 2.63 mV) ($P<0.05$). Interestingly, the rise in polymer-drug ratio from 6:1 to 7:1 resulted in no significant change in either of these particle characterisations ($P<0.05$), which was further reflected with their drug loading efficiency. However, a significant increase in drug loading was observed as the polymer drug ratio increased from 5:1 to 6:1 (92.37 ± 1.31 and 96.30 ± 0.93 % respectively) ($P<0.05$), with no further improvement in lansoprazole entrapment as the polymer-drug ratio was further increased to 7:1 ($P>0.05$). Statistically these results showed a significant improvement on the non-milled PLGA nanoparticles which ranged in size from 259-292 nm and achieved a maximum drug-loading efficiency of 80 % ($P<0.05$) (Table 7.3).

Table 7.8. Characterisation of nanoparticles prepared using milled PLGA (200 rpm, 1 hour). As the polymer-drug ratio increased from 5:1 to 6:1, a significant increased in particle size, particle charge and drug loading was observed ($P<0.05$), with no significant change as the polymer-drug ratio was further increased to 7:1 ($P>0.05$).

Polymer ratio	Particle size (nm)	PI	Zeta Potential (mV)	pH	LSP retention (%)
5:1	237.7 ± 7.44	0.07 ± 0.06	-14.78 ± 4.53	7.21 ± 0.06	92.37 ± 1.31
6:1	257.6 ± 8.40	0.10 ± 0.01	-30.56 ± 4.27	6.85 ± 0.10	96.30 ± 0.93
7:1	267.6 ± 10.05	0.14 ± 0.09	-30.60 ± 2.63	7.16 ± 0.05	95.38 ± 3.23

The milling of polymers prior to nanoparticle formation resulted in both PLGA and PCL exhibiting smaller nanoparticles with higher drug loading. This was attributed to the repeated mechanical impaction weakening the rigidity of the polymer chains (as seen with reduced T_m in the DSC study). The reduction in structural rigidity enabled the polymer to form tighter coils and therefore form smaller nanoparticles. This reduction in particle size was a direct result of the planetary mill causing a shortening of the polymer chains, thereby once the polymer was dissolved in acetone during the nanoparticle formation, shorter chain lengths were formed and ultimately forming smaller nanospheres once exposed to the surfactant solution. In contrast the non-milled polymers have a longer chain length due to their molecular weight, whereby the milling process bridges new bonds (weak) between the polymer chains and thus ultimately increasing their molecular weight.

The reduction in particle charge exhibited by milled polymers can be attributed to the partial masking of the polymer charge, even though pluronic F127 is a non-ionic surfactant. This has been supported by the work carried out by Mosqueira and co-workers (2000), who determined that the particle charge was influenced by the surfactant, oil and polymer molecular weight. With the latter it was expected that the higher the molecular weight of the polymer, the smaller the influence on particle charge for the same weight of the polymer. This was due to the fact that a smaller number of end groups are present in the larger polymer molecular weight. However in the present study, there was a decrease in the zeta potential, the reverse of what was expected, and thus concluded that the surfactant was acting as a masking agent of the end carboxyl groups. An alternate reasoning for the milled polymers exhibiting greater drug-loading efficiency was increased adsorption of lansoprazole molecules on the nanoparticle surface, which may attribute to the masking of the particle charge and thereby decreasing the extent of anionic charge exerted.

Milling has previously been used to study the effect of ball milling on the surface area of certain compounds, such as carbon. A study carried out by Chen and co-workers (1999) was one such study, where the effect of ball milling (wet and dry) was assessed with regard to the nano-porous structure and the changes in internal and external surface areas. By using a vertical planetary ball mill and a vibrating frame grinder (Pulverisette 0, Fritsch, Germany) it was found that approximately 50 % of the internal surface area was a result of the formation of nanosized pores. It was found that an initial increase in the surface area during the first stage of milling was a result of “particle fracturing induced by ball impaction”, after which the surface area began to decrease due to agglomeration of the particles. This can be related to the present study and can be clearly observed with the PLGA particles (Figure 7.7), where

the SEM photomicrographs clearly show the initial external surface area of PLGA to be flat and large, however after planetary milling at 200 rpm for 1 hour, the particles are seen to agglomerate together, thereby decreasing the external particle size. With regard to the internal surface area, both Chen and co-workers (1999) and Oberlain (1989) agreed that the nano-porous structure increased with extended milling times. It was deemed by both authors that the formation of these nano-porous structures was most likely to be linked to the formation of an amorphous phase, micro-pores formed during agglomeration of very fine particles during welding under the ball impacts. Thus in the current study it can be said that the increase in the internal particle size resulting from the hydrophobic nano-porous structure of PLGA formed after milling, resulted in increased areas of hydrophobic pockets within which the hydrophobic lansoprazole was able to bind to. This then results in increased drug loading efficiency from 80 % to approximately 95 %.

PCL-milled nanoparticles displayed a smaller increase in drug loading compared with PLGA-milled nanoparticles, with there being no significant difference between the 6:1 and 7:1 ratios (Table 7.7). This was possibly as a result of the particle fracturing being in balance with the formation of agglomerates, and thus the external surface area remained constant with no additional nano-porous structures being produced (Chen *et al*, 1999). The SEM (Figure 7.6) confirmed this, where no significant difference was observed between the milled and non-milled PCL.

7.3.4.3. Physiochemical analysis of milled PCL and milled PLGA nanoparticles

7.3.4.3.1. H¹-NMR

H¹-NMR was carried out in order to establish structural changes within the polymer chain according to the number of protons present. To some extent the scope and limitation of analysis of polymer composites using H¹-NMR spectroscopy depends upon the appearance of the non-superimposed signals of the components in the spectra. Therefore the first stage was to highlight the spectra of the pure components.

With F127 a sharp singlet peak was obtained at 3.50 ppm which had a broad base (Figure 7.10). The integration calculation indicates 12 H-ions to be present within this peak, thus the singlet corresponds to the main body of the F127 chain including the methyl side chain. At 1 ppm a doublet peak was observed which corresponds to the OH- groups present at the end of the chains. The NMR spectrum for lansoprazole shows; a single peak at 13.58 ppm

corresponding to the N-H chain on the cyclic amide group, a set of 6 peaks at 4.82 ppm corresponding to the cyclic chain of lansoprazole and a triplet peak at 7.70 ppm corresponding to the CH₃- methyl side group on the amide cyclic chain (Figure 7.11). The H¹-NMR spectrum for PCL shows a triplet at 3.95 ppm, a doublet at 2.25 ppm, a quartet at 1.56 ppm and a triplet at 1.29 ppm corresponding to its various carbonyl groups (Petrova *et al*, 2008), in total 1 polymer chain potentially holds 10 H-ions (Figure 7.12). The H¹-NMR spectrum for PLGA shows a large peak at 1.48 ppm corresponding to 37 H-ions, a large single peak at 3.36 ppm corresponding to approximately 14 H-ions and a doublet peak at 4.93 ppm corresponding to 23 H-ions and a further broad peak at 5.23 ppm indicating 12 H-ions are present, in total 1 polymer chain potentially holds 86 H-ions (Figure 7.13).

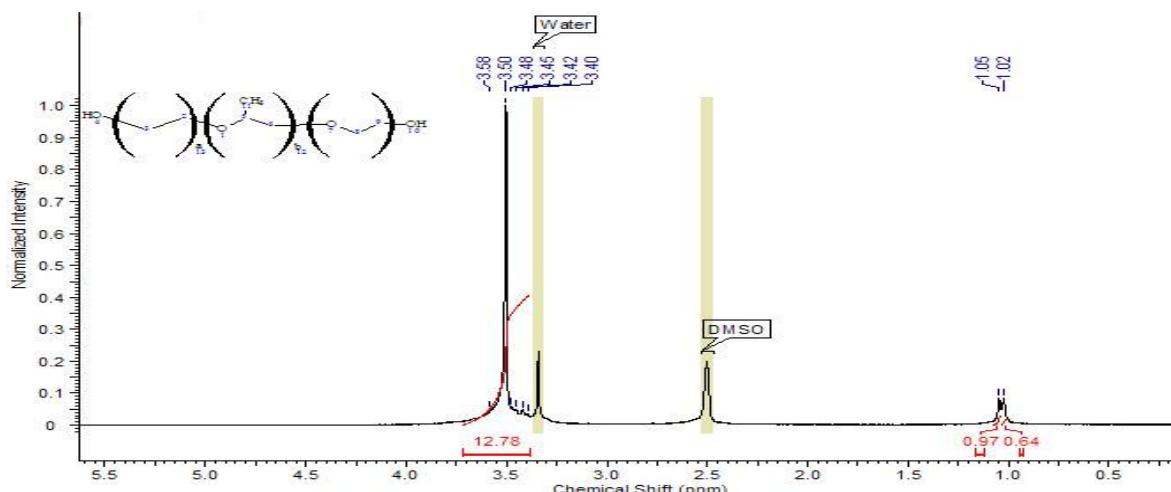


Figure 7.10. H¹-NMR spectrum (DMSO-D₆) of pure pluronic F127.

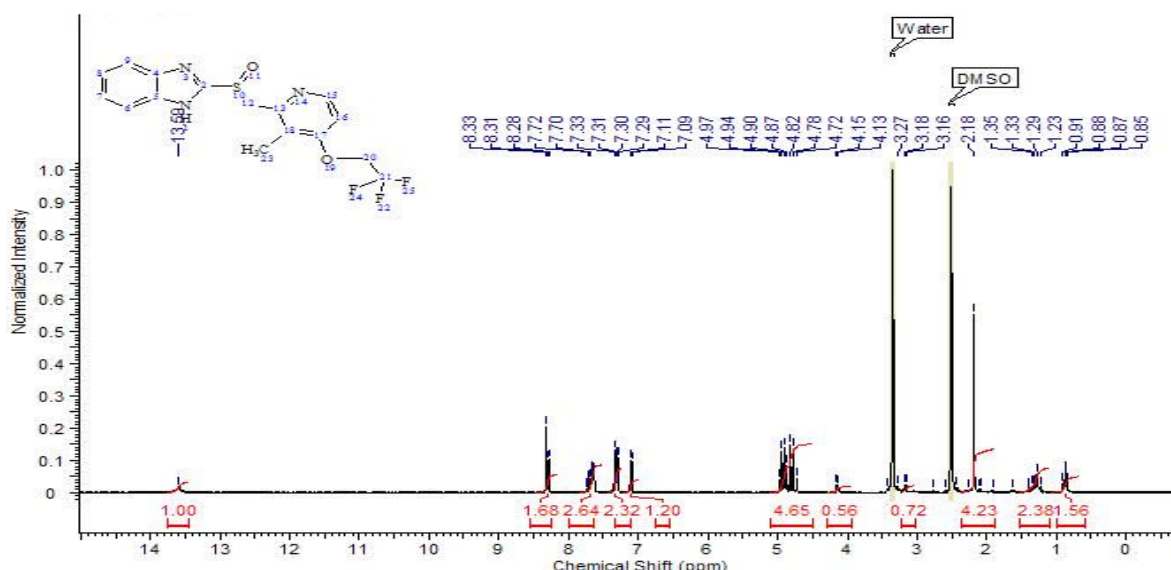


Figure 7.11. H¹-NMR spectrum (DMSO-D₆) of pure lansoprazole.

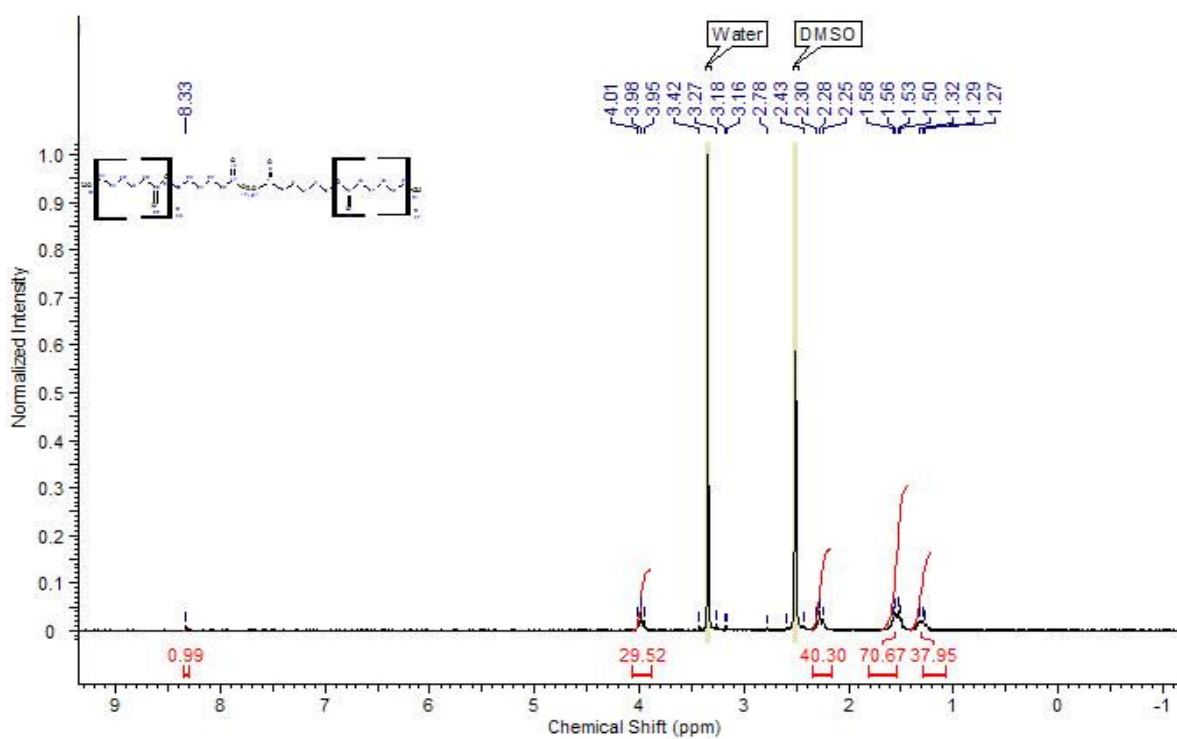


Figure 7.12. H^1 -NMR spectrum (DMSO- D_6) of pure PCL.

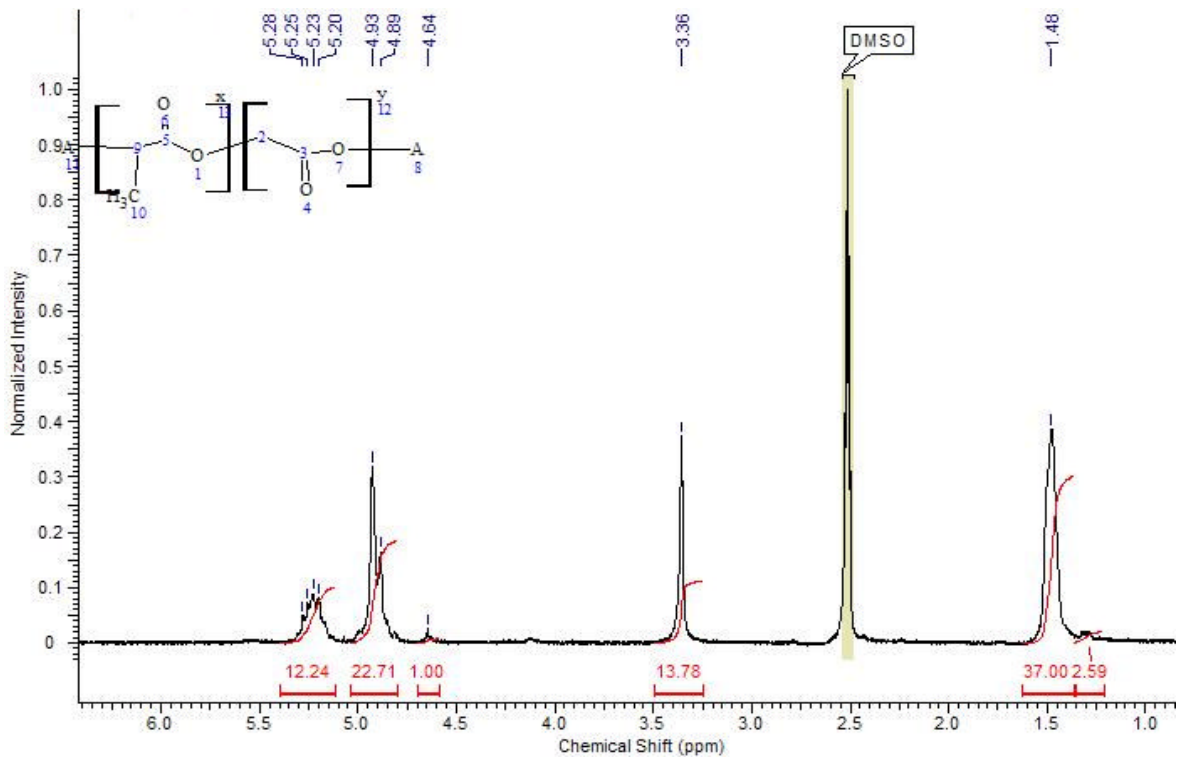


Figure 7.13. H^1 -NMR spectrum (DMSO- D_6) of pure PLGA.

PCL nanoparticles

By eliminating the known spectral peaks of the individual components of the nanoparticle, any interaction occurring in the physical mixture or the nanoparticle itself can be determined. The H^1 -NMR spectrum for the physical mixture of non-milled and milled PCL with lansoprazole showed similar profiles, with all of the protons being present (Figure 7.14 and 7.15). Therefore the results confirm that the process of milling does not cause any chemical change in the chemical chain but only aids in changing the chain length of the polymer and thus its molecular weight.

The NMR scans for PCL nanoparticles loaded with lansoprazole displayed the absence of the lansoprazole fingerprint (13.58, 1.48 and 2.18 ppm peaks are missing) (Figure 7.16). Therefore indicating lansoprazole to be fully incorporated into the core and not adsorbed onto the surface of the particle.

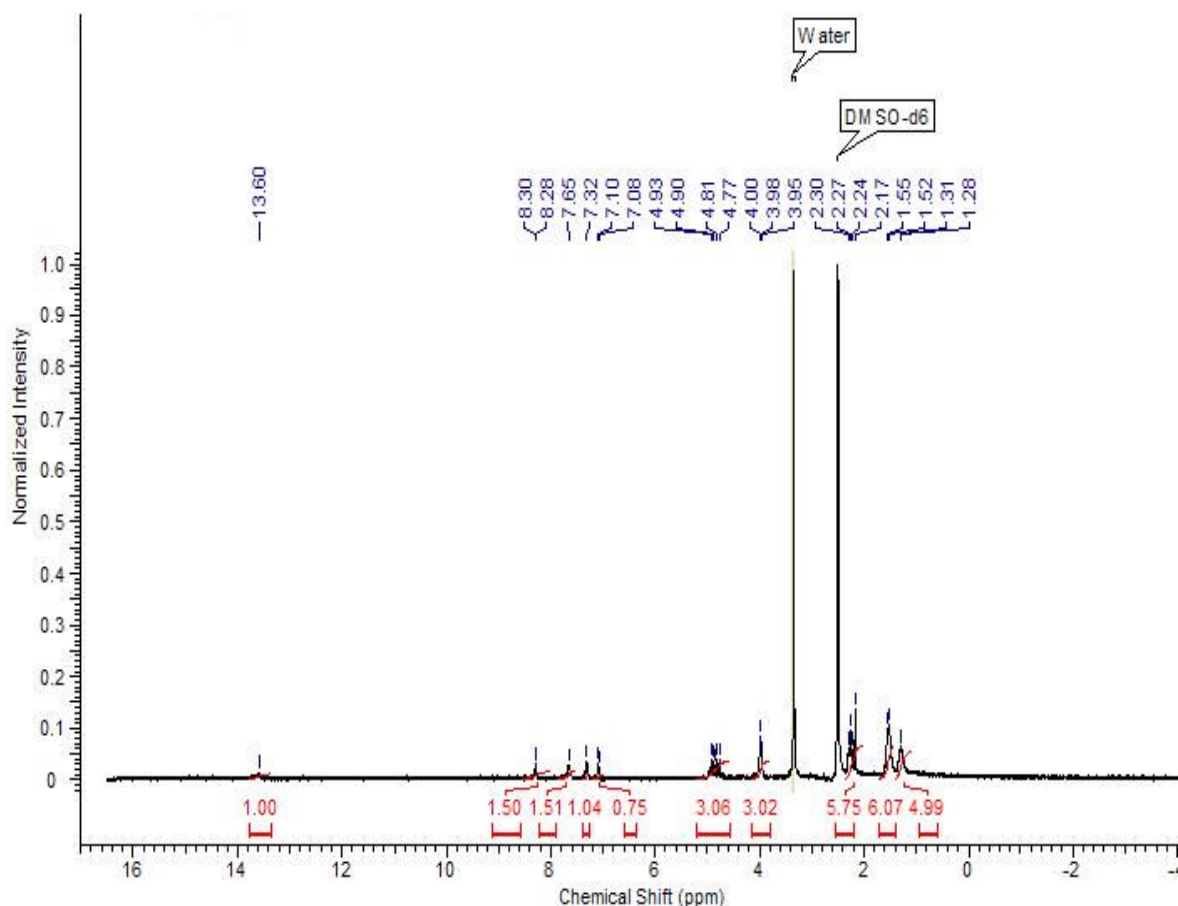


Figure 7.14. H^1 -NMR spectrum (DMSO-D_6) of physical mixture of PCL and lansoprazole.

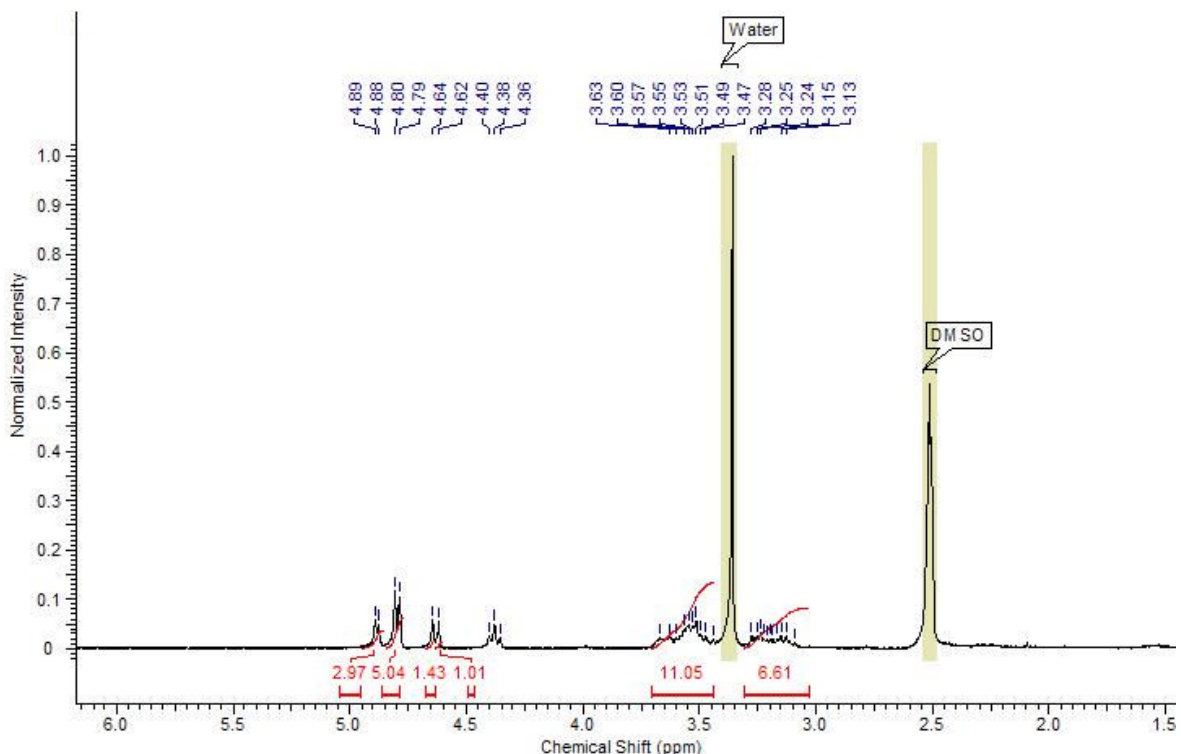


Figure 7.15. H^1 -NMR spectrum (DMSO- D_6) of physical mixture of milled PCL and lansoprazole.

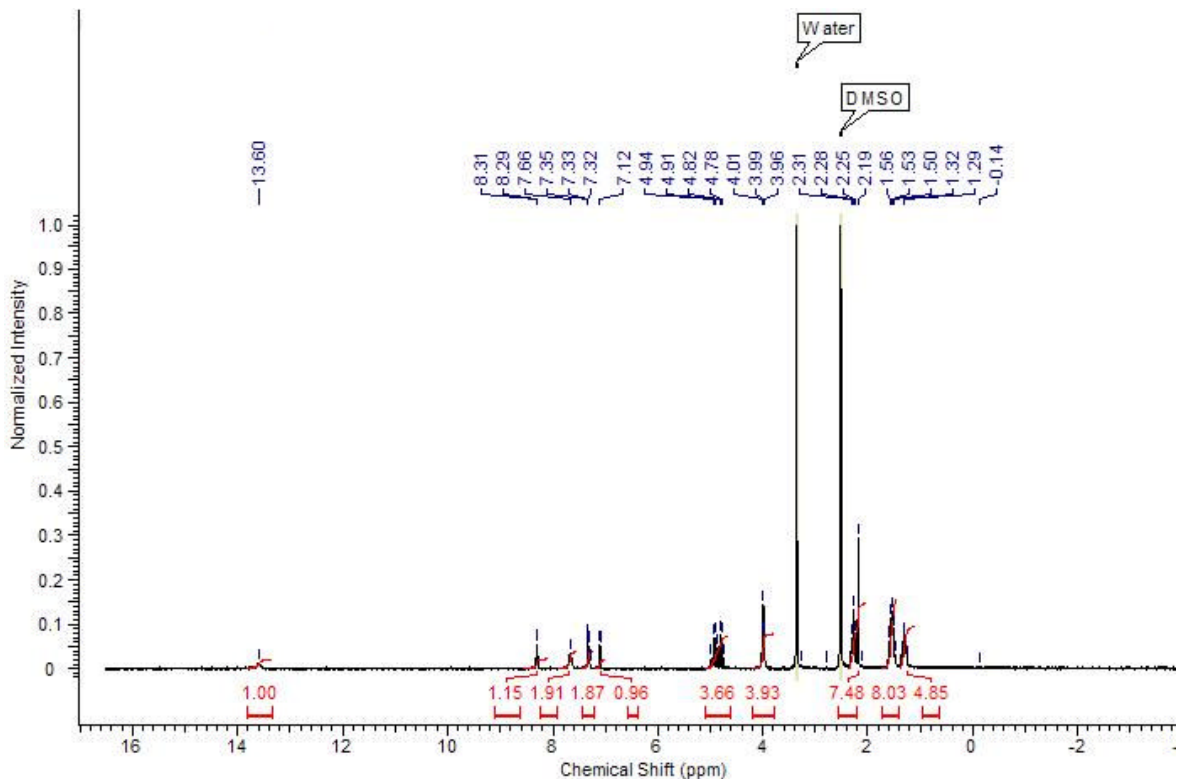


Figure 7.16. H^1 -NMR spectrum (DMSO- D_6) of PCL-coated lansoprazole-loaded nanoparticles.

PLGA nanoparticles

The $\text{H}^1\text{-NMR}$ spectra for the physical mixture of non-milled and milled PLGA with lansoprazole were distinctly different. The non-milled PLGA displayed a small single peak at 13.58 ppm that represents the -N-H group from the lansoprazole structure. Also at 8.29 ppm a small doublet peak was observed with further 2 smaller single peaks at 7.33 and 7.12 ppm. Multiple peaks are seen at 4.93 and 5.20 ppm equalling to 14 and 6 H-ions respectively. A new peak was observed at 2.18 ppm representing 2 H-ions, with the peak 1.47 ppm representing 20 H-ions, previously 37 H-ions with regard to the pure compound (Figure 7.17).

When the physical mixture of milled PLGA and lansoprazole was analysed (Figure 7.18), it could be observed that despite the peak specific to -N-H being present at 13.58 ppm, several other peaks were either not present or had a lower number of H-ions assigned to it. One particular example was the 20 H-ion large peak at 1.47 ppm, which was now representative of 1 H-ion. The NMR scans demonstrate significant differences between the physical mixture of milled and non-milled PLGA with lansoprazole.

The NMR scans for PLGA nanoparticles loaded with lansoprazole displayed the absence of the lansoprazole fingerprint (13.58, 1.48 and 2.18 ppm peaks are missing) (Figure 7.19). Thus indicating that lansoprazole had been fully incorporated into the core and not adsorbed onto the particle surface.

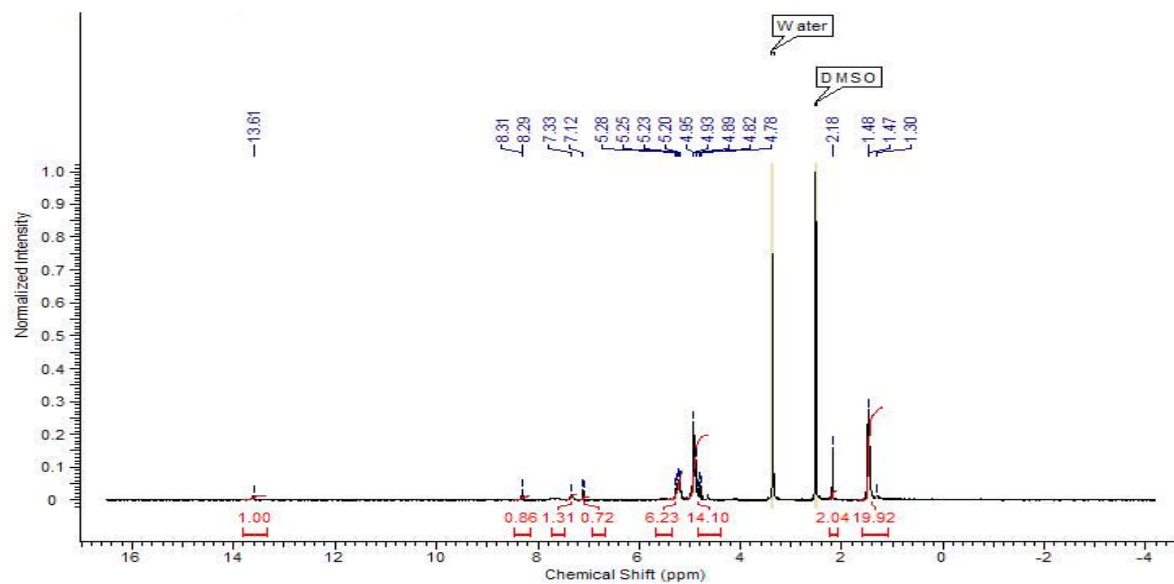


Figure 7.17. $\text{H}^1\text{-NMR}$ spectrum (DMSO-D_6) of physical mixture of PLGA and lansoprazole.

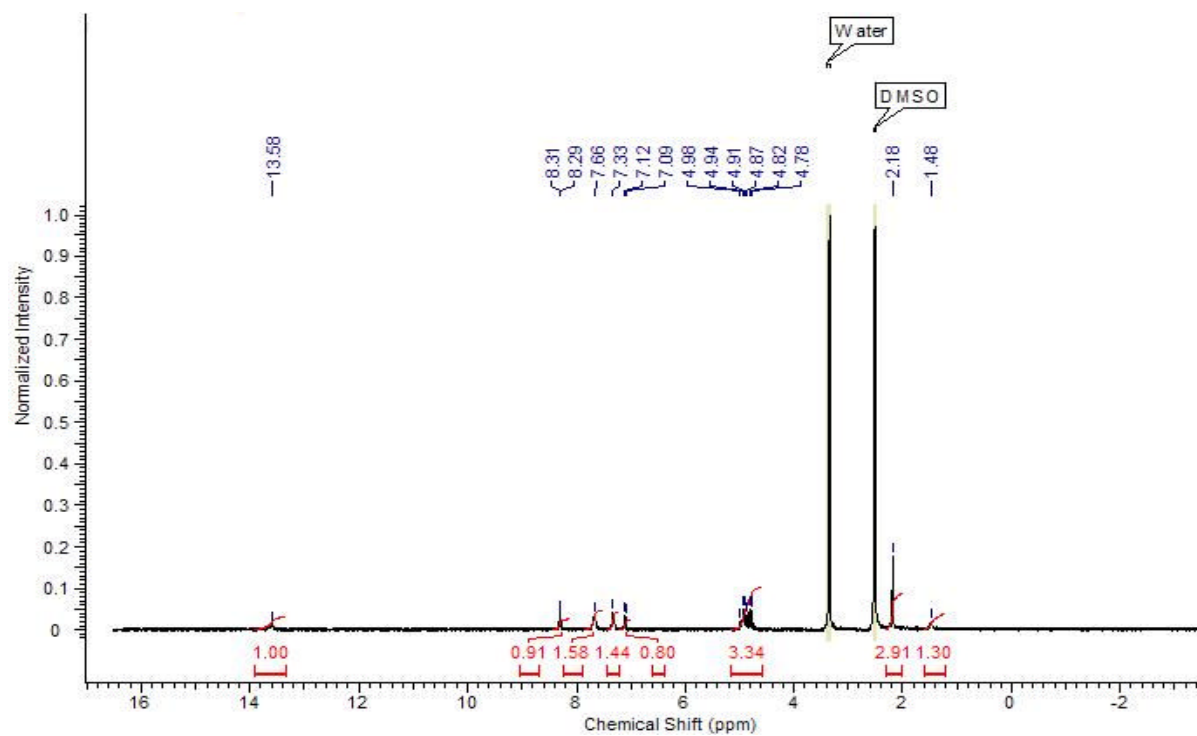


Figure 7.18. H^1 -NMR spectrum (DMSO- D_6) of physical mixture of milled PLGA and lansoprazole.

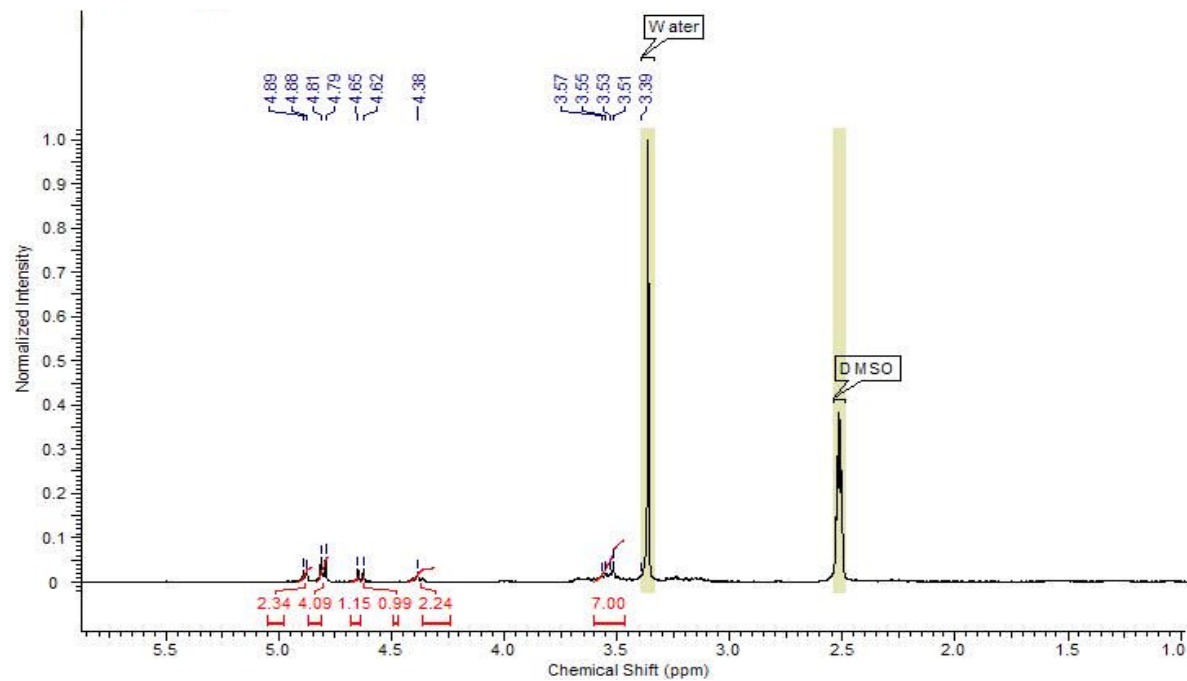


Figure 7.19. H^1 -NMR spectrum (DMSO- D_6) of PLGA-coated lansoprazole-loaded nanoparticles.

Therefore the NMR results establish the loading of lansoprazole to be within the core of the nanoparticles, and not adhered to the outside, with no interaction occurring between the polymers and the drug.

7.3.4.3.2. FTIR

FTIR was carried out in order to assess the bond integrity of the non-milled and milled polymers and respective nanoparticles. The scope and limitation of FTIR analysis depends upon the appearance of the non-superimposed transmittance spectrum, thus the first stage was to highlight the spectra of the pure components. The structural composition of pluronic F127, lansoprazole, PCL, PLGA and trehalose have been displayed in figure 7.1.

Figure 7.20 demonstrates the transmittance spectrum of trehalose, pluronic F127, PCL and lansoprazole. Trehalose showed a distinct broad peak at 3367 cm^{-1} corresponding to an –OH group, with pluronic F127 having two distinct transmittance peaks at 2890 and 1112 cm^{-1} , corresponding to a –C-H stretch and a –C-O bond respectively. Lansoprazole displayed transmittance peaks at 3222, 2983, 1580, 1282 and 1117 cm^{-1} , which denoted to the stretching vibrations of –NH, -CH₂-, the aromatic ring, C-N on the pyridyl ring and the ether bond respectively (Zhang *et al*, 2008). Further multiple transmittance peaks for lansoprazole were detected at 2930, 1127, 800 and 577 cm^{-1} , which correspond to its –C-H alkane, a –C=N alkyl halide, a –C-H, and a –C-S bonds.

PCL nanoparticles

PCL displayed a transmittance peak at 2994, 1726, 1243 and 1365cm^{-1} which corresponded to the –C-H stretch, -C=O, -C-O, and the –C-H (rock) respectively. The milled polymer displayed similar transmittance data with very slight deviation. When the PCL and milled PCL nanoparticles were analysed with FT-IR, they both displayed a similar transmittance profile (Table 7.9 and Figure 7.21). Both nanoparticle formulations demonstrated new transmittance peaks at 990 and 841 cm^{-1} , corresponding to a =C-H and an alkyl halide bond. This was indicative of a weak interaction (weak transmittance peak) occurring between the halide of lansoprazole and the double bonded carbon of PCL.

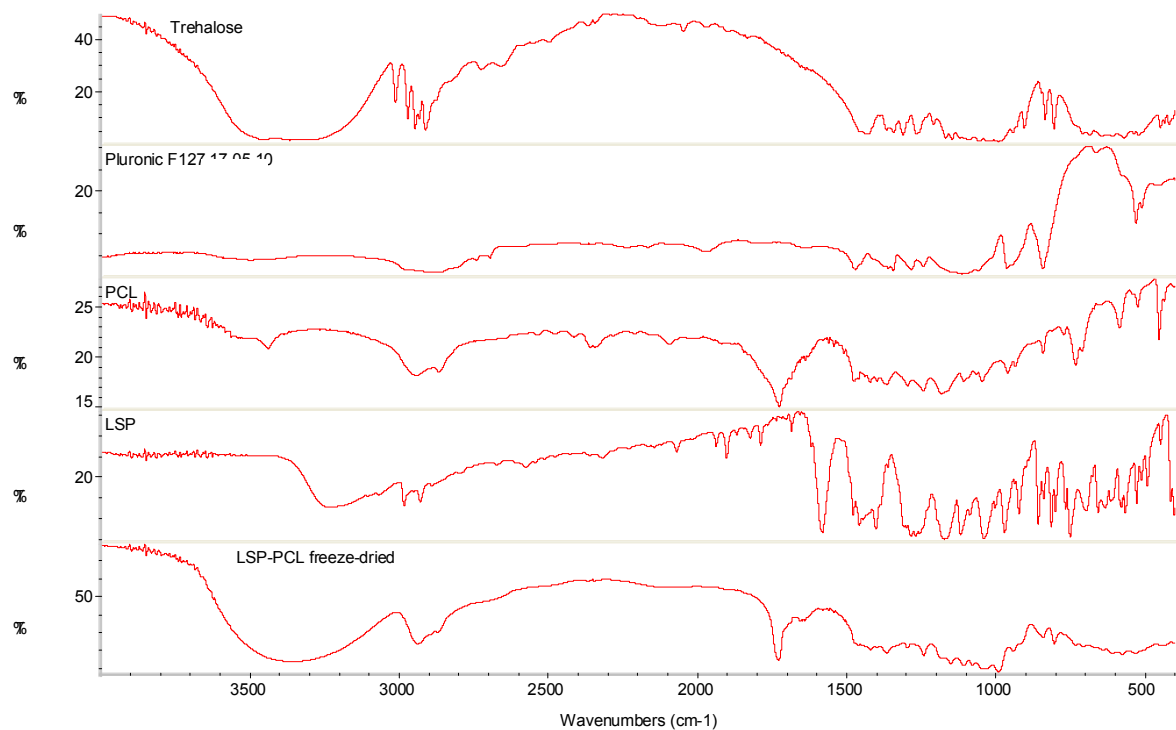


Figure 7.20. Comparison of FTIR spectrum for trehalose, pluronic F127, lansoprazole (LSP), standard PLGA and PLGA nanoparticles prepared at a 5:1 polymer drug ratio.

Table 7.9. Analysis of excipient interaction and chemical bond donation with PCL nanoparticles, prepared at a 5:1 polymer-drug ratio. A new bond formation was observed at 990 and 841 cm⁻¹ corresponding to a =C-H and an alkyl halide bond.

Peak No.	Wavelength/cm ⁻¹	Donated from	Bond
1	3350	Trehalose	O-H
2	2938	PCL, F127, LSP	C-H alkanes
3	1728	PCL	C=O
4	1365	PCL	C-H rock
5	1241	PCL	C-O
6	1150	LSP	C-N /alkyl halides -CH ₂ X
7	1107	LSP	C-O / C-N
8	990		=C-H
9	841		alkyl halide
10	803	LSP	C-H aromatic
11	575	LSP	C-Br stretch

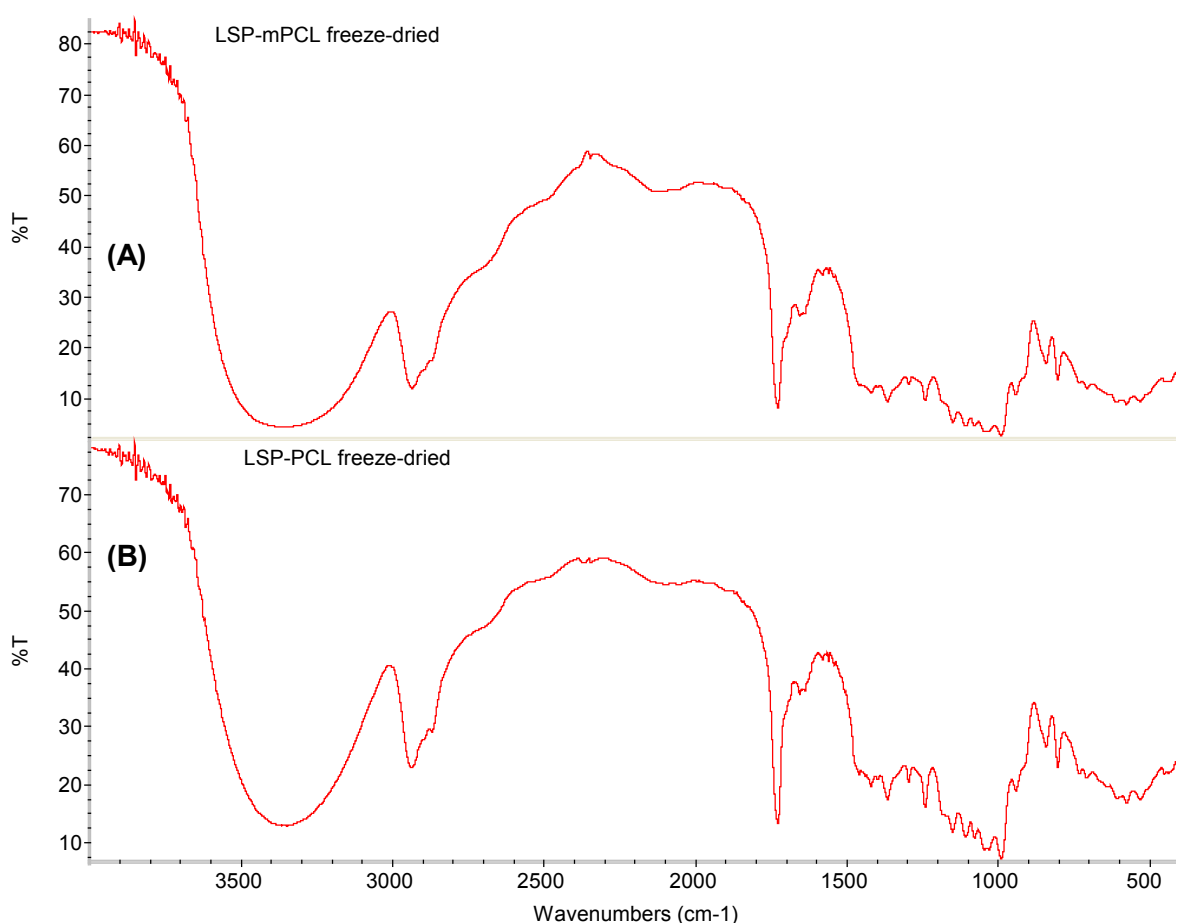


Figure 7.21. FTIR spectra of PCL nanoparticles prepared at a 5:1 polymer-drug ratio. No significant difference was observed in the transmittance peaks of (A) milled PCL and (B) non-milled PCL nanoparticles.

PLGA nanoparticles

PLGA displayed a transmittance peak at 2999, 3527, 1759, 1456 and 1182 cm^{-1} which correspond to $-\text{O-H}$, $-\text{O-H}$ (alcohol), $-\text{C=O}$ (ester), $-\text{CH}_3$, and $-\text{C-O-C-}$ (ester) bonds respectively (Figure 7.22). The milled polymer displayed similar transmittance data with very slight deviation. When non milled PLGA and milled PLGA nanoparticles were analysed with FTIR, they both displayed a similar transmittance profile (Table 7.10 and Figure 7.23). Both nanoparticle formulations demonstrated new transmittance peaks at 991 and 843 cm^{-1} , corresponding to a $=\text{C-H}$ and an alkyl halide bond (similar to the PCL nanoparticles). This was indicative of a weak interaction (weak transmittance peak) occurring between the halide (lansoprazole) and a double bonded carbon (PLGA).

Table 7.10. Analysis of excipient interaction and chemical bond donation with PLGA nanoparticles, prepared at a 5:1 polymer-drug ratio. A new bond formation was observed at 991 and 843 cm⁻¹ corresponding to a =C-H and an alkyl halide bond.

Peak No.	Wavelength/cm ⁻¹	Donated from	Bond
1	3392	PLGA/mPLGA/trehalose	O-H
2	2936	PLGA/mPLGA	CH ₃
3	1760	PLGA/mPLGA	C=O
4	1643	LSP	N-H bending
5	1428	PLGA/mPLGA	C-O-H bending
6	1149	LSP	C-N/alkyl halide -CH ₂ X
7	1103	LSP	C-O/C-N
8	1078	F127	C-O
9	1031	F127	C-O
10	991		=C-H
11	942	LSP	=C-H
12	843		Alkyl halide
13	803	LSP	C-H aromatic
14	576	LSP	C-BR stretch

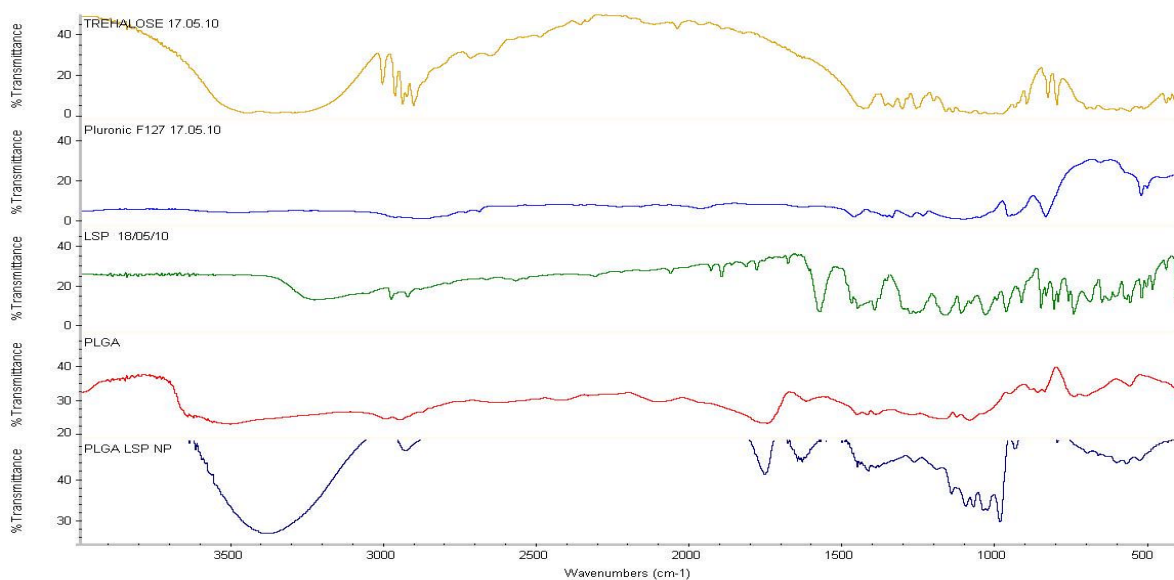


Figure 7.22. Comparison of FTIR spectrum for trehalose, pluronic F127, lansoprazole (LSP), standard PLGA and PLGA nanoparticles prepared at a 5:1 polymer drug ratio.

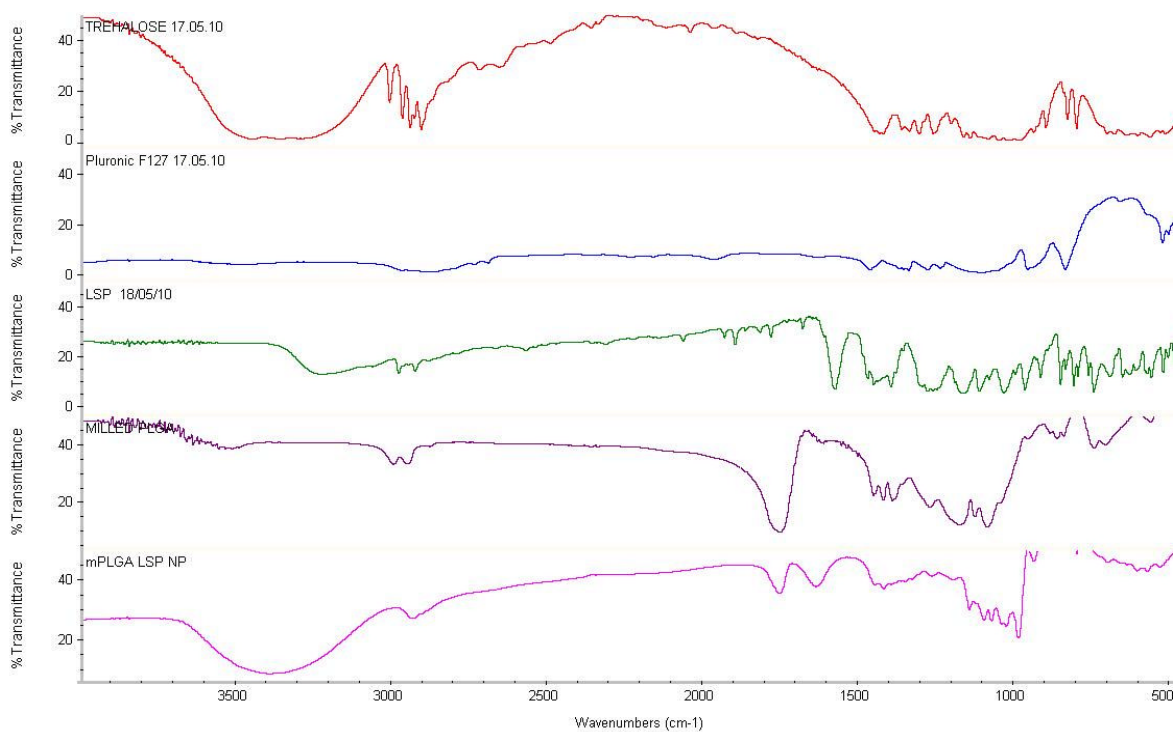


Figure 7.23. Comparison of FTIR spectrum for trehalose, pluronic F127, lansoprazole (LSP), milled PLGA and milled PLGA nanoparticles prepared at a 5:1 polymer drug ratio.

7.3.4.3.3. DSC

DSC was carried out to ascertain the thermodynamics of the nanoparticles and to confirm the absorption of lansoprazole into its hydrophobic core. The study was carried out using freeze-dried nanoparticles prepared with trehalose, which acts as a cryoprotectant (Cerimedo *et al*, 2008).

Milled PCL nanoparticles versus non-milled PCL nanoparticles

It was known that PCL and lansoprazole had on-set T_m of 62 and 180 °C respectively (Figure 7.8). Interestingly however the thermographs of non-milled and milled PCL nanoparticles at 5:1, 6:1 and 7:1 polymer-drug ratios (Figure 7.24 and 7.25) all display a single onset melting endotherm at 49 ± 3 °C with no enthalpic peak being observed for lansoprazole at 180 °C, therefore confirming the incorporation of lansoprazole into the hydrophobic core of the nanoparticle.

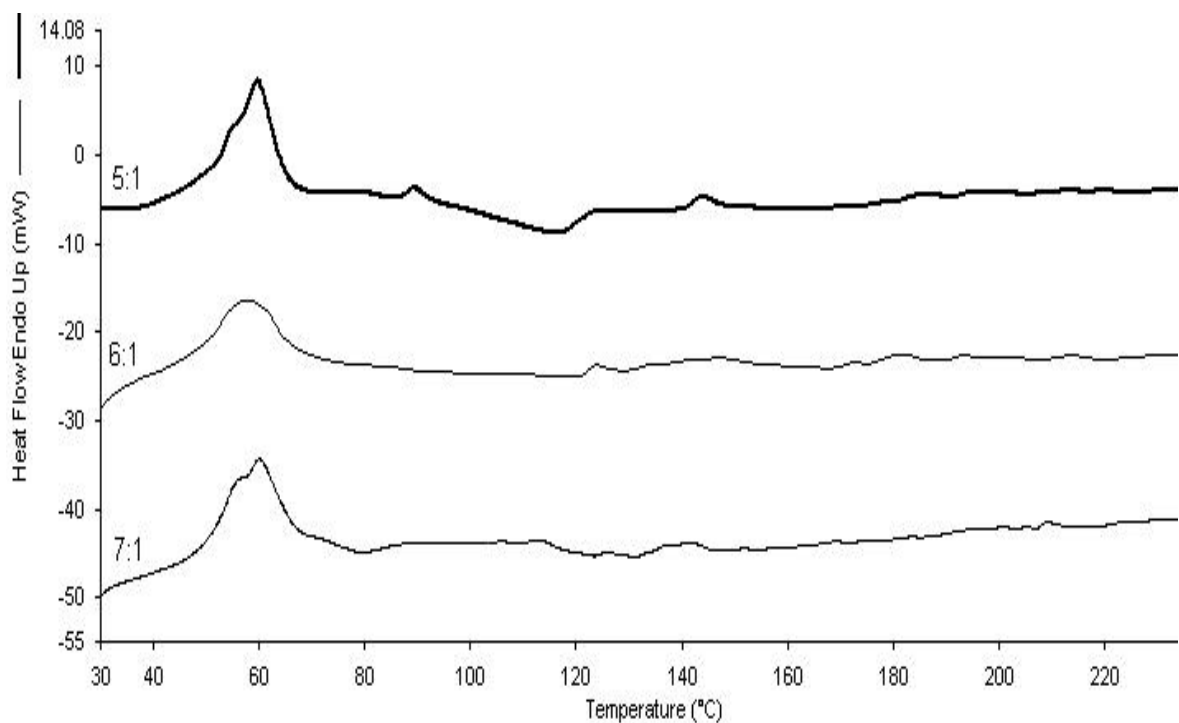


Figure 7.24. DSC thermogram of PCL lansoprazole nanoparticles at varying ratios, at a scan rate of $150\text{ }^{\circ}\text{C}.\text{min}^{-1}$. At all three ratios a melt is observed at $59\text{ }^{\circ}\text{C}$, and a subsequent crystallisation at $117\text{ }^{\circ}\text{C}$.

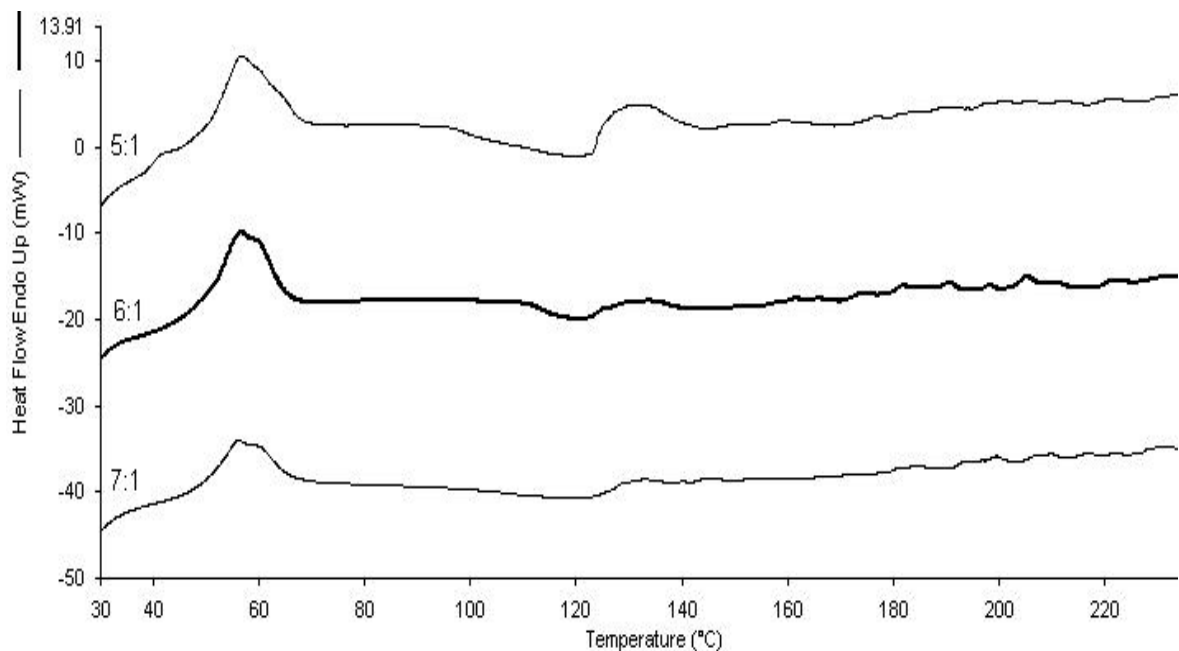


Figure 7.25. DSC thermogram of milled PCL lansoprazole nanoparticles at varying ratios, at a scan rate of $150\text{ }^{\circ}\text{C}.\text{min}^{-1}$. At all three ratios a melt is observed at $56\text{ }^{\circ}\text{C}$, and a subsequent crystallisation at $120\text{ }^{\circ}\text{C}$. Contrary to the non-milled PCL nanoparticles, immediately after the crystallisation a melt is observed at $129\text{ }^{\circ}\text{C}$.

Milled PLGA nanoparticles versus non-milled PLGA nanoparticles

It was known from previous studies that PLGA had on-set T_m of 33 °C which was observed as a small endothermic peak (Figure 7.8). However the DSC thermograms of the polymer in the milled and non-milled PLGA nanoparticles were masked by the presence of trehalose, which has a polymorphic crystalline pattern (Figure 7.26 and 7.27). Importantly however, the lansoprazole T_m was absent on both thermographs (at 180 °C), therefore confirming the drug to be fully incorporated into the hydrophobic matrix of the milled and non-milled PLGA nanoparticles.

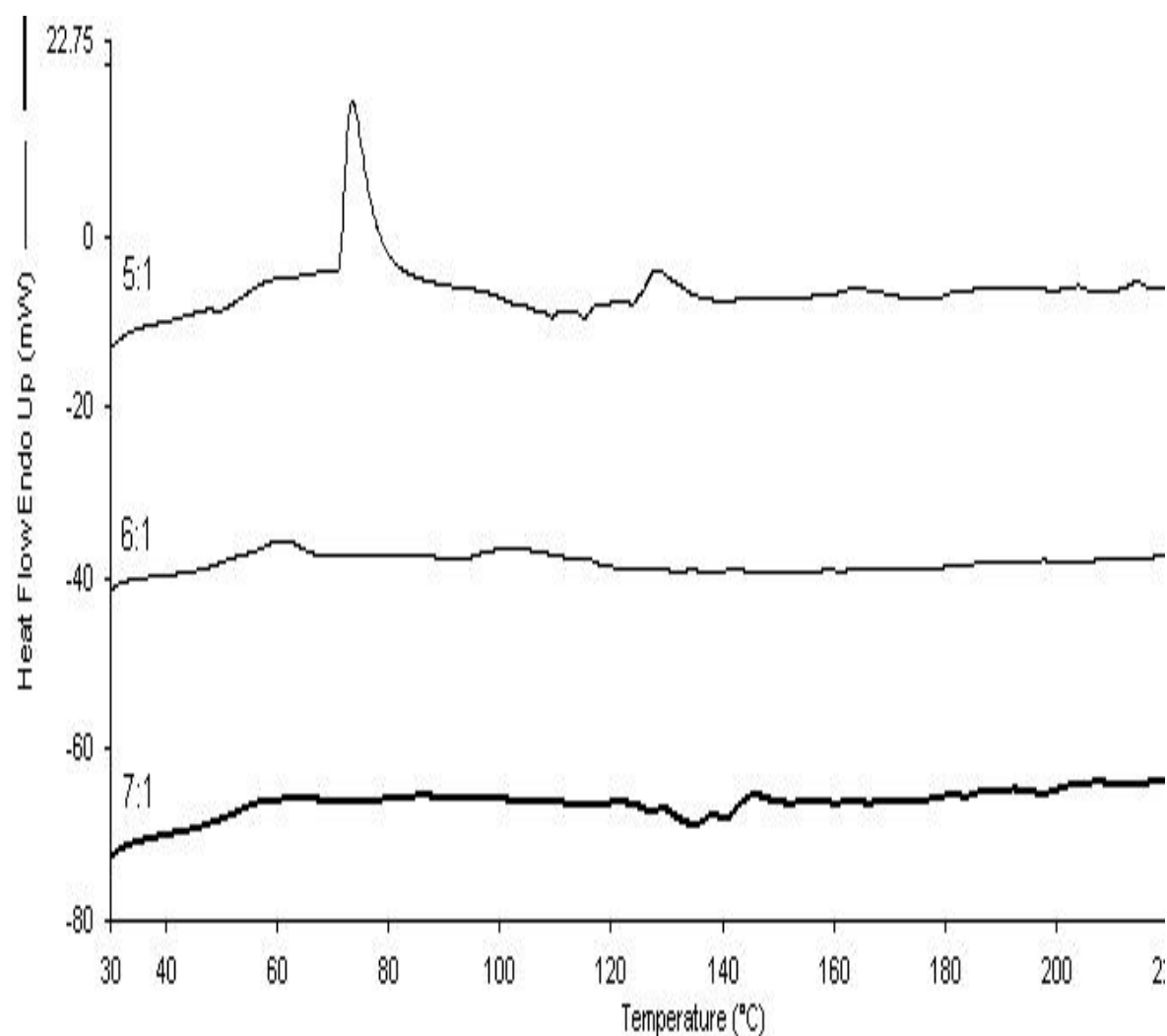


Figure 7.26. DSC thermogram for the milled PLGA nanoparticles at varying ratios, at a scan rate of $150 \text{ }^{\circ}\text{C}.\text{min}^{-1}$. For the 5:1 ratio, a melting peak is observed at 73 °C with an addition melt occurring at 128 °C.

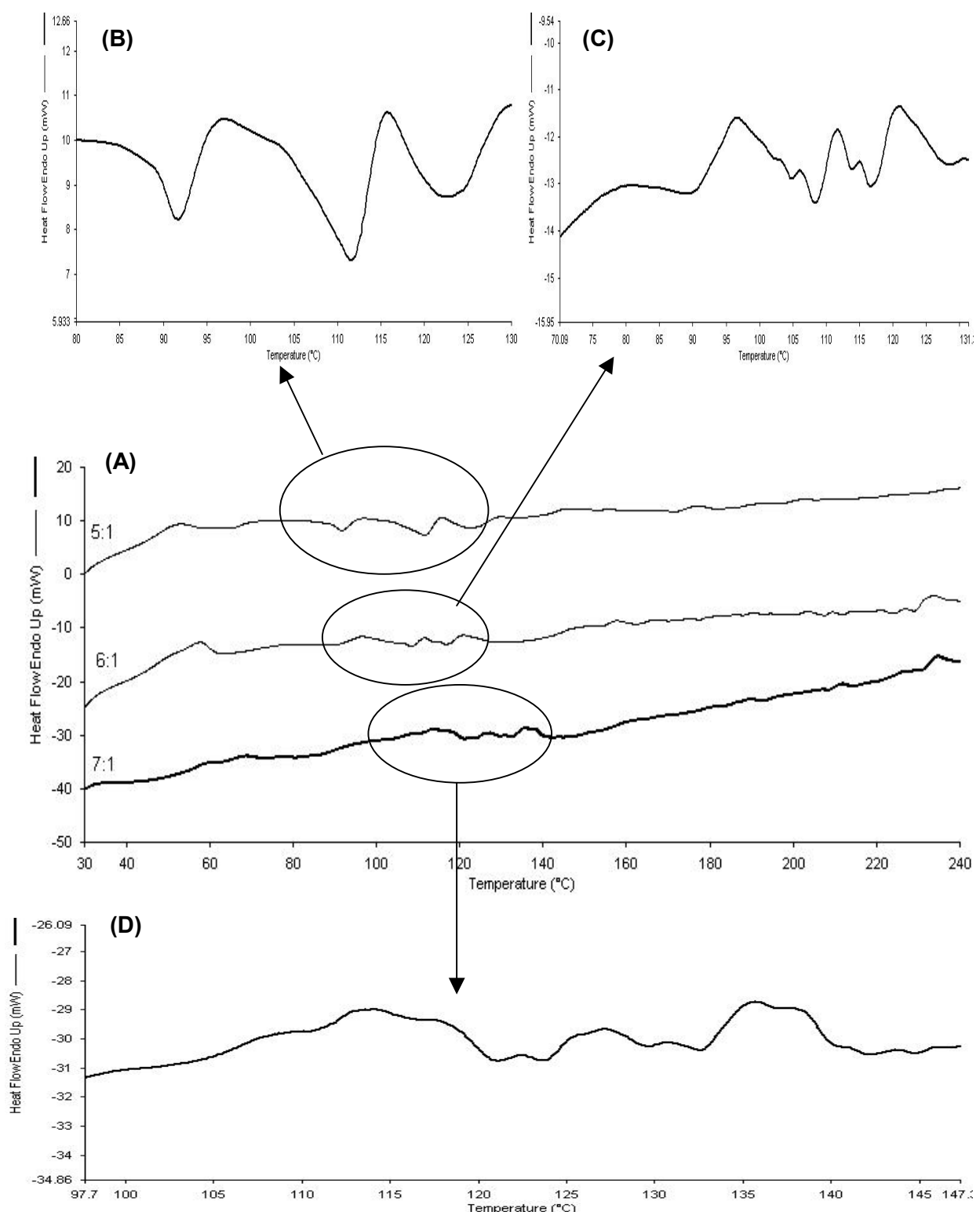


Figure 7.27. DSC thermogram for PLGA nanoparticles at varying polymer-drug concentrations, at a scan rate of $150\text{ }^{\circ}\text{C}.\text{min}^{-1}$. **(A)** The T_m of lansoprazole at $180\text{ }^{\circ}\text{C}$ was absent indicating complete absorption into the polymeric matrix. **(B)** Polymorphic crystallinity of trehalose detected at the 5:1 ratio. **(C)** Polymorphic crystallinity of trehalose detected at the 6:1 ratio. **(D)** Polymorphic crystallinity of trehalose detected at the 7:1 ratio.

7.3.5. *In Vitro* release study

The release study for the lansoprazole-loaded nanoparticles was carried out in two stages; the first stage was in 0.1 M HCl or pH 4.5 aimed at mimicking the acid in the stomach in the fasted and fed state respectively. The second phase was in the buffer at pH 6.8, aimed at mimicking the conditions within the small intestine.

7.3.5.1. Implications of the fasted state conditions (0.1 M HCl) on non-milled and milled polymeric nanoparticles

Figure 7.28 displays the release profile of lansoprazole from non-milled and milled PCL nanoparticles prepared at a polymer-drug ratio of 5:1. In the acid phase ~51 % of lansoprazole was released from the PCL nanoparticles, with the milled PCL nanoparticles displaying a relatively lower release profile (19-30 %). In the buffer stage, the drug was released from the nanoparticles at a steady rate, after an initial burst release of ~22 %. However, the release rate from the non-milled PCL nanoparticles was significantly higher than the release obtained from the milled PCL nanoparticles. At the 4 hour mark in the buffer

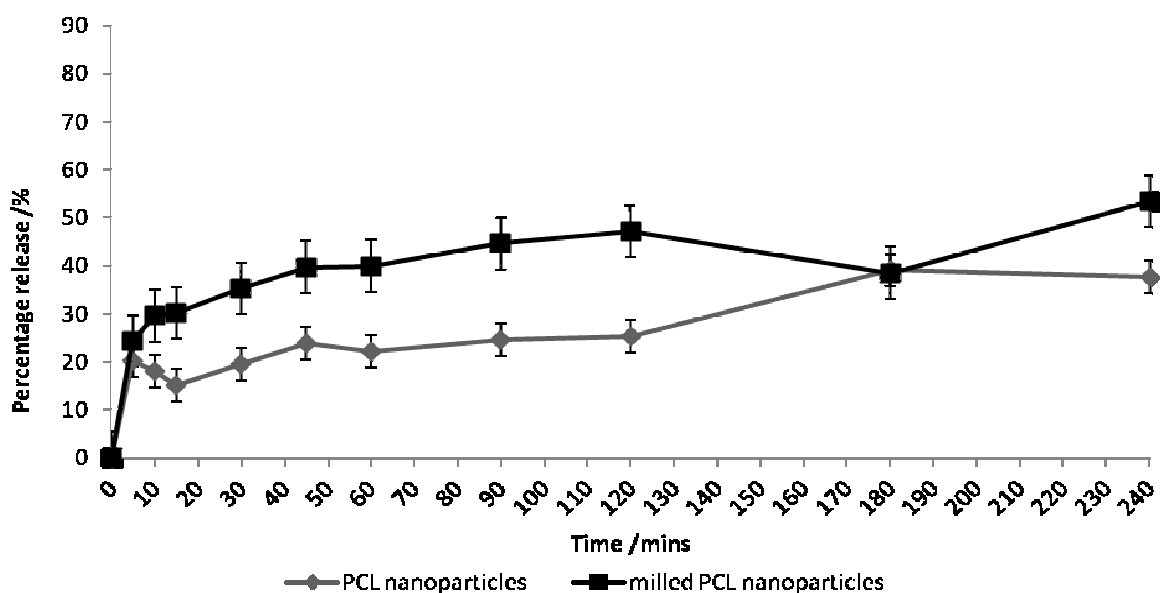


Figure 7.28. Release profile of milled and non-milled PCL nanoparticles (5:1 polymer-drug ratio) in the buffer phase when under fasting conditions. Milled PCL nanoparticles displayed a quicker release profile than non-milled PCL nanoparticles. At the 4 hour phase hour mark in the buffer phase, 37.70 ± 8.48 and 53.34 ± 28.59 % of lansoprazole from PCL and milled PCL nanoparticles had been released respectively. (n=3)

phase, 37.70 ± 8.48 and 53.34 ± 28.59 % of lansoprazole from PCL and milled PCL nanoparticles had been released respectively. At the 48 hour mark, lansoprazole increased to 49.27 ± 3.91 and 69.89 ± 29.88 % respectively. It was concluded that approximately 100 % had been released in total from the PCL nano-suspension, and 81-100 % from the milled PCL nano-suspension.

Figure 7.29 displays the release profile of lansoprazole from non-milled and milled PLGA nanoparticles prepared at a polymer-drug ratio of 5:1. In the acid phase 25-35 % of lansoprazole was released from the PLGA nanoparticles, with a greater proportion of lansoprazole being released from the milled PLGA nanoparticles (34-44 %). In the buffer stage, this trend continued in which the release rate of lansoprazole from milled PLGA nanoparticles was significantly higher than the release obtained from non-milled PLGA nanoparticles. Within the first 5 minutes a burst effect was observed, with non-milled PLGA releasing 6.28 ± 5.64 %, in comparison with milled PLGA nanoparticle releasing 26.49 ± 17.53 % lansoprazole. The burst effect was attributed to the adsorption of lansoprazole near the outer layers of the nanoparticle matrix (Magenheim *et al*, 1993; Singh

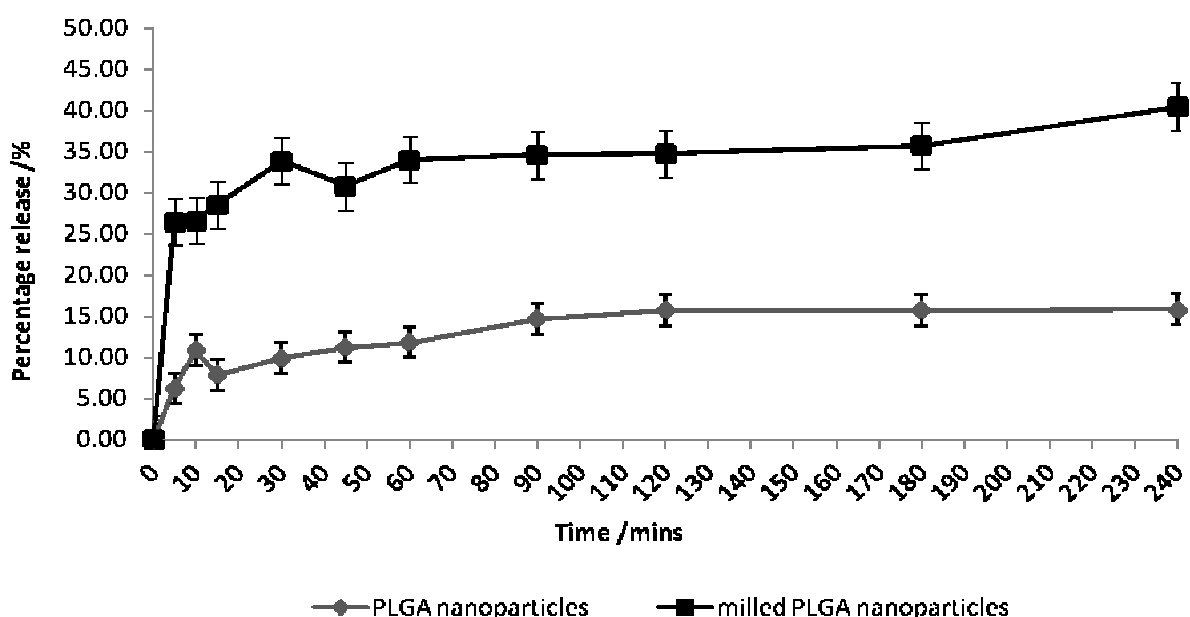


Figure 7.29. Release profile of milled and non-milled PLGA nanoparticles (5:1 polymer-drug ratio) in the buffer phase when under fasting conditions. Milled PLGA nanoparticles displayed a quicker release profile than non-milled PLGA nanoparticles. At the 4 hour phase hour mark in the buffer phase, 15.87 ± 9.05 and 40.34 ± 18.08 % of lansoprazole from PLGA and milled PLGA nanoparticles had been released respectively. ($n=3$)

and Lillard, 2009). After the burst affect, both nanoparticles released the drug at a steady increase. At the 4 hour mark in the buffer phase, $15.87 \pm 9.05\%$ of lansoprazole from PLGA nanoparticles was released, increasing to $27.56 \pm 14.05\%$ after 48 hours. In contrast, milled PLGA nanoparticles released $40.50 \pm 18.08\%$ of lansoprazole within 4 hours, with no further release by the 48 hour mark. It was concluded that approximately 33-52 % had been released in total from the PLGA nano-suspension, and 69-100 % from the milled PLGA nano-suspension.

7.3.5.2. Implications of the fed state conditions (pH 4.5) on milled and non-milled polymeric nanoparticles

Figure 7.30 displays the release profile of lansoprazole nanoparticles prepared from standard PCL and PLGA at a polymer-drug ratio of 5:1. In the acid phase (pH 4.5) $24.27 \pm 2.52\%$ of lansoprazole was released from the PCL nanoparticles, with PLGA nanoparticles exhibiting a lowered release profile ($11.28 \pm 2.42\%$). In the buffer stage, the drug was released from the nanoparticles at a slow steady rate, with no burst affect being observed. At the 48 hour mark in the buffer phase, 61.36 ± 6.53 and $42.74 \pm 8.57\%$ of lansoprazole from PCL and PLGA nanoparticles had been released respectively. It was thus concluded that approximately 85 % had been released in total from the PCL colloidal system, and approximately 53 % from the milled PCL matrix system.

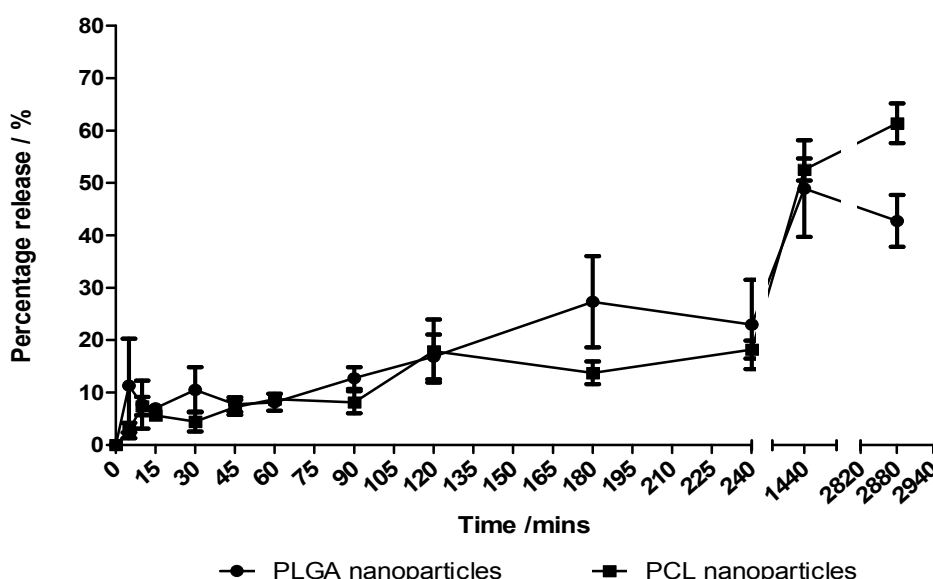


Figure 7.30. Release profile of PCL and PLGA nanoparticles (5:1 polymer-drug ratio) in the buffer phase, when under fed condition. Both polymers displayed a fairly similar release profile; slow and steady. At the 48 hour phase hour mark in the buffer phase, 61.36 ± 6.53 and $42.74 \pm 8.57\%$ of lansoprazole from PCL and PLGA nanoparticles had been released respectively. (n=3)

7.3.5.3. Fasting versus Fed conditions

The conditions of the stomach greatly influenced the release rate of lansoprazole from the nanoparticles. A greater proportion of the lansoprazole was released from the nanoparticles (standard and milled polymers) under fasted conditions (0.1 M HCl) than under fed conditions (pH 4.5). These variances can be attributed to the acidic environment degrading the outer layers of the polymer coat, and thus resulting in increased dispersion of lansoprazole into the acid environment. Therefore, these results highlight the importance of pre-drug delivery conditions, and can be recommended that for polymeric nanoparticle delivery the patient is medicated after food intake in order to reduce the degradative properties of the stomach environment.

In the second phase of the release study the nanoparticles were placed in buffer conditions (pH 6.8) for 48 hours, representing nanoparticles in the small intestine. The PCL and PLGA nanoparticles showed no significant difference in the initial rate of release, neither of which exhibited a burst affect, however after 48 hours the greatest lansoprazole release was exerted by the PCL matrix system. In contrast, under fasting conditions, milled and non-milled polymer nanoparticles exhibited a burst release of lansoprazole, which was associated with increased polymer degradation in the acid phase. This initial degradation of the polymer coat resulted in a smaller distance for the drug had to diffuse across, and thus causing the initial burst release affect.

Nanoparticles release their drug load either by diffusion or matrix erosion, with the method of release depending on the rate of matrix erosion. In the present study, lansoprazole was found to be diffusing through the matrix at a faster rate than the polymer was degrading, and therefore the rate of release in this system was concluded to be controlled by a diffusion process. Interestingly the rate of release was also controlled by a second factor: particle size of the colloidal system. The milled polymers produced smaller nanoparticles, thereby increasing their surface area-to-volume ratio. Hence the majority of the drug load was located nearer to the polymeric nanoparticle surface resulting in a faster drug release profile. The non-milled polymer nanoparticles displayed a significantly larger particle size, and therefore had a larger matrix system allowing a greater amount of drug to be encapsulated within a single nanoparticle. In a larger polymeric nanoparticle, longer time was required to degrade the polymer in order to release all of its drug contents, resulting in a slower release profile (Redhead *et al*, 2001; Singh and Lillard, 2009). The rate of release of lansoprazole can therefore be directly related to particle size and the rate of drug diffusion.

7.4. Conclusion

The current study showed that the solvent displacement and the emulsion diffusion techniques successfully produced polymeric nanoparticles; however the drug load was greatly influenced by the composition of the polymer and the polymer concentration. It was found that PCL nanoparticles decreased in drug loading with increasing polymer concentration, whereas PLGA nanoparticles remained relatively unaffected by the polymer-drug ratio. A third factor governing the loading efficiency of the nanoparticles was mechanical milling of the polymers prior to nanoparticle preparation. The process of milling altered the molecular weight of the polymers, and also changed the physical aspects of the PLGA polymer, making its less glassy in structure and more globular. Also the repeated mechanical impaction of the mill caused a weakening of the polymer chain, enabling increased flexibility of the polymer to coil into a more condensed particle. This in turn resulted in smaller particles with higher drug loading efficiency. Preparative polymer variables (molecular weight and concentration) are important factors for the formation of polymeric nanoparticles. The release kinetics of the drug was governed by the initial drug loading, higher the initial drug loading resulted in a faster drug release profile. The process of milling resulted in milled polymers nanoparticles having a greater drug loading efficiency and thus had a faster release profile than the non-milled polymer.

CHAPTER 8

General Conclusions

CHAPTER 8

General Conclusions

8.1. Summary of research findings

The thesis highlights the systematic approaches towards development of oral liquid formulation and overcoming barriers associated with poorly soluble drugs and drugs which are unstable in aqueous environments, in order to improve patient compliance along with providing alternative pharmaceutical preparations to potentially increase patent-life. By investigating the drug formulation criteria, the formulation parameters could be assessed and an oral liquid solution or suspension prepared. The investigation revealed that the stabilisation of poorly soluble drugs was attributed to reduced polarity and increasing potential hydrophobic binding constants, such as cyclodextrins and nanoparticles. Accordingly, research was carried out to explore and optimise simple approaches towards specific hydrophobic drug solubilisation and hydrophilic drug stabilisation, which could be easily scaled up for industrial manufacturing. As a result of this research, various excipients commonly used in the pharmaceutical industry were studied.

8.1.1. Formulation development and physicochemical investigation of a stable aqueous preparation of captopril

Hydrophilic drugs can hinder the development of aqueous preparations, particularly when challenged with instability and self-dimerisation issues. Captopril is one such drug that despite its hydrophilicity (160 mg.mL^{-1}) remains unstable in solution. The degradation of captopril is initiated by the ionisation of the carboxylic group, which in turn ionises the thiol group yielding the major degradation product captopril disulphide (oxygen-facilitated, first order, free radical oxidation).

EDTA and HP- β -CD were introduced into a solution of 1 mg.mL^{-1} and 5 mg.mL^{-1} captopril, in an attempt to stabilise the drug and to prevent the initiation of its degradation pathway. EDTA acts by a chelation mechanism: its protonated carboxyl group binds to the ionised thiol group of captopril preventing captopril dimerisation. The aromatic side chain and a carboxylic acid side group of captopril was found to be reversibly bound to the core of HP- β -CD, thereby forming a rigid structure. This steric hindrance resulted in a reduction in the sulphuric-like

odour normally associated with captopril. 1 mg.mL⁻¹ and 5 mg.mL⁻¹ captopril formulations comprising of EDTA and EDTA-HP-β-C-D were found to be stable for 12 months both chemically and organoleptically, when stored under 5 °C, 25 °C and 40 °C conditions (drug retention above 95 %).

8.1.2. Solubilisation and physicochemical analysis of gliclazide

Poorly soluble drugs display particular challenges when formulating an alternate dosage form to tablets, such as aqueous solutions/suspensions. Gliclazide has very poor water solubility (55 mg.L⁻¹) and is currently only available as a tablet. Enhancement of drug solubilisation can be carried out by adjusting the polarity of the medium (using a co-solvent system) or by adjustment of pH (using amino acids).

Gliclazide was solubilised (8 mg.mL⁻¹ dosage) using L-arginine, which was found to be stable chemically and organoleptically for 12 months when stored under 5 °C, 25 °C and 40 °C conditions (drug retention above 95 %). The stability was assessed by DSC, FTIR and H¹-NMR, and was found to be attributed to the intermolecular bonding (hydrogen bonding) between the 1:1 stereochemistry of L-arginine and gliclazide.

A second aqueous preparation of gliclazide (16 mg.mL⁻¹) was prepared using dual action of a co-solvent and a surfactant (CMC = 5 % w/v). This method of preparation was dependent upon two factors: (1) the dielectric constant (polarity) of the medium, and (2) the pH of the system (gliclazide concentration increased with increasing pH). The formulation was found to be stable, analytically and organoleptically, for 12 months when stored under 5 °C, 25 °C and 40 °C conditions (drug retention above 95 %).

8.1.3. Solubilisation and formulation of melatonin as a liquid oral dosage form

Photosensitive drugs, such as melatonin, hinder the development of new dosage forms by limiting the type of dosage forms available to patients. The rate of degradation increases exponentially when the drug compound has been solubilised in solution, exposing its chemical structure to the harmful UV rays. By temporarily binding melatonin to HP-β-CD, the cyclodextrin was able to successfully mask the affects of UV, thereby stabilising and preventing degradation in an aqueous environment.

The results showed that melatonin was solubilised in water to achieve a drug dosage concentration of 1 mg.mL^{-1} , by reducing the polarity of the aqueous medium using sorbitol and heat. Samples stored at 5°C were stable for up to 6 months ($93.63 \pm 1.12\%$), with samples stored at 25°C achieving a 12 month stability profile of $91.52 \pm 0.77\%$. However, aqueous preparations of 1 mg.mL^{-1} melatonin were only stable for 3 months at 40°C ($91.80 \pm 1.73\%$). This degradation was associated with: (1) the scavenging of hydroxide radicals ($\cdot\text{OH}$), (2) the formation of hydronium ions from tartaric acid, and (3) Le Chatelier's Principle.

8.1.4. Optimisation of an extraction protocol and development of an oral liquid formulation for L-arginine

In the developmental stages of drug formulation, the organoleptic properties are crucial in determining the acceptability of the drug formulation for the patient. For oral liquid preparations these properties include; pleasant smell, smooth consistency, and most importantly a palatable taste (not too sour or too sweet). A common organoleptic property associated with basic amino acids, particularly L-arginine, is extreme bitterness when in solution, which can affect the compliance issues associated with formulation and dosing.

The bitterness of L-arginine intensified as the concentration of the drug was increased, which was attributed to an increase in concentration of its guanidinium groups further increasing the alkalinity of the solution (100 mg.mL^{-1} : L-arginine in water = pH 11). The addition of 4 % (w/v) tartaric acid resulted in neutralising this bitterness and subsequently enabling a dosage of 100 mg.mL^{-1} to be prepared.

Extensive investigation of the analytical method resulted in the development of ninhydrin assay which was simple, reproducible and validated method for assessing the concentration of L arginine. Utilising this protocol, L-arginine was found to be stable in solution when stored for 12 months at 5°C , 25°C and 40°C (L-arginine retention was 95.86 ± 4.91 , 93.15 ± 2.82 , and $92.05 \pm 3.72\%$ respectively). However the organoleptic property (smell) of the formulation stored under accelerated conditions (40°C , 75 % humidity) decreased over time, which was attributed to the excipients in the formulation and not the amino acid.

8.1.5. Preservative Efficacy Test (PET)

Investigation of microbial contamination of pharmaceutical products is vital to the pharmaceutical industry and the World Health Organisation, as it can become a major cause

of product and economic losses, as well as deterioration in the patients' health or related side effects. Pharmaceutical preservatives that have been listed as GRAS are used to reduce the likelihood of microbial growth in aqueous systems. This is essential with preparations being stored in multi-dose containers that are susceptible to microbial contamination. Ideal preservative characteristics include broad spectrum of activity, active within the formulation at low concentration and effective within the pH range of the formulation.

A PET was carried out in accordance with the USP and BP guidelines, in order to evaluate the effectiveness of the preservative within the pharmaceutical preparation. Five specific microbes (*S.aureus*, *E.coli*, *P.aeruginosa*, *A.niger* and *C.albicans*) were used to challenge captopril (with (1) EDTA and (2) EDTA-HP β -CD), gliclazide (with (1) ethanol-F127 and (2) L-arginine), melatonin and L-arginine formulations. According to the BP (2009), the criteria of acceptance for oral preparations were a \log_{10} reduction of 3 and 1 for bacteria and fungi respectively, with no further increase in growth after 28 days incubation. The results revealed all of the formulations to have sufficient preservative activity against both bacterial as well as fungal microbes.

8.1.6. Solubilisation of a proton pump inhibitor (Lansoprazole) using nano-particulate delivery

Acid labile drugs are particularly difficult to formulate as suspension or solutions, as the exposure of the drug through the GIT has to be carefully considered during the formulation process. Lansoprazole has two major obstacles when formulating an oral suspension: (1) it is very poorly soluble (0.97 mg.L^{-1}), and (2) it undergoes degradation when exposed to acidic environments. Therefore the formulation strategy involved preparing a 1 mg.mL^{-1} suspension using nano-particulate delivery, with the aim that the nanoparticle protects the drug as it enters the stomach.

It was found that the composition of the polymer had an influence on the drug loading and the release rates, with PCL achieving a maximum of $85.57 \pm 1.80\%$ (5:1 polymer drug ratio) and PLGA achieving a maximum of 80 % (polymer ratio had no influence on drug loading). By milling the polymer prior to nanoparticle preparation, the drug loading increased to 91.87 ± 0.43 (7:1 polymer:drug ratio) and 96.30 ± 0.93 (6:1 polymer:drug ratio) for PCL and PLGA respectively. The increase in drug loading was attributed to the repeated mechanical impaction of the mill causing a weakening of the polymer chain and altering the molecular weight of the polymers. This resulted in increased flexibility of the polymers to coil into a

more condensed particle, thereby forming a higher concentration of smaller particles within solution and ultimately increasing the nanoparticle surface area available for drug loading.

REFERENCES

- Abdelwahed, W., Degobert, G., Stainmesse, S., Fessi, H. (2006). "Freeze-drying of nanoparticles: formulation, process and storage considerations." Adv Drug Deliver Rev **58**: 1688-1713.
- Aboellil, A. H., Al-Tuwaijri, M. M. Y. (2010). "Effect of some alternative medicine and biological factors on *Candida albicans* in Saudi Arabia." J. Yeast Fungal Res. **1**(6): 100-107.
- Abu-Shandi, K. H., Redel, E. (2009). "Quantification and Stability Evaluation of the Highly Specific Angiotensin-Converting Enzyme (ACE) Inhibitor Captopril in Human Plasma Using a Gas Chromatographic Method with N,N,N',N'-tetramethyl-2-butenediamide Derivatizing Agent." Jordan J Chem **4**(2): 183-194.
- Alkhamis, K. A., Allaboun, H., Al-momani, W.Y. (2003). "Study of the solubilisaiton of gliclazide by aqueous micellar solutions." J Pharm Sci **92**(4): 839-846.
- Altun, A., Ugar-Altun, B. (2007). "Melatonin: therapeutic and clinical utilisation." Int J Clin Pract **61**(5): 835-845.
- Amnon, B. (1997). "Mechanisms in disease: Melatonin in humans." New Engl J Medinine **336**(3): 186-195.
- Annapragada, A., Adjei, A. (1996). "Numerical simulation of milling processes as an aid to process design." Int J Pharm **136**: 1-11.
- Arayne, M. S., Sultana, N., Qureshi, F. (2007). "Nanoparticles in delivery of cariovascular drugs." Pak J Pharm Sci **20**(4): 340-348.
- Arias-Blanco, M. J., Moyano, J.R., Jose, I., Perez-Martinez, J.I., Gines, J.M. (1998). "Study of the inclusion of gliclazide in β -cyclodextrin." J Pharm Biomed Anal **18**(1-2): 275-279.
- Armstrong, D. W., DEmond, W. (1984). "Cyclodextrin bonded phases for the liquid chromatographic separation of optical, geometrical, and structural isomers." J Chromatogr Sci **22**(9): 411-415.
- Ashburn, T. T., Thor, K.B. (2004). "Drug repositioning: identifying and developing new uses for existing drugs." Nat Rev Drug Discov **3**: 673-683.

- Astray, G., Mejuto, J.C., Morales, J., Rial-Otero, R., Simal-Gándara, J. (2010). "Factors controlling flavors binding constants to cyclodextrins and their application in foods." *Food Res Int*: in press.
- Avdeef, A. (2003). *Absorption and drug development: solubility, permeability, and charge state*. New Jersey, USA, John Wiley & Sons Inc.
- Ayenew, Z., Puri, V., Kumar, L., Bansal, A.K. (2009). "Trends in pharmaceutical taste masking technologies: A patent review." *Recent Patents Drug Deliv Formulation* **3**: 29-39.
- Backensfeld, T., Muller, B.W., Kolter, K. (1991). "Interaction of NSA with cyclodextrins with cyclodextrins and hydroxypropyl cyclodextrin derivatives." *Int J Pharm* **74**: 85-93.
- Bamford, C. V., D'Mello, A., Nobbs, A.H., Dutton, L.C., Vickerman, M.M., Jenkinson, H.F. (2009). "Streptococcus gordonii modulates Candida albicans biofilm formation through intergeneric communication." *Infect Immun* **77**(9): 3696-3704.
- Barichello, J. M., Morishita, M., Takayama, K., Nagai, T. (1999). "Encapsulation of hydrophilic and lipophilic drugs in PLGA nanoparticles by the nanoprecipitation method." *Drug Dev Ind Pharm* **25**(4): 471-476.
- Bayomi, M. A., Abanumay, K.A., Al-Angary, A.A. (2002). "Effect of inclusion complexation with cyclodextrins on photostability of nifedipine in solid state." *Int J Pharm* **243**: 107-117.
- Beales, N. (2004). "Adaptation of microorganisms to cold temperatures, weak acid preservatives, low pH, and osmotic stress: A review." *Compr Rev Food Sci and Food Safety* **3**: 1-20.
- Bean, H. S. (1972). "Preservatives for pharmaceuticals." *J Soc Cosmet Chem* **23**: 703-720.
- Benita, S., Levy, M.Y. (1993). "Submicron emulsions as colloid drug carriers for intravenous administration: comprehensive physicochemical characterisation." *J Pharm Sci* **82**: 1069-1079.
- Berger-Gryllaki, M., Pdilsky, G., Widmer, N., Gloor, S., testa, B., Pannatier, A. (2007). "The developement of a stable oral solution of captopril for paediatric patients." *EJHP science* **13**(3): 67-72.

- Bertau, M., Jorg, G. (2004). "Saccharides as efficacious solubilisers for highly lipophilic compounds in aqueous media." Bioorg Med Chem **12**(11): 2973-2983.
- Bhattaram, V. A., et al. (2005). "Impact of pharmacometrics on drug approval and labeling decisions: A survey of 42 new drug applications." The AAPS J **7**(3): E503-E512.
- Bi, M., Singh, J. (1999). "HPLC method for quantification of arginine containing vasopressin." J Liq Chrom & Rel Technol **22**(4): 551-560.
- Biswal, S., Sahoo, J., Murthy, P.N. (2009). "Physiochemical properties of solid dispersions of gliclazide in polyvinylpyrrolidone K90." AAPS Pharm Sci Tech **10**(2): 329-334.
- Bonnefont-Rousselot, D., Collin, F., Jore, D., Gardes-Albert, M. (2011). "Reaction mechanism of melatonin oxidation by reactive oxygen species in vitro." J Pineal Res **50**(3): 328-335.
- Brewer, J. M., Roberts, C.W., Stimson, W.H., Alexander, J. (1995). "Accurate determination of adjuvant-associated protein or peptide by ninhydrin assay." Vaccine **13**: 1441-1444.
- Brewster, M. E., Loftsson, T. (2007). "Cyclodextrins as pharmaceutical solubilisers." Adv Drug Deliv Rev **59**: 645-666.
- Brown, M. E. (2001). Introduction to thermal analysis: techniques and applications. London, Kluwer Academic.
- Cabaleiro-Lago, C., Nilsson, M., Valente, A.J.M., Bonini, M., Soderman, O. (2006). "NMR diffusometry and conductometry study of the host-guest association between β -cyclodextrin and dodecane 1,12-bis(trimethylammonium bromide)." J Colloid Interface Sci **300**: 782-787.
- Campbell, D. B., Lavielle, R., Nathan, C. (1991). "The mode of action and clinical pharmacology of gliclazide: A review." Diabetics Res Clin Practice **14**(2): S21-S36.
- Cardinali, D. P., Pevet, P. (1998). "Basic aspects of melatonin action." Sleep Med Rev **2**(3): 175-190.
- CErimedo, M. S. A., Cerdeira, M., Candal, R.J., Herrera, M.L. (2008). "Microemulsion of a Low-trans fat in trehalose as affected by emulsifier type." J Am Oil Chem Soc **85**: 797-807.

- Chandra, R., Rustgi, R. (1998). "Biodegradable polymers." Progr Polym Sci **23**: 1273-1335.
- Chen, M.-C., Yeh, G.H.-C., Chiang, B.-H. (1996). "Antimicrobial and physiochemical properties of methylcellulose and chitosan films containing a preservative." J Food Process Pres **20**: 379-390.
- Chen, Y., Gerald, J.F., Chadderton, L.T., Chaffron, L. (1999). "Nanoporous carbon produced by ball milling." Appl Physics Lett **74**(19): 2782-2784.
- Chieng, N., Aaltonen, J., Saville, D., Rades, T. (2009). "Physical characterisation and stability of amorphous indomethacin and ranitidine hydrochloride binary systems prepared by mechanical activation." Eur J Pharm Biopharm **71**: 47-54.
- Chorilli, M., Leonardi, G.R., Salgado, H.R.N., Scarpa, M.V. (2011). "Evaluation of preservative effectiveness of liquid crystalline systems with retynil palmitate by the challenge test and D-value." J. AOAC Int. **94**(1): 118-127.
- Christensen, D., Foged, C., Rosenkrands, I., Nielsen, H.M., Andersen, P., Agger, E.M. (2007). "Trehalose preserves DDA/TDB liposomes and their adjuvant effects during freeze-drying." Biochimica et Biophysica Acta **1768**: 2120-2129.
- Conacher, M., Alexander, J., Brewer, J.M. (2001). "Oral immunisation with peptide and protein antigens by formulation in lipid vesicles incorporating bile salts (bilosomes)." Vaccine **19**(20-22): 2963-2974.
- Connors, K. A., Amidon, G.I., Stella, Z.J. (1986). Chemical stability of pharmaceuticals: A handbook for pharmacists. New York, Wiley Interscience.
- Corrigan, O. I., Li, X. (2009). "Quantifying drug release form PLGA nanoparticles." Eur J Pharm Sci **37**: 477-485.
- Cross, M. M. (1965). "Rheology of non-Newtonian fluids: a new flow equation for pseudoplastic systems." J Colloid Sci **20**: 417-426.
- Davis, S. S., Illum, L. (1988). "Polymeric microspheres as drug carriers." Biomaterials **9**: 111-115.
- Davis, T. M. E., Daly, F., Walsh, J.P., Illett, K.F., Beilby, J.P., Dusci, L.J., Barrett, P.H.R. (2000). "Pharmacokinetics and pharmacodynamics of gliclazide in caucasians and Australian Aborigines with type 2 diabetes." Brit J Clin Pharmcol **49**: 223-230.

- Derjaguin, B. V., and Landau, L.D. (1941). "Theory of stability of highly charged lyophobic sols and adhesion of highly charged particles in solution of electrolytes." *Acta Physiochim URSS* **14**(6): 633-652.
- Dupont, B. (2002). "Overview of teh lipid formulations of amphotericin B." *J Antimicrob Chemother* **S1**: 31-36.
- Emara, S., Morita, I., Tamura, K., Razee, S., Masujima, T., Mohamed, H.A., El-Gizawy, S.M., El-Rabbat, N.A. (2000). "Effect of cyclodextrins on the stability of adriamycin, adriamycinol, adriamycinone, and daunomycin." *Talanta* **51**: 359-364.
- EMEA (1995). Validation of analytical procedures: Text and methodology. CPMP/ICH/381/95.
- EMEA (2010). Revised priority list for studies into off-patent paediatric medicinal products. EMA/480197/2010.
- Faergemann, J., Runeman, B., Larko, O. (2000). "Experimental Candida albicans lesions in healthy humans: dependance on skin pH." *Acta Derm-venereol* **80**: 421-424.
- FDA (1998). Regulations Requiring Manufacturers to Assess the Safety and Effectiveness of New Drugs and Biological Products in Pediatric Patient, Federal Register. **63**: 66632-66672.
- FDA (2002). Best Pharmaceuticals for Children Act. **Pub. L. No. 107-109**.
- Fessi, H., Puisieux, F., Devissaguet, J.Ph., Ammoury, N., Benita, S. (1989). "Nanocapsule formation by interfacial polymer deposition following solvent displacement." *Int J Pharm* **55**: R1-R4.
- Field, L. D., Sternhell, S. (1989). *Analytical NMR*. Bath, UK, John Wiley & Sons.
- Firaji, A. H., Wipf, P. (2009). "Nanoparticles in cellular drug delivery." *Bioorg Med Chem* **17**: 2950-2962.
- Fleming, E. D. D., Ma, P. (2002). "Drug life-cycle technologies." *Nat Rev Drug Discov* **1**: 751-752.

- Florence, A. T., Hillary, A.M., Hussain, N., Jani, P.U. (1995). "Nanoparticles as carriers for oral peptide absorption: studies on particle uptake and fate." J Control Release **36**: 39-46.
- Florey, K., Ed. (1982). Analytical profiles of drug substances. Captopril. London, Academic Press.
- Forgo, P., Vincze, I., Kövér, E. (2003). "Inclusion complexes of ketosteroids with β -cyclodextrin." Steroids **68**: 321-327.
- Furr , J. R., Russell, A. D. (1972). "Factors influencing the activity of esters of *p*-hydroxybenzoic acid against *Serratia marcescens*." Microbios **5**: 189-198.
- Gallardo, V., Salcedo, J., Parera, A., Delgado, A. (1991). "Effect of the preservatives antipyrin, benzoic acid and sodium metabisulfite on properties of the nitrofurantoin/solution interface." Int J Pharm **71**(3): 223-227.
- Giam, J. A., McLachlan, A.J. (2008). "Extemporaneous product use in paediatric patients: a systematic review." Int J Pharm Practice **16**: 3-10.
- Gibaud, S., Demoy, M., Andreux, J.P., Weingarten, C., Gouritin, B., Couvreur, P. (1996). "Cells involved in the capture of nanoparticles in hematopoietic organs." J Pharm Sci **85**: 944-950.
- Govender, T., Stolnik, S., Garnett, M.C., Illum, L., Davis, S.S. (1999). "PLGA nanoparticles prepared by nanoprecipitation: drug loading and release studies of a water soluble drug." J Control Release **57**: 171-185.
- Grove, C., Liebenberg, W., Du Preez, J.I., Yang, W., De Villiers, M.M. (2003). "Improving the aqueous solubility of triclosan by solubilization, complexation, and in situ salt formation." J Cosmet Sci **54**: 537-550.
- Grubb, S. E. W., Murdocj, C., Sudbery, P.E., Saville, S.P., Lopez-Ribot, J.L., Thornhill, M.H. (2008). "*Candida albicans* - Endothelial cell interactions: a key step in th epathogenesis of systemic candidiasis." Infect Imun **76**(10): 4370-4377.

- Gubskaya, A. V., Lihnyak, Y.V., Blagoy, Y.P. (1995). "Effect of cryogrinding on physicochemical properties of drugs. I. Theophylline: evaluation of particle sizes and the degree of crystallinity, relation to dissolution parameters." *Drug Dev Ind Pharm* **21**: 1953-1964.
- Gupta, P. K., Ed. (2005). *Chapter 16: solutions and phase equilibria*. Remington: The science and practice of pharmacy., Lippincott Williams and Wilkins.
- Hans, M. L., Lowman, A.M. (2002). "Biodegradable nanoparticles for drug delivery and targeting." *Curr Opin Solid State Mater Sci* **6**: 319-327.
- Hardeland, R., Pandi-Perumal, S.R. (2005). "Melatonin, a potent agent in antioxidative defense: Actions as a natural food constituent, gastrointestinal factor, drug and prodrug." *Nutr & Metab* **2**(22): 1-15.
- Hardeland, R., Pandi-Perumal, S.R., Cardinali, D.P. (2006). "Melatonin." *Int J Biochem & Cell Bio* **38**: 313-316.
- Hattori, M. A., Del Ben, G.L., Carmona, A.K., Casarini, D.E. (2000). "Angiotensin I-Converting enzyme isoforms (high and low molecular weight) in urine of premature and full-term infants." *Hypertension* **35**: 1284-12990.
- Hey, E., Ed. (2007). *Neonatal formulary 5: drug use in pregnancy and first year of life*. Oxford, Blackwell publishers.
- Hillaert, S., Van den Bossche, W. (1999). "Determination of captopril and its degradation products by capillary electrophoresis." *J Pharmaceut Biomed* **21**(1): 65-73.
- Hillery, A. M., Florence, A.T. (1996). "The effect of adsorbed poloxamer 188 and 407 surfactants on the intestinal uptake of 60nm polystyrene particles after oral administration in the rat." *Int J Pharm* **132**: 123-130.
- Hiremath, S. N., Raghavendra, R.K., Sunil, F., Dhanki, L.S., Rampure, M.V., Swamy, P.V., Bhosale, U.V. (2008). "Dissolution enhancement of gliclazide by preparation of inclusion complexes with β -cyclodextrin." *Asian J Pharm* **2**(1): 73-76.
- Hong, S. S., Lee, S.H., Lee, Y.J., Chung, S.J.Lee, M.H., Shim, C.K. (1998). "Accelerated oral absorption of gliclazide in human subjects from a soft gelatin capsule containing a PEG 400 suspension of gliclazide." *J Control Release* **51**: 185-192.

- Huang, L.-F., Guo, F.-Q., Liang, Y.-Z., Li, B.Y., Cheng, B.-M. (2004). "Simultaneous determination of L-arginine and its mono- and dimethylated metabolites in human plasma by high-performance liquid chromatography–mass spectrometry." Anal Bioanal Chem **380**: 643-649.
- Ikeda, Y., Kimura, K., Hirayama, F., Arima, H., Uekama, K. (2000). "Controlled release of water-soluble drug, captopril, by a combination of hydrophilic and hydrophobic derivatives." J Control Release **66**: 271-280.
- Jurca, T., Vicas, L. (2010). "Complexes of the ACE-inhibitor captopril." Farmacia **58**(2): 198-202.
- Kabara, J. J., Ed. (1984). Chelating agents as preservative potentiators. Cosmetic and drug preservation: principles and practice. New York, Marcel Dekker Inc.
- Kabara, J. J., Orth, D.S. (1997). Preservative-free and self-preserving cosmetics and drugs: principles and practices. New York, USA, Marcel Dekker.
- Kant, A., Linforth, R.S.T., Hort, J., Taylor, A.J. (2004). "Effect of β -cyclodextrin on aroma release and flavour perception." J Agr Food Chem **50**: 7293-7298.
- Katzung, B. G., Masters, S.B., Trevor, A.J. (2009). Basic and Clinical Pharmacology. New York, McGraw-Hill Medical.
- Kayes, J. B. (1977). "Pharmaceutical suspensions: relation between zeta potential, sedimentation volume and suspension stability." J Pharm Pharmacol **29**(1): 199-204.
- Kayser, O., Olbrich, C., Croft, S.L., Kiderlan, A.F. (2003). "Formulation and biopharmaceutical issues in the development of drug delivery systems for antiparasitic drugs." Parasitol Res **90**: S63-S70.
- Kellaway, I. W., Najib, N.M. (1981). "Hydrophilic polymers as stabilizers and flocculants of sulphadimidine suspensions." Int J Pharm **9**: 59-66.
- Khan, M. A., Sastry, S.V., Vaithiyalingam, S.R., Agarwal, V., Nazzal, S., Reddy, I.K. (2000). "Captopril gastrointestinal therapeutic system coated with cellulose acetate pseudolatex: evaluation of main effects of several formulation variables." Int J Pharm **193**: 147-156.

- Kowalcuk, D., Pietras, R., Baran, J. (2007). "Spectrophotometric analysis of cefepime and L-arginine in the pharmaceutical preparation." Universitatis Mariae Curie-Sklodowska **10**(2): 83-87.
- Krebs, H. A., Wiggins, D., Stubbs, M., Sols, A., Bedoya, F. (1983). "Studies on the mechanism of the antifungal action of benzoate." Biochem. J. **214**(3): 657-663.
- Kristensen, S., Lao, Y.E., Brustugun, J., Braenden, J.U. (2008). "Influence of formulation properties on the chemical stability of captopril in aqueous preparation." Pharmazie **63**: 872-877.
- Kumar, R., Arora, V., Ram, V., Bhandari, A., Vyas, P. (2011). "Hypoglycemic and hypolipidemic effect of Allopolyherbal formulations in streptozotocin induced diabetes mellitus in rats." Int J Diabetes Mellitus: DOI: 10.1016/j.ijdm.2011.01.00.
- Kumari, A., Yadav, S.K., Yadav, S.C. (2010). "Biodegradable polymeric nanoparticles based drug delivery systems." Colloid Surface B **75**: 1-18.
- Kurrup, T. R. R., Wan, S.C., Chan, L.W. (1995). "Interactions of preservatives with macromolecules. Part II. Cellulose derivatives." Pharmaceutica Acta Helveticae **70**(2): 187-193.
- Kwon, H.-Y., Lee, J.-Y., Choi, S.-W., Jang, Y., Kim, J.-H. (2001). "Preperation of PLGA nanoparticles containing estrogen by emulsification-diffusion method." Colloid Surface A **182**: 123-130.
- Lawrence, M. J., Rees, G.D. (2000). "Microemulsion-based media as novel drug delivery systems." Adv Drug Del. Rev **45**: 89-121.
- Lee, B.-J., Min, G.-H. (1996). "Oral controlled release of melatonin using polymer-reinforced and coated alginate beads." Int J Pharm **144**: 37-46.
- Lee, B.-J., Choi, H.-G., Kim, C.-K., Parrott, K.A., Ayres, J.W., Sack, R.L. (1997). "Solubility and stability of melatonin in propylene glycol and 2-hydroxypropyl- β -cyclodextrin vehicles." Arch Pharm Res **20**(6): 560-565.
- Lee, S., Lee, J., Choi, Y.W. (2007). "Characterisation and evaluation of freeze-dried liposomes loaded with ascorbyl palmitate enabling anti-aging therapy of the skin." Bull Korean Chem Soc **28**(1): 99-102.

- Leroueil-Le Verger, M., FLuckiger, L., Kim, Y.-I., Hoffman, M., Maincent, P. (1998). "Preperation and characterisation of nanoparticles containing an antihypertensive agent." Eur J Pharm Biopharm **46**: 137-143.
- Leuner, C., Dressman, J. (2000). "Improving drug solubility for oral delivery using solid dispersions." Eur J Pharm Biopharm **50**: 47-60.
- Li, P. Z., L. (2003). "Solubilisation of flurbiprofen in pH-surfactant solutions." J Pharm Sci **92**(5): 951-956.
- Loftsson, T. (1995). "Effects of cyclodextrins on the chemical stability of drugs in aqueous solutions." Drug Stability **1**: 22-23.
- Lyklema, J., and Duval, J.F.L. (2005). "Hetero-interaction between Gouy-Stern double layers: Charge and potential regulation." Adv Colloid Interfac **114-115**: 27-45.
- MacFadyen, D. A., Fowler, N. (1950). "On the mechanism of the reaction of ninhydrin with alpha amino acids." J Biol Chem **186**: 1-12.
- Macgregor, D. R., Elliker, P.R. (1958). "A comparison of some properties of strains of *Pseudomonas aeruginosa* sensitive and resistant to quaternary ammonium compounds." Can J Microbiol **4**(499-503).
- Magenheim, B., Levy, M.Y., Benita, S. (1993). "A new in vitro technique for the evaluation of drug release profiles from colloidal carriers - ultrafiltration technique at low pressure." Int J Pharm **94**: 115-123.
- Marçon, F., Mathiron, D., Pilard, S., Lemaire-Hurtel, A.-S., Dubaele, J.-M., Djedaini-Pilard, F. (2009). "Development and formulation of a 0.2% oral solution of midazolam containing γ -cyclodextrin." Int J Pharm **379**: 244-250.
- Markowski, P., Baranowska, I., Braranowski, J., (2007). "Simultaneous determination of L-arginine and 12 molecules participating in its metabolic cycle by gradient RP-HPLC method application to human urine samples." Analytica Chimica Acta **605**: 205-217.
- Másson, M., Loftsson, T., Jónsdóttir, S., Fridriksdóttir, H., Petersen, D.S., (1998). "Stabilisation of ionic drugs through complexation with non-ionic and ionic cyclodextrins." Int J Pharm **164**: 45-55.

- Mayer, M., Meyer, B. (2000). "Mapping the active site of angiotensin-converting enzyme by transferred NOE spectroscopy." *J Med Chem* **43**: 2093-2099.
- Meyer, H. (1957). "The ninhydrin reaction and its analytical applications." *Biochem J* **67**(2): 333-340.
- Midmore, B. R., Hunter, R.J. (1988). "The effect of electrolyte concentration and co-ion type on the ζ -potential of polystyrene latices." *J Colloid Interface Sci* **122**(2): 521-529.
- Mielcarek, J., Daczkowska, E. (1999). "Photodegradation of inclusion complexes of israpidine with methyl- β -cyclodextrin." *J Pharmaceut Biomed* **21**: 393-398.
- Miller, T. E. (1969). "Killing and lysis of Gram-negative bacteria through the synergistic effect of hydrogen peroxide, ascorbic acid and lysozyme." *J. Bacteriol.* **98**(3): 949-955.
- Minami, M., Takahashi, H., Inagaki, H., Yamano, Y., Onoue, S., Matsumoto, S., Sasaki, T., Sakai, K. (2009). "Novel tryptamine-related substances, 5-sulphatoxydiacetyltryptamine, 5-hydroxydiacetyltryptamine, and reduced melatonin in human urine and the determination of those compounds, 6-sulphatoxymelatonin, and melatonin with fluorometric HPLC." *J Chromatography B* **877**(8-9): 814-822.
- Miyako, Y., Khalef, N., Matsuzaki, K., Pinal, R. (2010). "Solubility enhancement of hydrophobic compounds by cosolvents: Role of solute hydrophobicity on the solubilisation effect." *Int J Pharm* **393**: 48-54.
- Moghimi, S. M., Hawley, A.E., Christy, N.M., Gray, T., Illum, L. Davis, S.S. (1994). "Surface engineered nanospheres with enhanced drainage into lymphatics and uptake by macrophages of the regional lymph nodes." *FEBS Lett* **344**: 25-30.
- Mosqueira, V. C. F., Legrand, P., Pinto-Alphandary, H., Puisieux, F., Barratt, G. (2000). "Poly(DL-lactide) nanocapsules prepared by the solvent displacement process: influence of the composition on physicochemical and structural properties." *J Pharm Sci* **89**(5): 614-626.
- Moyano, J. R., Arias-Blanco, M.J., Gines, J.M., Giordano, F. (1997). "solid-state characterisation and dissolution characteristics of gliclazide- β -cyclodextrin inclusion complexes." *Int J Pharm* **148**(211-217).

- Mulla, H., Tofeig, M., Bu-Lock, F., Samani, N., Pandya, H.C. (2007). "Variations in captopril formulations used to treat children with heart failure: a survey in the United Kingdom." *Arch Dis Child* **92**: 409-411.
- Mulla, H., Hussain, N., Tanna, S., Lawson, G., Manktelow, B.N., Tuleu, C., Samani, N.J., Pandya, H.C. (2010). "Assessment of liquid captopril formulations used in children." *Arch Dis Child* **96**: 293-296.
- Muller, R. H. (1991). Charge determinations in:Colloidal carriers for controlled drug delivery and targeting, modification, characterisation and in vivo. Boca Raton, FL., CRC Press.
- Murakami, H., Kobayashi, M., Takeuchi, H., Kawashima, Y. (1999). "Preperation of poly(DL-lactide-co-glycolide) nanoparticles by modified spontaneous emulsification solvent diffusion method." *Int J Pharm* **187**: 143-152.
- Murray, P. R., Rosenthal, K.S., Kobayashi, G.S., Pfaller, M.A. (2002). Medical Microbiology. Missouri, USA, Mosby, Inc.
- Nahata, M. C. (1999). "Lack of paediatric drug formulations." *Paediatrics* **104**(3): 607-609.
- Nair, L. S., Laurencin, C.T. (2007). "Biodegradable polymers as biomaterials." *Progr Polym Sci* **32**: 762-798.
- Nakano, M. (2000). "Places of emulsions in drug delivery." *Adv Drug Del. Rev* **45**: 1-4.
- Narang, R., Narasimhan, B., Judge, V., Ohlan, S., Ohlan, R. (2009). "Evaluation of preservative effectiveness in an offcial antacid preperation." *Acta Pharmaceutica Sciencia* **51**: 225-229.
- Nguyen, T., Clare, B., Guo, W., Martinac, B. (2005). "The effects of parabens on the mechanosensitive channels of *E. coli*." *Eur. Biophys. J.* **34**: 389-395.
- Norris, D. A., Puri, N., Sinko, P.J. (1998). "The effect of physical barriers and properties on the oral absorption of particulates." *Adv Drug Del. Rev* **34**: 135-154.
- Oberlain, A. (1989). Chemistry of physics of carbon. New York, USA, Marcel Dekker.
- Okada, M. (2002). "Chemical synthesis of biodegradable polymers." *Progr Polym Sci* **27**: 87-133.

- Ozkan, Y., Atay, T., Dikmen, N., Isimer, A., Aboul-Enein, H.Y. (2000). "Improvement of water solubility and in vitro dissolution rate of gliclazide by complexation with β - cyclodextrin." Pharmaceutica Acta Helvetiae **74**: 365-370.
- Palmer, K. J., Brogden, R.N. (1993). "An update of its pharmacological properties and therapeutic efficacy in non-insulin-dependent diabetes mellitus." Drugs **46**: 93-125.
- Pearce, R. E., Rodrigues, A.D., Goldstein, J.A., Parkinson, A. (1996). "Identification of the human P450 enzymes involved in lansoprazole metabolism." J Pharmacol Exp Ther **277**: 805-816.
- Permyakov, E. A., Kretsinger, R.H. (2011). Calcium binding proteins. New Jersey, USA, John Wiley & Sons.
- Pieri, C., Mooni, F., Marra, M., Marcheselli, F., Recchioni, R. (1995). "Melatonin is an efficient antioxidant." Arch Gerontol Geriat **20**: 159-165.
- Prabha, S., Labhsetwar, V. (2004). "Critical determinants in PLGA/PLA nanoparticle-mediated gene expression." Pharm Res **21**: 354-364.
- Prabha, S., Labhsetwar, V. (2004b). "Nanoparticle-mediated wild-type p53 gene delivery results sustained antiproliferative activity in breast cells." Mol Pharmacol **1**: 211-219.
- Prasad, N., Strauss, D., Reichart, G. (1999). "Cyclodextrins inclusion for food, cosmetics and pharmaceuticals." Eur Patent **1084**: 625.
- Quintanar-Guerrero, D., Allemann, E., Fessi, H., Doelker, E. (1998). "Preparation techniques and mechanisms of formation of biodegradable nanoparticles from preformed polymers." Drug Dev Ind Pharm **24**: 1113-1128.
- Ramakrishnan, S., Prud'homme, R.K., (2000). "Effect of solvent quality and ions on the rheology and gelation of kappa-carrageenan." J Rheology **44**(4): 885-896.
- Redhead, H. M., Davis, S.S., Illum, L. (2001). "Drug delivery in poly(lactide-co-glycolide) nanoparticles surface modified with poloxamer 407 and poloxamine 9028: in vitro characterisation and in vivo evaluation." J. Control Release **70**: 353-363.
- Reiter, R. J. (1991). "Pineal melatonin: cell biology of its synthesis and of its physiological interactions." Endocr Rev **12**: 151-180.

- Rezzani, R., Rodella, L.F., Fraschini, F., Gasco, M.R., Demartini, G., Musicanti, C., Reiter, R.J. (2009). "Melatonin delivery in solid lipid nanoparticles: prevention of cyclosporine A induced cardiac damage." J Pineal Res **46**: 255-261.
- Rose, N. R., Barron, A.L. (1983). Microbiology: basic principles and clinical applications. London, Macmillan.
- Rouini, M.-R., Mohajer, A., Tahami, M.-H. (2003). "A simple and sensitive HPLC method for determination of gliclazide in human serum." J Chromatography B **785**: 383-386.
- Rowe, R. C., Sheskey, P.J., Owen, S.C. (2006). Handbook of Pharmaceutical excipients. London, Pharmaceutical Press.
- Rubino, J. T., Ed. (2002). cosolvents and colsolvency. Encyclopedia of pharmaceutical technology., Marcel Dekker, Inc.
- Russell, A. D., Chopra. I. (1996). Understanding antimicrobial action and resistance. London, Ellis Horwood.
- Saez, A., Guzman, M., Molpeceres, J., Aberturas, M.R. (2000). "Freeze-drying of polycaprolactone and poly (_{D,L}-lactide-glycolic) nanoparticles induce minor particle size changes affecting the oral pharmacokinetics of loaded drugs." Eur J Pharm Biopharm **50**: 379-387.
- Sam, W. J., Ho, P.C. (1998). "Stability of captopril in invert sugar solution." J Clin Pharm Ther **23**: 451-456.
- Scheler, S., Saupe, S., Herre, A., Fahr, A. (2010). "Preservation of liquid drug preparations for oral administration." J Pharm Sci **99**(1): 357-367.
- Schwartz, A. M., Perry, J.W. (1949). Surface active agents: Their chemistry and technology. New York, Interscience Publishers, Inc.
- Seedher, N., Bhatia, S. (2003). "Solubility enhancement of Cox-2 Inhibitors using various solvent systems." AAPS Pharm Sci Tech **4**(3): 1-9.
- Seedher, N., Kanojia, M. (2009). "Co-solvent solubilisation of some poorly-soluble antidiabetic drugs." Pharm Dev Technol **14**(2): 185-192.

- Serajuddin, A. T. M. (2007). "Salt formation to improve drug solubility." Adv Drug Deliv Rev **59**: 603-616.
- Shabir, A., Mohammed, A. (2010). "Exploring the use of cyclodextrins as carriers in paediatric formulations." Brit J Clin Pharm **2**: 275-278.
- Shenoy, B. C., Rao, A. A. G., Rao, R. M. R. (1984). "Structure and stability of glycoamylase II from *Aspergillus niger*: a circular dichroism study." J. Biosci. **6**(5): 601-611.
- Shewale, B. D., Fursule, R.A., Sapkal, N.P. (2008). "Effect of pH and hydroxypropyl- β -cyclodextrin on solubility and stability of gliclazide." Int J Health Res **1**(2): 95-99.
- Shiri, N., Furuta, T., Xiao, F., Kajimura, M., Hanai, H., Ohashi, K., Ishizaki, T. (2002). "Comparison of Lansoprazole and famotidine for gastric acid inhibition during the daytime and night-time in different CYP2C19 genotype groups." Ailment Pharmacol Ther **16**: 837-846.
- Singh, M., Sharma, R., Banerjee, U.C. (2002). "Biotechnological applications of cyclodextrins." Biotechnol Adv **20**: 341-359.
- Singh, R., Lillard Jr., J.W. (2009). "Nanoparticle-based targeted delivery." Exp. Mol. Pathol. **86**: 215-223.
- Smith, A. P., Spontak, R.J., Ade, H. (2001). "On the similarity of macromolecular responses to high-energy processes: mechanical milling vs. irradiation." Polym Degrad Stabil **72**: 519-524.
- Soni, M. G., Burdock, G.A., Taylor, S. L., Greenberg, N. A. (2001). "Safety assessment of propyl paraben: a review of published literature." Food Chem. Toxicol. **39**: 513-532.
- Sortino, S., Scaiano, J.C., DE Guidi, G., Monti, S. (1999). "Effect of β -cyclodextrin complexation on the photochemical and photosensitizing properties of tolmetin: a steady-state and time-resolved study." Photochem Photobiol **70**: 549-556.
- Stahl, P. H., Wermuth, C.G. (2002). Handbook of Pharmaceutical Salts: Properties, selection and use. Chester, England, Wiley-VCH.

- Stamkulov, N. S., Mussabekov, K.B., Aidarova, S.B., Luckham, P.F. (2009). "Stabilisation of emulsions by using a combination of an oil soluble ionic surfactant and water soluble polyelectrolytes. I: Emulsion stabilisation and Interfacial tension measurements." Colloids Surface A **335**(1): 103-106.
- Starcher, B. (2001). "A ninhydrin-based assay to quantitate the total protein content of tissue samples." Anal Biochem **292**(1): 125-129.
- Stella, V., Rao, V.M., Zia, Z.V. (1999). "Mechanisms of drug release from cyclodextrin complexes." Adv Drug Del. Rev **36**: 3-16.
- Strand, S. P., Varum, K.M., Osgaard, K. (2003). "Interaction between chitosan and bacterisal suspension - adsorption and flocculation." Colloid Surface B **27**(1): 71-81.
- Strickley, R. G. (2004). "Solubilising excipients in oral and injectable formulations." Pharm Res **21**(2): 201-230.
- Tung, H.-H., Waterson, S., Reynolds, S.D. (1991). Formation and resolution of ibuprofen lysinate. U. S. Patent. **4994604**: 3.
- Tursilli, R., Casolari, A., Iannuccelli, V., Scalia, S. (2006). "Enhancement of malatonin photostability by encapsulation in lipospheres." J Pharm Biomed Anal **40**: 910-914.
- Van Natta, F. J., Hill, J.W., Carruthers, W.H. (1934). "Polymerization and ring formation, ϵ -caprolactone and its polymers." J Am Chem Soc **56**: 455-459.
- Varshosaz, J., Talari, R., Mostafavi, S.A., Nokhodchi, A. (2008). "Dissolution enhancement of gliclazide using in situ micronization by solvent change method." Powder Technol **187**: 222-230.
- Vemula, V. R., Lagishetty, V., Lingala, S. (2010). "Solubility enhancement techniques." Int J Pharmceut Sci Rev Res **5**(1): 41-51.
- Verwey, E. J. W., Overbeek, J.T.G. (1948). Theory of the stability of lyophobic colloids. New York, Dover Publications, Inc.
- Villiers, V. M., Tiedt, L.R. (1996). "An analysis of fine grinding and aggregation of poorly soluble drug powders in a vibrating mill." Pharmazie **51**: 564-567.

- Waldhauser, F. W., M., Lieberman, H.R., Deng, M.H., Lynch, H.J., Wurtman, R.J. (1984). "Bioavailability of oral melatonin in humans." Neuroendocrinology **39**: 307-313.
- Wallmark, B., Sachs, G., Mardh, S, Fellenenius, E. (1983). "Inhibition of gastric (H⁺ and K⁺)-ATPase by the substituted benzimidazole, picoprazole." Biochem Biophys Acta **728**: 31-38.
- Willmott, G. R., Vogel, R., Yu, S.S.C., Groenewegen, L.G., Roberts, G.S., Kozak, D., Anderson, W., Trau, M. (2010). "Use of tunable nanopore blockade rates to investigate colloidal dispersions." J Physics: Condens Matter **22**(45): 1-19.
- Wong, S. M., Kellaway, I.W., Murdan, S. (2006). "Enhancement of the dissolution rate and oral absorption of a poorly water soluble drug by formation of surfactant-containing microparticle." Int J Pharm **317**: 61-68.
- Woodruff, M. A., Hutmacher, D.W. (2010). "The return of the forgotten polymer - Polycaprolactone in the 21st century." Progr Polym Sci DOI: [10.1016/j.progpolymsci.2010.04.002](https://doi.org/10.1016/j.progpolymsci.2010.04.002).
- Wu, Y., Hussain, M., Fassihi, R. (2005). "Development of a simple analytical methodology for determination of glucosamine release from modified release matrix tablets." J Pharmaceut Biomed **38**: 263-269.
- Yoshitani, R. S., Cooper, E.S. (2007). "Pharmaceutical reformulation: The growth of life cycle management." Hous J Health L & Pol'y **7**: 379-410.
- Zani, F., Minutello, A, Maggi, L., Santi, P., Mazza, P. (1997). "Evaluation of preservative effectiveness in pharmaceutical products: the use of a wild strain of *Pseudomonas cepacia*." J. Appl. Microbiol. **83**(3): 322-326.
- Zhang, X., Sun, N., Wu, B., Lu, Y., Guan, T., Wu, W. (2008). "Physical characterisation of Lansoprazole/PVP solid dispersion prepared by fluid-bed coating technique." Powder Technol **182**: 480-485.
- Zheng, Y. J., Keeney, M.P. (2006). "Taste masking analysis in pharmaceutical formulation development using an electronic tongue." Int J Pharm **310**: 118-124.

Zhu, A., Ji, J., Lin, R., Gao, C., Feng, L., Shen, J. (2002). "Surface engineering of poly(dl-lactic acid) by entrapment of alginate-amino acid derivatives for promotion of chondrogenesis." Biomaterials **23**: 3141-3148.